MASSEY UNIVERSITY
TE KUNENGA KI PŪREHUROA
UNIVERSITY OF NEW ZEALAND

Historical biogeography of marine ray-finned fishes (Actinopterygii) of the Southwest Pacific

A thesis submitted in partial fulfilment of the requirements for the degree of

Doctor of Philosophy

in

Marine Evolutionary Ecology

at Massey University, Auckland, New Zealand

André Philippe SAMAYOA

February 2023

Thesis abstract

Current environmental and anthropogenic pressures are driving significant biodiversity loss and range shifts in marine environments. Understanding how biodiversity is generated and how it responded to past environmental changes is fundamental to inform future management strategies for marine resources. As the largest ubiquitous taxonomic group among marine vertebrates, ray-finned fishes (Actinopterygii) represent the best model to understand the generation of biodiversity and the processes that shaped contemporary geographic patterns in the sea. In this sense, centers of marine endemism are of evolutionary value as they translate evolutionary and ecological mechanisms that drive biodiversity dynamics. In the Pacific Ocean, endemism centers for marine fishes are mainly located in remote oceanic islands at the periphery of the tropical West Pacific which harbors the highest levels of biodiversity. Biogeographic research suggests that marine fish endemism in the oceanic islands of the Central Pacific originated via multiple independent jump-dispersal colonization events, and that the islands have acted as sources of new unique biodiversity. However, as the evolutionary setting starts to be revealed for marine fish endemism in the Pacific, processes that generate and maintain biodiversity in other peripheral islands remain unknown. My thesis aims to fill this gap by studying the origin, evolution, and processes that have shaped endemism and biodiversity of marine fishes in the Southwest Pacific. I examined the historical biogeography of the region´s marine fish fauna using open-access molecular data to infer evolutionary histories, and geographic distribution information to assess spatial patterns of endemism and biodiversity. Data were analyzed across three research projects based on time-calibrated phylogenies, probabilistic biogeographic modeling, and statistical analysis of phylogenetic measures of endemism and biodiversity. My results confirm the role of the subtropical islands of the Southwest Pacific as sources of new unique biodiversity, identify mainland Australia as the major source of endemic lineages, highlight the significance of jump-dispersal and vicariance in shaping

endemism patterns, and reveal that the processes shaping patterns of endemism and biodiversity differ at local scales. My thesis contributes to the understanding of unique contemporary biogeographic patterns in the marine fish fauna of the Southwest Pacific.

Keywords

Biodiversity – biogeography – endemism – evolution – marine ray-finned fishes – molecular phylogenetics – Southwest Pacific

Declaration by author

The research carried out for my doctoral thesis has been used in whole or in part for this qualification only. The research is my original work, except as indicated by appropriate attribution in the text and/or acknowledgments; quotation marks have been used where required; and I take responsibility for the content and quality of this thesis. I have clearly stated the contribution of others in jointly authored works, which can be found at the end of each chapter. The “Statement of Contribution to Doctoral Thesis Containing Publications (DRC16)”, has been completed for each research chapter within the thesis, and is included in the electronic copy at the start of each chapter.

Publications during candidature

Peer-reviewed journal article, included in this thesis:

Samayoa, A.P., Struthers, C.D., Trnski, T., Roberts, C.D. & Liggins, L. (2022). Molecular phylogenetics reveals the evolutionary history of marine fishes (Actinopterygii) endemic to the subtropical islands of the Southwest Pacific. *Molecular Phylogenetics and Evolution*. 176, 107584.

https://doi.org/10.1016/j.ympev.2022.107584

Article submitted for publication in a peer-reviewed journal, included in this thesis:

Samayoa A.P., Aguirre, J.D., Delrieu-Trottin, E., & Liggins, L. In press. The origins of marine fishes endemic to subtropical islands of the Southwest Pacific. *Journal of Biogeography*.

Acknowledgments

No PhD is easy, less in a foreign land, and even less during a pandemic. Away from my relatives in Guatemala, Spain, and France, I landed in New Zealand without realizing how my Kiwi adventure would be a terrifying roller-coaster of emotions. Yes, it was extremely hard to focus on my PhD during the first year, locked thousands of kilometers away from my loved ones, fearing for their health as for mine. Yes, it was very difficult to be thousands of kilometers from my academic hub once I was able to work overseas for the remaining two years. Yes, it required a significant amount of courage to keep working while the whole world was constantly adapting to ever-daily changing rules. But, yes, I felt an explosion of colorful emotions when I could overturn all sorts of difficulties, pushing my PhD progress toward success.

I deeply thank and owe my achievement to: my two sons, for their patience when dad worked with “his fishes”; my mum, whose unconditional love has always been present; Rosa, who has been courageous from the beginning until the end; Libby, my main Supervisor, for believing in me from the beginning, for her natural care towards her students, for being assertive in every single feedback, and for supporting me in working overseas; Dave and Adam, my Co-Supervisors, for their insatiable enthusiasm when discussing research; Linh Mills, my stability in the country when things did go wrong; to colleagues that worked in Ōtehā Rohe; co-authors and scientists in New Zealand and abroad, for their constructive comments; and all my friends in the past and present, in New Zealand and across the globe, thanks for bearing with me in my doctoral quest.

This special moment is dedicated to my sons, Nico and Om, two wonderful pillars that bring light to my heart: dreams come true, build your path along caring people that will support you in every possible way. Never stop dreaming, live for it.

Table of Contents

1. General introduction

1. 1. Literature review

1. 1. 1. Biogeographic patterns in the sea

Marine organisms are not uniformly distributed in the sea realm, a phenomenon resulting from the effect of ecological and evolutionary mechanisms (Costello and Chaudhary, 2017). Biogeography studies the distribution of living organisms and the mechanisms influencing their distribution, traditionally aiming to identify “hotspots”, geographic locations with high levels of biodiversity, given the value in protecting such places in the face of the ongoing biodiversity loss (Norman, 2003). Although it is worth noting that a hotspot can be defined either by its number of total species (Reid, 1998) or of range-restricted species only (Myers, 1990), we currently have an advanced understanding of the geographic distribution of the most diverse terrestrial (Myers et al., 2000) and marine (Roberts et al., 2002) regions.

In the marine environment, cross-taxon species richness concentrates in tropical ecosystems, peaks at the edges of warm waters, and dips at the equator following a bimodal latitudinal distribution (Chaudhary et al., 2016). This latitudinal gradient seems shaped by the strong influence of temperature, as shown by the symmetrical thermal gradient along latitude (Chaudhary et al., 2017), and the ongoing poleward range shifts of marine species caused by equatorial warming conditions (Chaudhary et al., 2021). Within tropical ecosystems, it is largely accepted that the diversity of marine coastal species is higher at the intersection of the East Indian and West Pacific Oceans (Tittensor et al., 2010), a region known as the Indo-Australian Archipelago of long-lasting interest for biogeographers (Lohman et al., 2011). However, despite the large consensus in the biogeographic value of the Indo-Pacific, determining the mechanisms underpinning the tropical hotspot has been a challenging task, traditionally spinning around three major hypotheses (Bellwood et al., 2012): the Center of Origin – species

originate in the tropical Indo-Pacific and spread outwards (Briggs, 2003); the Center of Overlap – the Indo-Pacific is the meeting area where the ranges of nearby species overlap (Woodland, 1983); and the Center of Accumulation/Survival – species originate at the periphery of the Indo-Pacific and spread inwards (Barber and Bellwood, 2005, Ladd, 1960). However, neither "Center-of" hypothesis fully explains the tropical "bullseye" pattern, with more recent data suggesting that processes referred to in each hypothesis interact over multiple spatio-temporal scales (Cowman, 2014).

Centers of endemism concentrate species found nowhere else (Myers et al., 2000), and as a scale-dependent pattern, endemism requires an *a priori* definition of the spatial framework where species are range-restricted (Daru et al., 2020). Marine endemism has not only value for conservation due to the higher extinction risks of range-restricted species (Manes et al., 2021), but also for evolutionary biologists, given that endemism sheds light on processes generating biodiversity (Bellwood and Meyer, 2009). In marine (Cowman et al., 2017) and terrestrial (Orme et al., 2005) species, evidence shows that hotspots of species richness and endemism do not always overlap, an indication that these patterns originate from different processes. Centers of endemism are often located in oceanic islands characterized by relatively low species richness (Kier et al., 2009), a pattern to be explained by models that derive from early island biogeographic theory that predicts species richness as a function of immigration, speciation, and extinction (MacArthur and Wilson, 1963, MacArthur and Wilson, 1967). Despite numerous oceanic island models proposed by theoreticians and empiricists, most models follow the principle that island endemism arises from highly dispersing colonizers, subsequent diversification events driven by geographic and/or ecological isolation, and eventual increase in endemism richness (Dawson, 2016, Hachich et al., 2015, Pinheiro et al., 2017, Whittaker et al., 2008, Whittaker et al., 2010). This theoretical framework brings together two processes belonging to two traditionally opposed views as to the main mechanism shaping biogeographic patterns (Wiens and Donoghue,

2004): rare long-distance dispersal (jump-dispersal) and geographic separation of two populations by a land or marine barrier (vicariance; see Cowman and Bellwood, 2013, for a review of barriers in the sea). In the last few decades, methodological progress has generated empirical data that supports the interaction of both processes over time in the generation of contemporary biogeographic patterns (Sanmartín, 2012), demonstrating how technological advances facilitate the study of historical processes that shape the distribution of marine organisms, contributing to the expansion of biogeographic theory.

1. 1. 2. Investigating the history of biogeographic patterns

Historical biogeography focuses on evolutionary processes (e.g., speciation, extinction) over geological time to explain the geographic distribution of organisms through time and space (Crisci, 2001), requiring a sound understanding of the evolutionary history of biodiversity and contemporary range information (Ronquist and Sanmartín, 2011). The technological innovations of the 20th century have improved methods to infer the evolutionary trajectories of living organisms using molecular sequences, resulting in the substantial integration of phylogenetic trees in historical biogeographic methods (Posadas et al., 2006). For marine biodiversity, the incorporation of range information has been slow, given the sampling bias towards terrestrial ecosystems (Hughes et al., 2021) and coastal areas (Hortal et al., 2015), leaving vast open-water regions unsampled. To fill this gap, recent modeling techniques generate probabilistic maps for benthic and pelagic taxa (Kaschner et al., 2019), combining environmental variables with occurrence data from web-based repositories (e.g., Ocean Biogeographic Information System, www.obis.org; and Global Biodiversity Information Facility, www.gbif.org).

Phylogenetic and range information are the basis of countless historical biogeographic methods (Crisci, 2001), which, until recent decades, excluded ecological explanations (e.g., dispersal ability, competition) for contemporary biogeographic patterns. To address calls to unify historical and ecological perspectives (Crisp et al., 2011, Ebach, 2004, Wiens and Donoghue, 2004), recent approaches integrate

evolutionary and ecological processes, leading to a more dynamic methodological approach in biogeographic research (Sanmartín, 2012). In my doctoral thesis, I acknowledge the plurality of historical biogeographic methods, referring the reader to the reviews by Crisci (2001), Posadas et al. (2006), and Sanmartín (2012), for detailed information on each methodological approach. Hereby, I rather focus on the more integrative tools and methods that can infer both evolutionary and ecological processes underlying biogeographic patterns.

Time is a fundamental feature in historical biogeography. Consequently, dating the geological and speciation events can unveil the evolutionary processes that organisms underwent to display their current spatial distribution (Hedges, 1996, Hunn and Upchurch, 2001). Molecular phylogenies can include a time framework for branching patterns by constraining specific nodes to fossil ages, allowing the estimation of absolute divergence timings (Gandolfo et al., 2008). For endemism patterns, time-calibrated phylogenies could indicate if an endemic lineage diverged after (neoendemic) or before (paleoendemic) the emergence of an island, recognizing an endemism center as a 'cradle' for biodiversity, or a 'museum' for the remnant population of a previously widespread taxon (Gillespie and Roderick, 2002). The combination of time-calibrated phylogenies and range information for terminal taxa is key for the estimation of ancestral ranges and the geographic origin of biodiversity (Sanmartín, 2012). Recently developed methods parametrize processes shaping range evolution (e.g., vicariance and jump-dispersal) along the phylogenetic tree (Matzke, 2013, Matzke, 2014), estimate parameters under a maximum-likelihood framework (Ree et al., 2005), and infer the most likely range at each ancestral node (Ree and Smith, 2008). Probabilistic biogeography allows the explicit testing of evolutionary and ecological hypotheses regarding the processes shaping modern-day biogeographic patterns (Lamm and Redelings, 2009), significantly clarifying the prevalence of jump-dispersal and vicariant events during range evolution (Matzke, 2014). Measuring the evolutionary differences between lineages

within a phylogenetic tree can further highlight evolutionary and ecological mechanisms creating species assemblages (Cadotte et al., 2010), resulting in the development of phylogenetic metrics that translate distinct evolutionary aspects of the biodiversity's history (Tucker et al., 2017). Contrasting the spatial distribution of phylogenetic measures of diversity and endemism with species richness is a proven approach to infer the evolutionary and ecological processes shaping richness hotspots (Pavoine and Bonsall, 2011), and to quantitatively distinguish centers of neo- and paleoendemism (Mishler et al., 2014).

Overall, these methods depart from traditional vicariance-vs-dispersal and evolutionary-vs-ecological biogeographic dichotomies, and are considered sensible approaches to enhance our understanding of the patterns of marine biodiversity through time and space under a more dynamic biogeographic approach.

1. 1. 3. The biogeography of marine fishes in the Pacific

Ray-finned fishes (Actinopterygii) belong to one of the largest taxonomic groups in the animal kingdom with over 34,500 valid species and 4,950 valid genera (Fricke et al., 2022). Due to a wide range of phenotypic traits, actinopterygians are evenly distributed between freshwater and marine environments (Seehausen and Wagner, 2014), with marine ray-finned fishes (hereby "marine fishes") spreading from tropical to polar latitudes (Lin et al., 2021), and inhabiting the top 75% of the oceans' depths (Yancey et al., 2014). Marine fishes are fundamental for ecosystem function, occupying a wide array of trophic positions and dietary niches (Hayden et al., 2019), and for human consumption (Natale et al., 2013). Because the elevated actinopterygian diversity seems to provide resilience to current climatic pressures (Duffy et al., 2016), marine fishes represent the best model to understand how marine biodiversity originates and persists over time if we are to determine future biodiversity patterns in the face of increasing environmental changes.

The Pacific Ocean is the largest body of seawater in the globe, and includes part of the Indo-Australian Archipelago which hosts the highest diversity of coastal marine fishes in the world (Cowman, 2014). The biogeography of marine fishes in the Pacific is characterized by high species richness/low endemism in the western tropical “bullseye”, and low species richness/high endemism in the oceanic islands at the periphery of the richness hotspot (Cowman et al., 2017). Recent works investigating the historical biogeography of marine fishes (Gaboriau et al., 2018, Miller et al., 2018, Pellissier et al., 2014, Siqueira et al., 2016) suggest that the geographic distribution of actinopterygians in the Indo-Pacific emerged from: the stability of tropical ecosystems during glaciations within the last 34 Ma, providing sufficient time for speciation and persistence of old lineages over time; elevated diversification driven by the high topographic variability of reef habitats; the interaction of mechanisms invoked in each of the three “Center-of” hypotheses (see Bellwood et al., 2012) over distinct geological timings; and the contribution of peripheral regions in generating and maintaining biodiversity.

The significant role that peripheral oceanic islands play in the dynamics of marine fish biodiversity is explicitly acknowledged in the “biodiversity feedback” model (Bowen et al., 2013), a biogeographic hypothesis in which the tropical Indo-Pacific exports biodiversity, but also imports biodiversity produced in peripheral islands. More regional evidence supports the model by highlighting the role of peripheral islands as engines for biodiversity origination, as reported for Hawaii (Hodge et al., 2014) and Easter Island (Rapa Nui) (Delrieu-Trottin et al., 2019). In both cases, biogeographic analyses suggest that the conjunct action of vicariant and colonization events shaped contemporary patterns of insular biodiversity and endemism, a conclusion congruent with the current historical biogeographic philosophy that recognizes the relevance of both vicariant and dispersal arguments in the explanation of biogeographic patterns (Sanmartín, 2012). However, despite significant progress in understanding the role of oceanic islands in

shaping spatial patterns of marine fish biodiversity, many remote islands that lie at the periphery of the Pacific Ocean remain understudied by biogeographers.

1. 1. 4. The Southwest Pacific

In this thesis, the “Southwest Pacific” is defined as the southwestern quadrant of the Pacific Ocean, bounded by latitudes 20°S-55°S and longitudes 150°E-165°W. It is a geologically active region (Neall and Trewick, 2008) characterized by two continental fragments of Gondwanan origin, Australia and Zealandia, and by the Australian-Pacific plate boundary that crosses New Zealand between the North and South Islands. Consequently, major landmasses include the continental islands of mainland Australia (eastern segment), and the aerial sections of Zealandia that comprise Aotearoa New Zealand (North Island, South Island, Stewart Island, the Chatham Islands, and several smaller islands) and New Caledonia (Trewick et al., 2007). Additionally, the Southwest Pacific harbors recently emerged oceanic islands of volcanic origin, with estimated ages of 23.8-1 Ma for subantarctic islands (Quilty, 2007, Scott and Turnbull, 2019), and 6.9-2.58 Ma for subtropical islands (Brook, 1998b, Jones and McDougall, 1973, McDougall et al., 1981). Most outlying islands sit on Zealandia (Mortimer et al., 2017), except the Kermadec Archipelago/Rangitāhua on the Kermadec Ridge (Brook, 1998b) and Macquarie Island on the Macquarie Ridge (Quilty, 2007). Politically, Australia administers the subtropical Lord Howe Island and Norfolk Island, and the subantarctic Macquarie Island. New Zealand’s outlying territories include subtropical Rangitāhua, as well as the subantarctic Bounty Islands/Moutere Hauriri, Antipodes Islands/Moutere Mahue, Snares Islands/Tini Heke, Auckland Islands/Motu Maha, and Campbell Island/Motu Ihupuku.

Surface currents in the Southwest Pacific follow the anti-clockwise movement of the South Pacific Gyre (Ganachaud et al., 2014): the main flow moves west at low latitudes as the South Equatorial Current, reaches mainland Australia through the Coral Sea, becomes the East Australian Current at 15°S to then flow southward along the

eastern Australian coastline, branches eastward between 32°S-34°S as the Tasman Front, crosses Norfolk, and reaches the North Island of New Zealand, becoming the East Auckland Current. Additionally, two independent currents from the East Australian Current flow east across the high latitudes of the Southwest Pacific (Nelson and Cooke, 2001): the Subtropical Front (ca. 43°S-45°S) that follows a convoluted path around the southern tip of New Zealand's South Island to then reach the Chatham Islands; and the Subantarctic Front (ca. 52°S) that flows around the southernmost continental segment of Zealandia to meet the Subtropical Front south of the Chathams. The three major eastward currents of the Southwest Pacific are distinguished by their physicochemical characteristics (Lorrey et al., 2012): the Tasman Front carries highly saline warm water which is poor in nutrients; the Subantarctic Front is a nutrient-rich, cold-water mass with lower salinity; and the Subtropical Front separates both other currents.

The Southwest Pacific hosts an exceptionally rich marine biodiversity resulting from the high species richness and endemism in New Zealand, and to a lesser extent, Australia (Briggs and Bowen, 2012, Costello et al., 2017). Both countries are considered the best taxonomically studied regions in the West Pacific (Costello et al., 2010), exemplified by the elevated completeness of New Zealand's inventory of marine species (Mora et al., 2008) which include 17,135 taxa and 4,315 undescribed species according to Gordon et al. (2010). For fish diversity, Roberts et al. (2020) report 1,296 species, of which 1,085 are marine actinopterygians. As high marine fish biodiversity seems linked to habitat complexity (Leprieur et al., 2016), New Zealand's marine richness might result from the extensive Zealandian continental shelf which likely provides abundant habitats for diversification (Gordon et al., 2010). Within the Southwest Pacific, taxonomic data point to the subtropical islands of Lord Howe, Norfolk, and Rangitāhua as centers of endemism, with an overall 4.6% endemism rate for coastal marine fishes (Francis, 1993), although recent surveys report the same figure for Rangitāhua alone (Trnski et al., 2015). The marine fish communities in the three island groups are a mixture of tropical,

subtropical, and temperate species (Francis and Duffy, 2015), a similarity likely explained by the predominant eastward oceanic currents of the region (Trnski and de Lange, 2015).

Overall, the contemporary spatial patterns of marine fish biodiversity and endemism are broadly understood in the Southwest Pacific. However, the evolutionary value of regional actinopterygians, and key biogeographic locations, have just started to be revealed (Delrieu-Trottin et al., 2018, Eme et al., 2020, Liggins et al., 2022). A comprehensive historical framework is needed to inform biogeographers, evolutionary biologists, ecologists, and conservationists about the relevance of the processes shaping the biogeography of marine fishes in the Southwest Pacific, if we are to determine how marine biodiversity will evolve in times of heavy biodiversity loss and intense anthropogenic pressure.

1. 2. Rationale and objectives

In the face of biodiversity loss in the sea, intense anthropogenic pressure on fish communities, and the immediate changes in biodiversity patterns due to climate change, it is imperative to pay attention to the spatial patterns of marine fishes in the Southwest Pacific and the underlying shaping processes if we are to understand the evolution of marine biodiversity in the region, and inform future management strategies for marine resources.

This thesis addresses the following questions:

Q1 - What is the origin of marine fish endemism in the region?

Q2 - What evolutionary and ecological processes shape endemism patterns in marine fishes in the region?

Q3 - What is the role of oceanic islands in promoting endemism of marine fishes in the region?

Q4 - Are patterns of marine fish endemism and elevated biodiversity shaped by the same processes?

My aims were:

A1 - To determine the geographic origin of marine fish taxa endemic to the subtropical oceanic islands of the Southwest Pacific

A2 - To establish the role of these oceanic islands in promoting endemism in the region

A3 - To identify biogeographic processes that have generated these endemism patterns in the region

A4 - To contrast the spatial patterns of marine fish endemism and biodiversity in the Southwest Pacific

A5 - To contrast the historical processes responsible for contemporary patterns of marine fish endemism and biodiversity

1. 3. Thesis structure

This thesis is composed of five chapters. This chapter (Chapter 1) introduces the theoretical framework from where my research derives, and presents the aims of the doctoral thesis. Chapter 5 summarizes my major findings and the main contributions of the present thesis, while proposing directives for future work. Three research chapters compose the main body text of the thesis, and are hereby presented in publishable format: one chapter has been published in *Molecular Phylogenetics and Evolution* (Chapter 2), another is submitted for peer-review in the *Journal of Biogeography* (Chapter 3), and the last chapter is intended to be submitted to the *New Zealand Journal of Marine and Freshwater Research* for peer-review (Chapter 4).

Chapters 2 to 4 are written as independent publishable research articles, resulting in the repetition of some methodological detail within the thesis, particularly between Chapters 2 and 3. As papers are co-authored, I use “we” and “our” in Chapters 2 to 4 to be inclusive of co-authors (see “Declaration by Author” on page iv). My proportional contribution is indicated in the Statement of Contribution form (DRC16) at the beginning of each chapter.

Chapter 2 addresses aims A1 and A2. The chapter’s objectives were to understand the evolutionary relationships of taxa endemic to the subtropical islands of the Southwest Pacific, to determine the role of the islands in the establishment of endemism in the region, and to qualitatively determine the origin of endemic taxa of the Southwest Pacific. The research is based on the inference of time-calibrated phylogenies to estimate the divergence time of endemic lineages, and contrast them with the ages of the islands they are endemic to. The chapter also includes the qualitative association of the phylogenetic placement of endemics and congeners with their geographic distribution to identify affinities of endemic taxa with fauna found in other marine regions.

Chapter 2 is an introduction to the marine fish taxa endemic to the remote islands of the Southwest Pacific and begins the present thesis with a qualitative analysis of the origin of endemism in the region.

Chapter 3 addresses aims A1, A2, and A3. The chapter's objectives were to examine the biogeographic and evolutionary processes that have shaped marine fish endemism in the Southwest Pacific, and to quantitatively determine the biogeographic origin of endemism in the Southwest Pacific. The biogeographic analysis relies on a probabilistic approach to range evolution modeling which simulates key biogeographic mechanisms. Chapter 3 is a natural continuation of the previous chapter by using a quantitative approach to reveal the geographic location of endemic lineage origination and the processes that gave rise to contemporary endemism patterns in the Southwest Pacific.

Chapter 4 addresses aims A2, A3, A4, and A5. The chapter's objectives were to describe and contrast the spatial patterns of biodiversity and endemism in marine fishes in Aotearoa New Zealand, and to propose hypotheses for the evolutionary and ecological processes shaping both biogeographic patterns. The work used a set of taxonomic and phylogenetic indices to characterize biodiversity and endemism, and to reveal historical processes responsible for the spatial patterns of phylogenetic metrics. Chapter 4 closes the thesis by examining the spatial patterns of endemism on a larger geographic scale, and contrasting processes responsible for endemism and biodiversity patterns in marine fishes. The study comprises remote oceanic islands examined in the previous chapters, and expands to all main and offshore islands of New Zealand, one of the most comprehensively studied areas in the Southwest Pacific from both taxonomic and phylogenetic perspectives.

2. Molecular phylogenetics reveals the evolutionary history of marine fishes (Actinopterygii) endemic to the subtropical islands of the Southwest Pacific

MASSEY UNIVERSITY
TE KUNENGA KI PŪREHUROA
UNIVERSITY OF NEW ZEALAND

GRADUATE RESEARCH SCHOOL

STATEMENT OF CONTRIBUTION
DOCTORATE WITH PUBLICATIONS/MANUSCRIPTS

We, the student and the student's main supervisor, certify that all co-authors have consented to their work being included in the thesis and they have accepted the student's contribution as indicated below in the Statement of Originality.

Student name:	André Philippe SAMAYOA
Name and title of main supervisor:	Dr. Libby Liggins
In which chapter is the manuscript/published work?	Chapter 2
What percentage of the manuscript/published work was contributed by the student?	75%

Describe the contribution that the student has made to the manuscript/published work:

Data curation, data analysis, results interpretation, original manuscript draft, review and final editing of manuscript, corresponding author.

Please select one of the following three options:

- (●) The manuscript/published work is published or in press

  Please provide the full reference of the research output:

  Samayoa, A.P., Struthers, C.D., Trnski, T., Roberts, C.D. & Liggins, L. (2022). Molecular phylogenetics reveals the evolutionary history of marine fishes (Actinopterygii) endemic to the subtropical islands of the Southwest Pacific. Molecular Phylogenetics and Evolution. 176, 107584. https://doi.org/10.1016/j.ympev.2022.107584

- ( ) The manuscript is currently under review for publication

  Please provide the name of the journal:

- ( ) It is intended that the manuscript will be published, but it has not yet been submitted to a journal

Student's signature:	André Philippe SAMAYOA Digitally signed by André Philippe SAMAYOA Date: 2022.10.26 14:58:49 +02'00'	Main supervisor's signature:	Libby Liggins Digitally signed by Libby Liggins Date: 2022.10.27 10:33:32 +13'00'

This form should be placed at the beginning of each relevant thesis chapter.

2.1. Abstract

Remote oceanic islands of the Pacific host elevated levels of actinopterygian (ray-finned fishes) endemism. Characterizing the evolutionary histories of these endemics has provided insight into the generation and maintenance of marine biodiversity in many regions. The subtropical islands of Lord Howe, Norfolk, and Rangitāhua (Kermadec) in the Southwest Pacific are yet to be comprehensively studied. Here, we characterize the spatio-temporal diversification of marine fishes endemic to these Southwest Pacific islands by combining molecular phylogenies and the geographic distribution of species. We built Bayesian ultrametric trees based on open-access and newly generated sequences for five mitochondrial and ten nuclear loci, and using fossil data for time calibration. We present the most comprehensive phylogenies to date for marine ray-finned fish genera, comprising 34 species endemic to the islands, including the first phylogenetic placements for 11 endemics. Overall, our topologies confirm the species status of all endemics, including three undescribed taxa. Our phylogenies highlight the predominant affinity of these endemics with the Australian fish fauna (53%), followed by the East Pacific (15%), and individual cases where the closest sister taxon of our endemic is found in the Northwest Pacific and wider Indo-Pacific. Nonetheless, for a quarter of our focal endemics, their geographic affinity remains unresolved due to sampling gaps within their genera. Our divergence time estimates reveal that the majority of endemic lineages (67.6%) diverged after the emergence of Lord Howe (6.92 Ma), the oldest subtropical island in the Southwest Pacific, suggesting that these islands have promoted diversification. However, divergence ages of some endemics pre-date the emergence of the islands, suggesting they may have originated outside of these islands, or, in some cases, ages may be overestimated due to unsampled taxa. To fully understand the role of the Southwest Pacific subtropical islands as a ‘cradle’ for diversification, our study advocates for further regional surveys focused on tissue collection for DNA analysis.

2.2. Introduction

Marine biodiversity is being lost at an accelerated rate, driven by anthropogenic pressures such as overharvesting (Costello et al., 2010), habitat fragmentation (Lotze et al., 2006), and climate change (Beaugrand et al., 2015). In particular, endemic species are more vulnerable to extinction than widespread taxa because of their restricted spatial distribution (Norman, 2003) and specialist niche requirements (Le Feuvre et al., 2021). For this reason, areas of high endemism have been of great research interest, shedding light on how biodiversity is generated and maintained (Bowen et al., 2013), and therefore how it is best conserved (Moritz, 2002). Molecular phylogenetics has been crucial in characterizing the evolutionary history of endemic species in these regions, and, consequently, the macroevolutionary processes that have given rise and maintained unique regional biodiversity (Bellwood and Meyer, 2009). Still, many regions are yet to be comprehensively researched (Hortal et al., 2015), and the evolutionary history of their endemic species characterized. Such understanding is increasingly urgent as pressures on biodiversity continue to escalate (Nunez et al., 2019).

Marine actinopterygians (ray-finned fishes) have been extensively studied in the last decade, providing comprehensive knowledge of their evolutionary relationships and temporal diversification patterns globally (Alfaro et al., 2018, Betancur-R et al., 2013, Betancur-R et al., 2015, Betancur-R et al., 2017, Hughes et al., 2018, Matschiner et al., 2017, Mirande, 2017, Near et al., 2013, Near et al., 2012, Rabosky, 2020, Rabosky et al., 2018). In particular, the deep nodes in the phylogeny of all marine ray-finned fishes have been the subject of intense research; however, towards the tips of the phylogeny, our understanding of the evolutionary relationships among finer taxonomic units (e.g. genera and species) diminishes, and a bias toward the most speciose, conspicuous, and easy to study taxa, increases (Cowman, 2014). This phylogenetic knowledge gap is exacerbated by survey efforts that tend to favor easy-to-access regions with substantial research resources, delaying comprehensive species inventories and associated

phylogenetic research in more isolated areas (Hortal et al., 2015). However, it is in isolated oceanic islands that the highest proportions of endemic marine fishes are observed (Van Der Meer et al., 2015), highlighting the importance of turning our attention to these remote centers of endemism to better understand the evolutionary and ecological processes shaping their biodiversity.

Within the Indo-Pacific Ocean, the tropical latitudes are widely recognized as hosting the highest levels of marine biodiversity, where the Coral Triangle represents the region's "bullseye" (Hoeksema, 2007). Synthetic literature has discussed the evolutionary and ecological processes that have formed and maintained this unique pattern (Cowman, 2014, Gaboriau et al., 2018), including the role of diversification in peripheral regions (Bowen et al., 2013). At the periphery of the Pacific Ocean, there tend to be geographically isolated islands characterized by elevated rates of endemism and low species richness (Cowman et al., 2017). For instance, Juan Fernández and Desventuradas in the East Pacific have the highest proportion of endemic coastal marine fishes (61.5%, Friedlander et al., 2016), followed by the Hawaiian archipelago in the Central North Pacific (25%, Randall, 2007), Rapa Nui (Easter Island) (21.7%, Randall and Cea, 2011), and the Marquesas Islands in the Central Pacific (13.7%, Delrieu-Trottin et al., 2015). Studies that combine the checklist of a region's marine fish fauna and the available molecular data in a phylogenetic framework have unveiled biogeographic patterns and the origin of species and biogeographic patterns in tropical areas (e.g. Hodge and Bellwood, 2016), including in the peripheral islands of Hawaii (Hoban and Williams, 2020, Hodge et al., 2014) and Rapa Nui (Delrieu-Trottin et al., 2019) providing a general understanding of the evolutionary histories of the fish fauna.

The Southwest Pacific harbors peripheral oceanic islands where the fish fauna is relatively understudied from an evolutionary perspective (Liggins et al., 2022). Lord Howe Island and Norfolk Island of Australia, and Rangitāhua (the Kermadec Islands) of New Zealand (Aotearoa) straddle subtropical waters (29°-32°S, Francis, 1993) (Fig. 1)

and are geologically young. Their estimated age of emergence due to intense volcanic activity is 6.92 Ma for Lord Howe (McDougall et al., 1981), 3.05 Ma for Norfolk (Jones and McDougall, 1973), and the Early Pleistocene (i.e. no older than 2.58 Ma) for Rangitāhua (Brook, 1998b). Because of their geographic position, the marine fish fauna is characterized by a mixture of tropical, subtropical, and temperate species (Francis and Duffy, 2015) and the overall rate of endemism for coastal fishes across the three island groups has been reported at 4.6% with individual rates in the 1.2-2.1% range (Francis, 1993). However, since these early studies, there have been several surveys and expeditions to the islands, resulting in the addition of further taxa to the fish checklists and the description of new endemic species (Francis, 2019). In particular, Rangitāhua has been the subject of intense sampling which has led to recent comprehensive checklists for its marine fauna and flora (Duffy and Ahyong, 2015), and its coastal fishes with an updated endemicity rate of 4.6% for this group (Trnski et al., 2015).

As a result of decades of field work, specimen curation, and laboratory work, we live in an age where it is easy to access large volumes of molecular, biological, and ecological information (Allendorf et al., 2010, Hoban et al., 2021). Nevertheless, the rates at which data are being generated, and ulteriorly analyzed differ considerably, increasing the amount of information yet to be evaluated (Hortal et al., 2015). Phylogenetic analyses are one means to summarize molecular data that has been accumulated across disparate taxa and research groups, helping to quickly contextualize new information that becomes available (Antonelli et al., 2017). Therefore, based on recent updates to species checklists for Lord Howe, Norfolk, and Rangitāhua, the acquisition of specimens endemic to the islands, the accumulation of open-access molecular sequences, and phylogenetic knowledge of marine fishes, we are well-placed to improve our understanding of how marine endemism has evolved in these peripheral islands of the Pacific.

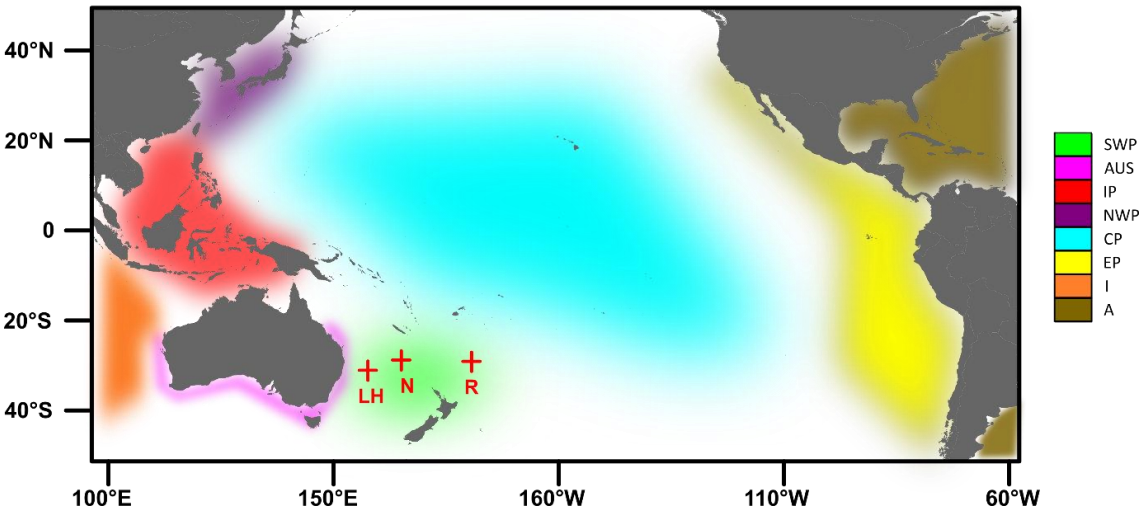

Fig. 1. Geographic location of Lord Howe Island (LH), Norfolk Island (N), and Rangitāhua (the Kermadec Islands) (R) in the Southwest Pacific region. The color palette illustrates the geographic regions defined in our study to classify the origin of sampled taxa: SWP: Southwest Pacific; AUS: Australian coasts; IP: Indian Ocean and West Pacific, centered in the Coral Triangle; NWP: Northwest Pacific; CP: Central Pacific; EP: East Pacific; I: Indian Ocean only; A: Atlantic Ocean.

In this study, we build the most comprehensive multi-locus time-calibrated phylogenies to date for marine ray-finned fishes occurring in the Southwest Pacific and endemic to the islands of Lord Howe Island, Norfolk Island, and/or Rangitāhua, to shed light on their evolutionary history. Firstly, we aimed to corroborate the species status of each endemic by phylogenetically placing it alongside its presumed sister taxa using molecular sequences. Secondly, we characterized the geographic origin of marine fish endemism in the Southwest Pacific region by associating each taxon to its range within each topology. Finally, we provide a temporal context for diversification in the Southwest Pacific region by estimating the divergence times of these endemic lineages using fossil-based calibration points. Our study generates new knowledge regarding the phylogenetic relationships of fishes endemic to the subtropical islands of the Southwest Pacific, and helps to highlight persisting gaps in taxonomic sampling that preclude definitive dating, the inference of their biogeographic origins, and modes by which endemic species evolved in the Southwest Pacific.

2.3. Materials and methods

2.3.1. Taxonomic sampling and study approach

We focused on marine fish taxa that are distributed in at least one of the three oceanic islands of Lord Howe, Norfolk, and Rangitāhua, and occurring in areas within the Southwest Pacific region (i.e. not occurring beyond Aotearoa New Zealand mainland, New Caledonia, and the east coast of Australia; Fig. 1), but not being widespread throughout the Southwest Pacific. We assembled a list of 60 taxa based on this criterion (hereafter "endemic taxa") using checklists from recent expeditions to Rangitāhua (Duffy and Ahyong, 2015, Francis and Duffy, 2015, Roberts et al., 2015, Trnski et al., 2015), and the most up-to-date checklist for Lord Howe, Norfolk, and Rangitāhua (Francis, 2019). This initial list was further refined according to DNA sequence data availability to select the endemics for subsequent analysis. For instance, we only kept endemics for which we had access to either DNA sequences or tissue for DNA extraction and sequencing. For the selected endemics, we also required that several sister taxa within their genus (and/or family) had either molecular sequences or tissues available, that could be used to phylogenetically place the endemics. The list of all sister taxa was built based on searches through World Register of Marine Species (WoRMS; WoRMS Editorial Board, 2021). To retrieve existing sequences for endemics and sister taxa, we searched the open-access sequence repositories of the National Center for Biotechnology Information (NCBI; www.ncbi.nlm.nih.gov/) and the Barcode of Life Data System (BOLD; www.barcodinglife.org). For endemics and sister taxa without available sequence information, we requested tissues from existing collections to generate novel sequences. For each endemic, the current valid scientific and vernacular names, and geographic distribution information were retrieved from the Eschmeyer's Catalog of Fishes (Fricke et al., 2021), Fishbase (Froese and Pauly, 2021), and faunal checklists of the Southwest Pacific (Francis, 2019, Duffy and Ahyong, 2015, Roberts et al., 2015, Roberts et al., 2020) and Australia (Fishes of Australia; http://fishesofaustralia.au.net).

For each sister taxon, taxonomic validity and their geographic range were verified using the Eschmeyer's Catalog of Fishes and FishBase. The final list of endemics for subsequent analysis included 34 taxa (Table 1).

The selection of outgroup taxa for phylogenetic analyses included representatives of related genera within the family of the endemics, related families of the same order, and members of related orders, based on the hypothetical evolutionary relationships among species in published literature and global phylogenies of ray-finned fishes (Alfaro et al., 2018, Betancur-R et al., 2017, Hughes et al., 2018, Matschiner et al., 2017, Near et al., 2013, Near et al., 2012, Rabosky et al., 2018). We specifically aimed for taxa for which fossil data are available according to Matschiner et al. (2017) to inform inference of time-calibrated trees. When possible, endemic and sister taxa that shared fossil calibration points with other endemic and sister taxa were grouped in a single phylogeny to use the same outgroup taxa. Consequently, the 34 endemics were analyzed in 13 phylogenies (Table 1). In our taxonomic sampling strategy, *Notocirrhitus splendens* represented an exceptional case within the NEMOGOCHIA phylogeny (naming as described below), since it is both a monotypic genus that we identify as an endemic – distributed in East Australia, Lord Howe, Norfolk, and Rangitāhua – and a representative of the family Cirrhitidae which has been consistently used as an outgroup to root trees of Aplodactylidae (Burridge, 2000b), Chironemidae (Burridge et al., 2006), and Cheilodactylidae/Latridae (Burridge and Smolenski, 2004, Ludt et al., 2019). Given that we had no available sequences for all the presumed sister taxa of *N. splendens*, and that missing species overestimate divergence times among phylogenetic congeners (Hodge and Bellwood, 2016), we opted to use this endemic as an outgroup in the phylogeny and exclude it from our final list of focal endemics.

Table 1. The 34 marine fish taxa included in our study that are endemic to the subtropical islands of Lord Howe, Norfolk, and/or Rangitāhua (Kermadec) in the Southwest Pacific. Current valid scientific and vernacular names; associated range (AUS: eastern coast of Australia; NC: New Caledonia; LH: Lord Howe; N: Norfolk; R: Rangitāhua - Kermadec Islands; NZ: mainland New Zealand); genus assessed and, in brackets, the number of taxa represented in the phylogeny over the total number of species in the genus; and the name of the phylogeny it is included in. The GAMS phylogeny includes *Girella*, *Atypichthys*, *Microcanthus*, and *Scorpis*. The HL phylogeny includes *Hypoplectrodes* and *Lepidoperca*. The NEMOGOCHIA phylogeny includes *Nemadactylus*, *Morwong*, *Goniistius*, *Chironemus*, and *Aplodactylus*. *Lepidoperca inornata* was selected as an endemic associated with Rangitāhua as it occurs along the Kermadec Ridge. *Girella fimbriata*, *Morwong fuscus*, and *Upeneus francisi* were not considered in mainland New Zealand, as their occurrence in northern locations is rare (Middleton et al., 2021, Middleton et al., in review).

ENDEMIC SPECIES	RANGE						GENUS	PHYLOGENY NAME
	AUS	NC	LH	N	R	NZ		
Arripis trutta (Forster, 1801) - Kahawai	X		X	X	X	X	*Arripis* (4/4)	Arripis
Arripis xylabion Paulin, 1993 - Northern kahawai			X	X	X	X		
Capromimus abbreviatus (Hector, 1875) - Capro dory					X	X	*Capromimus* (1/1)	Capromimus
Chromis abyssicola Allen & Randall, 1985 - Deepwater demoiselle				X	X	X	*Chromis* (85/110*-59/84**)	Chromis
Chromis dispila Griffin, 1923 - Twospot demoiselle					X	X		
Chromis hypsilepis (Günther, 1867) - Onespot demoiselle	X		X	X		X		
Chromis kennensis Whitley, 1964 ^^ - Yellowspot Puller	X	X	X	X	X			
Chromis nitida (Whitley, 1928) - Barrier reef chromis	X		X					
Enneapterygius kermadecensis Fricke, 1994 - Kermadec triplefin					X		*Enneapterygius* (27/63)	Enneapterygius
Eviota kermadecensis Hoese & Stewart, 2012 - Feathery goby					X		*Eviota* (62/117)	Eviota
Flexor incus Conway, Stewart & Summers 2018 - Kermadec clingfish		X	X		X		*Flexor* (1/1)	Flexor
Girella cyanea Macleay, 1881 - Bluefish	X		X	X	X	X	*Girella* (16/17)	GAMS
Girella fimbriata (McCulloch, 1920) - Caramel drummer					X			
Atypichthys latus McCulloch & Waite, 1916 - Mado			X	X	X	X	*Atypichthys* (2/2)	
Microcanthus joyceae Whitley, 1931 - East-Australian stripey	X	X	X	X			*Microcanthus* (2/2)	
Scorpis violacea (Hutton, 1873) - Blue maomao	X		X	X	X	X	*Scorpis* (4/5)	
Hypoplectrodes sp. A (*sensu* Roberts et al., 2015:1189) - Eyebrow perch	X		X	X	X	X	*Hypoplectrodes* (9/11^)	HL
Hypoplectrodes sp. C (*sensu* Roberts et al., 2015:1192) - Kermadec halfbanded perch					X			
Lepidoperca inornata Regan 1914 - Plain perch					X	X	*Lepidoperca* (8/10)	
Kathetostoma binigrasella Gomon & Roberts, 2011 - Banded stargazer					X	X	*Kathetostoma* (7/8)	Kathetostoma
Nemadactylus douglasii (Hector, 1875) - Porae	X				X	X	*Nemadactylus* (7/8)	NEMOGOCHIA
Nemadactylus n. sp. (*sensu* Roberts et al., 2015:1357) - King tarakihi	X		X	X	X	X		
Morwong ephippium (McCulloch & Waite, 1916) - Painted moki	X		X	X	X	X	*Morwong* (2/2)	
Morwong fuscus (Castelnau, 1979) - Red morwong	X		X					
Goniistius francisi (Burridge, 2004) - Masked morwong		X	X	X	X		*Goniistius* (9/9)	
Goniistius vestitus (Castelnau, 1879) - Crested morwong	X	X	X	X				
Chironemus marmoratus Günther, 1860 - Hiwihiwi	X		X			X	*Chironemus* (6/6)	
Chironemus microlepis Waite, 1916 - Northern kelpfish			X	X	X			
Aplodactylus etheridgii (Ogilby, 1889) - Notch-head marblefish			X	X	X	X	*Aplodactylus* (5/5)	
Optivus agastos Gomon, 2004 - Violet roughy	X	X	X				*Optivus* (3/3)	Optivus
Optivus elongatus (Günther, 1859) - Slender roughy					X	X		
Parma alboscapularis Allen & Hoese, 1975 - Black angelfish			X	X	X	X	*Parma* (7/10)	Parma

Table 1. *(continued)*

ENDEMIC SPECIES	RANGE						GENUS	PHYLOGENY NAME
	AUS	NC	LH	N	R	NZ		
Parma kermadecensis Allen, 1987 - Kermadec scalyfin					X			
Upeneus francisi Randall & Guézé, 1992 - Bartail goatfish			X	X	X		*Upeneus* (29/37)	Upeneus

Chromis sensu lato* and ***Chromis sensu stricto* as in Tang et al. (2021); ^includes the eight taxa from WoRMS and the unnamed species A, B, and C; ^^found also in Tonga (Iwatsubo and Motomura, 2013).

2.3.2. DNA sequence retrieval and generation

We extracted DNA sequences from NCBI and BOLD for 389 of the 401 species that comprise ingroups and outgroups for the 13 phylogenies. To do this, an automated sequence search was facilitated through the 'regPhylo' package (Eme et al., 2019) for R v.3.6.3 (R Core Team, 2020) using RStudio v.1.2.5033 (RStudio Team, 2019) following the functions 'GetSeqInfo_NCBI_taxid' to search NCBI and 'GetSeq_BOLD' to search BOLD. As a general rule, a locus was retained for phylogenetic analysis when it was represented in at least 50% of the ingroup and outgroup species list per phylogeny (see Tables 2.1S-2.13S). Loci were exceptionally retained for phylogenetic analysis when they covered unique ingroup species despite not reaching the 50% threshold, or when they were the only nuclear loci and nearly covered 50%. Overall, we downloaded sequences for five mitochondrial markers (the 12S and 16S non-coding ribosomal RNA regions, the non-coding D-loop, and the two coding COI and Cytb) and ten nuclear loci (protein-coding regions RAG1, RAG2, Tmo-4C4, H3, MYH6, PLAGL2, ENC1, GLYT, SH3PX3, and Ptr) to be used in the 13 phylogenies (Table 2). Previous studies have revealed that some fish sequences sourced from NCBI and BOLD are assigned to species identities incorrectly (e.g. Liggins et al., 2022, Tang et al., 2021) which can impact phylogenetic inferences. In our study, we minimized the probability of incorporating sequences from misidentified taxa by: not using "blacklisted" sequences identified in previous studies (Eme et al., 2020, Eme et al., 2019, Tang et al., 2021);

ensuring most accessed sequences were supported by vouchers and/or isolate numbers where these metadata were provided; verifying that taxa fell within expected taxonomic groups and positions during phylogenetic inference; and where we encountered discrepancy, we preferentially used sequences included in peer-reviewed reputable phylogenies, or those we knew had corresponding voucher specimens under the authors' care (e.g. Eme et al., 2020, Eme et al., 2019).

Table 2. Gene regions used for the inference of the 13 phylogenies. The GAMS phylogeny includes *Girella*, *Atypichthys*, *Microcanthus*, and *Scorpis*; the HL phylogeny includes *Hypoplectrodes* and *Lepidoperca*; the NEMOGOCHIA phylogeny includes *Nemadactylus*, *Morwong*, *Goniistius*, *Chironemus*, and *Aplodactylus*. Sizes (bp) of mitochondrial (italic) and nuclear (regular text) loci are provided in brackets. The total length of the concatenated sequences used in phylogenetic analysis is provided in the last column.

PHYLOGENY NAME	Gene regions (bp)	Concatenated alignments (bp)
Arripis	*16S (1643), COI (651), Cytb (1138)*	3432
Capromimus	*12S (561), 16S (501), COI (651)*, GLYT (843), H3 (310), MYH6 (777), PLAGL2 (789), SH3PX3 (708)	5140
Chromis	*12S (652), 16S (550), COI (539), Cytb (576)*, RAG1 (897)	3214
Enneapterygius	*12S (167), COI (649)*	816
Eviota	*12S (147), COI (1548*), Ptr (594)	2289
Flexor	*12S (350), COI (648)*, ENC1 (741), MYH6 (658)	2397
GAMS	*16S (479), COI (651), Cytb (420)*, RAG1 (1371), RAG2 (765), Tmo-4C4 (477)	4163
HL	*COI (650)*	650
Kathetostoma	*16S (530), COI (650), Cytb (368), D-loop (357)*, ENC1 (747), RAG1 (1257)	3909
NEMOGOCHIA	*16S (571), COI (650), Cytb (327)*, RAG1 (1410)	2958
Optivus	*COI (651), Cytb (1134)*, MYH6 (729)	2514
Parma	*16S (544), COI (648), Cytb (699)*, RAG1 (1457), Tmo-4C4 (511)	3859
Upeneus	*12S (170), COI (651)*	821

For species that had no sequence information available in NCBI and BOLD, or from collaborators, we accessed tissue from within curated collections of the Museum of New Zealand Te Papa Tongarewa (NMNZ, The National Fish Collection), Auckland Museum Tāmaki Paenga Hira (AIM), Massey University, and the Australian Museum (AMS) to generate novel sequences. All DNA extraction, PCR, and sequencing preparation for the focal taxa was carried out at Massey University Auckland. Genomic DNA was extracted using the DNeasy Blood and Tissue kit (Qiagen, Valencia, CA). To amplify a portion of the COI gene region, we used the primer combination named Fish

COI-2 cocktail (Ivanova et al., 2007) or FishF1 and FishR1 or FishR2 (Ward et al., 2005); for the RAG1 gene region, we used Rag1F1 and Rag1R1 (López et al., 2004); and for the 12S gene region, we used 12S53F and 12S613R, and 12S489F and 12S991R to amplify two fragments (McCord and Westneat, 2016). All PCRs were conducted using either the MyTaq™ or MyFi™ DNA polymerase kits (Bioline, Australia Pty Ltd, Alexandria, NSW) as per the kit instructions. For the Fish COI-2 primer cocktail, PCR was performed with a denaturation at 94°C for 1 min, followed by an initial 5 cycles (94°C for 30 secs, 50°C for 40 secs, 72°C for 1 min), followed by 35 cycles (94°C for 30 secs, 54°C for 40 secs, 7 °C for 1 min), then a final extension at 72°C for 10 mins (as per Ivanova et al., 2007). Using FishF1 and FishR1 or FishR2, PCR was performed with a denaturation at 95°C for 2 mins, followed by 35 cycles (95°C for 45 secs, 54°C for 45 secs, 72°C for 1 min), then a final extension at 72°C for 5 mins. For the rag 1 and 12S gene regions, PCR was performed with a denaturation at 94°C for 5 mins, followed by 40 cycles (94°C for 30 secs, 50°C for 30 secs, 72°C for 45 secs), then a final extension at 72°C for 3 mins. Following PCR, a 1% agarose gel was run using 2 µL of PCR product and 1 µL of GelRed, alongside a BioLabs Quick Loading DNA Ladder to ensure PCR products were of the right size and sufficient concentration. PCR products were then purified using the ExoSap reagents and protocol (Thermo Fisher Scientific, West Palm Beach, FL) and sent for forward and reverse sequencing (Macrogen, Korea). Quality control of the received sequences was carried out using Geneious v.9.0.5 (https://www.geneious.com). All sequence chromatographs were inspected by eye and poor-quality nucleotide bases and primer sequences were trimmed before the alignment of the forward and reverse sequence (where available) to check for consensus. All generated sequences are deposited in NCBI (Accessions: ON368279-91 [CO1], ON387613-7 [12S]) and metadata uploaded to the Genomic Observatories MetaDatabase (GEOME; Deck et al., 2017, Riginos et al., 2020; accessioned at https://n2t.net/ark:/21547/ECL2 [CO1] and https://n2t.net/ark:/21547/EBx2 [12S]).

2.3.3. Maximum likelihood phylogenetic inference

The ‘regPhylo’ package was used to perform sequence alignment, trimming, partitioning, and to build a guide tree for a maximum likelihood (ML) inference in RAxML (Stamatakis, 2014). The best sequence per locus per taxon was selected using the median length option of the ‘SelBestSeq’ function. The absence of stop codons in protein-coding sequences and general alignment quality were checked in Geneious v.9.1.8. Multiple sequence alignments were run by calling MAFFT (Katoh et al., 2002) from ‘regPhylo’. Alignments were trimmed with the ‘Filtering.align.Trimal’ function that calls the program TrimAl (Capella-Gutiérrez et al., 2009) after which we opted for the output from the automated1 option that selects the best-trimmed alignment based on a heuristic approach. All alignments were visually inspected, and manual trimming was required for Cytb and 12S sequences. To aid in the alignment, trimming, and sequence selection: for Cytb, we used a reference sequence that includes adjacent gene regions (accession number GU135519, recommended by Li et al., 2018); and for 12S, we used a reference sequence (accession number AP019333) to help identify the two subregions of the gene region, choosing the subregion with the maximum overlap among taxa for subsequent analysis. The accession numbers for all sequences (retrieved and novel) used in subsequent phylogenetic analyses are included as Supplementary Material.

For each phylogeny, aligned sequences were concatenated in multilocus supermatrices using the ‘Align.Concat’ function (exceptionally not applied for the COI-based HL phylogeny, see Table 2), after which the program PartitionFinder2 (Lanfear et al., 2017) was called from ‘regPhylo’ to partition our alignments with the following options: branch lengths linked; greedy search; all models; and AICc model selection criterion. The option RAxML was additionally set to ‘True’ as this fits the best partitioning scheme according to the substitution models implemented in the program. The function ‘ConstraintTaxo2newick’ was used to build a multifurcating tree based on soft constraints derived from previously published phylogenies and ready to use in a rapid bootstrap

analysis in RAxML (as in Eme et al., 2019, Eme et al., 2020). The program RAxML was run as a command-line interface selecting the GTRGAMMA model of substitution with the autoMRE option which selects the best number of bootstrap replicates to compute bootstrap values for each node. The inference included the partitioning scheme and the guide tree from the previous steps. The best tree was rerooted in Dendroscope v.3.5.9 (Huson and Scornavacca, 2012) using the hypothetical most distantly related taxon per phylogeny. The final rooted tree and bootstrap support values per node were visualized in FigTree v.1.4.4.

2.3.4. Bayesian estimates of divergence times

BEAST2 (Bouckaert et al., 2019) was used to infer the 13 time-calibrated trees based on the same partitioning scheme we employed during the ML inference. A GTR+G substitution model with four categories of evolutionary rates was set for each subset after selecting the Standard GTR model in the SSM package for BEAUTi (Bouckaert and Xie, 2017). Trees and an uncorrelated relaxed clock model were linked across subsets. A Birth-Death speciation model was assumed in all cases and hard constraints were introduced based on the nodes that displayed 100 bootstrap support on the ML tree with a log-normal distribution prior on each one.

The CA package of Matschiner et al. (2017) for BEAUti was used to include fossil constraints based on the fossil records of the selected taxa from the initial taxonomic sampling and the parameters indicated by the authors (diversification rate of 0.041-0.081; turnover rate of 0.0011-0.37; sampling rate of 0.0066-0.01806). The maximum and minimum ages per fossil (Table 2.14S) were set according to the first occurrence of each fossil as indicated in the supporting material of Matschiner et al. (2017). In addition, we opted to include two of the fossils used by Frédérich et al. (2013) to calibrate their pomacentrid tree (*Morone* †sp. considered a relevant upper boundary at 74 Ma to root the tree; and *Chromis* †*savornini* to date the origin of the genus *Chromis*, using the age range 5.332-7.246 Ma as indicated in Fossilworks at http://fossilworks.org). The use of

fossils as primary calibration points was preferred over other methods for divergence time estimations, as this approach avoids the additional errors from the use of secondary calibrations and the circularity of using geological calibration events (Powell et al., 2020, Sauquet, 2013).

For each phylogeny, three independent BEAST2 analyses were run with the BEAGLE package (Ayres et al., 2012) for performance improvement. The chain length of every run was set to 70,000,000 steps, with samples taken every 7,000 iterations, and discarding the first 10% as burn-in. The program Tracer v.1.7.1 (Rambaut et al., 2018) was used to verify effective mixing of the chains, appropriate burn-in, and that each run reached convergence by ensuring that the effective sample size (ESS) computed for every parameter yielded values of over 200. The log and tree files of the three BEAST2 analyses were combined with LogCombiner v.2.6.3 (Bouckaert et al., 2019). The posterior probability of the trees was summarized in a Maximum Clade Credibility Tree in TreeAnnotator v.2.6.3 (Bouckaert et al., 2019). The mean node heights and 95% highest probability density were visualized with FigTree v.1.4.4.

2.4. Results

Evolutionary relationships were inferred for 34 ray-finned fish species endemic to the Southwest Pacific islands of Lord Howe, Norfolk, and Rangitāhua. Novel sequences were generated for seven species previously unrepresented in open-access sequence repositories (*Enneapterygius kermadecensis*, *Eviota kermadecensis*, *Hypoplectrodes huntii*, *Hypoplectrodes* sp. C, *Optivus elongatus*, *Parma kermadecensis*, and *Upeneus francisi*) based on tissues within New Zealand collections, and for three species (*Hypoplectrodes maccullochi*, *Hypoplectrodes nigroruber* and *Lepidoperca brochata*) based on the tissue loans from the Australian Museum, six of which were endemics of the Southwest Pacific islands. We generated additional 12S sequences for *Chromis abyssicola*, *Chromis dispila*, and *Chromis hyspilepis*, and COI for *Flexor incus* and *Parma alboscapularis* to inform phylogenetic analyses. Except for the COI-based “HL”

phylogeny, all phylogenetic inferences were based on concatenated multi-locus sequences between 816-5140 bp (Table 2). The evolutionary relationships among species within each endemic's genus are summarized in 13 phylogenies spanning 21 genera (Fig. 2, Fig. 2.1S-2.13S). Two phylogenies correspond to the monotypic genera *Capromimus* and *Flexor*, and include all sister taxa with available molecular data at the order and subfamily levels, respectively. Eight genera (*Aplodactylus*, *Arripis*, *Atypichthys*, *Chironemus*, *Goniistius*, *Microcanthus*, *Morwong*, and *Optivus*) are fully resolved with all current valid species included in each phylogeny. Four genera are almost fully resolved with all species per genus sampled except for one, due to missing sequences and unavailable tissues: the Atlantic representatives *Nemadactylus vemae* and *Kathetostoma cubana*, and the Pacific taxa *Girella simplex* and *Scorpis chilensis* are absent within their genus' phylogenies. The remaining genera are missing two or more species. We also report the geographic distribution for each species included in the phylogenetic trees (Fig. 2, Tables 2.1Sa-2.13Sa).

The generation of the *Arripis* time-calibrated tree involved five primary calibration points located at deep evolutionary positions (Table 2.14S) given that the genus is placed at basal nodes within Scombriformes (Matschiner et al., 2017, Sanciangco et al., 2016): the three most closely related orders (Ophidiiformes, Batrachoidiformes, and Gobiiformes; Alfaro et al., 2018, Betancur-R et al., 2017, Hughes et al., 2018, and Matschiner et al., 2017), and two more distant orders (Lampriformes, the only outgroup lacking fossils, and Myctophiformes; Matschiner et al., 2017) were required to correctly root and calibrate the final version of our tree (Fig. 2.1S). The monophyly of *Arripis* is strongly supported by both ML and Bayesian inferences (BI) (BS=100; PP=1; Fig. 2.1S) based on a 3432 bp concatenated sequence of three mitochondrial markers (Table 2). The endemics *A. trutta* and *A. xylabion* sit in a well-supported clade (BS=97; PP=1) that includes *A. truttacea* (Australia). All species are distributed between Australia and New

Zealand. With all congeners sampled, the first lineage split is estimated to have occurred 8.87 Ma, and the divergence of both endemics from *A. truttacea* at 0.332 Ma.

The monotypic *Capromimus* lies outside its presumed confamilials within Zeniontidae appearing as the sister taxon of all members of the Oreosomatidae family (Fig. 2.2S). The phylogenetic position of the endemic *C. abbreviatus* is consistent in all our tree inferences with strong support in the BI (PP>0.99) and is based on the 5140 bp concatenated sequence of three mitochondrial and five nuclear markers. The estimated divergence time of the endemic's lineage is 14.18 Ma based on our list of sampled taxa.

The "Chromis" phylogeny was inferred using a 3214 bp concatenated sequence of four mitochondrial loci and one nuclear locus (Table 2). Our initial phylogenies included all species named under the *Chromis* genus prior to Tang et al. (2021) (i.e. *Chromis sensu lato*) (results not shown). Based on their study and our data, we observed that all our focal endemics were placed within the *Chromis sensu stricto* clade, thus opting to update our phylogenies by including only strict *Chromis* taxa. Final results (Fig. 2.3S) show highly-supported sister taxa relationships at terminal positions for four endemics: *C. nitida* (endemic)/*C. fumea* (Indo-Pacific) (BS=100; PP=1); *C. dispila*/*C. hypsilepis* (both endemic) (BS=66; PP>95); and *C. abyssicola* (endemic)/*C. mamatapara* (East Pacific) (BS=92; PP>99). The position of *C. kennensis* was poorly supported (BS=56; PP>0.16). All endemics consistently belong to a clade of 19 taxa across our inferences with strong support in the BI tree (PP>0.81). Based on our genus coverage (59/84 species), the estimated divergence ages are 1.33 Ma for *C. abyssicola*, 2.72 Ma for *C. nitida*, 3.94 Ma for the clade of endemics *C. dispila*/*C. hypsilepis*, and 5.34 for *C. kennensis*.

The phylogeny of *Enneapterygius* is based on two mitochondrial loci (COI and Cytb) analyzed as a supermatrix of 816 bp (Table 2), including 27 of 63 described species to date. The ML phylogeny (Fig. 2.4S) shows extremely weak support at deep and intermediate nodes. However, the nodes at the terminal clades *Enneapterygius*

similis/*E. bahasa*, *Enneapterygius rubicauda*/*E. flavoccipitis*, *Enneapterygius paucifasciatus*/*E. pyramis*, and *Enneapterygius kermadecencis*/*E. williamsi*/*E. nigricauda*/*E. randalli* show support values of over 89. The BI chronogram supports the monophyly of the members of the Tripterygiidae family (PP=1) which includes the 27 species of *Enneapterygius* and the two taxa of *Helcogramma*. Only four nodes are supported by PP values of over 0.70: *Enneapterygius gruschkai*/*E. abeli*/*E. philippinus* (0.7655); *Enneapterygius flavoccipitis*/*E. rubicauda* (0.7977); *Enneapterygius paucifasciatus*/*E. pyramis* (0.7062); and *Enneapterygius kermadecensis*/*E. williamsi* (0.7103). In all our trees, the endemic *Enneapterygius kermadecensis* is grouped with *E. williamsi* (Central Pacific), and *E. pusillus* is consistently placed closer to the genus *Helcogramma* than to other *Enneapterygius* taxa. The lineage including *Enneapterygius kermadecensis* is estimated to have diverged 8.93 Ma from its closer congeners within our dataset.

Phylogenetic relationships within *Eviota* were inferred based on 62 of its 117 valid species to date. We used the concatenation (2289 bp) of two mitochondrial and one nuclear locus (Table 2). The monophyly of the genus is supported in our Bayesian phylogeny (PP>0.96; Fig. 2.5S). Intermediate nodes are characterized by low BS and PP values, both increasing when approaching terminal positions. The endemic *Eviota kermadecensis* is consistently located within its genus as the sister taxon of *E. distigma* and *E. herrei* (both from the Indo-Pacific), albeit in poorly supported phylogenetic positions. Given our taxonomic sampling, the lineage represented by *Eviota kermadecensis* is estimated to have diverged 20.97 Ma.

Evolutionary relationships of *Flexor* were inferred from a supermatrix of 2397 bp encompassing two mitochondrial and two nuclear loci (Table 2). The monotypic genus is placed within its own family in a clade supported by a PP of 0.99 (Fig. 2.6S). In both the ML and BI topologies, the endemic *F. incus* is grouped with *Lepadichthys trishula*, *Aspasmichthys ciconiae*, and *Aspasma minima* (BS=32; PP=0.72), all Northwest Pacific

taxa. In both inferences, the monophyly of the Diademichthyinae subfamily *sensu* Conway et al. (2020) is supported by BS=100 and PP=1 where the pair *Aspasmogaster tasmaniensis* and *Aspasmogaster ciconiae* are the sister taxa of the subfamily members with the same support values. Based on the taxa sampled in our analysis, the lineage represented by *F. incus* is estimated to have diverged 13.46 Ma.

Our GAMS phylogeny includes the genera *Girella*, *Atypichthys*, *Microcanthus*, and *Scorpis*, and is based on the concatenated sequence (4163 bp) of three mitochondrial and three nuclear loci (Table 2). All current valid species within each genus were sampled except in *Girella* (16/17) and *Scorpis* (4/5). *Girella*, *Microcanthus*, and *Atypichthys* appear monophyletic across all analyses (Fig. 2.7S) with BS values of 95-99 and PP of 0.97-1. *Scorpis* is a strongly supported clade (BS=100; PP=1) when *S. aequipinnis*, *S. lineolata*, and *S. violacea* are considered. *S. georgiana* is consistently positioned outside its presumed congeners. Given our taxonomic coverage, the endemics *G. cyanea*, *G. fimbriata*, *A. latus*, *M. joyceae*, and *S. violacea* are located within their genus members in respective sister taxa relationships with *G. albostriata* (Southeast Pacific), *G. nebulosa* (Southeast Pacific), *A. strigatus* (Australia), *M. strigatus* (Indo-Pacific), and *S. lineolata* (Southwest Pacific), and estimated divergence times of 3.77 Ma, 2.12 Ma, 2.56 Ma, 2.99 Ma, and 3.35 Ma.

The HL phylogeny includes *Hypoplectrodes* and *Lepidoperca* using a 650 bp sequence of COI (Table 2). Both genera are nearly-fully resolved, and their monophyly is supported in our ML and BI analyses (BS=100 both cases; PP>0.93 *Hypoplectrodes*; PP=1 *Lepidoperca*; see Fig. 2.8S). All species occur in waters of Australia or the Southwest Pacific region, except *H. semicinctum* that inhabits remote oceanic islands of the Southeast Pacific. Species sampled within *Hypoplectrodes* include six of the eight described species and the three undescribed taxa: *H.* sp. A (not valid as *H. coronatus* in Roberts et al., 2015), *H.* sp. B (not valid as *H. dimidius* in Roberts et al., 2015), and *H.* sp. C (not valid as *H. igneus* in Roberts et al., 2015). The endemic *H.* sp. A has a weakly

supported placement (BS=46; PP=0.4909) as the ancestor of the monophyletic clade (BS=100; PP=1) formed by *H. maccullochi*, *H.* sp. B, *H. jamesoni*, *H.* sp. C, *H. cardinalis*, and *H. semicinctum*. Within this clade, the endemic *H.* sp. C displays a variable position across our trees. The phylogenetic relationships among *Lepidoperca* congeners are constant in our analyses, with the endemic *L. inornata* and *L. pulchella* (Australia) forming a highly supported clade (BS=80; PP>0.98) nested in a larger well-supported clade (BS=100; PP=1) that includes *L. tasmanica* and *L. filamenta*. Based on our species coverage, the estimated divergence times are 10.26 Ma for *H.* sp. A, 1.58 Ma for *H.* sp. C, and 1.56 for *L. inornata*.

The monophyly of the genus *Kathetostoma* is well supported in our analyses (BS=77; PP=1; see Fig. 2.9S). There are no differences among the ML and BI topologies which are based on the concatenated sequence (3909 bp) of four mitochondrial and two nuclear markers (Table 2), and seven of the eight current valid species. Phylogenies are characterized by a clade of two taxa (*K. albiguttata* and *K. averruncus*) geographically distributed in the Atlantic and East Pacific regions, and a clade of five species found in Australia and Southwest Pacific (Fig. 2). In the second group, the Australian *K. laeve* is the sister taxon of the remaining four taxa. In our dataset, the endemic lineage representing *K. binigrasella* is estimated to have diverged 6.98 Ma from its congeners.

Our NEMOGOCHIA phylogeny includes the closely related genera *Nemadactylus*, *Morwong*, *Goniistius*, *Chironemus*, and *Aplodactylus* based on a concatenated sequence (2958 bp) of four mitochondrial loci and one nuclear locus. Our initial taxonomic search included all *Cheilodactylus* species within Cheilodactylidae prior to the nomenclature revision of Ludt et al. (2019). Based on their work, our final species list included taxa reassigned to Latridae, specifically the genera *Pseudogoniistius*, *Goniistius*, and *Morwong*. Our focal endemics spanned five genera, of which four were fully resolved and one (*Nemadactylus*) missed one species. Overall, the monophyly of *Aplodactylus*, *Chironemus*, *Morwong*, and *Nemadactylus* is highly supported in our ML

and BI trees (BS=96-100; PP=0.99-1; see Fig. 2.10S). The genus *Goniistius* forms a supported monophyletic clade in our ML tree only (BS=89; PP=0.48 respectively). The two valid *Morwong* species are both considered endemics and are included in our study with an estimated divergence time of 8.51 Ma. Within *Chironemus*, *C. microlepis* is consistently grouped with *C. marmoratus*, both of which are closely related to *C. bicornis* from the Southeast Pacific (BS=75; PP>0.99). Based on all sampled congeners, the endemics are estimated to have diverged 13.61 Ma. Within the fully resolved *Aplodactyus*, *A. etheridgii* is constantly coupled with *A. lophodon* from Australia (BS=56; PP>0.94) with a divergence time of 11.18 Ma. Within *Goniistius*, *G. vestitus* forms a moderately supported sister taxa relationship with *G. gibbosus* from Australia (BS=73; PP=0.69). The position of *G. francisi* varies across our analyses but remains closely related to a clade formed by *G. vestitus*, *G. vittatus*, *G. zebra*, and *G. plessisi*. The estimated divergence times of *G. vestitus* and *G. francisi* are 8.53 Ma and 6.54 Ma respectively. For the near complete phylogeny of *Nemadactylus*, *Pseudogoniistius nigripes* consistently appears as the sister taxon (BS=58; PP>0.99). *Nemadactylus douglasii* (estimated age: 4.29 Ma) forms a strongly supported clade (BS=96; PP=1) with *N. valenciennesi* (Australia). *Nemadactylus* n. sp. (not valid as *N. rex* in Roberts et al., 2015, and Ludt et al., 2019; estimated age: 1.56 Ma) is the ancestor in a well-supported clade (BS=97; PP=1) that includes *N. monodactylus*, *N. bergi*, *N. gayi*, and *N. macropterus*.

The fully-resolved genus *Optivus* is monophyletic in our phylogenies (BS=99; PP=1) with its three valid species displaying the same positions in the ML and BI topologies (Fig. 2.11S), based on a 2514 bp concatenated sequence of two mitochondrial loci and one nuclear locus (Table 2). The endemics *O. elongatus* and *O. agastos* form a monophyletic clade (BS=99; PP>0.99) with an estimated divergence time of 0.589 Ma. Both occur in the Southwest Pacific while the basal *O. agrammus* occurs in Australia.

The *Parma* phylogeny includes 7 of the 10 recognized *Parma* species, all of which are geographically restricted to Australia and the Southwest Pacific. The monophyly of the genus is highly supported (BS=100; PP=1) with *Mecaenichthys immaculatus* appearing as the sister taxon (Fig. 2.12S). ML and BI trees were inferred from a sequence of 3859 bp that concatenates three mitochondrial and two nuclear loci (Table 2). Based on our taxonomic sampling, the endemics *P. alboscapularis* and *P. kermadecensis* consistently form a clade across all our inferences, albeit with low node support (BS=40; PP=0.33). The estimated age of both endemics is 5.1 Ma.

The relationships within *Upeneus* are based on 29 of 37 described species, and the 821 bp concatenated sequence of two mitochondrial loci (Table 2). Based on the number of sampled taxa, our ML and BI results indicate that the genus is monophyletic (BS=100; PP=1) with *U. parvus* (Atlantic) as the sister taxon of its remaining congeners (Fig. 2.13S). In our dataset, the endemic *U. francisi* (estimated age: 3.65 Ma) is weakly (BS=44; PP=0.41) but consistently positioned within its genus as the base of the clade *U. lombok*/*U. pori*, all three forming a weak but consistent clade (BS=44; PP=0.49) that diverges from *U. australiae* (Australia).

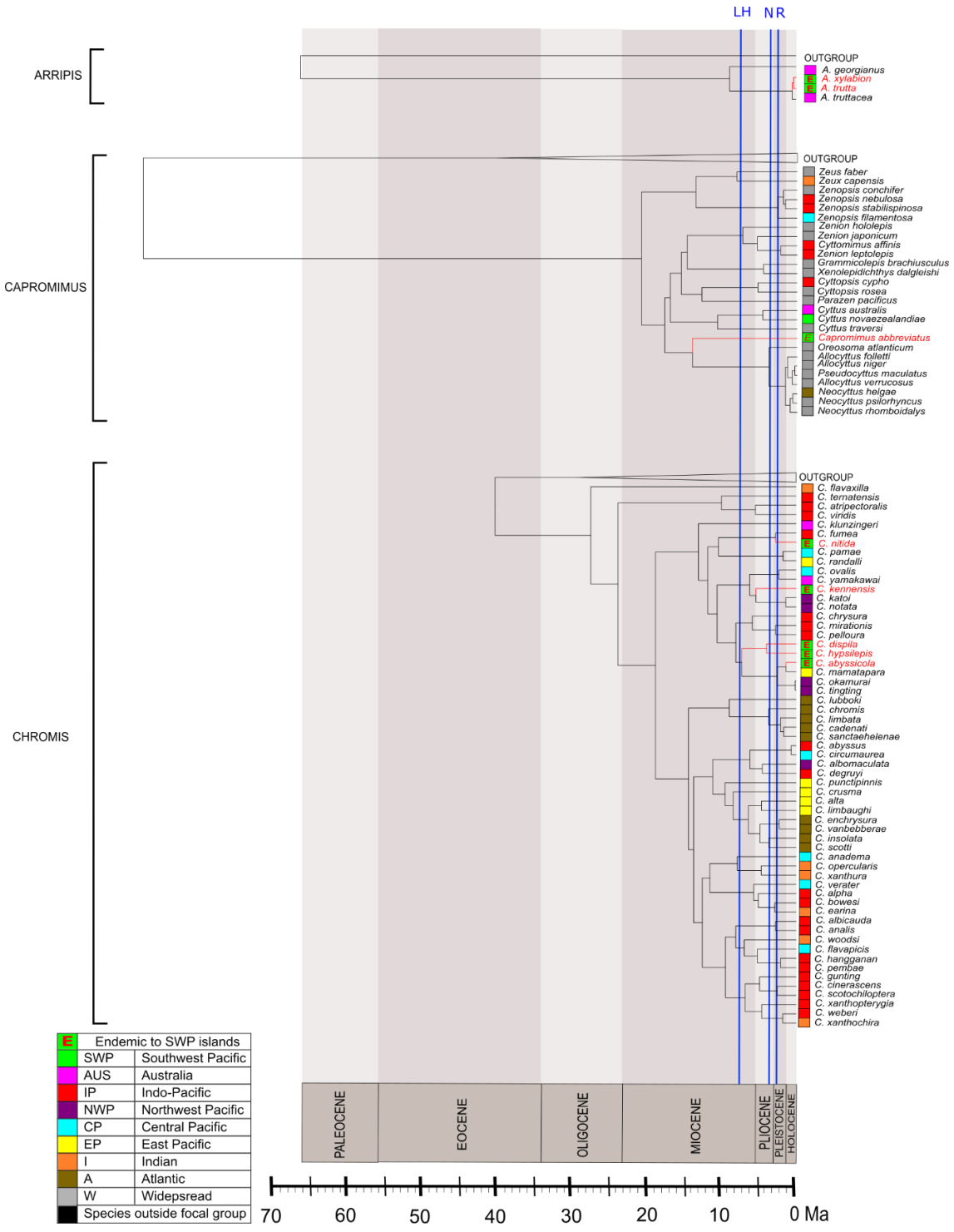

Fig. 2. Molecular placing of 34 marine fish species endemic to the Southwest Pacific islands across 13 time-calibrated Bayesian trees. An endemic's phylogenetic position is displayed as a red branch. Phylogenies and the ages of focal islands (vertical blue lines: LH: Lord Howe; N: Norfolk; R: Rangitāhua - the Kermadecs) are placed on a temporal axis in million years (Ma). Colored squares at the tips of the trees illustrate the range of each taxon following the colored geographic regions of Fig. 1, except for grey (widespread species) and black (outside focal taxonomic group). Squares for the focal endemic taxa are indicated with a red 'E' over the SWP green background. Species omnipresent in the SWP, or restricted to New Zealand mainland, New Caledonia, and/or the east/south of Australia retain the SWP green color.

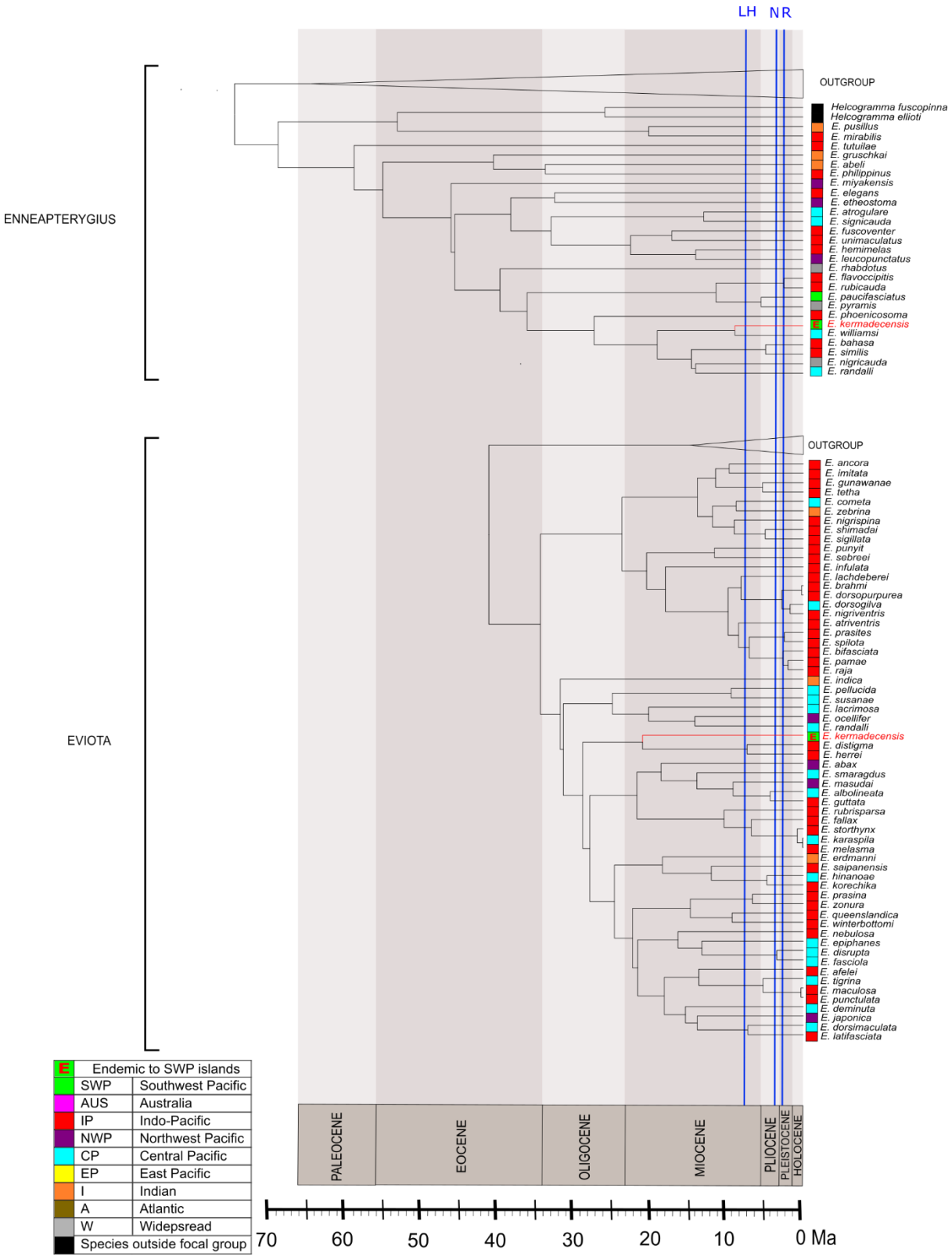

Fig. 2. *(continued)*

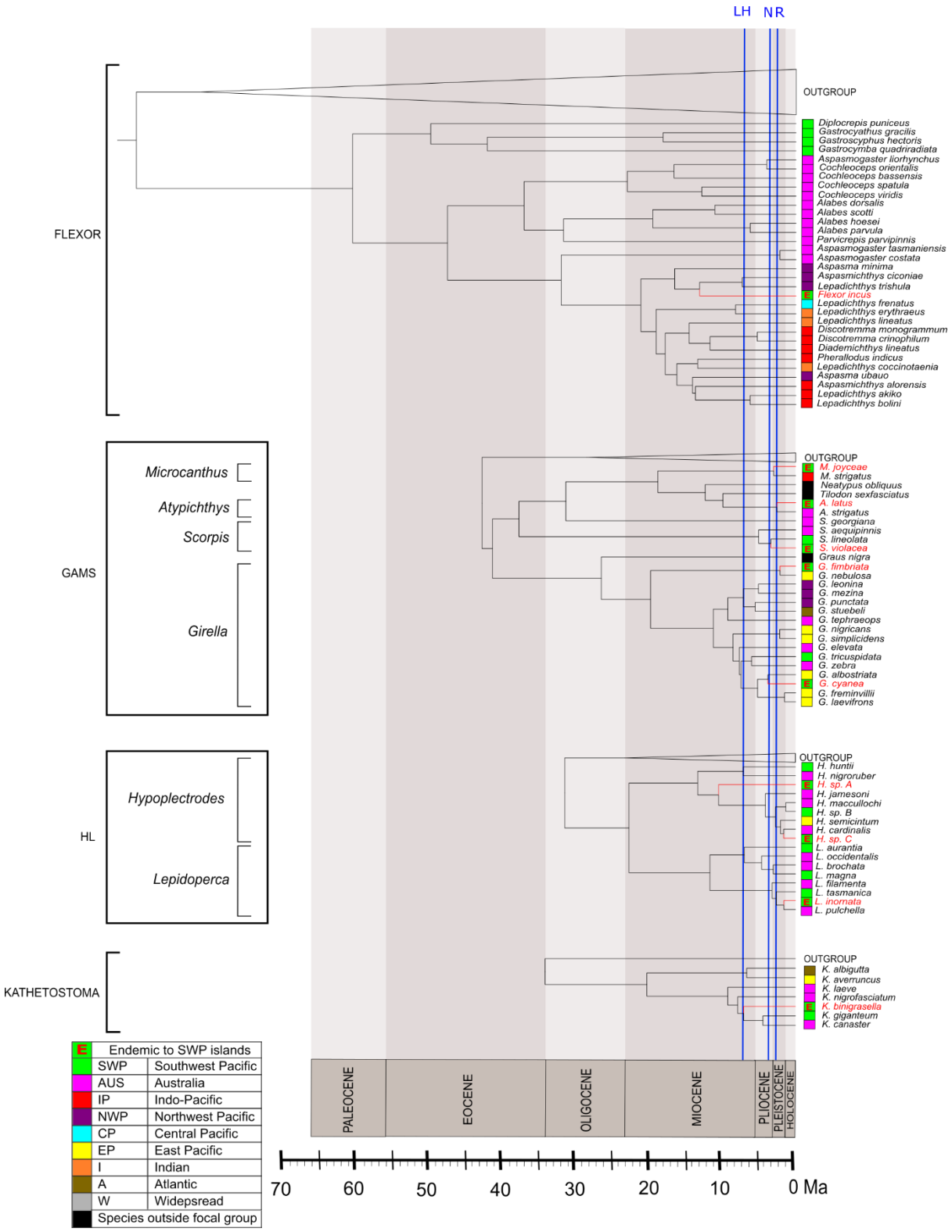

Fig. 2. *(continued)*

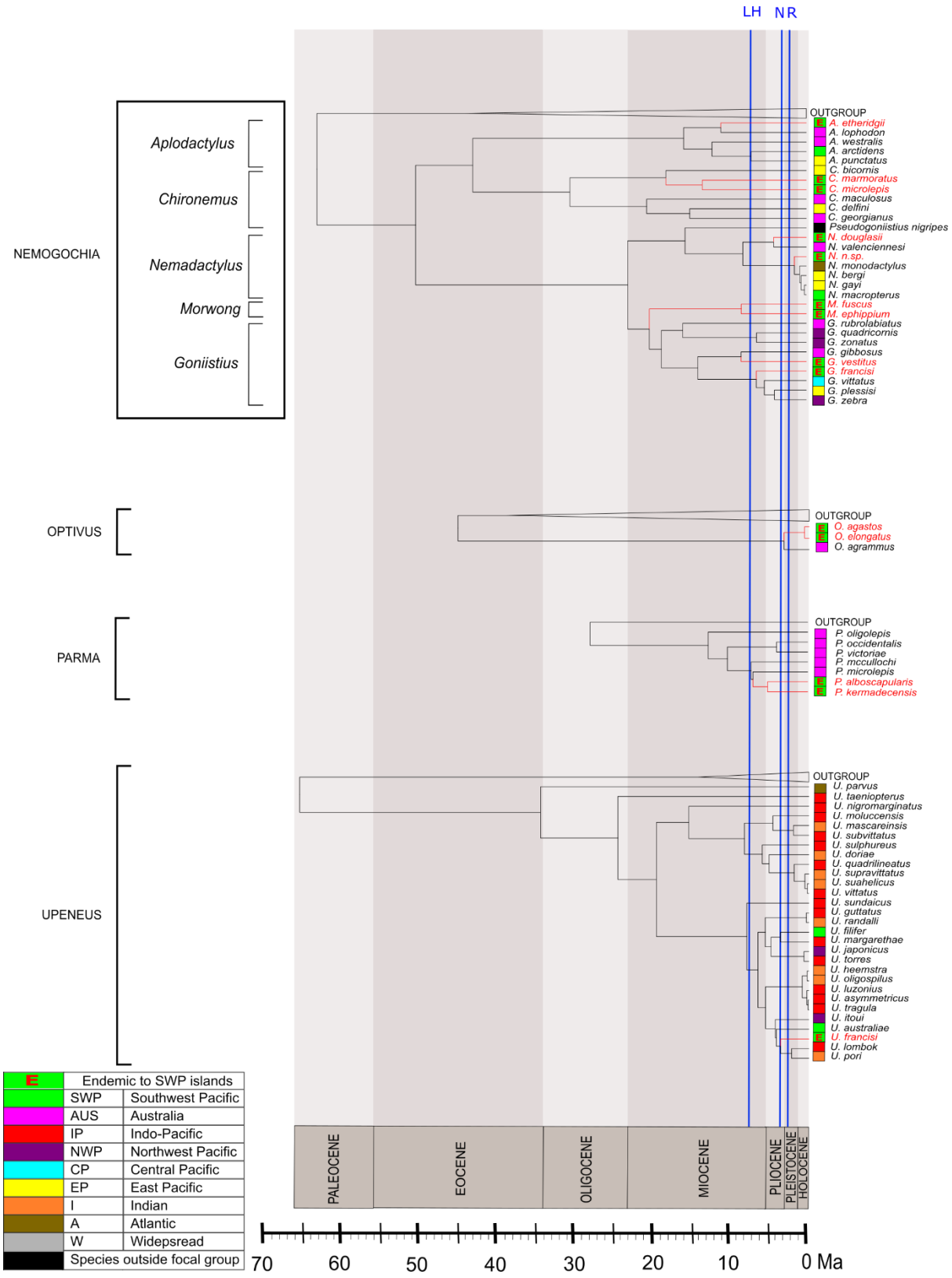

Fig. 2. *(continued)*

2.5. Discussion

Understanding the evolutionary history of endemic species in remote islands has provided insight as to how marine biodiversity is generated and maintained (Bowen et al., 2013), and, in particular, molecular phylogenies have helped illuminate the evolutionary trajectories of endemic marine fishes (Bellwood and Meyer, 2009). Here we present the first comprehensive molecular phylogenies for 21 marine fish genera that encompass 34 taxa endemic to the subtropical islands of Lord Howe, Norfolk, and Rangitāhua in the Southwest Pacific, helping to refine the recent evolutionary histories and patterns for marine ray-finned fishes in the region. Our analyses confirm the species status of all focal endemics by placing them in time-calibrated phylogenies including all relevant sister taxa where DNA sequences could be retrieved or generated. Below we discuss the spatial and temporal diversification patterns of marine fish endemics in the Southwest Pacific based on our results.

2.5.1. Phylogenetic placement of endemic taxa

We provide the first published placement within a molecular phylogeny for 11 species endemic to the subtropical islands of the Southwest Pacific and smaller areas within (*Arripis xylabion*, *Enneapterygius kermadecensis*, *Eviota kermadecensis*, *Atypichthys latus*, *Lepidoperca inornata*, *Hypoplectrodes* sp. A, *Hypoplectrodes* sp. C, *Nemadactylus* n.sp., *Optivus elongatus*, *Parma kermadecensis*, and *Upeneus francisi*), and the first comprehensive molecular phylogenies for four of the studied genera (*Enneapterygius*, *Lepidoperca*, *Hypoplectrodes*, and *Upeneus*). Our molecular results and phylogenetic analyses for three endemics (*Hypoplectrodes* sp. A, *Hypoplectrodes* sp. C, and *Nemadactylus* n. sp.) will support their formal species description, and for *Arripis xylabion* (Paulin, 1993), we provide new knowledge of its evolutionary relationship to other taxa, previously undescribed based on either molecular or morphological studies.

For some endemic species already described using phenotypic traits, we found that their suggested sister taxon relationships were not completely corroborated by our

molecular and phylogenetic inference. For instance, *U. francisi* and 16 other congeners belong to the "*japonicus* group" (Uiblein and Motomura, 2021) based on morphometric, meristic, and color characters (Uiblein and Heemstra, 2010). In our ML and BI phylogenies, however, the 10 "*japonicus* group" species with available sequences (*U. asymmetricus*, *U. australiae*, *U. francisi*, *U. guttatus*, *U. itoui*, *U. japonicus*, *U. lombok*, *U. parvus*, *U. pori*, and *U. torres*) do not cluster, and *U. francisi* has a constant close kinship with only three of its presumed sister taxa (*U. australiae*, *U. lombok*, and *U. pori*). Similarly for *Eviota kermadecensis*, while Hoese and Stewart (2012) related the endemic to *E. abax* and *E. masudai* within the group I defined by Lachner and Karnella (1980), our phylogenies reveal a closer relationship with different congeners (*E. distigma* and *E. herrei*) within group I (Fig. 2.5S). For *Enneapterygius kermadecensis*, we found complete disagreement between taxon relationships suggested by our results and former meristic studies (Fricke, 1994): the endemic was originally placed within a complex that included *E. hemimelas*, *E. bichrous* (synonym of *E. flavoccipitis*), and *E. niger*, whereas our analyses do not show a phylogenetic closeness between any of these taxa and *E. kermadecensis*. As the original taxonomic relationships for these taxa were described based on phenotypic similarities, these incongruences could be indicative of homoplasy, rather than homology in the meristic traits among the originally proposed sister taxa. However, particularly for the *Enneapterygius* and *Eviota* genera for which taxonomic sampling was not comprehensive, the inclusion of further taxa and more gene regions to support some of the weakly supported nodes may change the topology of the phylogeny, and the divergence date of the endemic lineages.

Twenty-three of the endemic taxa included in our study had previously been included in a molecular phylogeny. For two taxa (*Kathetostoma binigrasella* and *Microcanthus joyceae*), we present their accepted binomial name in a time-calibrated tree for the first time, as they were officially named, or resurrected, following their previous inclusion in a phylogeny: *K. binigrasella* was named the "banded giant stargazer

of New Zealand" in the phylogenetic inference of Smith et al. (2006) before its formal description by Gomon and Roberts (2011), and; *M. joyceae* was resurrected by Tea and Gill (2020) after providing molecular and morphological evidence that the Southwest population of *M. strigatus* deserved distinct species status. For these species, and the remaining 21 focal endemics, our phylogenetic inferences are congruent with previously reported topologies. Nonetheless, our analyses have extended previous phylogenetic studies through the inclusion of more taxa for several taxonomic groups, including *Arripis* (previously studied by Sanciangco et al., 2016), *Chromis sensu lato* and *Parma* (most recently studied by McCord et al., 2021, and Tang et al., 2021), *Girella* and *Scorpis* (previously studied by Beldade et al., 2021, and Knudsen et al., 2019), *Nemadactylus* (previously studied by Ludt et al., 2019), *Optivus* (previously studied by Ghedotti et al., 2021), the subfamily Diademichthyinae (including *Flexor incus*, previously studied by Conway et al., 2020), and the order Zeiformes (including *Capromimus abbreviatus*, previously studied by Grande et al., 2018). Furthermore, our time-calibrated phylogenies based on fossils provide a temporal context for the evolutionary history of several taxonomic groups previously without any divergence time estimates (*Goniistius* and *Morwong*, Ludt et al., 2019; *Aplodactylus*, Burridge, 2000b), and corroborate divergence time estimates based on other methods (*Chironemus*, Burridge et al., 2006; *Nemadactylus*, Papa et al., 2021). Overall, our standardized methodological approach to phylogenetic analysis has made use of all available data and collections to present the most comprehensive understanding of the evolutionary history of the endemic Southwest Pacific fish fauna to date. Our research has also highlighted persisting gaps in taxonomic sampling, representation, and consequently our knowledge of this regional fish fauna.

2.5.2. Resolution and accuracy of evolutionary relationships

The 13 phylogenies presented in this study recover the molecular data and metadata available in open-access repositories for 389 of our total set of 401 fish species. As we

endeavored to include all known valid taxa, our results directly reflect the sequence availability in these groups and portray the repercussions of taxonomic gaps in analysis. In our case, we acknowledge three inherent caveats that affect the resolution and robustness of our inferred phylogenies.

Firstly, the taxonomic coverage is disparate across the 21 genera. Eight are fully sampled (*Aplodactylus*, *Arripis*, *Atypichthys*, *Chironemus*, *Goniistius*, *Microcanthus*, *Morwong*, and *Optivus*), and four are nearly fully sampled missing one species each: *Kathetostoma* and *Nemadactylus* are missing their Atlantic member (likely not affecting our inferred patterns within the Pacific), and *Girella* and *Scorpis* are missing one Pacific member (which should not significantly impact our inferences, but the possibility cannot be ruled out), whereas coverage is only partial for *Hypoplectrodes* (82%), *Lepidoperca* (80%), *Upeneus* (78%), *Chromis* (70%), *Parma* (70%), *Eviota* (53%), and *Enneapterygius* (43%). Having included all species that have sequences in the open-access repositories, our results highlight the need to increase the collection and preservation of specimens for DNA analysis, in particular for the most speciose genera. Missing taxa are a source of divergence time overestimations (Hodge and Bellwood, 2016), so great care should be taken in the interpretation of our incompletely sampled phylogenies.

Secondly, each phylogeny was inferred with a variable number of gene regions (Table 2), ranging between one (“HL”) and eight (“Capromimus”) with a mean of four. Four phylogenies were based on mitochondrial loci only, and the rest in a combination of both mitochondrial and nuclear loci, illustrating the traditional prevalence of mitochondrial markers due to their evolutionary properties (Wilson et al., 1985) and the tendency to examine multiple loci over this single locus (Brito and Edwards, 2009). Within mitochondrial loci, COI occurs in all inferences, followed by Cytb and 16S in seven phylogenies, 12S in six, and the D-loop in one. COI has been the marker of choice for species delimitation, including fishes, owing to its almost-universal resolution power for

closely allied taxa (Hebert et al., 2003). For nuclear loci, RAG1 was most commonly used (four phylogenies), followed by MYH6 (three), Tmo-4C4 (two), and seven other regions were used in one phylogeny each. In contrast to phylogenies based on a single locus or the mitochondrial locus, our inferences that include multiple loci are expected to provide better inferences for closely related species given that: a multilocus approach increases species delimitation success (Dupuis et al., 2012); concatenation counteracts the heterogeneity of single-locus inferences (Roe et al., 2010); and the integrative analysis of nuclear and mitochondrial markers leads to more informative and better well-resolved topologies (Rubinoff and Holland, 2005).

Thirdly, we report missing data values per phylogeny between 0% (HL) and 43% (*Enneapterygius*) with an average of 29% across all phylogenies. We generally included loci that covered a minimum of 50% of species within a phylogeny to avoid elevating levels of missing data. However, adding genes can improve poorly supported nodes, even when that gene region is not represented in a high proportion of taxa (Jiang et al., 2014). As a consequence, some of the low support values, particularly at intermediate nodes of our ML topologies, might have been improved with the inclusion of further gene regions albeit with an increase in the percent missing data across our multilocus supermatrices. Nonetheless, our inferred trees largely agree with previously published phylogenies, and divergence time estimates using an uncorrelated log-normal clock in BEAST, as is our case, are relatively insensitive to varying degrees of missing data (Zheng and Wiens, 2015).

2.5.3. Geographic affinities of endemic taxa

Despite contrasting topologies and ranges of included taxa (Fig. 2), the majority of our focal endemics are most closely related to Australian taxa, followed by East Pacific species (Table 3). We also found individual cases where an endemic is closely related to taxa found throughout the broader Indo-Pacific region and the Northwest Pacific.

However, the geographic affinity of a quarter of the endemics analyzed here remains unresolved.

Table 3. Geographic affinity of the 34 endemics based on our study. Number, percentage, and taxa allocated to each presumed geographic region following those shown in Fig. 1 and Fig. 2.

GEOGRAPHIC AFFINITY	NUMBER OF TAXA	TAXA
AUSTRALIA	18/34 - 53%	*Aplodactylus etheridgii, Arripis trutta, Arripis xylabion, Atypichthys latus, Goniistius francisi, Goniistius vestitus, Hypoplectrodes* sp.A*, Hypoplectrodes* sp.C*, Kathetostoma binigrasella, Lepidoperca inornata, Nemadactylus douglasii, Nemadactylus* n.sp.*, Optivus agastos, Optivus elongatus, Parma alboscapularis, Parma kermadecensis, Scorpis violacea, Upeneus francisi*
EAST PACIFIC	5/34 - 15%	*Chironemus marmoratus, Chironemus microlepis, Chromis abyssicola, Girella cyanea, Girella fimbriata*
INDO-PACIFIC	1/34 - 3%	*Chromis nitida*
NORTHWEST PACIFIC	1/34 - 3%	*Flexor incus*
NOT YET RESOLVED*	9/34 - 26%	*Capromimus abbreviatus, Chromis dispila, Chromis hypsilepis, Chromis kennensis, Enneapterygius kermadecensis, Eviota kermadecensis, Microcanthus joyceae, Morwong ephippium, Morwong fuscus*

*Geographic origin not yet resolved due to incomplete taxonomic sampling.

2.5.3.1. Australia

Our findings indicate a geographic affinity between 18 of our endemics and Australia mainland. Nine species are distributed in six genera that include sampled taxa only found in the Southwest Pacific and the larger Australia region. For fully sampled genera (*Arripis*, *Atypichthys*, and *Optivus*), the geographic affinity is clearly illustrated by the divergence of the endemics from taxa distributed in Australia, including its western coasts (Fig. 2; Tables 2.1S,2.7S,2.11S). For the partially sampled *Parma*, despite missing two taxa, all described members are restricted to New Zealand and Australia (Tang et al., 2021), and *P. oligolepis* (East Australia) appears as the sister taxon of all congeners. For the partially sampled *Lepidoperca* and *Scorpis*, missing taxa are distributed in other oceanic regions (*L. coatsii*: Atlantic and Indian; *S. chilensis*: East Pacific), adding a small degree of uncertainty to our inferences. However, we still detect

an affinity with Australia as *L. inornata* forms a strongly supported clade (BS=80; PP>0.98) with *L. pulchella* from New South Wales and Victoria, and *S. violacea* descends from congeners of Australia and New Zealand mainland.

Seven further endemics are proximal to Australian taxa, but the ranges of sampled congeners extend to other oceanic regions. The phylogenetic placements of *A. etheridgii*, *G. vestitus*, and *N. douglasii* are consistent across our analyses forming well-supported clades with *A. lophodon*, *G. gibbosus*, and *N. valenciennesi* respectively, all three restricted to Australian coasts. The placement of *K. binigrasella* persists also in all our analyses, deriving from *K. nigrofasciatum* found in Australia mainland. A more subtle affinity is detected for three endemics that represent consistent single lineages that descend from Australia and/or Southwest Pacific congeners: *U. francisi* splits from *U. australiae* (Australia and New Caledonia); *N.* n.sp. from the clade *N. valenciennesi* (Australia)/*N. douglasii* (Southwest Pacific); and *H.* sp. A from the clade *H. nigroruber* (Australia)/*H. huntii* (New Zealand). An even more subtle affinity is observed for two endemics placed within clades that descend from Australian taxa, but their phylogenetic position within the clade is variable: the species *G. rubrolabiatus*, found in Australia, appears in our ML phylogeny as the sister taxon of all its congeners, including the endemic *G. francisii*, and is the oldest *Goniistius* lineage in our BI tree; and the clade *H.* sp. C/ *H. jamesoni*/*H. cardinalis*/*H. semicinctum*/*H. maccullochi*/*H.* sp. B diverges from *H.* sp. A, for which we have previously inferred an Australian affinity.

The strong geographic affinity between our focal endemics and Australia is likely determined by the regional oceanography, climate similarity, and past geological events. Our results show that in at least 15 of the 18 endemics with an Australian affinity, there is a direct or indirect evolutionary divergence from a taxon restricted to mainland Australia, suggesting eastward dispersal. It has been proposed that this movement is facilitated by the Tasman Front, a branch of the East Australia Current, which likely transports larvae in an eastward flow, connecting East Australia, Lord Howe, Norfolk,

and Rangitāhua (Trnski and de Lange, 2015). This route has been previously suggested to influence the biogeography and species distributions of the region's marine fish fauna (Francis, 1993), as well as the region's coastal corals (Brook, 1999), echinoderms (Bronstein et al., 2019), and marine mollusks (Brook, 1998a). Additionally, environmental factors could also explain affinities between Australia and the islands of the Southwest Pacific. For instance, Wicks et al. (2010) reported similarities in the hydrodynamics (e.g. wave energy) of coastal sites in Southeast Australia and Rangitāhua, and suggested it had a role in shaping the similar coral assemblages they observed. Furthermore, sea surface temperature is known to shape the range boundaries of marine fauna (Stuart-Smith et al., 2017) and is often approximated by latitude. In the Southwest Pacific, our focal islands sit in a subtropical belt shared with Australia mainland and no other major landmass regionally, resulting in similar marine fish biota within this same marine climate zone. Lastly, historical events have likely also influenced the current regional biogeography. For 15 of the 18 endemics with an Australian affinity, the closest sister taxon inhabits temperate waters which clearly points to the temperate Australian coasts as a significant origin of biodiversity. Divergence time estimates for these taxa range from 11.17 Ma (*Aplodactylus etheridgii*) to 0.332 Ma (*Arripis trutta* and *Arripis xylabion*) (Table 4), a timing that coincides with the global cooling phase that started in the Middle Miocene (ca. 15 Ma), witnessing a major influence of cooler waters at mid-latitudes in the Southwest Pacific (Nelson and Cooke, 2001) and the receding of tropical and subtropical marine taxa to lower latitudes in both hemispheres (Flower and Kennett, 1994). The expansion of cold marine conditions to lower latitudes would have facilitated the northward input of cold-water temperate Australian fishes into modern-day subtropical latitudes where they would have found suitable habitats, a process that would have resulted in independent lineage diversification events at different time scales. Two other endemics (*Hypoplectrodes* sp. C and *Atypichthys latus*) are closely related to subtropical Australian species, and one (*Upeneus francisi*) to a tropical Australian taxon. All three have recent diversifications (3.65-1.58 Ma) (Table 4), exemplifying that

diversification from warmer Australian latitudes has been occurring over more contemporary time scales.

2.5.3.2. East Pacific

Several of our Southwest Pacific endemics had a geographic affinity with remote insular territories of Chile in the Southeast Pacific, namely Juan Fernández and Desventuradas (*C. marmoratus*, *C. microlepis*, *G. cyanea*) and Rapa Nui (*C. abyssicola*, *G. fimbriata*). For instance, *C. abyssicola* and *G. cyanea* are consistently grouped with East Pacific congeners, however, we currently lack additional congenerics to confidently infer the East Pacific as their geographic origin in both cases. Using meristic traits, the pomacentrid was initially allied with species from West Australia, Japan, and Hawaii (Allen and Randall, 1985), but molecular evidence brought by Tang et al. (2021) and our study (Fig. 2.3S; Table 2.3S) groups it with its congener from Rapa Nui (*C. mamatapara*). Since around one-third of *Chromis sensu stricto* species are missing in our phylogeny, however, we refrain from further biogeographic inferences. For the girellid, we present the most comprehensively sampled time-calibrated molecular phylogeny to date for its genus (16/17 taxa), finding that *G. cyanea* is grouped with *G. albostriata* (Juan Fernández and Desventuradas), a similar result to the 16S topology of Beldade et al. (2021). All our topologies show that this clade is in a sister-taxa relationship with the clade *G. freminvillii*/*G. laevifrons*, both from the East Pacific, and that both clades descend from Southwest Pacific taxa (*G. tricuspidata*, *G. zebra*, and *G. elevata*). Our current data is insufficient to confidently establish if *G. cyanea* diverged from its closest phylogenetic neighbors from the Southeast, or its Southwest ancestors giving rise to its Southeast congeners. For the remaining endemics with East Pacific affinities, our time-calibrated trees show that they are chronological descendants of Southeast Pacific taxa (Fig. 2): *C. marmoratus* and *C. microlepis* diverge from *C. bicornis* (Juan Fernández and Desventuradas), and the clade *G. fimbriata* (endemic)/*G. nebulosa* (Rapa Nui) from *Graus nigra* (Southeast Pacific). Our confidence in these inferred patterns are supported

by: previous phylogenies of *Chironemus* (Burridge et al., 2006) and *Girella* (Knudsen et al., 2019, Knudsen and Clements, 2016); *Chironemus* is fully sampled; and *Girella* is missing only one species.

The presence of congeners at the longitudinal extremes of the Pacific implies trans-oceanic dispersal events, a pattern reported in other marine fishes (Robertson et al., 2004, Rosenblatt and Waples, 1986). In their phylogenetic analysis of the *Cirripictes alboapicalis* complex distributed across the South Pacific, Delrieu-Trottin et al. (2018) describe similar patterns. Their results highlight evolutionary proximity between Rangitāhua and Rapa Nui clades, despite the presence of other clades within the species complex occupying intervening islands of French Polynesia. Such patterns indicate that chance colonization among these island groups, followed by allopatry, may have occurred in the evolutionary history of several fishes. For *C. marmoratus*, *C. microlepis*, and *G. fimbriata*, our analysis suggests that these Southwest Pacific endemic lineages originated in the East Pacific: their divergence postdates the estimated ages of eastern taxa, implying westward dispersal via the warm low latitude South Equatorial Current, and eventual spreading along the East Australian Current. Endemics with an East Pacific affinity and their closest sister taxon diverged between 13.61 Ma (*C. marmoratus* and *C. microlepis*) and 1.33 Ma (*C. abyssicola*), and are mostly subtropical, implying in our case that organisms with similar climatic adaptations to the subtropics have dispersed since the Mid-Miocene across the Pacific as independent events at different times. This inferred pattern is counter to the eastward colonization routes inferred for the same trans-Pacific congeners within *Chironemus* (Burridge et al., 2006), but also *Nemadactylus* (Burridge, 1999), the flat oyster (Ó Foighil et al., 1999), and other marine taxa (Waters, 2008), presumably facilitated by the West Wind Drift that flows in a clockwise rotation around Antarctica and dominates at higher latitudes. Determining the prevalence of westward dispersal of subtropical taxa, the species groups that are advected, and the

periods when this dispersal has been the most influential in shaping the biodiversity in the Southwest Pacific requires further examination across broader taxonomic groups.

2.5.3.3. Indo-Pacific, Northwest Pacific, and unresolved affinities

The only endemic that displays a geographic affinity with the Indo-Pacific belongs to *Chromis* (Table 3), a genus characterized by its reef-associated species mostly found in the tropical latitudes of the Indo-Pacific. We recover the monophyletic clade (BS=99; PP=1) between *C. nitida* and *C. fumea* (Indo-Pacific) from previous molecular phylogenies (Frédérich et al., 2013, McCord et al., 2021, Tang et al., 2021), pointing to a geographic closeness between our Southwest Pacific endemic and its tropical congener. Although there is dispersal and ongoing colonization of the subtropical Southwest islands by tropical fishes (Duffy and Ahyong, 2015, Liggins et al., 2020), the speciose genus *Chromis* is poorly sampled in our analysis (Table 1). For this reason, we only provisionally associate a tropical affinity to the *Chromis* endemic, anticipating that the inclusion of further taxa may alter this inference.

The sole endemic of our dataset with an anti-equatorial affinity is *Flexor incus*, showing a proximal association with temperate taxa from the Northwest Pacific (Fig. 2; Table 2.6S). Previously known as *Aspasmogaster* sp. (Francis and Duffy, 2015, Roberts et al., 2009, Stewart, 2015, Trnski et al., 2015), the endemic was presumed linked to Indo-Pacific taxa based on its formal description (Conway et al., 2018), but was later grouped with *Aspasmichthys ciconiae* (Northwest Pacific) within the Diademichthyinae subfamily using molecular evidence (Conway et al., 2020). Our results recover this trend with the association of *F. incus* with two further Northwest Pacific taxa, suggesting an anti-equatorial origin and the dispersal of organisms from the Northern to the Southern Hemisphere. This trans-equatorial north-to-south pathway has been previously reported in girellids (Beldade et al., 2021), and the opposite south-to-north in microcanthids (Tea et al., 2019). Similar to these studies, we presume that oceanic connectivity between northern and southern regions happened during periods of global climatic change.

However, whereas Beldade et al. (2021) and Tea et al. (2019) describe connectivity within the Pleistocene, our estimated age of *F. incus* (ca. 13.5 Ma) suggests that the Mid-Miocene, when there was a major global cooling phase, may have also been a period of trans-equatorial connectivity (i.e. the Middle Miocene Climatic Transition, Crame, 2018).

Lastly, we were unable to address a biogeographic pattern for nine endemics due to unclear evolutionary relationships (Table 3). The monotypic *Capromimus* is placed among Zeiformes species, missing six taxa required to fully sample the Order. The endemic is the sole sister taxon of Oreosomatidae outside its presumed confamilials (Fig. 2.2S), as already reported by Grande et al. (2018), with no distinct closeness to other species, nor a clear divergence from a specific geographic region (Fig. 2). In the case of *Chromis dispila*, *Chromis hypsilepis*, *Morwong ephippium*, *Morwong fuscus*, and *Microcanthus joyceae*, each forms a monophyletic clade with a congener, but there is still insufficient ancestral evidence to infer their geographic affinities. Both *Chromis* endemics are sister taxa to each other, also reported by McCord et al. (2021) and Tang et al. (2021), but there is no clear ancestor to associate them with (Fig. 2 and Fig. 2.3S). Similarly, both *Morwong* endemics form a sister taxa relationship (BS=100; PP>0.98; Fig. 2.10S) within the resurrected genus (Ludt et al., 2019), but with unclear ancestral taxa to relate with. *Microcanthus joyceae* is the assumed ancestor within its clade with *M. strigatus* (Tea et al., 2019), but our topologies show *Microcanthus* as the basal genus within our fully sampled Microcanthidae. Since we did not aim for inter-genus relationships, we lack evidence for the ancestry of the family, the genus, and ultimately, the endemic. Lastly, the three endemics *Chromis kennensis*, *Enneapterygius kermadecensis*, and *Eviota kermadecensis* appear as single lineages within poorly sampled genera, impeding the inference of a clear geographic affinity (Table 1). Nonetheless, our time-calibrated phylogeny for the *Enneapterygius* genus shows that *E. kermadecensis* forms a moderately supported clade with *E. williamsi* (PP=0.71), suggesting an association with a tropical species found in Tonga, Vanuatu, and New

Caledonia. The geographic affinity of *Eviota kermadecensis* is more diffuse as its closest taxa vary across our trees, and although it consistently appears as the sister taxon of a clade of Indo-Pacific congeners (*E. distigma* and *E. herrei*), we encourage conservative interpretation of these patterns until further taxonomic sampling can be undertaken to resolve its geographic affinities.

2.5.4. Temporal diversification of endemic taxa

Based on our analyses, 23 of our 34 (67.6%) endemics are neo-endemics estimated to have diverged at, or after, the emergence of the oldest island in the Southwest Pacific (6.92 Ma for Lord Howe in McDougall et al., 1981; Table 4). A divergence age that postdates the emergence of an island is indicative of a diversification event after the formation of the oceanic element, suggesting that the remote volcanic islands of the Southwest Pacific have provided a suitable habitat for the generation of unique evolutionary lineages of marine fishes. Furthermore, for 19 of the 34 endemics analyzed, their clades were not fully sampled and so our divergence time estimates may be overestimated, meaning the first island emergence may be even more important in driving species origination in the region, or that the younger islands are more important than currently suggested by our time estimates. Our conclusions add the Southwest Pacific islands to the list of peripheral islands in the Pacific that export marine biodiversity (Bowen et al., 2013, Cowman et al., 2017), confirming the role of these topographical features in providing the opportunity for origination and hosting unique taxa found nowhere else. Moreover, the Southwest Pacific islands likely continue to promote contemporary diversification in “Oceanic” *Chrysiptera* (*sensu* Tang et al., 2021). The significant morphological divergence of the “Rangitāhua demoiselle” (formerly recognized as *C. rapanui*) from *C. rapanui* of Rapa Nui, and congeners of neighboring regions, suggest that this taxon should be considered a very recent neoendemic of Rangitāhua (Liggins et al., 2022).

Table 4. Mean node age and confidence interval (Ma) for the 34 endemics investigated in this study. The dashed line separates species based on our threshold of 6.92 Ma for the maximum geological age of our focal islands of the Southwest Pacific.

SPECIES	Ma	CONFIDENCE INTERVALS
*Arripis trutta**	0.3316	0.0276 - 0.7643
*Arripis xylabion**	0.3316	0.0276 - 0.7643
*Optivus agastos**	0.5894	0.025 - 1.447
*Optivus elongatus**	0.5894	0.025 - 1.447
Chromis abyssicola^^	1.3287	0.4658 - 2.3425
Nemadactylus n.sp.^	1.5559	0.5458 - 2.8226
Lepidoperca inornata^^	1.5646	0.3202 - 3.1078
Hypoplectrodes sp. C^^	1.5831	0.3218 - 3.1659
Girella fimbriata^	2.1243	0.6036 - 3.9862
*Atypichthys latus**	2.5647	0.172 - 6.2026
Chromis nitida^^	2.7212	1.2932 - 4.4505
*Microcanthus joyceae**	2.9897	0.8873 - 5.6315
Scorpis violacea^	3.3464	1.1055 - 5.9461
Upeneus francisi^^	3.6506	1.1718 - 6.6257
Girella cyanea^	3.7686	1.1038 - 6.7333
Chromis dispila^^	3.9381	1.8694 - 6.1324
Chromis hypsilepis^^	3.9381	1.8694 - 6.1324
Nemadactylus douglasii^	4.2883	1.9409 - 7.0924
Parma alboscapularis^^	5.1040	2.2551 - 8.1674
Parma kermadecensis^^	5.1040	2.2551 - 8.1674
Chromis kennensis^^	5.3413	2.6805 - 8.4153
*Goniistius francisi**	6.5410	2.2662 - 12.2732
Kathetostoma binigrasella^	6.9795	4.3927 - 11.4104
*Morwong ephippium**	8.5109	2.6548 - 15.9602
*Morwong fuscus**	8.5109	2.6548 - 15.9602
*Goniistius vestitus**	8.5287	3.7424 - 14.2155
Enneapterygius kermadecensis^^	8.9317	4.3217 - 14.3042
Hypoplectrodes sp. A^^	10.2637	3.7005 - 18.1031
*Aplodactylus etheridgii**	11.1763	5.6481 - 18.0152
Flexor incus‡	13.4632	6.2634 - 21.1712
*Chironemus marmoratus**	13.6110	5.2852 - 22.8507
*Chironemus microlepis**	13.6110	5.2852 - 22.8507
Capromimus abbreviatus‡	14.1837	5.2581 - 23.5608
Eviota kermadecensis^^	20.9723	11.3006 - 31.5149

*Fully sampled genera; ^Nearly-fully sampled genera (one species missing); ^^Partially sampled genera (two or more missing taxa); ‡ Monotypic.

For 32.4% of our focal endemics, their divergence times pre-date the emergence of the subtropical Southwest Pacific islands. As suggested, these cases could be due to the overestimation of node ages caused by missing taxa within genera (*Hypoplectrodes*: 18%; *Eviota*: 47%; *Enneapterygius*: 57%), the subfamily Diademichthyinae for *F. incus* (missing six of 23 members), and the Zeiformes for *C. abbreviatus* (missing six of 27 members). However, it is also plausible that our divergence estimates are close to real ages, and that these species could have found suitable habitats in either emerged islands (that are now submerged or on a mainland) or former seamounts in the vicinity of our focal islands, resulting in older endemic taxa than the islands they are endemic to (Heads, 2011). In the case of the fully sampled *Morwong* and *Goniistius*, the closeness of the endemics' estimated age (ca. 8.5 Ma) to our Lord Howe's threshold (6.92 Ma) might indicate that their representatives could have settled in nearby oceanic formations before the actual emergence of the islands. For *F. incus* (estimated age:13.5 Ma), it was initially described only in Rangitāhua (Conway et al., 2018) of ca 2.5 Ma age, but is recently reported in Lord Howe and New Caledonia (Fujiwara et al., 2021) of much older ages of 6.92 Ma and 37 Ma respectively (Grandcolas et al., 2008), suggesting that the endemic originated outside our focal islands. A similar scenario might be hypothesized for endemics whose range also includes New Zealand mainland (*A. etheridgii* and *C. abbreviatus*) and Australia mainland (*Hypoplectrodes* sp. A), with these two locations acting as the main center of origination in each case. Finally, if we consider our estimates close to real ages for the fully sampled *Chironemus*, our much older estimated ages imply that *C. marmoratus* and *C. microlepis* diverged well before the emergence of the islands and that their current ranges are relicts of a much wider past range. Since both taxa seem to have diverged from a Southeast congener, our results suggest the splitting of an ancestral chironemid lineage, with a trans-Pacific distribution rather than the westward colonization route solely hypothesized on geographic affinities. A similar example of paleo-endemism is reported for the Kermadec Islands giant limpet (*Scutellastra kermadecensis*), in which case fossil evidence suggested that climatic

fluctuations altered its former widespread range, reducing it to its current restricted distribution in Rangitāhua (Fleming, 1973).

2.6. Conclusions

Our molecular phylogenetic analysis provides the most comprehensive understanding of the evolutionary histories of endemic ray-finned fishes in the Southwest Pacific islands to date. From our general work, further research can be undertaken to understand the biogeography and evolution of marine ray-finned fishes at finer spatial and temporal scales. While we confirm the species status of our focal endemics by phylogenetically positioning them within their sister taxa, and have fully sampled eight genera, presenting the first inferences on the geographic origin and diversification timings of endemism in the Southwest Pacific islands, we also highlight some limitations. Multiple genera have a large number of missing taxa, although some require only a single species to achieve complete taxonomic representation. This limitation would benefit from the provisioning of suitable DNA samples in specimen collections, and increased collection effort, in particular in Norfolk and Lord Howe islands. Additionally, we find that four of our phylogenies are solely covered by mitochondrial loci, emphasizing the necessity to include more nuclear markers, and the importance of high-throughput technologies that increasingly enable the parallel sequencing of thousands of homologous gene regions across taxa (Faircloth et al., 2020, Tea et al., 2022). By closing the divide between scientific expeditions, specimen collection, DNA sample preparation, and increasing locus coverage, we will learn more about the formation and maintenance of marine ray-finned fish diversity in the Southwest Pacific.

2.7. Authors' contributions

André P. Samayoa: Investigation, Data curation, Formal analysis, Validation, Writing – original draft, Writing – review & editing. **Carl D. Struthers:** Resources, Writing – review & editing. **Thomas Trnski:** Resources, Writing – review & editing. **Clive D. Roberts:** Writing – review & editing. **Libby Liggins:** Conceptualization, Data curation, Funding

acquisition, Project administration, Supervision, Resources, Validation, Writing – review & editing.

2.8. Acknowledgments

We are grateful to the following colleagues for their role in this research: Giacomo Bernardi (University of California Santa Cruz), Kendall Clements (University of Auckland), and co-authors for sharing 16S sequences for *Girella*; Amanda Hay (Australian Museum) for facilitating tissue loans; Diane Pitassy (Smithsonian Institution), Richard Pyle (Bishop Museum), and Luis Rocha (California Academy of Sciences) for providing information on specimens within their institute's fish collections and for searching potentially usable tissues; José I. Carvajal for laboratory assistance and analysis advice; and J. David Aguirre (Massey University), Erwan Delrieu-Trottin (Université Montpellier II), and Adam N. H. Smith (Massey University) for helpful feedback during discussions of the project. We additionally thank two anonymous reviewers and the editor for their constructive insights. This research was a continuation of the collaboration between Massey University and Te Papa Tongarewa founded by Marti J. Anderson and Clive D. Roberts and funded by a Royal Society of New Zealand Te Apārangi Marsden Grant (15-MAU-132). We wish to thank and acknowledge mana whenua (the traditional owners) of Rangitāhua, the Māori iwi of Ngāti Kuri for their support, and the New Zealand Department of Conservation for sampling permission (Authorisation number: 47976 MAR). Expeditions to Rangitāhua were made possible by the crew of the RV Braveheart, Stoney Creek Shipping Company. These expeditions were supported by Natural History New Zealand and the New Zealand on Air Platinum Fund, the Auckland Museum Institute, Auckland Museum, C&L Gregory Trust, the Pew Charitable Trusts, the School of Natural Sciences Massey University, and the National Institute of Water and Atmospheric Research Ltd Core Funded Coasts & Oceans Programme 2: Biological Resources subcontract for fundamental knowledge of marine fish biodiversity with the Museum of New Zealand Te Papa Tongarewa, Museum of New

Zealand Te Papa Tongarewa Collection Development fund: AP's 4788 and 4862. André P. Samayoa is supported by a Massey University Doctoral Scholarship; Libby Liggins is supported by a Rutherford Discovery Fellowship (RDF-20-MAU-001). Ongoing biodiversity research of Rangitāhua is supported by a New Zealand Ministry of Business, Innovation, and Employment Endeavour Research Fund ''Te Mana o Rangitāhua'' (69495-ENDRP-AWMMU2001).

2.9. Supplementary material

Alignments and tree files can be found online at https://doi.org/10.17632/cmz9gjd97g.1.

Table 2.1Sa. "Arripis" phylogeny: list of species and ranges.

Species	Range
Arripis georgianus	West, South, and East Australia
Arripis trutta	Southwest Pacific: East Australia, New Zealand, and Rangitāhua
Arripis truttacea	West, South, and East Australia
Arripis xylabion	Southwest Pacific: Lord Howe Island, Norfolk Island, Rangitāhua and north New Zealand
Porichthys myriaster	East Pacific
Porichthys plectrodon	Atlantic
Gobius fallax	Atlantic
Gobius incognitus	Mediterranean
Gobius vittatus	Mediterranean
Odontobutis platycephala	Northwest Pacific: Korea
Odontobutis obscura	Northwest Pacific: Japan and Korea
Odontobutis interrupta	Northwest Pacific: Korea
Lamprogrammus niger	Circumglobal
Lampris guttatus	Mediterranean
Neoscopelus microchir	Circumglobal
Diaphus splendidus	Circumglobal
Myctophum affine	Atlantic

Table 2.1Sb. “Arripis” phylogeny: accession numbers.

Species	16s	co1	cytb
Arripis georgianus	DQ532841	B:2987828	KF656685
Arripis trutta	GU018105	EF6092901	KF656677
Arripis truttacea	KR153522	B:2987838	KF656681
Arripis xylabion	NA	NA	KF656682
Porichthys myriaster	NA	NC_006920	NC_006920
Porichthys plectrodon	NA	B:2843747	NA
Gobius fallax	FJ460199	MT670216	KR811066
Gobius incognitus	NA	MT884425	KR811059
Gobius vittatus	GQ485305	MT670267	NA
Odontobutis platycephala	MN416814	NC_010199	NC_010199
Odontobutis obscura	AB095531	JX679046	KF415618
Odontobutis interrupta	NA	HQ536410	NC_027583
Lamprogrammus niger	KJ010661	MT323243	NA
Lampris guttatus	DQ027908	JF931919	JF931960
Neoscopelus microchir	KC441992	KF489670	NC_003180
Diaphus splendidus	AP002923	MT323688	NC_003164
Myctophum affine	AP002922	MF041688	NC_003163

Table 2.2Sa. “Capromimus” phylogeny: list of species and ranges.

Species	Range
Cyttus australis	Australia: NSW, VIC, TAS, SA
Cyttus novaezealandiae	Southwest Pacific: New Zealand and Australia
Cyttus traversi	Southern hemisphere, except South America
Cyttomimus affinis	West Pacific, antiequatorial
Zenion hololepis	Circumglobal
Zenion japonicum	Pacific Ocean
Zenion leptolepis	Indo-Pacific
Capromimus abbreviatus	Southwest Pacific: Rangitāhua and New Zealand mainland
Grammicolepis brachiusculus	Circumglobal
Xenolepidichthys dalgleishi	Atlantic and Indo-Pacific
Allocyttus folletti	North Pacific
Allocyttus niger	Southern oceans
Allocyttus verrucosus	Southern oceans
Neocyttus helgae	Northeast Atlantic
Neocyttus psilorhynchus	South Pacific
Neocyttus rhomboidalis	Southern oceans
Oreosoma atlanticum	Southern oceans, except South America
Pseudocyttus maculatus	Southern oceans
Cyttopsis cypho	Indo-Pacific
Cyttopsis rosea	Circumglobal, except East Pacific
Parazen pacificus	West Atlantic and Indo-Pacific
Zenopsis conchifer	Circumglobal
Zenopsis filamentosa	Central Pacific: Japan, Fiji, and Tonga
Zenopsis nebulosa	Indo-Pacific widespread
Zenopsis stabilispinosa	Indo-Pacific from West Australia to South China
Zeus capensis	South Africa: Indian coast up to Atlantic
Zeus faber	East Atlantic and Indo-Pacific
Percopsis transmontana	Northeast Atlantic
Aphredoderus sayanus	Atlantic Ocean
Polymixia lowei	West Atlantic
Polymixia japonica	West Pacific, from New Zealand to Japan
Polymixia nobilis	Atlantic Ocean

Table 2.2Sb. “Capromimus” phylogeny: accession numbers.

Species	12s	16s	co1	glyt	h3	myh6	plagl2	sh3px3
Cyttus australis	KY873646	EU848425	B:2941283	KY873763	KY873805	KY873856	KY873911	KY873960
Cyttus novaezealandiae	KY873648	KY873692	B:2914515	KY873765	KY873807	KY873858	KY873913	KY873962
Cyttus traversi	KY873649	KY873693	B:2754976	KY873766	KY873808	KY873859	KY873914	KY873963
Cyttomimus affinis	NA	NA	B:3214762	KF139724	NA	NA	NA	NA
Zenion hololepis	KY873667	KY873713	MG856787	KY873787	KY873828	KY873878	KY873932	KY873981
Zenion japonicum	KY873668	KY873714	KY873736	KY873789	KY873830	KY873880	KY873934	KY873983
Zenion leptolepis	NA	NA	MN915266	NA	NA	NA	NA	NA
Capromimus abbreviatus	KY873643	KY873686	B:2914393	KY873758	KY873802	KY873853	KY873906	KY873954
Grammicolepis brachiusculus	KY873651	KY873695	B:4306633	KY873768	KY873810	KY873861	KY873916	KY873965
Xenolepidichthys dalgleishi	KY873665	KY873711	MG856726	KY873785	KY873826	KY873876	KY873931	KY873979
Allocyttus folletti	KY873637	JX121802	GU440211	KY873753	KY873797	KY873847	KY873901	NA
Allocyttus niger	NA	GU018085	B:2914206	NA	NA	NA	NA	NA
Allocyttus verrucosus	KY873639	KY873683	B:2910204	KY873754	KY873799	KY873850	KY873904	KY873953
Neocyttus helgae	KY873653	KY873697	DQ108079	KY873770	KY873812	KY873863	KY873918	KY873967
Neocyttus psilorhynchus	KY873655	KY873699	B:3002097	KY873772	KY873813	KY873864	KY873919	KY873968
Neocyttus rhomboidalis	KY873656	KY873700	B:2914871	KY873773	KY873814	KY873865	KY873920	KY873969
Oreosoma atlanticum	KY873658	KY873703	KY873732	KY873776	KY873817	KY873868	KY873923	KY873972
Pseudocyttus maculatus	KY873664	GU018092	EU074570	KY873783	KY873824	KY873874	KY873929	KY873977
Cyttopsis cypho	NA	KY873688	B:2804637	NA	NA	NA	NA	NA
Cyttopsis rosea	KY873645	KY873689	KP266756	KY873762	JX121714	JX190465	KY873910	KY873959
Parazen pacificus	KY873662	KY873708	B:2804903	KY873781	KY873821	KY873871	KY873927	KY873976
Zenopsis conchifer	KY873672	KY873718	B:3227976	KY873791	KY873831	JX190466	JX190589	KY873985
Zenopsis filamentosa	NA	NA	LC430166	NA	NA	NA	NA	NA
Zenopsis nebulosa	KY873673	KY873719	LC430165	KY873792	KY873832	KY873883	KY873937	KY873986
Zenopsis stabilispinosa	NA	NA	LC430124	NA	NA	NA	NA	NA
Zeus capensis	KY873674	GU946631	JF494808	KY873793	KY873833	KY873884	KY873938	KY873987
Zeus faber	KY873676	AF221896	KF489469	JX190323	KY873834	JQ939540	JX190590	JX190988
Percopsis transmontana	KY873632	KY873678	NC_003168	KY873743	JX121710	KC826898	JX459167	JX459150
Aphredoderus sayanus	DQ533156	FJ215096	MT456238	JX190317	DQ028082	EU001908	JX190586	JX459152
Polymixia lowei	KY873630	AY538966	B:2859192	MH917490	NA	MH917535	MH917580	MH917662
Polymixia japonica	KY873629	DQ532939	KF930291	MH917475	DQ533436	MH917519	MH917563	MH917650
Polymixia nobilis	NA	MH917411	NA	MH917502	NA	MH917544	MH917588	MH917677

Table 2.3Sa. “Chromis” phylogeny: list of species and ranges.

Species	Range
Chromis abyssicola	Southwest Pacific: Norfolk Ridge, Kermadec Ridge, and New Zealand
Chromis abyssus	Indo-Pacific: Indonesia, Palau, Vanuatu
Chromis albicauda	Indo-Pacific
Chromis albomaculata	Northwest Pacific: Japan
Chromis alpha	Indo-Pacific
Chromis alta	East Pacific
Chromis anadema	Central Pacific: Pitcairn, Gambier, Society, Marquesas, Mariana, Palau, and South Japan
Chromis analis	Indo-Pacific
Chromis atripectoralis	Indo-Pacific
Chromis bowesi	Indo-Pacific
Chromis cadenati	Atlantic Ocean
Chromis chromis	Atlantic Ocean
Chromis chrysura	Indo-Pacific
Chromis cinerascens	Indo-Pacific
Chromis circumaurea	Central Pacific: Marshall and Mariana Islands
Chromis crusma	East Pacific
Chromis degruyi	Indo-Pacific
Chromis dispila	Southwest Pacific: Rangitāhua and New Zealand
Chromis earina	Indian Ocean
Chromis enchrysura	Atlantic Ocean
Chromis flavapicis	Central Pacific: Marquesas Islands
Chromis flavaxilla	Indian Ocean
Chromis fumea	Indo-Pacific
Chromis gunting	Indo-Pacific
Chromis hangganan	Indo-Pacific
Chromis hypsilepis	Southwest Pacific: Lord Howe, Norfolk, Southeast Australia, and New Zealand mainland
Chromis insolata	Atlantic Ocean
Chromis katoi	Northwest Pacific: Japan
Chromis kennensis	Southwest Pacific: East Australia, Coral Sea, Lord Howe, Norfolk, Rangitāhua, New Caledonia, and Tonga
Chromis klunzingeri	Southwest Australia
Chromis limbata	Atlantic Ocean
Chromis limbaughi	East Pacific
Chromis lubbocki	Atlantic Ocean
Chromis mamatapara	East Pacific
Chromis mirationis	Indo-Pacific
Chromis nitida	Southwest Pacific: East Australia and Lord Howe
Chromis notata	Northwest Pacific: China, Korea, Japan, and north of Vietnam
Chromis okamurai	Northwest Pacific: Japan
Chromis opercularis	Indian Ocean
Chromis ovalis	Central Pacific: Hawaii
Chromis pamae	Central Pacific: Pitcairn
Chromis pelloura	Indian Ocean
Chromis pembae	Indian Ocean
Chromis punctipinnis	East Pacific
Chromis randalli	East Pacific
Chromis sanctaehelenae	Atlantic Ocean
Chromis scotochiloptera	Indo-Pacific
Chromis scotti	Atlantic Ocean
Chromis ternatensis	Indo-Pacific
Chromis tingting	Northwest Pacific: Japan
Chromis vanbebberae	Atlantic Ocean
Chromis verater	Central Pacific: Johnston Atoll and Hawaii
Chromis viridis	Indo-Pacific
Chromis weberi	Indo-Pacific
Chromis woodsi	Indian Ocean
Chromis xanthochira	Indian Ocean
Chromis xanthopterygia	Indian Ocean
Chromis xanthura	Indian Ocean
Chromis yamakawai	Northwest Pacific: Japan
Stegastes nigricans	Indo-Pacific
Lepidozygus tapeinosoma	Indo-Pacific
Semicossyphus pulcher	East Pacific
Centropyge bicolor	Indo-Pacific
Dicentrarchus punctatus	Atlantic Ocean

Table 2.3Sb. “Chromis” phylogeny: accession numbers.

Species	12s	16s	co1	cytb	rag1
Chromis abyssicola	ON387613	NA	MN915255	NA	MN918524
Chromis abyssus	NA	NA	B:2684073	NA	NA
Chromis albicauda	LC499304	KC767731	MW630785	MW630996	MW631399
Chromis albomaculata	LC579140	NA	KU944386	NA	NA
Chromis alpha	FJ616313	FJ616421	B:10878062	NA	FJ616640
Chromis alta	JQ707030	JQ707065	JQ707133	MW630997	MW631400
Chromis anadema	NA	NA	NC_026075	LC259485	NA
Chromis analis	AF081223	FJ616423	B:3214864	NA	FJ616642
Chromis atripectoralis	FJ616316	JF457368	B:4146283	JF458034	MW631401
Chromis bowesi	NA	NA	MH170479	NA	NA
Chromis cadenati	NA	NA	GQ341589	NA	NA
Chromis chromis	FJ616317	EF489735	MN402507	EF489748	AY208640
Chromis chrysura	LC104613	JF457373	B:3215604	JF458038	MW631402
Chromis cinerascens	LC104616	B:13478007	B:10647686	MW631000	MW631403
Chromis circumaurea	NA	NA	B:2684085	NA	NA
Chromis crusma	NA	NA	B:2878395	NA	NA
Chromis degruyi	NA	NA	EU358590	NA	NA
Chromis dispila	ON387614	MW630398	MN915256	MW631001	MN918525
Chromis earina	NA	NA	B:2672058	NA	NA
Chromis enchrysura	JQ707036	JQ707071	MT726977	MT720929	MW631405
Chromis flavapicis	NA	NA	MK566866	KM455538	NA
Chromis flavaxilla	NA	NA	MF123813	NA	NA
Chromis fumea	LC327121	KC767733	KU944417	EU267219	NA
Chromis gunting	NA	NA	MH170474	NA	NA
Chromis hangganan	NA	NA	MH170476	NA	NA
Chromis hypsilepis	ON387615	MW630399	MW630792	MW631003	NA
Chromis insolata	MW630208	MW630400	B:2843200	MW631004	MW631406
Chromis katoi	LC499559	NA	NA	NA	NA
Chromis kennensis	NA	NA	NA	AY208530	NA
Chromis klunzingeri	NA	MN473598	NA	NA	NA
Chromis limbata	NA	EF489738	NA	EF392577	NA
Chromis limbaughi	NA	NA	B:2843201	NA	NA
Chromis lubbocki	NA	NA	MT726967	NA	NA
Chromis mamatapara	NA	NA	MN708011	NA	NA
Chromis mirationis	LC069646	NA	MK777551	NA	NA
Chromis nitida	MW630209	MZ366552	MW630794	MW631005	AY208638
Chromis notata	LC519420	KC767732	KU944401	EU267220	NA
Chromis okamurai	LC499303	NA	B:4720504	NA	NA
Chromis opercularis	FJ616320	JF457388	JF493178	JF458053	FJ616647
Chromis ovalis	NA	NA	NA	KU843486	NA
Chromis pamae	NA	NA	MK117066	NA	NA
Chromis pelloura	NA	NA	MF123816	NA	NA
Chromis pembae	NA	NA	HQ561507	NA	NA
Chromis punctipinnis	FJ616322	FJ616430	JQ934972	MW631006	MW631407
Chromis randalli	MK100717	MK100711	MT726968	MK100727	MK100752
Chromis sanctaehelenae	NA	NA	MT726969	NA	NA
Chromis scotochiloptera	NA	NA	MK059781	NA	NA
Chromis scotti	NA	NA	B:2734313	NA	NA
Chromis ternatensis	FJ616324	FJ616432	FJ583147	JF458059	MW631408
Chromis tingting	NA	KF957467	MN166324	NA	NA
Chromis vanbebberae	NA	NA	MT726973	MT720927	NA
Chromis verater	NA	NA	NA	KP183437	NA
Chromis viridis	JN935818	JF457397	JQ431635	MH743475	MW631409
Chromis weberi	LC104618	FJ616434	B:2824886	MW631009	MW631410
Chromis woodsi	NA	NA	HM421816	NA	NA
Chromis xanthochira	FJ616327	JF457403	JF434914	JF458075	FJ616654
Chromis xanthopterygia	NA	NA	NA	AY208538	NA
Chromis xanthura	LC104634	JF457405	MK658437	LC259483	MW631411
Chromis yamakawai	LC499560	NA	NA	NA	NA
Stegastes nigricans	FJ616389	JF457654	B:10967882	JF458265	MW631458
Lepidozygus tapeinosoma	FJ616349	FJ616457	MW630829	MW631040	MW631440
Semicossyphus pulcher	AY279644	AY279747	JQ934977	EU601405	FJ616726
Centropyge bicolor	LC579131	FJ616501	MZ771337	KJ148824	FJ616720
Dicentrarchus punctatus	KJ168066	AF247437	NC_026075	AF240740	NA

Table 2.4Sa. “Enneapterygius” phylogeny: list of species and ranges.

Species	Range
Enneapterygius abeli	West Indian
Enneapterygius atrogulare	Central Pacific: Tonga, Coral Sea, and East Australia
Enneapterygius bahasa	West Pacific
Enneapterygius elegans	Indo-Pacific
Enneapterygius etheostoma	Northwest Pacific: Japan, Korea, China, and Vietnam
Enneapterygius flavoccipitis	Indo-Pacific
Enneapterygius fuscoventer	Pacific Ocean: West and Central
Enneapterygius gruschkai	West Indian
Enneapterygius hemimelas	Indo-Pacific
Enneapterygius kermadecensis	Southwest Pacific: Rangitāhua
Enneapterygius leucopunctatus	Northwest Pacific: Japan
Enneapterygius mirabilis	Indo-Pacific: PNG and north Australia
Enneapterygius miyakensis	Northwest Pacific: Japan
Enneapterygius nigricauda	Pacific Ocean
Enneapterygius paucifasciatus	Southwest Pacific: New Caledonia
Enneapterygius philippinus	Indo-Pacific
Enneapterygius phoenicosoma	West Pacific
Enneapterygius pusillus	Indian Ocean
Enneapterygius pyramis	Pacific Ocean
Enneapterygius randalli	Central Pacific: French Polynesia
Enneapterygius rhabdotus	Pacific Ocean
Enneapterygius rubicauda	West Pacific
Enneapterygius signicauda	Central Pacific: Vanuatu, Tonga, and American Samoa
Enneapterygius similis	West Pacific
Enneapterygius tutuilae	Indo-Pacific
Enneapterygius unimaculatus	West Pacific
Enneapterygius williamsi	Central Pacific: Vanuatu, Tonga, and New Caledonia
Helcogramma fuscopinna	Indo-Pacific
Helcogramma ellioti	Indo-Pacific
Salarias alboguttatus	Indo-Pacific
Entomacrodus nigricans	Atlantic: Caribbean
Ophioblennius atlanticus	East Atlantic
Gramma loreto	West Atlantic
Opistognathus aurifrons	West Atlantic
Dicentrarchus punctatus	East Atlantic

Table 2.4Sb. “Enneapterygius” phylogeny: accession numbers.

Species	12s	co1
Enneapterygius abeli	NA	B:2824967
Enneapterygius atrogulare	NA	B:2820581
Enneapterygius bahasa	LC579180	NA
Enneapterygius elegans	NA	KP194474
Enneapterygius etheostoma	NA	KU944790
Enneapterygius flavoccipitis	LC499335	NA
Enneapterygius fuscoventer	LC340220	NA
Enneapterygius gruschkai	NA	B:2824969
Enneapterygius hemimelas	LC499334	B:10878116
Enneapterygius kermadecensis	NA	ON368280
Enneapterygius leucopunctatus	LC579347	NA
Enneapterygius mirabilis	LC499337	NA
Enneapterygius miyakensis	LC104697	NA
Enneapterygius nigricauda	NA	JQ431709
Enneapterygius paucifasciatus	NA	B:4146329
Enneapterygius philippinus	LC278068	KP194912
Enneapterygius phoenicosoma	LC499339	NA
Enneapterygius pusillus	NA	MF123873
Enneapterygius pyramis	NA	MK658450
Enneapterygius randalli	NA	MK658027
Enneapterygius rhabdotus	NA	MK566897
Enneapterygius rubicauda	LC499338	NA
Enneapterygius signicauda	LC340219	NA
Enneapterygius similis	LC146283	NA
Enneapterygius tutuilae	LC340217	B:10877970
Enneapterygius unimaculatus	LC499372	NA
Enneapterygius williamsi	NA	B:10878114
Helcogramma fuscopinna	NA	B:2825119
Helcogramma ellioti	NA	B:2672834
Salarias alboguttatus	NA	KP194608
Entomacrodus nigricans	NA	B:2843322
Ophioblennius atlanticus	NA	FJ583755
Gramma loreto	LC026666	JQ840515
Opistognathus aurifrons	LC026674	JF297892
Dicentrarchus punctatus	NA	KJ168066

Table 2.5Sa. “Eviota” phylogeny: list of species and ranges.

Species	Range
Eviota abax	Northwest Pacific: Korea and Japan
Eviota afelei	West Pacific: PNG to Japan and French Polynesia
Eviota albolineata	Central Pacific: Society Islands, Line Islands, and Tuamotu Archipelago
Eviota ancora	Indo-Pacific: Indonesia and south of Japan
Eviota atriventris	Indo-Pacific
Eviota bifasciata	Indo-Pacific
Eviota brahmi	Indo-Pacific: PNG
Eviota cometa	Central Pacific: Fiji and Tonga
Eviota deminuta	Central Pacific: Marquesas Islands
Eviota disrupta	Central Pacific: Fiji, Samoa, Tonga, and French Polynesia
Eviota distigma	Indo-Pacific
Eviota dorsimaculata	Central Pacific: Marquesas Islands
Eviota dorsogilva	Central Pacific: Fiji
Eviota dorsopurpurea	Indo-Pacific: PNG
Eviota epiphanes	Central Pacific: Hawaii and Kiritimati Island
Eviota erdmanni	Indian: south of Flores Island
Eviota fallax	West Pacific: Indonesia to Japan
Eviota fasciola	Central Pacific: Kiribati, Micronesia, south of Japan, Fiji, Tonga, New Caledonia, and PNG
Eviota gunawanae	Indo-Pacific: West Papua, Indonesia
Eviota guttata	Indian Ocean
Eviota herrei	Indo-Pacific
Eviota hinanoae	Central Pacific: French Polynesia, Fiji, Tonga, and Niue
Eviota imitata	Indo-Pacific: West Papua, Indonesia
Eviota indica	Indian Ocean
Eviota infulata	Indo-Pacific
Eviota japonica	Northwest Pacific: Japan
Eviota karaspila	Central Pacific: Fiji
Eviota kermadecensis	Southwest Pacific: Rangitāhua
Eviota korechika	Indo-Pacific
Eviota lachdeberei	Indo-Pacific
Eviota lacrimosa	Central Pacific: Marquesas Islands
Eviota latifasciata	Indo-Pacific
Eviota maculosa	Indo-Pacific
Eviota masudai	Northwest Pacific: Japan
Eviota melasma	Indo-Pacific
Eviota nebulosa	Indo-Pacific
Eviota nigrispina	West Pacific: Indonesia to Japan
Eviota nigriventris	Indo-Pacific
Eviota ocellifer	Northwest Pacific: Japan
Eviota pamae	Indo-Pacific: Indonesia
Eviota pellucida	Central Pacific: Marshall Islands, Mariana Islands, Micronesia, and south Japan
Eviota prasina	Indo-Pacific
Eviota prasites	Indo-Pacific
Eviota punctulata	Indo-Pacific
Eviota punyit	Indo-Pacific
Eviota queenslandica	Indo-Pacific
Eviota raja	Indo-Pacific: Raja Ampat Islands, Indonesia
Eviota randalli	Central Pacific: Fiji, American Samoa, and Tahiti
Eviota rubrisparsa	Indo-Pacific
Eviota saipanensis	West Pacific: Micronesia to Vietnam
Eviota sebreei	Indo-Pacific
Eviota shimadai	Indo-Pacific: Indonesia, Palau, and Japan
Eviota sigillata	Indo-Pacific
Eviota smaragdus	Central Pacific: Micronesia, Guam, Tonga, Samoa, Fiji, Vanuatu, to Norfolk and south Japan
Eviota spilota	Indo-Pacific
Eviota storthynx	Indo-Pacific
Eviota susanae	Central Pacific: Hawaii
Eviota tetha	Indo-Pacific: Indonesia
Eviota tigrina	Central Pacific: Tonga
Eviota winterbottomi	Indo-Pacific: Indonesia, Palau, and Vietnam
Eviota zebrina	Indian Ocean
Eviota zonura	Indo-Pacific
Odontobutis platycephala	Northwest Pacific: Korea
Odontobutis obscura	Northwest Pacific: Korea and Japan
Odontobutis interrupta	Northwest Pacific: Korea
Porichthys plectrodon	Atlantic Ocean
Porichthys notatus	East Pacific
Lepophidium profundorum	Atlantic Ocean
Lamprogrammus niger	Circumglobal

Table 2.5Sb. “Eviota” phylogeny: accession numbers.

Species	12s	co1	ptr
Eviota abax	LC506686	NA	KT266376
Eviota afelei	NA	MK658430	NA
Eviota albolineata	NA	JQ431732	JX483966
Eviota ancora	NA	KP013213	NA
Eviota atriventris	LC499593	KP013229	KP013364
Eviota bifasciata	LC340261	KP013242	KP013327
Eviota brahmi	NA	KJ439708	KJ439734
Eviota cometa	NA	MK712448	MK712478
Eviota deminuta	NA	MK566909	NA
Eviota disrupta	NA	JQ431734	NA
Eviota distigma	LC515657	JQ431736	NA
Eviota dorsimaculata	NA	MK566911	NA
Eviota dorsogilva	NA	KJ439724	KJ439752
Eviota dorsopurpurea	NA	KJ439703	KJ439727
Eviota epiphanes	NA	MK567497	NA
Eviota erdmanni	NA	KX432252	KX432253
Eviota fallax	NA	KP013253	KP013337
Eviota fasciola	LC340268	B:2672175	KP013369
Eviota gunawanae	NA	MK712458	MK712477
Eviota guttata	LC499464	MF123881	KP013376
Eviota herrei	LC385305	NA	NA
Eviota hinanoae	NA	KC807365	NA
Eviota imitata	NA	MF049074	MF049070
Eviota indica	NA	KY675827	NA
Eviota infulata	NA	MK658659	JX483959
Eviota japonica	LC385197	AP019334	NA
Eviota karaspila	NA	KP013292	KP013372
Eviota kermadecensis	ON387616	ON368281	NA
Eviota korechika	LC499465	NA	NA
Eviota lachdeberei	NA	KP013257	KP013340
Eviota lacrimosa	NA	MK566915	NA
Eviota latifasciata	LC499498	KP013246	KP013331
Eviota maculosa	NA	MH940308	MH940324
Eviota masudai	LC519467	NA	NA
Eviota melasma	LC458197	B:2672177	JX483960
Eviota nebulosa	NA	KP194977	NA
Eviota nigrispina	NA	KP013283	NA
Eviota nigriventris	LC579288	KJ439721	KJ439749
Eviota ocellifer	AP019333	AP019333	NA
Eviota pamae	NA	KP013264	KP013347
Eviota pellucida	LC499468	NA	NA
Eviota prasina	NA	B:2755040	NA
Eviota prasites	LC579305	KP194974	KP013375
Eviota punctulata	LC552559	JX483985	MH940321
Eviota punyit	NA	KT327060	KT327052
Eviota queenslandica	LC499470	KP194943	JX483961
Eviota raja	NA	KP013274	KP013356
Eviota randalli	NA	MK658454	NA
Eviota rubrisparsa	NA	KP013287	KP013367
Eviota saipanensis	LC049737	KP013293	KP013373
Eviota sebreei	NA	KT327053	KT327042
Eviota shimadai	LC579289	KP013265	KP013349
Eviota sigillata	NA	B:2825015	JX483971
Eviota smaragdus	LC146319	NA	NA
Eviota spilota	NA	JX483976	JX483967
Eviota storthynx	LC579302	NA	NA
Eviota susanae	NA	B:12634930	NA
Eviota tetha	NA	KP013248	MK712474
Eviota tigrina	NA	MH940298	MH940313
Eviota winterbottomi	NA	MZ422020	JX483974
Eviota zebrina	NA	MF123886	MK712472
Eviota zonura	NA	B:2672179	KP013371
Odontobutis platycephala	KM030426	NC_010199	NA
Odontobutis obscura	LC278148	AF391330	NA
Odontobutis interrupta	KM030424	HQ536410	NA
Porichthys_notatus	LC091844	FJ165037	JX190741
Porichthys_plectrodon	LC091841	MT582566	NA
Lepophidium profundorum	DQ533225	KF930038	NA
Lamprogrammus niger	NA	MT323243	NA

Table 2.6Sa. “Flexor” phylogeny: list of species and ranges.

Species	Range
Flexor incus	Southwest Pacific: Rangitāhua, Lord Howe, New Caledonia
Aspasma minima	Northwest Pacific: Korea and Japan
Aspasma ubauo	Northwest Pacific: Korea and Japan
Lepadichthys akiko	Indonesia
Lepadichthys bolini	Indo-Pacific
Lepadichthys coccinotaenia	Southwest Indian
Lepadichthys erythraeus	Red Sea
Lepadichthys frenatus	Central Pacific: Tonga, Fiji, Vanuatu, and Northeast Australia
Lepadichthys lineatus	Indian Ocean
Lepadichthys trishula	Northwest Pacific: Japan
Discotrema crinophilum	Indo-Pacific
Discotrema monogrammum	Indo-Pacific
Diademichthys lineatus	Indo-Pacific
Aspasmichthys alorensis	Indonesia
Aspasmichthys ciconiae	Northwest Pacific: Korea and Japan
Pherallodus indicus	West and Central Pacific
Alabes dorsalis	South and Southeast Australia
Alabes hoesei	Southeast to Southwest Australia
Alabes parvula	East Australia
Alabes scotti	Southeast Australia
Aspasmogaster costata	Australia
Aspasmogaster liorhynchus	Southeast to Southwest Australia
Aspasmogaster tasmaniensis	Southeast to Southwest Australia
Cochleoceps bassensis	Southeast Australia
Cochleoceps orientalis	Australia
Cochleoceps spatula	Southeast to Southwest Australia
Cochleoceps viridis	Australia: WA
Diplocrepis puniceus	Southwest Pacific: New Zealand mainland
Gastrocyathus gracilis	Southwest Pacific: New Zealand mainland
Gastrocymba quadriradiata	Southwest Pacific: New Zealand mainland
Gastroscyphus hectoris	Southwest Pacific: New Zealand mainland
Parvicrepis parvipinnis	Southeast to Southwest Australia
Salarias alboguttatus	West tropical Pacific
Entomacrodus nigricans	West Atlantic
Ophioblennius atlanticus	East Atlantic
Gramma loreto	West Atlantic
Opistognathus aurifrons	West Atlantic
Dicentrarchus punctatus	East Atlantic, Mediterranean

Table 2.6Sb. “Flexor” phylogeny: accession numbers.

Species	12s	co1	enc1	myh6
Flexor incus	NA	ON368279	MT569724	MT569770
Aspasma minima	NA	NC_008130	NA	NA
Aspasma ubauo	MT541780	NA	NA	NA
Lepadichthys akiko	NA	MT053034	MT569669	MT569731
Lepadichthys bolini	NA	MT053035	MT569671	MT569734
Lepadichthys coccinotaenia	NA	MT053036	NA	NA
Lepadichthys erythraeus	NA	MN560936	NA	NA
Lepadichthys frenatus	KY656408	MK658644	NA	KY686123
Lepadichthys lineatus	KY126074	B:3336567	KT266283	MT569733
Lepadichthys trishula	NA	NA	NA	MT569732
Discotrema crinophilum	EF031222	KY656438	MT569668	KY686124
Discotrema monogrammum	EF031230	NA	NA	NA
Diademichthys lineatus	KY656407	KY656436	MT569667	KY686122
Aspasmichthys alorensis	NA	MT053013	MT569661	MT569727
Aspasmichthys ciconiae	NA	MT053014	MT569662	MT569728
Pherallodus indicus	NA	MT053042	NA	MT569747
Alabes dorsalis	NA	B:10697666	MT569664	MT569730
Alabes hoesei	KY656412	KY656441	NA	KY686127
Alabes parvula	NA	NA	MT569665	NA
Alabes scotti	KY126073	B:4293902	NA	NA
Aspasmogaster costata	KY656414	B:2820479	MT569672	KY686129
Aspasmogaster liorhynchus	NA	MT053015	NA	MT569735
Aspasmogaster tasmaniensis	NA	MT053016	MT569673	MT569736
Cochleoceps bassensis	NA	MT053017	NA	MT569737
Cochleoceps orientalis	KY656411	KY656440	MT569674	KY686126
Cochleoceps spatula	NA	MT053018	NA	MT569738
Cochleoceps viridis	NA	MT053019	MT569675	MT569739
Diplocrepis puniceus	NA	MT053023	NA	MT569740
Gastrocyathus gracilis	NA	MT053026	NA	MT569741
Gastrocymba quadriradiata	NA	MT053027	NA	MT569742
Gastroscyphus hectoris	NA	MT053028	MT569676	MT569743
Parvicrepis parvipinnis	KY656413	B:2820772	MT569677	MT569744
Salarias alboguttatus	NA	KP194608	MG779108	MG779146
Entomacrodus nigricans	DQ143880	B:2843322	KF678528	KF139990
Ophioblennius atlanticus	AY098805	FJ583755	JX188983	JX189749
Gramma loreto	NA	JQ840515	JX188886	JQ939496
Opistognathus aurifrons	NA	JF297892	JX188902	JX189682
Dicentrarchus punctatus	NA	KJ168066	NA	NA

Table 2.7Sa. “GAMS” phylogeny (*Girella*, *Atypichthys*, *Microcanthus*, *Scorpis*): list of species and ranges.

Species	Range
Girella albostriata	Southeast Pacific: Desventuradas and Juan Fernández
Girella cyanea	Southwest Pacific: South Australia, Lord Howe, Norfolk, Rangitāhua, and New Zealand
Girella elevata	East Australia
Girella fimbriata	Southwest Pacific: Rangitāhua
Girella freminvillii	East Pacific: Galápagos
Girella laevifrons	Southeast Pacific: Peru and Chile
Girella leonina	Northwest Pacific: China and Japan
Girella mezina	Northwest Pacific: China and Japan
Girella nebulosa	Southeast Pacific: Rapa Nui
Girella nigricans	Northeast Pacific: Mexico and United States
Girella punctata	Northwest Pacific: China and Japan
Girella simplicidens	Northeast Pacific: Gulf California
Girella stuebeli	East Atlantic: Cape Verde
Girella tephraeops	Australia: WA
Girella tricuspidata	Southwest Pacific: Southeast Australia to New Zealand
Girella zebra	West, South and Southeast Australia
Graus nigra	Southeast Pacific: Chile
Atypichthys latus	Southwest Pacific: Southeast Australia, Lord Howe, Norfolk, Rangitāhua, and New Zealand
Atypichthys strigatus	East and Southeast Australia
Microcanthus joyceae	Southwest Pacific: East Australia, Lord Howe, Norfolk, and New Caledonia
Microcanthus strigatus	Indo-West Pacific, except Southwest Pacific
Neatypus obliquus	West and South Australia
Tilodon sexfasciatus	West, South, and Southeast Australia
Scorpis aequipinnis	West, South, Southeast, and East Australia
Scorpis georgiana	West and South Australia
Scorpis lineolata	Southwest Pacific: Southeast Australia and New Zealand
Scorpis violacea	Southwest Pacific: Australia, Lord Howe, Norfolk, Rangitāhua, and New Zealand
Kyphosus elegans	East Pacific
Kyphosus hawaiiensis	Hawaii
Kuhlia malo	Central Pacific: Society Islands
Kuhlia mugil	Indo-Pacific
Rhynchopelates oxyrhynchus	Northwest Pacific: Vietnam to Japan
Terapon puta	Indo-Pacific
Pelates quadrilineatus	Indo-Pacific
Oplegnathus woodwardi	Australia mainland up to New Zealand
Oplegnathus punctatus	West and Central Pacific
Nannoperca obscura	Southeast Australia
Scomber scombrus	Northern oceans
Hyperoglyphe antarctica	Southern circumglobal

Table 2.7Sb. “GAMS” phylogeny (*Girella*, *Atypichthys*, *Microcanthus*, *Scorpis*): accession numbers.

Species	16s	co1	cytb	rag1	rag2	tmo4c4
Girella albostriata	Beldade*	NA	NA	NA	NA	NA
Girella cyanea	Beldade*	NA	KC136395	JX908435	KC130527	KC130611
Girella elevata	Beldade*	NA	NA	NA	NA	NA
Girella fimbriata	Beldade*	B:2914609	KC136518	JX908419	KC130443	KC130547
Girella freminvillii	Beldade*	B:2843344	NA	NA	NA	NA
Girella laevifrons	Beldade*	MT080290	NA	NA	NA	NA
Girella leonina	Beldade*	KX494865	KX494865	NA	NA	NA
Girella mezina	Beldade*	KU944190	NA	JQ353029	NA	NA
Girella nebulosa	Beldade*	NA	KC136517	JX908377	KC130539	KC130604
Girella nigricans	Beldade*	GU440329	NA	JX908426	KC130518	KC130595
Girella punctata	Beldade*	MK560639	NC_013137	KC442214	KC130506	KC130637
Girella simplicidens	Beldade*	NA	KC136553	JX908450	KC130499	KC130597
Girella stuebeli	Beldade*	NA	NA	NA	NA	NA
Girella tephraeops	Beldade*	NA	NA	NA	NA	NA
Girella tricuspidata	Beldade*	DQ107783	KC136536	JX908480	KC130442	KC130651
Girella zebra	Beldade*	DQ107787	KC136370	JX908429	KC130447	KC130568
Graus nigra	Beldade*	NA	KC136425	JX908471	KC130465	KC130654
Atypichthys latus	AY530859	NA	NA	NA	NA	NA
Atypichthys strigatus	EF616973	B:2820485	KC136476	JX908483	KC130459	KC130610
Microcanthus joyceae	MK855349	MK871478	NA	JX908390	KC130466	NA
Microcanthus strigatus	MK855361	MK871506	NA	NA	NA	NA
Neatypus obliquus	NA	B:2804839	NA	NA	NA	NA
Tilodon sexfasciatus	NA	B:2755511	NA	NA	NA	NA
Scorpis aequipinnis	KX234683	DQ107772	NA	NA	NA	NA
Scorpis georgiana	NA	B:10013576	NA	NA	NA	NA
Scorpis lineolata	LC020588	DQ107777	KC136485	JX908461	KC130533	KC130607
Scorpis violacea	NA	NA	KC136465	JX908397	KC130440	KC130660
Kyphosus elegans	MH933932	B:2998773	KC136565	JX908403	KC130546	KC130650
Kyphosus hawaiiensis	NA	MG816699	KC136500	JX908423	KC130456	KC130656
Kuhlia malo	HE798359	HE798219	NA	NA	NA	HE798289
Kuhlia mugil	HE798381	B:2825147	AY116003	KF017126	KC130543	HE798311
Rhynchopelates oxyrhynchus	AP006811	KY372106	NA	JQ769453	JQ769497	JN688854
Terapon puta	KC774745	B:5303886	KF999869	JQ769462	JQ769506	NA
Pelates quadrilineatus	JN688788	KC970410	KF999858	JQ769448	JQ769493	JN688855
Oplegnathus woodwardi	DQ532924	DQ107729	KC136482	JX908475	KC130490	KC130613
Oplegnathus punctatus	HQ018811	NC_013143	NC_013143	EU167854	JQ769470	NA
Nannoperca obscura	JF519733	NC_015545	GQ470915	NA	HQ713637	NA
Scomber scombrus	NA	KX782980	NA	KF141355	DQ874765	DQ388099
Hyperoglyphe antarctica	AB642286	B:2820585	KC136576	JX908464	KC130446	KC130548

*Sequence provided by authors from Beldade et al. (2021).

Table 2.8Sa. “HL” phylogeny (*Hypoplectrodes*, *Lepidoperca*): list of species and ranges.

Species	Range
Lepidoperca aurantia	Southwest Pacific: New Zealand
Lepidoperca brochata	Australia: New South Wales
Lepidoperca filamenta	Australia: South and West
Lepidoperca inornata	Southwest Pacific: New Zealand and Rangitāhua (Kermadec Ridge)
Lepidoperca magna	Southwest Pacific: Australia and New Zealand (North Island)
Lepidoperca occidentalis	Australia: South and West
Lepidoperca pulchella	Australia: New South Wales and Victoria
Lepidoperca tasmanica	Southwest Pacific: Tasmania and New Zealand (South Island)
Hypoplectrodes cardinalis	West Australia
Hypoplectrodes huntii	Southwest Pacific: New Zealand
Hypoplectrodes jamesoni	Australia: Queensland to New South Wales
Hypoplectrodes maccullochi	Australia: Queensland, New South Wales, Victoria, and Tasmania
Hypoplectrodes nigroruber	Australia: East, South, and West
Hypoplectrodes semicinctum	Southeast Pacific: Juan Fernández and Desventuradas Islands
Hypoplectrodes sp. A	Southwest Pacific: East Australia, Lord Howe, Norfolk, Rangitāhua, and New Zealand mainland (Three Kings to Gisborne)
Hypoplectrodes sp. B	Southwest Pacific: northern mainland New Zealand
Hypoplectrodes sp. C	Southwest Pacific: Rangitāhua
Epinephelus aeneus	Atlantic Ocean
Epinephelus adscensionis	Atlantic Ocean
Epinephelus rivulatus	Indo-Pacific
Gobius incognitus	Mediterranean
Odontobutis interrupta	Northwest Pacific: Korea

Table 2.8Sb. “HL” phylogeny (*Hypoplectrodes*, *Lepidoperca*): accession numbers.

Species	co1
Lepidoperca aurantia	B:2914747
Lepidoperca brochata	ON368287
Lepidoperca filamenta	B:10565366
Lepidoperca inornata	B:2755176
Lepidoperca magna	B:2820692
Lepidoperca occidentalis	B:2755180
Lepidoperca pulchella	B:10258342
Lepidoperca tasmanica	B:11567001
Hypoplectrodes cardinalis	B:10270928
Hypoplectrodes huntii	ON368282
Hypoplectrodes jamesoni	B:2618665
Hypoplectrodes maccullochi	ON368283
Hypoplectrodes nigroruber	ON368284
Hypoplectrodes semicinctum	ON368285
Hypoplectrodes sp. A	MN123383
Hypoplectrodes sp. B	MN123384
Hypoplectrodes sp. C	ON368286
Epinephelus aeneus	KT805239
Epinephelus adscensionis	B:2771516
Epinephelus rivulatus	B:2801568
Gobius incognitus	MT884425
Odontobutis interrupta	HQ536410

Table 2.9Sa. “Kathetostoma” phylogeny: list of species and ranges.

Species	Range
Kathetostoma albigutta	West Atlantic
Kathetostoma averruncus	East Pacific: California, Galápagos, and Peru
Kathetostoma binigrasella	Southwest Pacific: Rangitāhua and New Zealand
Kathetostoma canaster	Southeast to Southwest Australia
Kathetostoma giganteum	Southwest Pacific: New Zealand
Kathetostoma laeve	Australia: East, Southeast, South, Southwest
Kathetostoma nigrofasciatum	South to West Australia
Xenocephalus armatus	Southwest Pacific: Southeast Australia to New Zealand
Pleuroscopus pseudodorsalis	Southern Atlantic, Indian, Pacific
Ammodytes hexapterus	Arctic
Acropoma japonicum	West Pacific
Pristiapogon exostigma	Indo-Pacific
Pristiapogon kallopterus	Indo-Pacific
Nannoperca obscura	Southeast Australia
Percalates novemaculeata	Southeast Australia
Percalates colonorum	Southeast Australia

Table 2.9Sb. “Kathetostoma” phylogeny: accession numbers.

Species	16s	co1	cytb	d-loop	enc1	rag1
Kathetostoma albigutta	NA	B:2859071	DQ165282	DQ165317	NA	NA
Kathetostoma averruncus	NA	MF956743	DQ165280	DQ165315	JX188980	JX189908
Kathetostoma binigrasella	NA	MN123388	DQ165269	DQ165308	NA	NA
Kathetostoma canaster	EU848426	B:2755159	DQ165275	DQ165310	NA	NA
Kathetostoma giganteum	GU018120	B:2914683	DQ165256	DQ165291	NA	NA
Kathetostoma laeve	KR153507	B:2820682	DQ165277	DQ165312	NA	NA
Kathetostoma nigrofasciatum	NA	B:2755161	DQ165278	DQ165313	NA	NA
Xenocephalus armatus	NA	B:2755563	NA	NA	NA	NA
Pleuroscopus pseudodorsalis	NA	B:2755362	NA	NA	NA	NA
Ammodytes hexapterus	KJ010574	B:4177175	KR422494	NA	KF139576	KF141166
Acropoma japonicum	DQ790843	KT718497	AB104911	NA	NA	KF017118
Pristiapogon exostigma	NA	JQ349730	EU380960	NA	AB893563	AB893443
Pristiapogon kallopterus	NA	B:3215655	KM455442	NA	AB893565	KT266395
Nannoperca obscura	JF519733	KJ669545	GQ470915	NA	NA	NA
Percalates novemaculeata	EF120873	DQ107936	NA	AF012458	KF139541	JQ353038
Percalates colonorum	AY254555	DQ107939	AY577775	EU886375	KF139540	KF017132

Table 2.10Sa. “NEMOGOCHIA” phylogeny (*Nemadactylus*, *Morwong*, *Goniistius*, *Chironemus*, *Aplodactylus*): list of species and ranges.

Species	Range
Goniistius francisi	Southwest Pacific: Lord Howe, Norfolk, Rangitāhua, and New Caledonia
Goniistius gibbosus	Australia: WA
Goniistius plessisi	Rapa Nui
Goniistius quadricornis	Northwest Pacific: Japan
Goniistius rubrolabiatus	West and South Australia
Goniistius vestitus	Southwest Pacific: Australia, New Caledonia, Lord Howe, and Norfolk
Goniistius vittatus	Central Pacific: Hawaii
Goniistius zebra	Northwest Pacific: Japan
Goniistius zonatus	Northwest Pacific: China, Japan, and Korea
Morwong ephippium	Southwest Pacific: Southeast Australia, Lord Howe, Norfolk, Rangitāhua, and New Zealand mainland
Morwong fuscus	Southwest Pacific: East Australia and Lord Howe
Nemadactylus bergi	Southeast Pacific and Southwest Atlantic
Nemadactylus douglasii	Southwest Pacific: Southeast Australia, Rangitāhua, and New Zealand (North Island)
Nemadactylus gayi	Southeast Pacific: Juan Fernández and Desventuradas
Nemadactylus macropterus	Southwest Pacific: southern Australia and mainland New Zealand
Nemadactylus monodactylus	South Atlantic: Tristan da Cunha
Nemadactyus n.sp.	Southwest Pacific: Southeast Australia, Lord Howe, Norfolk, Rangitāhua, and New Zealand (North Island)
Nemadactylus valenciennesi	West, South, and Southeast Australia
Pseudogoniistius nigripes	West, South, and Southeast Australia, and New Zealand
Chironemus bicornis	Southeast Pacific: Juan Fernández and Desventuradas
Chironemus delfini	Southeast Pacific: Juan Fernández
Chironemus georgianus	West, South, and Southeast Australia
Chironemus maculosus	West, South, and Southeast Australia
Chironemus marmoratus	Southwest Pacific: East Australia, Lord Howe, and New Zealand
Chironemus microlepis	Southwest Pacific: Lord Howe, Norfolk, and Rangitāhua
Aplodactylus arctidens	Southwest Pacific: Southeast Australia and New Zealand
Aplodactylus etheridgii	Southwest Pacific: Lord Howe, Norfolk, Rangitāhua, and New Zealand
Aplodactylus lophodon	South Australia
Aplodactylus punctatus	East Pacific: Peru to Chile
Aplodactylus westralis	Australia: WA
Cirrhitichthys falco	Indo-Pacific
Neocirrhites armatus	West Pacific
Notocirrhitus splendens	Southwest Pacific: Southeast Australia, Lord Howe, Norfolk, and Rangitāhua
Enoplosus armatus	West, South, and Southeast Australia
Nannoperca obscura	South Australia

Table 2.10Sb. “NEMOGOCHIA” phylogeny (*Nemadactylus*, *Morwong*, *Goniistius*, *Chironemus*, *Aplodactylus*): accession numbers.

Species	16s	co1	cytb	rag1
Goniistius francisi	NA	MN123305	NA	NA
Goniistius gibbosus	NA	B:2804708	AF067085	NA
Goniistius plessisi	NA	NA	AF092165	NA
Goniistius quadricornis	JQ178233	B:4720592	AF092163	KF017131
Goniistius rubrolabiatus	NA	NA	AF092909	NA
Goniistius vestitus	NA	NA	AF092166	NA
Goniistius vittatus	NA	NA	AY303768	NA
Goniistius zebra	NA	NA	AF092164	NA
Goniistius zonatus	HQ018815	JF952747	AF092162	KF017130
Morwong ephippium	NA	NA	AF092159	NA
Morwong fuscus	NA	B:2820635	AF092158	NA
Nemadactylus bergi	NA	EU074497	AF067092	NA
Nemadactylus douglasii	EU848430	B:2918461	AF067090	NA
Nemadactylus gayi	NA	NA	AF067095	NA
Nemadactylus macropterus	LC020572	B:2755258	AF067091	NA
Nemadactylus monodactylus	NA	NA	AF067094	EU167819
Nemadactyus n.sp.	NA	FOAE237-06	NA	NA
Nemadactylus valenciennesi	EU848449	B:2918475	AF067089	NA
Pseudogoniistius nigripes	KR153503	MN123306	AF092160	NA
Chironemus bicornis	DQ462669	NA	NA	NA
Chironemus delfini	DQ462667	NA	NA	NA
Chironemus georgianus	DQ462673	B:2754934	NA	KT883712
Chironemus maculosus	LC020589	B:2755506	NA	KT883713
Chironemus marmoratus	DQ462671	B:2820544	AF092167	EU167820
Chironemus microlepis	DQ462674	NA	NA	NA
Aplodactylus arctidens	EF120862	B:2918314	AF092157	EU167743
Aplodactylus etheridgii	NA	B:2914223	AF133066	KT883730
Aplodactylus lophodon	NA	B:2820561	AF133068	NA
Aplodactylus punctatus	DQ462677	B:2878311	AY074890	NA
Aplodactylus westralis	NA	NA	AF133067	NA
Cirrhitichthys falco	NA	B:10878253	NA	NA
Neocirrhites armatus	NA	B:10878251	JX645665	NA
Notocirrhitus splendens	NA	JX645656	AF067084	NA
Enoplosus armatus	DQ532873	B:2820582	NA	NA
Nannoperca obscura	NA	NC_015545	KC286021	NA

Table 2.11Sa. “Optivus” phylogeny: list of species and ranges.

Species	Range
Optivus agastos	Southwest Pacific: East Australia, Lord Howe, and New Caledonia
Optivus agrammus	West and South Australia
Optivus elongatus	Southwest Pacific: Rangitāhua and New Zealand mainland
Hoplostethus japonicus	Northwest Pacific: Japan
Diretmoides veriginae	Indo-Pacific
Diretmus argenteus	Circumglobal
Anomalops katoptron	West Pacific: Japan to Australia
Monocentris japonica	Indo-Pacific
Anoplogaster cornuta	Circumglobal
Polymixia lowei	West Atlantic
Polymixia japonica	West Pacific: Japan to New Zealand
Polymixia nobilis	Northern Atlantic

Table 2.11Sb. “Optivus” phylogeny: accession numbers.

Species	co1	cytb	myh6
Optivus agastos	HM902629	NA	NA
Optivus agrammus	B:2839479	NA	NA
Optivus elongatus	ON368288	NA	NA
Hoplostethus japonicus	NC_003187	NC_003187	NA
Diretmoides veriginae	B:2804671	NC_008126	NA
Diretmus argenteus	B:2914542	NC_008127	KF139985
Anomalops katoptron	FJ582852	NC_008128	KF139921
Monocentris japonica	B:5841487	NC_004392	JX190476
Anoplogaster cornuta	MH777666	KR422525	KC827343
Polymixia lowei	B:2859192	NC_003181	MH917535
Polymixia japonica	KF930291	NC_002648	MH917519
Polymixia nobilis	NA	DQ197980	MH917544

Table 2.12Sa. “Parma” phylogeny: list of species and ranges.

Species	Range
Parma alboscapularis	Southwest Pacific: Lord Howe, Rangitāhua, north New Zealand
Parma kermadecensis	Southwest Pacific: Rangitāhua
Parma mccullochi	Western Australia
Parma microlepis	Southeast Australia
Parma occidentalis	Western Australia
Parma oligolepis	East Australia
Parma victoriae	West, South, and East Australia
Mecaenichthys immaculatus	Southeast Australia
Ptychochromis oligacanthus	Indian Ocean: Madagascar
Gramma loreto	West Atlantic
Semicossyphus pulcher	East Pacific
Centropyge bicolor	Indo-Pacific
Dicentrarchus punctatus	East Atlantic

Table 2.12Sb. “Parma” phylogeny: accession numbers.

Species	16s	co1	cytb	rag1	tmo4c4
Parma alboscapularis	MW630433	ON368289	MW631043	MW631444	MW631633
Parma kermadecensis	NA	ON368290	NA	NA	NA
Parma mccullochi	MN473747	NA	NA	NA	NA
Parma microlepis	MW630434	MW630834	MW631044	MW631445	MW631634
Parma occidentalis	MN473748	NA	NA	NA	NA
Parma oligolepis	NA	MW630835	MW631045	MW631446	NA
Parma victoriae	MW630435	MW630836	MW631046	NA	NA
Mecaenichthys immaculatus	FJ616458	MW630831	MW631041	MW631442	MW631631
Ptychochromis oligacanthus	AY279667	AY263874	NA	KF557090	NA
Gramma loreto	AY539053	AY662751	NA	MW631387	MW631581
Semicossyphus pulcher	AY279747	JQ934977	MH767448	FJ616726	EU601305
Centropyge bicolor	FJ616501	FJ582947	KJ148824	FJ616720	NA
Dicentrarchus punctatus	AF247437	NC_026075	AF240740	NA	DQ388114

Table 2.13Sa. “Upeneus” phylogeny: list of species and ranges.

Species	Range
Upeneus asymmetricus	Indo-Pacific
Upeneus australiae	Southwest Pacific: Australia and New Caledonia
Upeneus doriae	Northwest Indian
Upeneus filifer	Southwest Pacific: Australia, Coral Sea, and New Caledonia
Upeneus francisi	Southwest Pacific: Lord Howe, Norfolk, and Rangitāhua
Upeneus guttatus	Indo-Pacific
Upeneus heemstra	West Indian
Upeneus itoui	Northwest Pacific: Japan
Upeneus japonicus	Northwest Pacific: Japan, Korea, Russia, down to Philippines and Malaysia
Upeneus lombok	Indo-Pacific
Upeneus luzonius	Indo-Pacific
Upeneus margarethae	Indo-Pacific
Upeneus mascareinsis	Southwest Indian
Upeneus moluccensis	Indo-Pacific
Upeneus nigromarginatus	Indo-Pacific: Philippines
Upeneus oligospilus	Northwest Indian
Upeneus parvus	West Atlantic
Upeneus pori	West Indian
Upeneus quadrilineatus	Indo-Pacific
Upeneus randalli	Northwest Indian
Upeneus suahelicus	West Indian
Upeneus subvittatus	Indo-Pacific
Upeneus sulphureus	Indo-Pacific
Upeneus sundaicus	Indo-Pacific
Upeneus supravittatus	Indian Ocean
Upeneus taeniopterus	Indo-Pacific
Upeneus torres	Indo-Pacific
Upeneus tragula	Indo-Pacific
Upeneus vittatus	Indo-Pacific
Aeoliscus strigatus	Indo-Pacific
Centriscus scutatus	Indo-Pacific

Table 2.13Sb. “Upeneus” phylogeny: accession numbers.

Species	12s	co1
Upeneus asymmetricus	NA	GU673369
Upeneus australiae	NA	B:11566976
Upeneus doriae	NA	KU499744
Upeneus filifer	NA	B:2619094
Upeneus francisi	ON387617	ON368291
Upeneus guttatus	LC036893	HM422398
Upeneus heemstra	NA	KC147810
Upeneus itoui	LC327113	NA
Upeneus japonicus	AB972201	JQ681335
Upeneus lombok	NA	HM902439
Upeneus luzonius	NA	GU673242
Upeneus margarethae	NA	KC147805
Upeneus mascareinsis	NA	KC147807
Upeneus moluccensis	LC499293	KR861567
Upeneus nigromarginatus	NA	KP331449
Upeneus oligospilus	NA	MT076735
Upeneus parvus	NA	B:2859311
Upeneus pori	NA	B:2801523
Upeneus quadrilineatus	LC499295	B:2619099
Upeneus randalli	NA	MT076738
Upeneus suahelicus	NA	KP293707
Upeneus subvittatus	AB972200	KY372343
Upeneus sulphureus	LC036892	KY372353
Upeneus sundaicus	LC499363	GU673373
Upeneus supravittatus	NA	KP293722
Upeneus taeniopterus	NA	B:2825668
Upeneus torres	NA	B:2744551
Upeneus tragula	LC036879	B:3962274
Upeneus vittatus	LC036890	JF493908
Aeoliscus strigatus	LC104456	B:3281345
Centriscus scutatus	LC026586	JN312879

Table 2.14S. List of fossils used as primary calibration points for each of the 13 phylogenies. Crown nomenclature, clade number, ages, and fossil names with associated references follow Matschiner et al. (2017). †Indicates extinction of both genus and species when placed in front of genus, and of species only within an extant genus when placed between genus and species. *ID number in Fossilworks.

PHYLOGENY	CROWN	CLADE NUMBER	AGES (Ma)	FOSSIL	REFERENCE
Arripis	Myctophata	77	83.5 - 70.6	†*Sardinioides* spp.	van der Marck (1858)
				†*Sardinius cordieri*	Agassiz (1839)
				†*Tachynectes* spp.	van der Marck (1863)
	Scombriformes	103	66.043 - 56.6	†*Eutrichiurides opiensis*	Leriche (1906)
				†*Sphyraenodus multidentatus*	Dartevelle & Casier (1959)
				†*Ardiodus mariotti*	White (1931)
	Ophidiimorpharia	100	57.23 - 55.8	†*Eolamprogrammus senectus*	Danil'chenko (1968)
	Gobiiformes	220	33.9 - 30.7	*"Gobius" gracilis*	Laube (1901)
	Batrachoidimorpharia	104	7.246 - 5.332	*Halobatrachus didactylus*	Bloch & Schneider (1801)
Capromimus	Polymixiacea	80	96.0 - 93.5	†*Homonotichthys rotundus*	Smith Woodward (1902)
	Zeariae	83	76.4 - 69.2	†*Cretazeus rinaldii*	Tyler et al. (2000)
	Percopsiaria	81	66.043 - 61.1	†*Mcconichthys longipinnis*	Grande (1988)
Chromis	Moronidae + Lobotidae	174	74.0 - 74.0	*Morone* †sp	Nolf & Dockery (1990)
	Pomacentridae	226	49.4 - 49.1	†*Palaeopomacentrus orphae*	Bellwood & Sorbini (1996)
				†*Lorenzichthys olihan*	Bellwood (1999)
	Chromis	356949 *	7.246 - 5.332	*Chromis* †*savornini*	Arambourg (1927)
Enneapterygius	Moronidae + Lobotidae	174	74.0 - 74.0	*Morone* †sp	Nolf & Dockery (1990)
	Blenniidae	233	49.4 - 49.1	†?*Oncolepis isseli*	Bassani (1898)
	Tripterygiidae	231	7.246 - 5.332	†*Tripterygion pronasus*	Arambourg (1927)
Eviota	Ophidiimorpharia	100	57.23 - 55.8	†*Eolamprogrammus senectus*	Danil'chenko (1968)
	Gobiiformes	220	33.9 - 30.7	†"*Gobius" gracilus*	Laube (1901)
	Batrachoidimorpharia	104	7.246 - 5.332	†*Halobatrachus didactylus*	Bloch & Schneider (1801)
Flexor	Moronidae + Lobotidae	174	74.0 - 74.0	*Morone* †sp	Nolf & Dockery (1990)
	Blenniidae	233	49.4 - 49.1	†?*Oncolepis isseli*	Bassani (1898)
GAS	Scombriformes	103	66.043 - 56.6	†*Eutrichiurides opiensis*	Leriche (1906)
				†*Sphyraenodus multidentatus*	Dartevelle & Casier (1959)
				†*Ardiodus mariotti*	White (1931)
	Percichthyidae + Perciliidae	139	58.7 - 55.8	†*Percichthys lonquimayensis*	Chang et al (1978)
	Kyphosidae	137	49.4 - 49.1	*?Pelates* †*quindecemalis*	Agassiz (1834)
HL	Gobiiformes	220	33. 9 - 30.7	†"*Gobius" gracilus*	Laube (1901)
	Epinephelidae	118	15.97 - 13.65	†*Epinephelus casotti*	Costa (1858)
Kathetostoma	Percichthyidae + Perciliidae	139	58.7 - 55.8	†*Percichthys lonquimayensis*	Chang et al (1978)
	Acropomatidae	161	49.4 - 49.1	*Acropoma* †*lepidotus*	Agassiz (1836)
	Apogonoidei	218	49.4 - 49.1	†*Apogon spinosus*	Agassiz (1836)
NEMOGOCHIA	Percichthyidae + Perciliidae	139	58.7 - 55.8	†*Percichthys lonquimayensis*	Chang et al (1978)
	Enoplosidae	138	49.4 - 49.1	*Enoplosus* †*pygopterus*	Agassiz (1836)
Optivus	Polymixiacea	80	96.0 – 93.5	†*Homonotichthys rotundus*	Smith Woodward (1902)
Parma	Moronidae + Lobotidae	174	74.0 - 74.0	*Morone* †sp	Nolf & Dockery (1990)
	Pomacentridae	226	49.4 - 49.1	†*Palaeopomacentrus orphae*	Bellwood & Sorbini (1996)
				†*Lorenzichthys olihan*	Bellwood (1999)

Table 2.14S. *(continued)*

PHYLOGENY	CROWN	CLADE NUMBER	AGES (Ma)	FOSSIL	REFERENCE
Upeneus	Centriscidae	106	55.964 - 55.788	†*Gerpegezhus paviai*	Bannikov & Carnevale (2012)
				†*Lorenzichthys olihan*	Bellwood (1999)
	Mulloidei + allies	112	49.4 - 49.1	†*Pterygocephalus paradoxus*	Agassiz (1839)

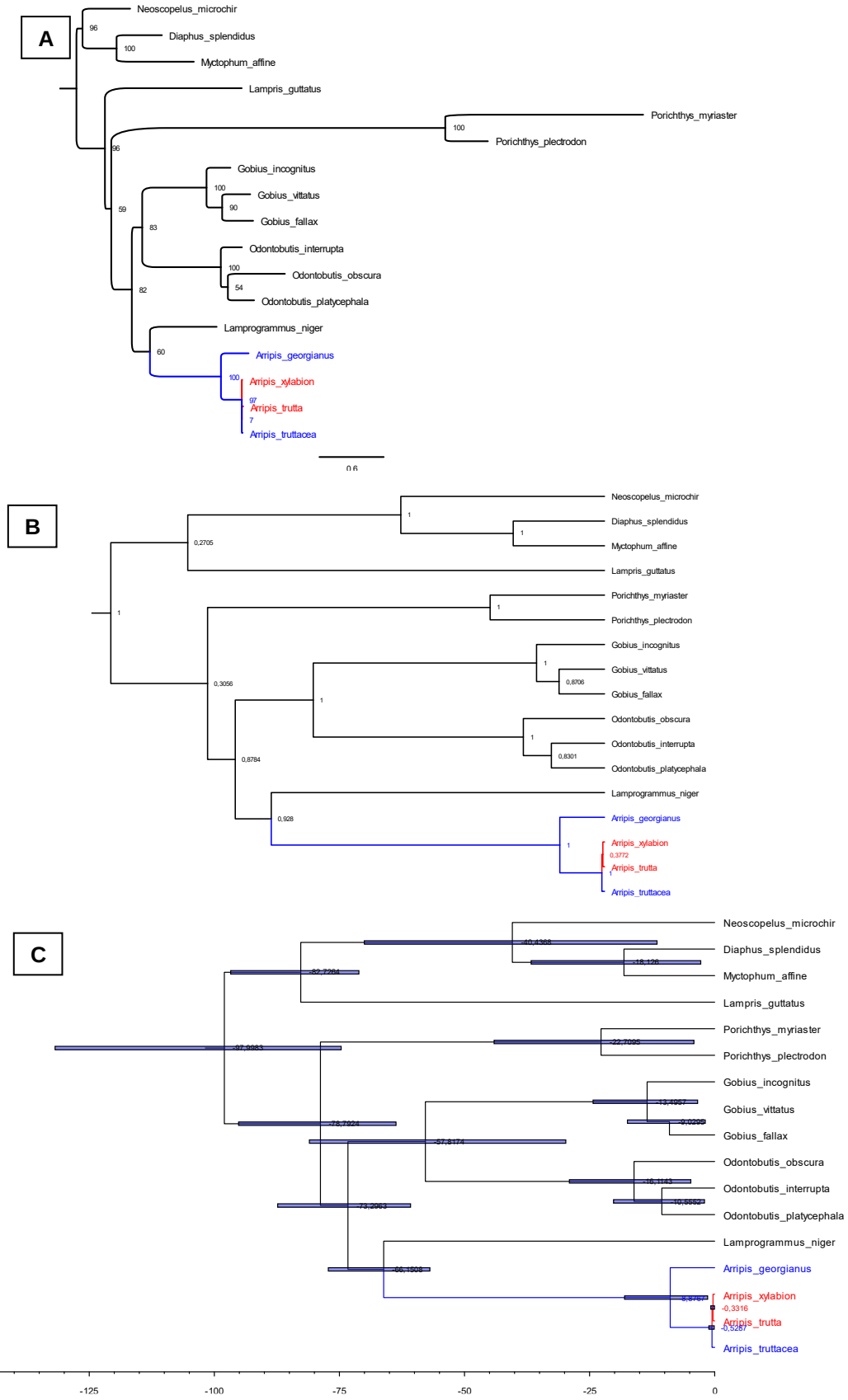

Figure 2.1S. Maximum-Likelihood phylogeny (**A**), Bayesian Inference with posterior probabilities (**B**), and time-calibrated tree (**C**) of the "Arripis" phylogeny. The red branches show the two endemics' position in the phylogeny and blue branches highlight their congeners within the same genus.

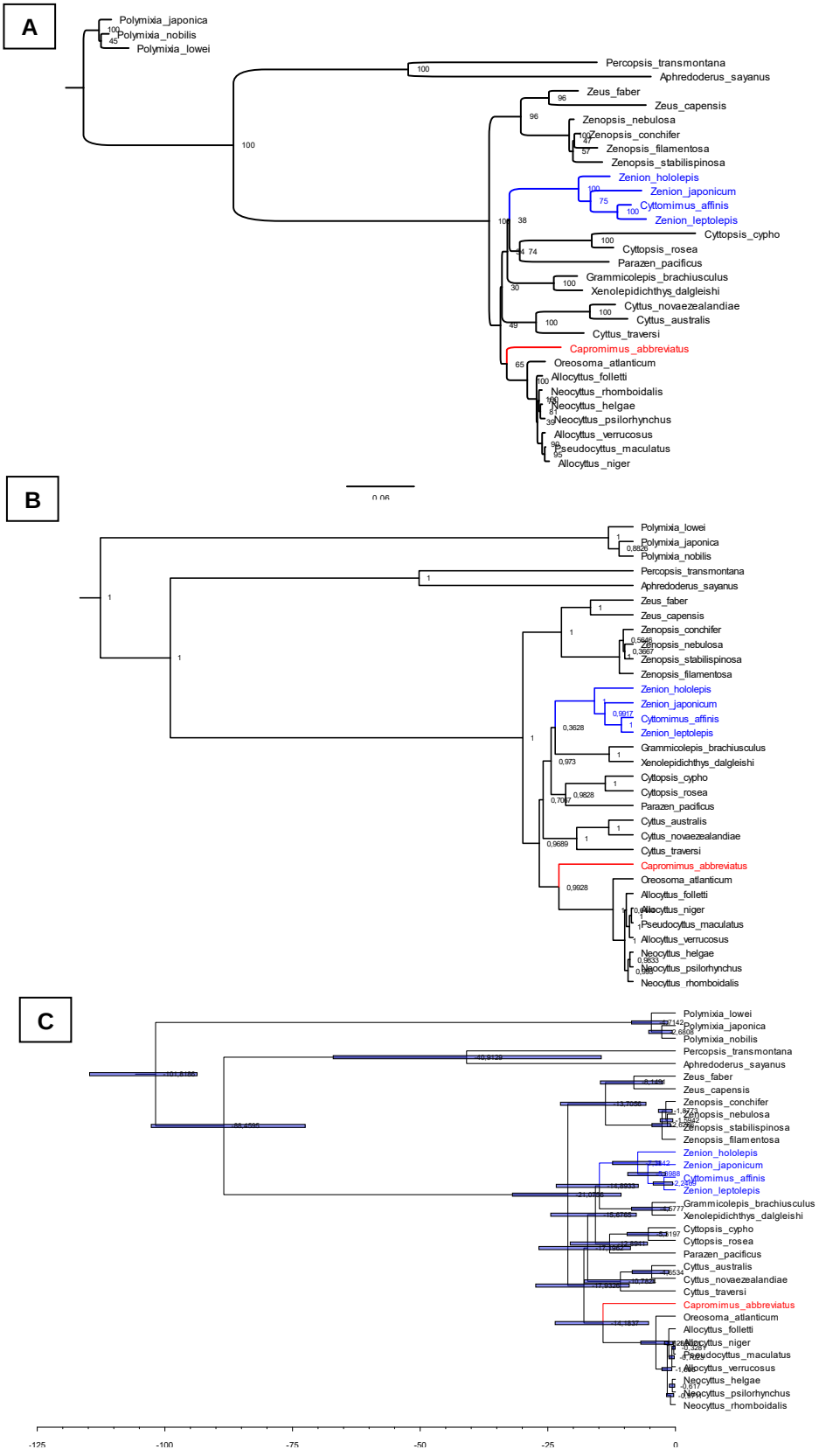

Figure 2.2S. Maximum-Likelihood phylogeny (**A**), Bayesian Inference with posterior probabilities (**B**), and time-calibrated tree (**C**) of the “Capromimus” phylogeny. The red branch shows the position of the monotypic endemic genus in the phylogeny and blue branches highlight the sampled endemic’s congeners within its family (Zeniontidae) as per the current taxonomic classification.

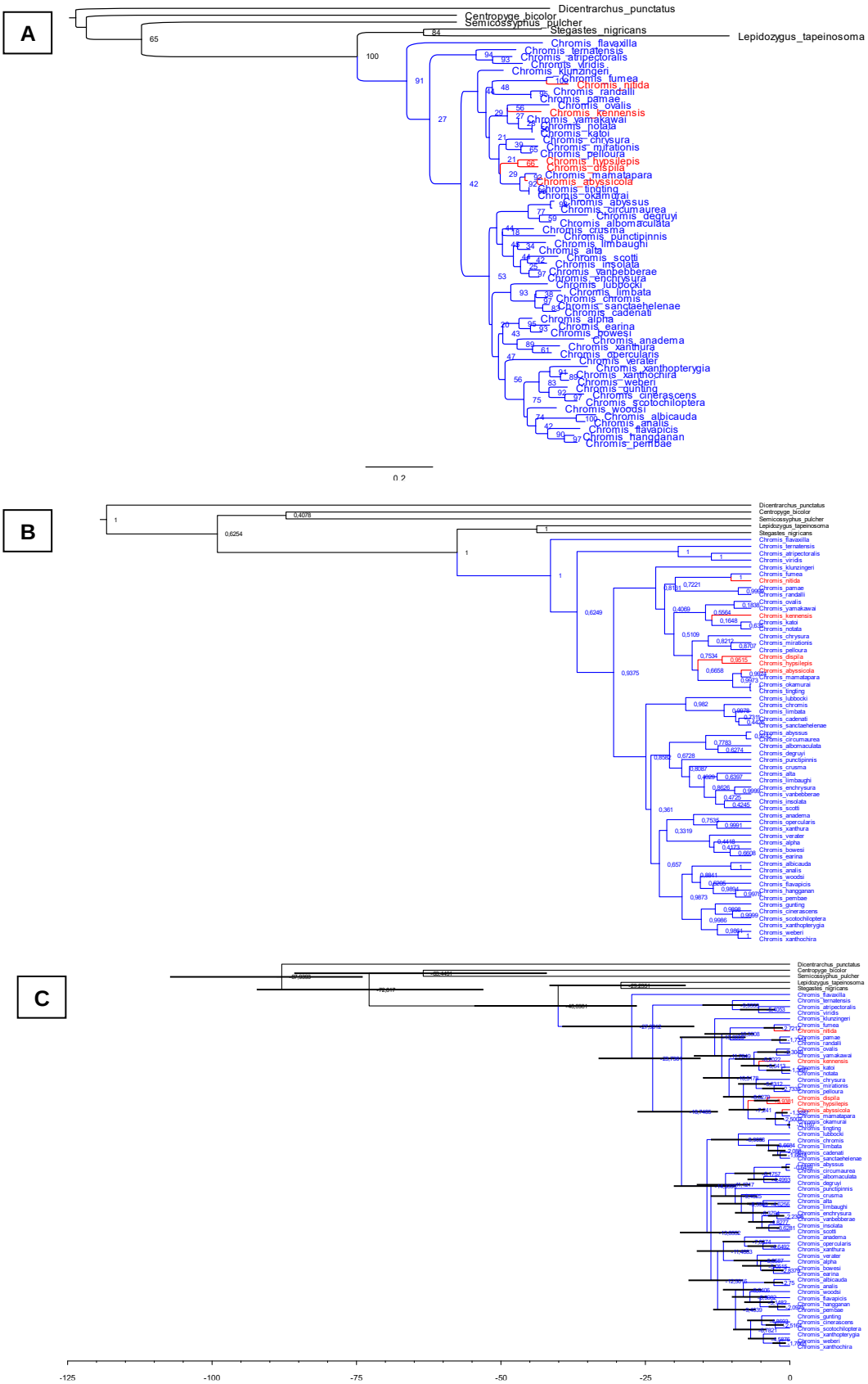

Figure 2.3S. Maximum-Likelihood phylogeny (**A**), Bayesian Inference with posterior probabilities (**B**), and time-calibrated tree (**C**) of the "Chromis" phylogeny. The red branches show the five endemics' position in the phylogeny, and blue branches highlight their congeners within *Chromis sensu stricto* (Tang et al., 2021).

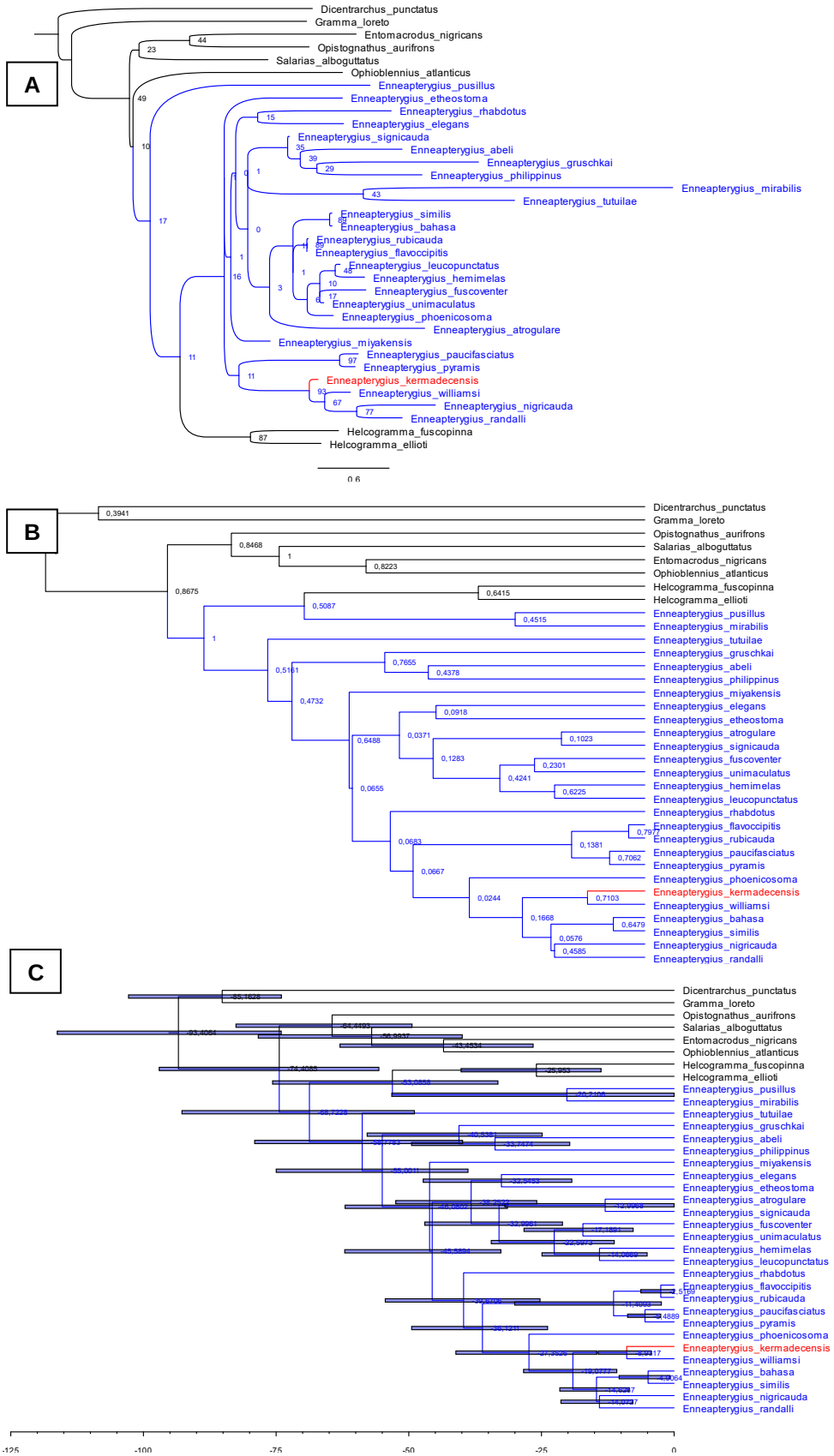

Figure 2.4S. Maximum-Likelihood phylogeny (**A**), Bayesian Inference with posterior probabilities (**B**), and time-calibrated tree (**C**) of the "Enneapterygius" phylogeny. The red branch shows the endemic's position in the phylogeny and blue branches highlight its congeners within the same genus.

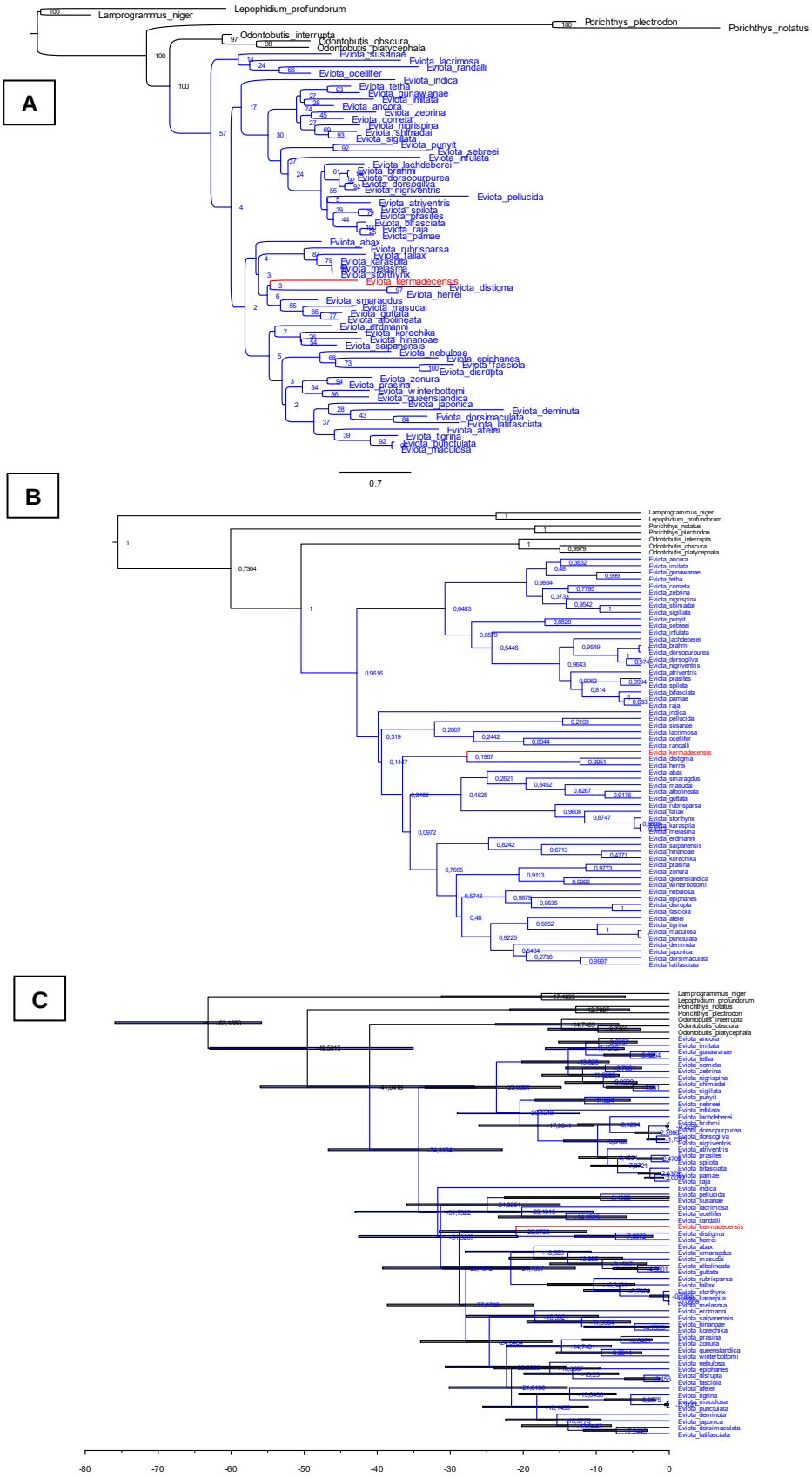

Figure 2.5S. Maximum-Likelihood phylogeny (**A**), Bayesian Inference with posterior probabilities (**B**), and time-calibrated tree (**C**) of the “Eviota” phylogeny. The red branch shows the endemic’s position in the phylogeny and blue branches highlight its congeners within the same genus.

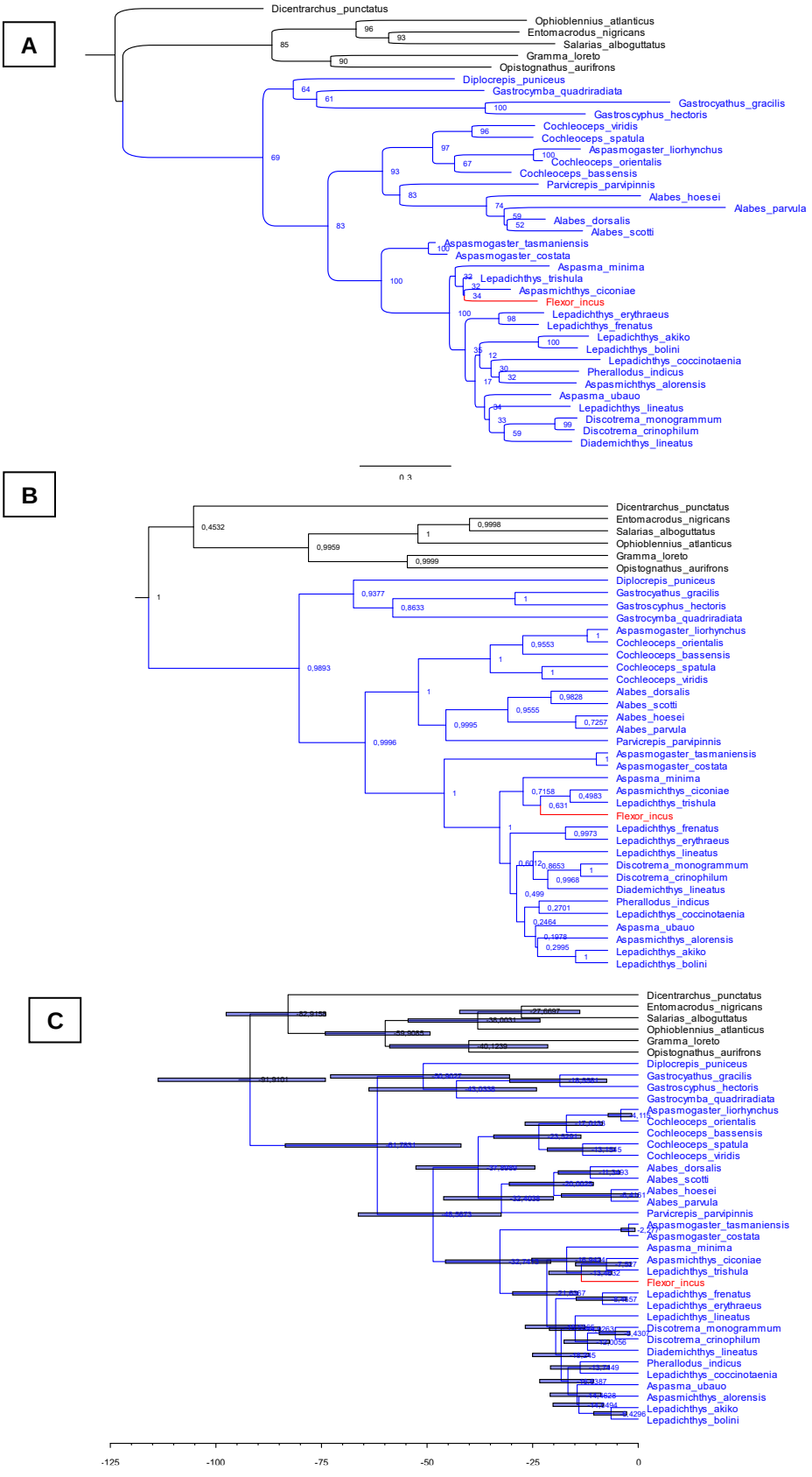

Figure 2.6S. Maximum-Likelihood phylogeny (**A**), Bayesian Inference with posterior probabilities (**B**), and time-calibrated tree (**C**) of the "Flexor" phylogeny. The red branch shows the position of the monotypic endemic genus in the phylogeny and blue branches highlight the sampled taxa within the endemic's family (Gobiesocidae).

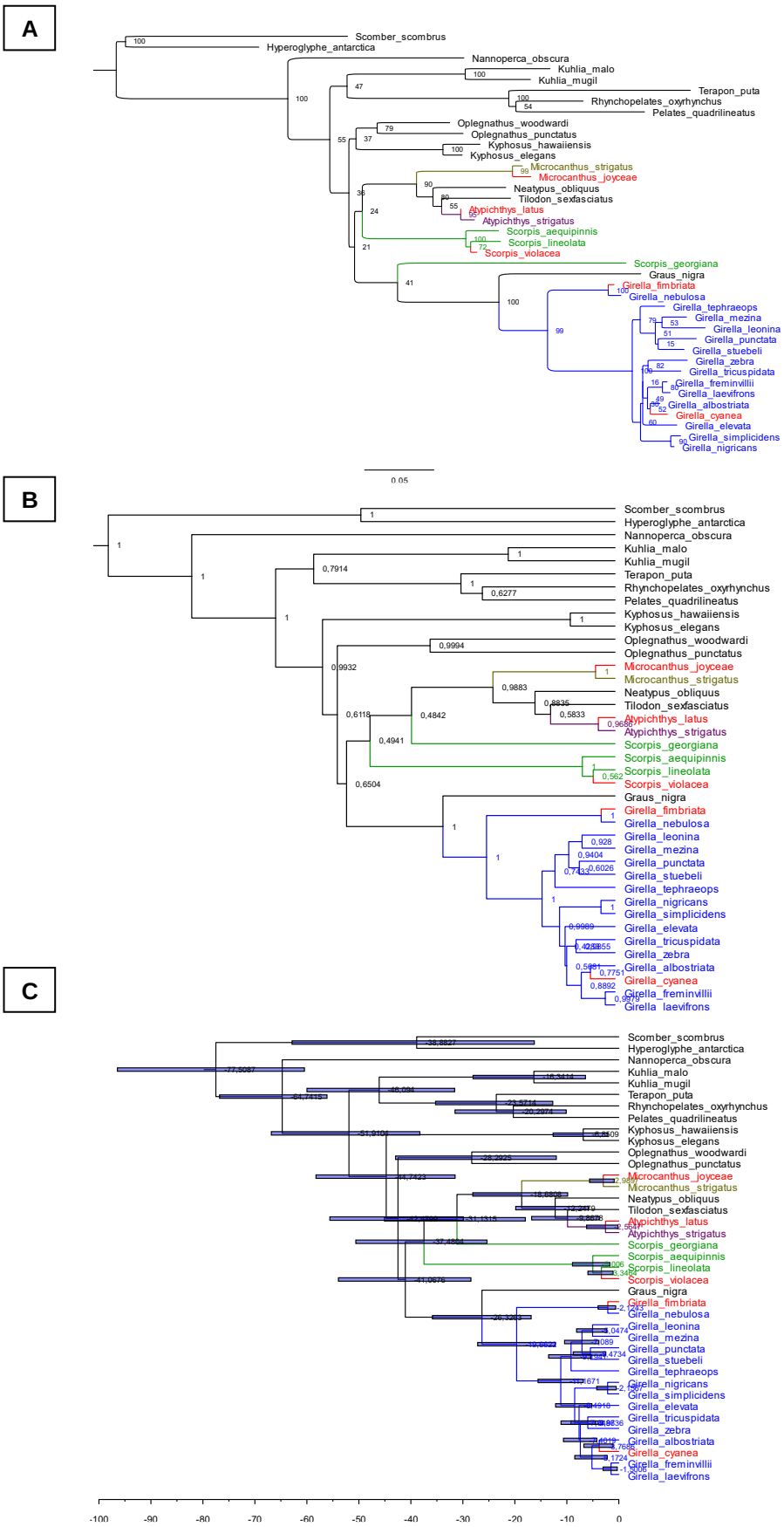

Figure 2.7S. Maximum-Likelihood phylogeny (**A**), Bayesian Inference with posterior probabilities (**B**), and time-calibrated tree (**C**) of the "GAMS" phylogeny. The red branches show the five endemics' position in the phylogeny. Blue (*Girella*), purple (*Atypichthys*), brown (*Microcanthus*), and green (*Scorpis*) branches highlight the endemics' congeners within the same genus.

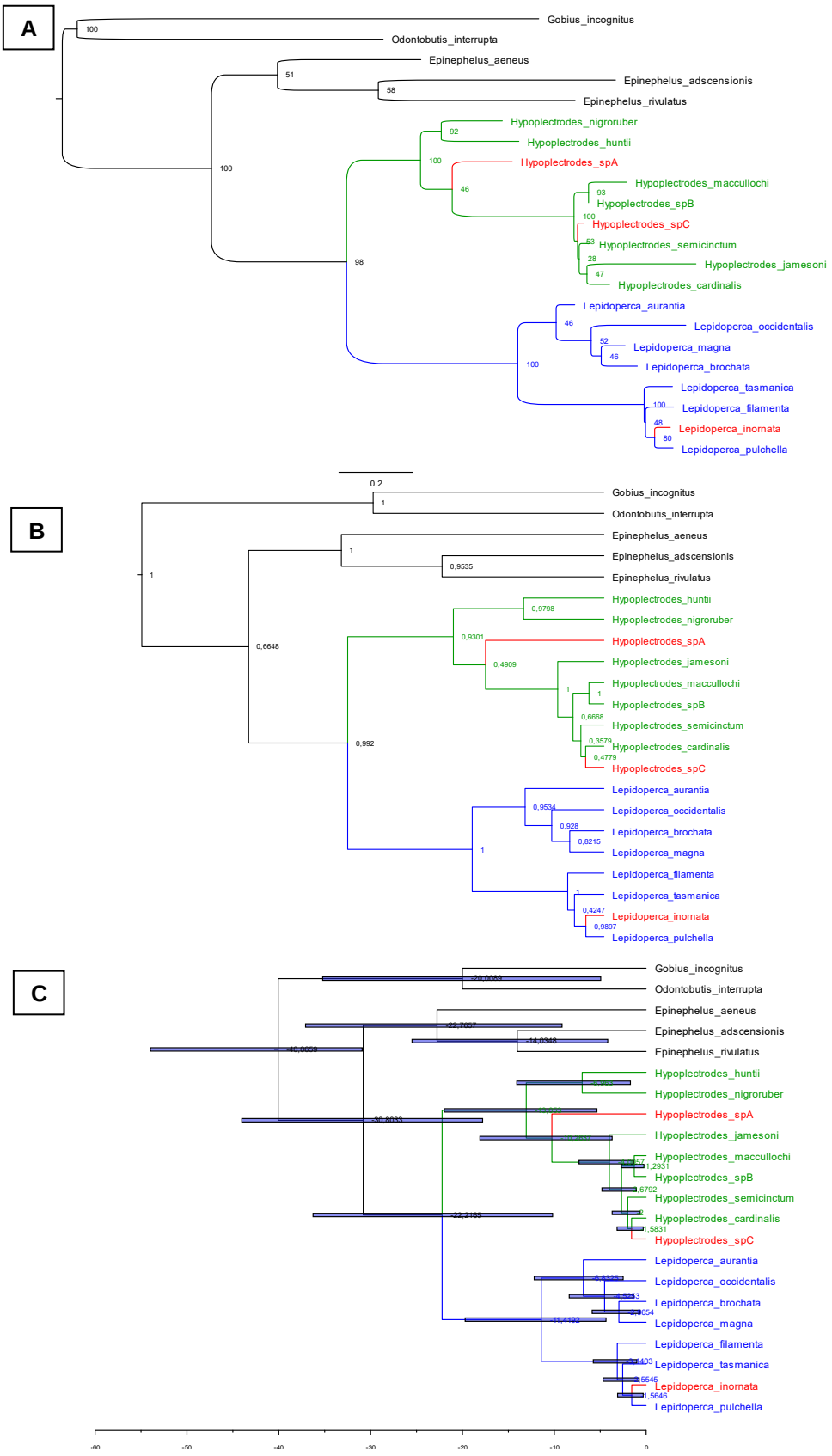

Figure 2.8S. Maximum-Likelihood phylogeny (**A**), Bayesian Inference with posterior probabilities (**B**), and time-calibrated tree (**C**) of the "HL" phylogeny. The red branch shows the endemics' position in the phylogeny. Blue (*Lepidoperca*) and green (*Hypoplectrodes*) branches highlight the congeners within the same genus.

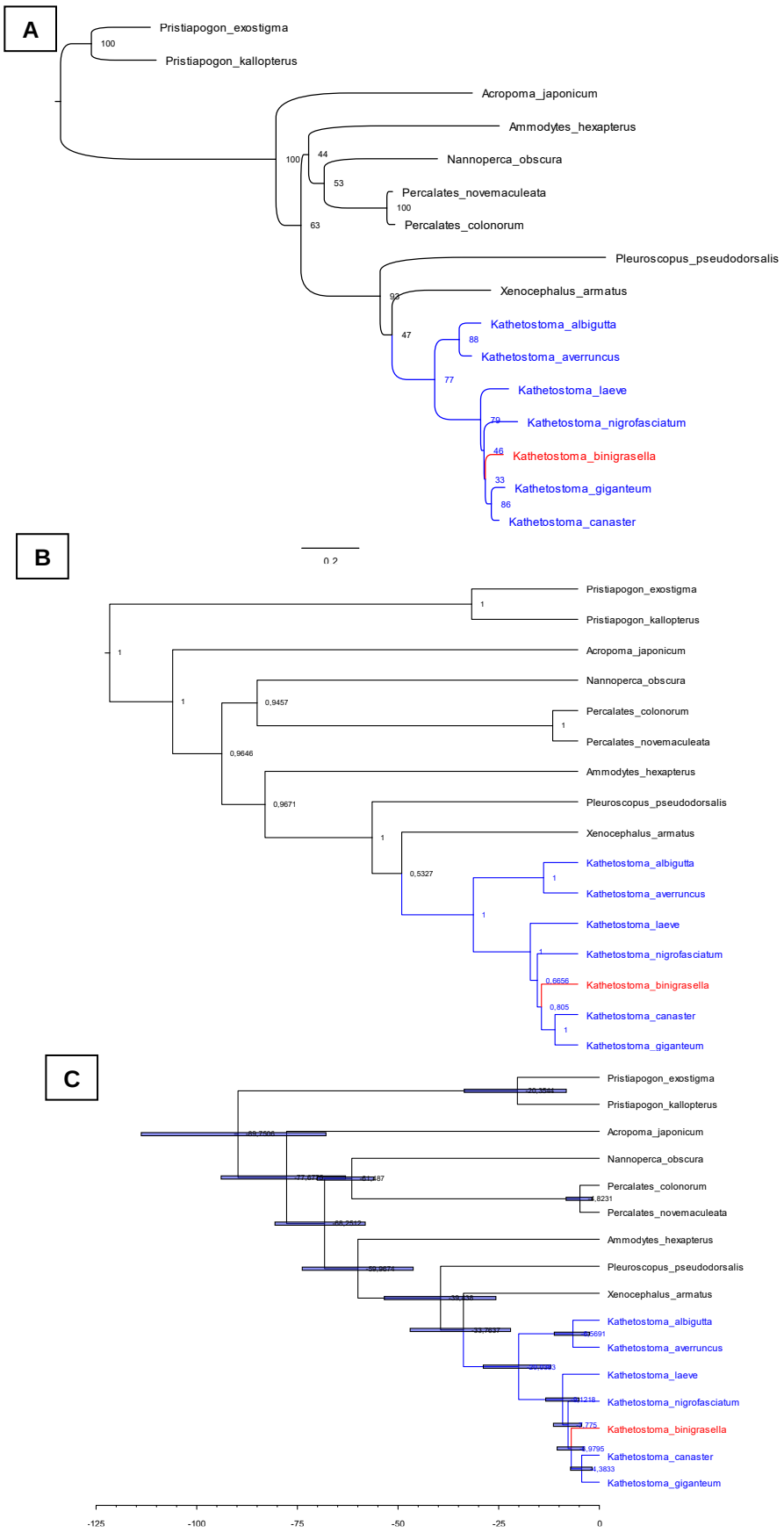

Figure 2.9S. Maximum-Likelihood phylogeny (**A**), Bayesian Inference with posterior probabilities (**B**), and time-calibrated tree (**C**) of the “Kathetostoma” phylogeny. The red branch shows the endemic’s position in the phylogeny and blue branches highlight its congeners within the same genus.

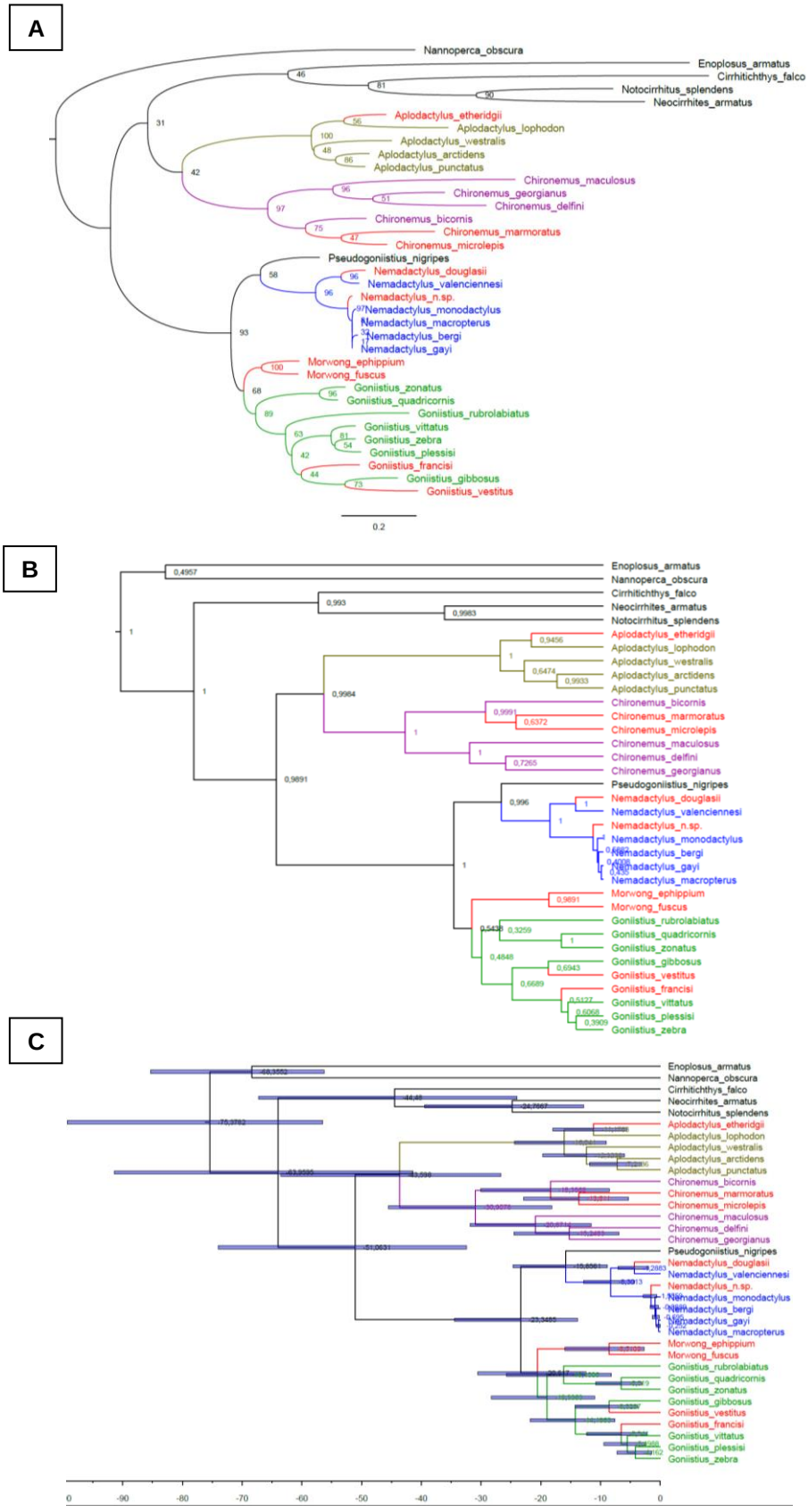

Figure 2.10S. Maximum-Likelihood phylogeny (**A**), Bayesian Inference with posterior probabilities (**B**), and time-calibrated tree (**C**) of the "NEMOGOCHIA" phylogeny. The red branches show the ten endemics' position in the phylogeny. The genus *Morwong* is illustrated as a red clade since its two single members are described as endemic in our study. Blue (*Nemadactylus*), green (*Goniistius*), purple (*Chironemus*), and brown (*Aplodactylus*) branches highlight an endemic's congeners within its genus.

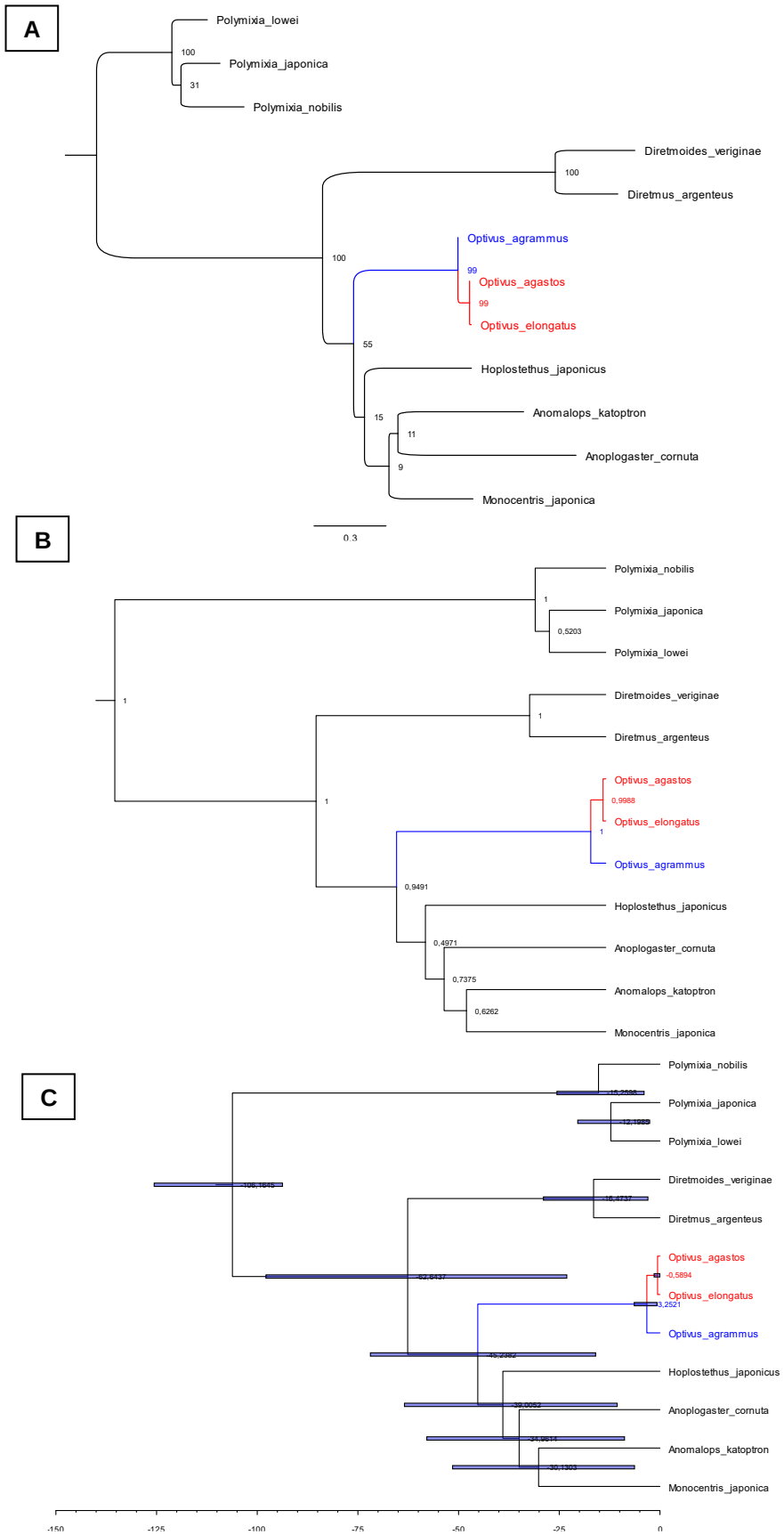

Figure 2.11S. Maximum-Likelihood phylogeny (**A**), Bayesian Inference with posterior probabilities (**B**), and time-calibrated tree (**C**) of the "Optivus" phylogeny. The red branches show the two endemics' position in the phylogeny and the blue branch highlights their congener within the same genus.

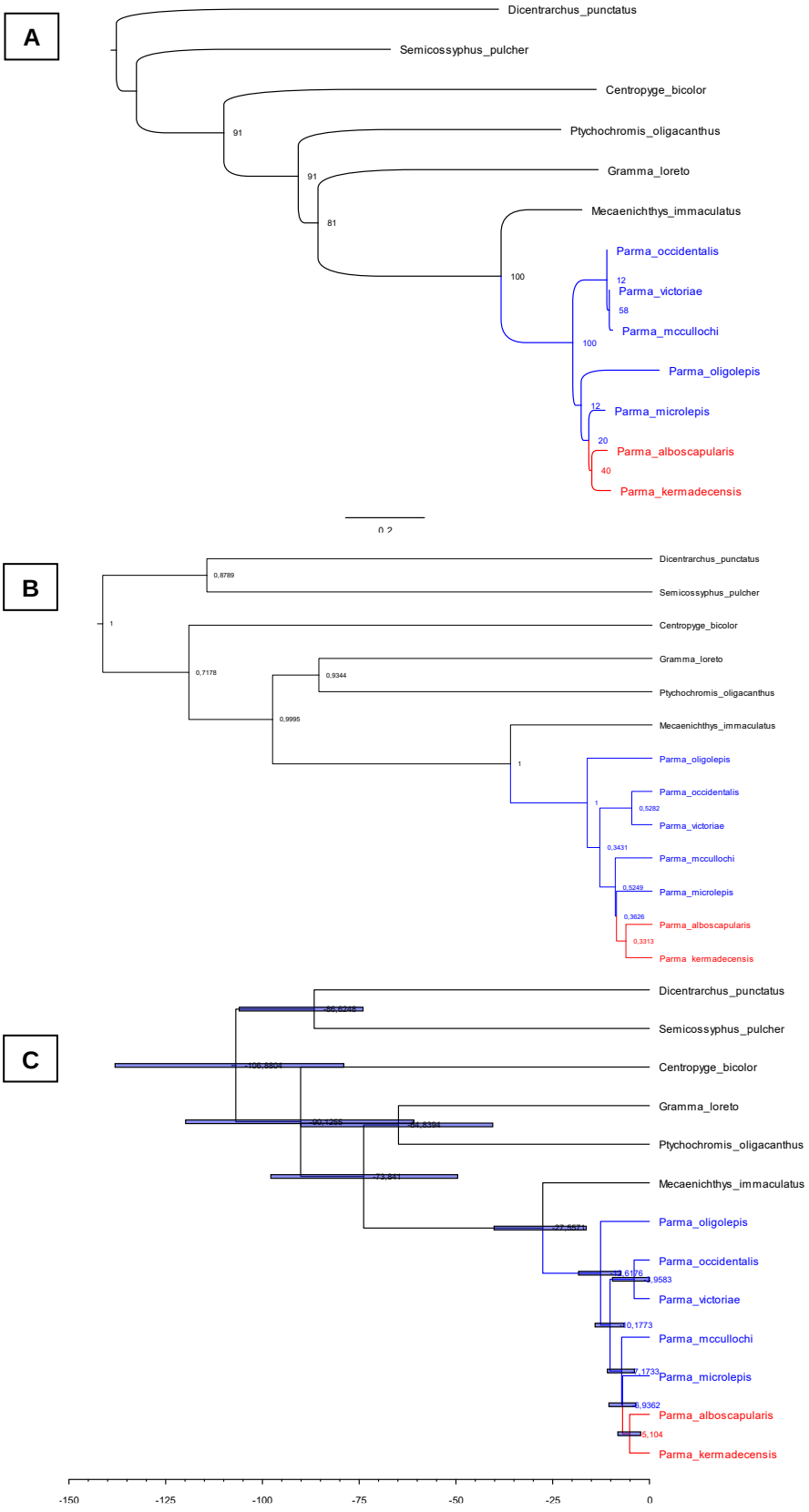

Figure 2.12S. Maximum-Likelihood phylogeny (**A**), Bayesian Inference with posterior probabilities (**B**), and time-calibrated tree (**C**) of the “Parma” phylogeny. The red branches show the position of the two endemics in the phylogeny and blue branches highlight the congeners within the same genus.

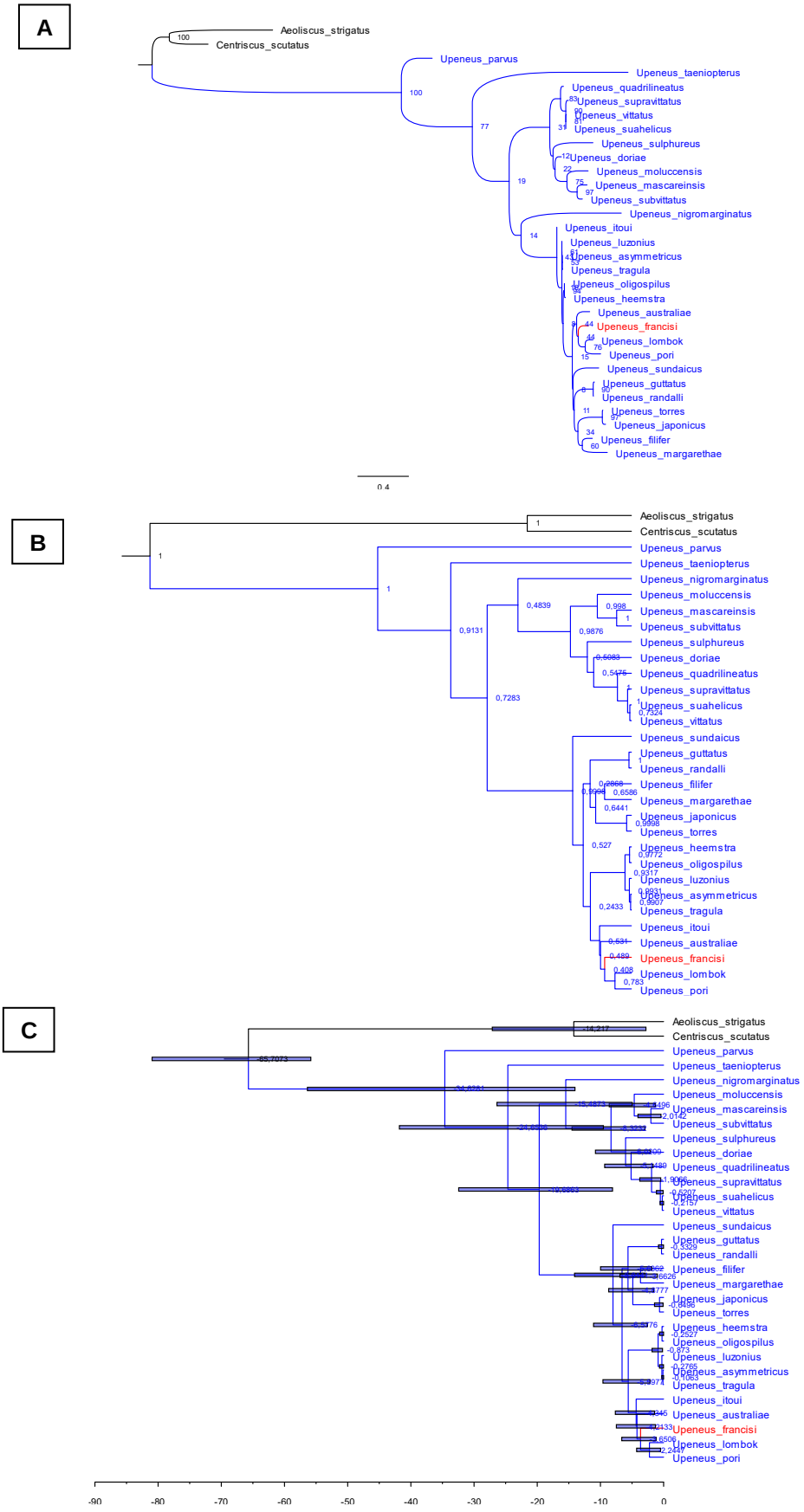

Figure 2.13S. Maximum-Likelihood phylogeny (**A**), Bayesian Inference with posterior probabilities (**B**), and time-calibrated tree (**C**) of the "Upeneus" phylogeny. The red branch shows the endemic's position in the phylogeny and blue branches highlight its congeners within the same genus.

3. The origins of marine fishes endemic to subtropical islands of the Southwest Pacific

MASSEY UNIVERSITY
TE KUNENGA KI PŪREHUROA
UNIVERSITY OF NEW ZEALAND

GRADUATE RESEARCH SCHOOL

STATEMENT OF CONTRIBUTION
DOCTORATE WITH PUBLICATIONS/MANUSCRIPTS

We, the student and the student's main supervisor, certify that all co-authors have consented to their work being included in the thesis and they have accepted the student's contribution as indicated below in the Statement of Originality.

Student name:	André Philippe SAMAYOA
Name and title of main supervisor:	Dr. Libby Liggins
In which chapter is the manuscript/published work?	Chapter 3
What percentage of the manuscript/published work was contributed by the student?	75%

Describe the contribution that the student has made to the manuscript/published work:
Study conception, sampling design, data analysis, results interpretation, original manuscript draft, review and final editing of chapter manuscript, corresponding author.

Please select one of the following three options:

- ○ The manuscript/published work is published or in press
  Please provide the full reference of the research output:
- ◉ The manuscript is currently under review for publication
  Please provide the name of the journal:
  Journal of Biogeography
- ○ It is intended that the manuscript will be published, but it has not yet been submitted to a journal

Student's signature:	André Philippe SAMAYOA Digitally signed by André Philippe SAMAYOA Date: 2022.10.26 15:03:40 +02'00'	Main supervisor's signature:	Libby Liggins Digitally signed by Libby Liggins Date: 2022.10.27 10:35:18 +13'00'

This form should be placed at the beginning of each relevant thesis chapter.

3.1. Abstract

Aim: Lineages colonizing subtropical oceanic islands often have to overcome geographic isolation and novel climate stressors to found new populations. Historical and ecological factors influence the success of colonization and subsequent diversification, leaving a signal in the genetic constitution of the diverged, range-restricted taxa. Here, we examined the historical biogeography of endemic marine fishes to quantify the role of geographic proximity and climate differences in determining colonization, and the underlying mechanisms of speciation.

Location: Subtropical islands of the Southwest Pacific

Taxa: 30 endemic marine ray-finned fishes from 17 genera.

Methods: Using parametric biogeographical history models, we estimated the ancestral geographic ranges for 144 species based on time-calibrated phylogenies that included endemic species and their closest sister taxa, linking terminal nodes with geographic distribution classified into 14 biogeographic areas.

Results: Ancestral range estimations revealed most species originated in Australia (66%), while only 10% and 7% originated in northern tropical Pacific locations and the East Pacific respectively, with 17% of species-range estimations being inconclusive. Vicariant events alone were identified as the most likely process shaping range evolution in 57% of the 14 best-fitting models, dispersal alone was the favored for 14% of species, and both processes had a role for the remaining 29% of species. Across all phylogenies, likelihood-ratio tests confirmed that geographic distance and climate differences constrained dispersal in 73% and 33% of species respectively.

Main conclusions: Marine fishes endemic to subtropical islands of the Southwest Pacific originated by vicariant and jump-dispersal events mainly from ancestral populations in mainland Australia. Geographic distance and climatic differences are significant taxon-specific factors influencing the dispersal of marine fishes in the region.

3.2. Introduction

The relative importance of vicariance and dispersal have been at the center of vigorous debates regarding the major forces governing geographic patterns of marine biodiversity and endemism (Wiens and Donoghue, 2004). While vicariance considers the sole action of geological events as the source of population differentiation and species diversification, the movement of individuals from a source population to new habitats across great distances (jump-dispersal) can also generate strong population and species diversification. In the last two decades, empirical evidence shows that jump-dispersal is a more prevalent process in marine biogeography than considered during the late 20th century (Sanmartín, 2012, Waters, 2008, Waters and Roy, 2004). Jump-dispersal results in limited gene flow between the original and new populations leading to founder-event speciation (Matzke, 2014, Templeton, 2008). Consequently, any factor affecting dispersal is likely altering the probabilities of colonization and eventual diversification of range-restricted biodiversity. Geographic isolation (Dalongeville et al., 2018, Jones et al., 2009) and environmental conditions (Stuart-Smith et al., 2017) can influence dispersal and hence the geographic distribution of marine organisms (Lester et al., 2007). Determining the prevalence of jump-dispersal and factors affecting dispersal probabilities in the sea is essential to better understand marine biogeographic patterns.

An approach that has significantly improved our understanding of processes shaping biogeographic patterns is the combination of geographic information and molecular phylogenies. Parametric methods allow the explicit testing of models that represent distinct biogeographic hypotheses (Lamm and Redelings, 2009) using procedures that: parametrize anagenetic (dispersal, extinction, range switching) and cladogenetic (vicariance, founder event) processes along a time-calibrated tree (Sanmartín, 2012), as well as the effect of geographic and environmental distances (Van Dam and Matzke, 2016); estimate parameters in a maximum-likelihood framework (Ree et al., 2005); and infer ranges at each ancestral node (Ree and Smith, 2008). A number

of studies have used this methodology to reveal the origin of evolutionary lineages in marine fishes: the ancestral Tethys Sea for syngnatharians (Santaquiteria et al., 2021), the Central Pacific for pomacanthids (Baraf et al., 2019), and the Indo-Pacific for the clade Gobiidae-Gobionellidae (Thacker, 2015) and for herbivorous groups in the Atlantic (Siqueira et al., 2019). Further evidence shows that both vicariance and jump-dispersal are relevant in the biogeography of marine fishes (Delrieu-Trottin et al., 2019, Piñeros et al., 2019). However, few of these studies have integrated distance parameters in their range evolution models to explicitly test the effect of geographic distance and climatic differences.

The Indo-Australian Archipelago (IAA) harbors the greatest levels of marine fish biodiversity in the Indo-Pacific (Hoeksema, 2007), whereas peripheral isolated islands have low species richness but high endemism (Allen, 2008, Hughes et al., 2002). Phylogenetic evidence suggests that high species richness in the center of the IAA is the result of multiple independent events (Cowman et al., 2017), in keeping with our understanding that the biogeographic history of this fauna has been long and complex (Miller et al., 2018). However, relatively less is known about the origins of endemism at the periphery of the Indo-Pacific (Bowen et al., 2013). In the Central Pacific, biogeographic analyses suggest a complex scenario where endemic lineages of Hawaii derive from allopatric speciation mainly driven by geologic events that influenced ocean circulation, with endemism generated in two temporal waves (0-3 and 8-12 Ma) from various geographic origins (Hodge et al., 2014). In the Southeast Pacific, seven of nine parametric models for reef fishes endemic to Easter Island (Rapa Nui), point to jump-dispersal as the main driver of endemism, in some cases via stepping-stone colonization routes within the Pacific (Delrieu-Trottin et al., 2019). Nevertheless, Hawaii and Rapa Nui are the most peripheral of the island groups in the Indo-Pacific, and the likely drivers of endemism in other peripheral islands remain unexplored.

The islands of Lord Howe, Norfolk, and Rangitāhua (the Kermadec Islands) lie in subtropical (29°S-31°S) waters of the Southwest Pacific (Francis, 1993), and have been relatively understudied by evolutionary biologists and biogeographers (Liggins et al., 2022). Of volcanic origin, the islands are geologically young with estimated ages of 6.9 Ma for Lord Howe (McDougall et al., 1981), 3.05 Ma for Norfolk (Jones and McDougall, 1973), and 2.58 Ma for Rangitāhua (Brook, 1998). The overall endemism rate for marine fishes across all three island groups is 4.6% (Francis, 1993), with local communities including a mixture of tropical, subtropical, and temperate species (Francis and Duffy, 2015). In the last decade, regional expeditions and collections of specimens have improved our knowledge of the regional fish fauna (Duffy and Ahyong, 2015, Francis, 2019), and the recent reconstruction of multi-locus time-calibrated phylogenies for 34 endemic marine fishes suggests that the origination of these three island groups had a role in generating novel biodiversity in the region (Samayoa et al., 2022).

Here, we examine the historical biogeography of 30 marine fishes endemic to the subtropical islands of the Southwest Pacific using a parametric modeling approach based on previously inferred molecular phylogenies. First, we determine the significance of vicariance and jump-dispersal as biogeographic processes shaping endemism patterns in the region. Given the suggested role of these islands in generating biodiversity (Samayoa et al., 2022), we hypothesized that founder-event speciation models would be favored. Second, we examine the influence of geographic proximity of source locations and their climate on dispersal probabilities. We hypothesized that lineages from geographically close locations of similar climate would be more successful in colonizing the subtropical islands of the Southwest Pacific prior to taxonomic diversification. Third, we use the estimated biogeographic origins and ancestral ranges to infer colonization routes for each endemic species, and then, using a comparative approach, we describe common patterns of origination and range evolution in the region. We hypothesized that marine fish endemism in the relatively young and volcanic

subtropical islands of the Southwest Pacific originated mainly from old continental islands in the region, such as Australia. Our study proposes a biogeographic scenario where multiple independent processes shaped contemporary endemism patterns in marine fishes of the Southwest Pacific, and where dispersal may be constrained by geographic distances and climate zone differences depending on the taxa examined, providing a new understanding of the evolution of marine fishes endemic to the peripheral islands of the Indo-Pacific.

3.3. Materials and methods

3.3.1. Time-calibrated phylogenies

Our analyses were based on the time-calibrated trees and sequence data presented in Samayoa et al. (2022). Taxa were defined as endemic to the Southwest Pacific when they occurred in at least one of the subtropical islands of Lord Howe, Norfolk, and Rangitāhua, without extending beyond Aotearoa New Zealand mainland, New Caledonia, and the East coast of mainland Australia. For biogeographic analysis, we included all phylogenies from Samayoa et al. (2022) except those where taxonomic sampling was low – two monotypic genera and two genera that only included around 50% of known congeners – to reduce biases in our inferences, as missing taxa can result in overestimation of divergence times (Hodge and Bellwood, 2016). We used the 'ape' package (Paradis and Schliep, 2019) for R v.3.6.3 (R Core Team, 2020) using RStudio v.1.2.5033 (RStudio Team, 2019) to prune a clade containing only the sister taxa relevant to our endemic/s, resulting in 14 clades (comprising a single genus, or multiple genera) to analyze 30 endemics across 17 genera (Table 5). For three clades, we included the most proximate sister taxon of the focal genus based on previous phylogenetic studies: *Pseudogoniistius nigripes* for *Nemadactylus* (Ludt et al., 2019); *Graus nigra* for *Girella* (Knudsen et al., 2019); and *Mecaenichthys immaculatus* for *Parma* (McCord et al., 2021). For three other clades, we grouped genera when we had certainty that they were sister to each other and/or that we had all intermediate phylogenetic taxa. For instance,

we grouped *Microcanthus* and *Atypichthys* in the same clade along with *Neatypus obliquus* and *Tilodon sexfasciatus*, which all form a consistent group of taxa within Microcanthidae (Tea and Gill, 2020). Two further clades were formed by the grouping of two genera each, as each pair consistently forms a clade in previous molecular phylogenies, resulting in our clustering of *Chironemus* and *Aplodactylus* (Ludt et al., 2019, Sanciangco et al., 2016) in one clade, and *Goniistius* and *Morwong* (Ludt et al., 2019) in another clade.

Table 5. Name of clades, number of taxa included per clade, and endemic taxa examined in this study. Species in bold are restricted to the subtropical islands (Lord Howe, Norfolk, and/or Rangitāhua). ^*Chromis sensu stricto* as in Tang et al. (2021).

Genus/Genera included	Taxa	Taxa endemic to the Southwest Pacific
Optivus	3	*Optivus agastos, O. elongatus*
Arripis	4	*Arripis trutta, A. xylabion*
Scorpis	4	*Scorpis violacea*
Atypichthys - Microcanthus	6	*Atypichthys latus, Microcanthus joyceae*
Kathetostoma	7	*Kathetostoma binigrasella*
Nemadactylus	8	*Nemadactylus douglasii, N.* n. sp.
Lepidoperca	8	*Lepidoperca inornata*
Parma	8	*Parma alboscapularis,* ***P. kermadecensis***
Hypoplectrodes	9	*Hypoplectrodes* sp. A, ***H.* sp. C**
Chironemus - Aplodactylus	11	*Chironemus marmoratus,* ***C. microlepis, Aplodactylus etheridgii***
Goniistius - Morwong	11	*Goniistius francisi, G. vestitus, Morwong ephippium, M. fuscus*
Girella	17	*Girella cyanea,* ***G. fimbriata***
Chromis	19^	*Chromis abyssicola, C. dispila, C. hypsilepis, C. kennensis, C. nitida*
Upeneus	29	***Upeneus francisi***

3.3.2. Geographic distributions

We defined 14 areas based on marine biogeographic regionalizations suggested by Kulbicki et al. (2013) and Bowen et al. (2016), distinguishing each of the three subtropical islands of the Southwest Pacific and the subtropical and temperate climate zones for mainland Aotearoa New Zealand and Australia (according to Commonwealth of Australia, 2012, and New Zealand Department of Conservation, 2019) (Table 6). To define the area/s that each taxon occupied, we referenced their occurrence data in OBIS

(https://obis.org), Fishes of Australia (http://fishesofaustralia.au.net), the Catalog of Fishes (Fricke et al., 2021), Fishbase (Froese and Pauly, 2021), faunal checklists of the Southwest Pacific (Duffy and Ahyong, 2015, Francis, 2019), and expert consultation. Within clades, taxa were coded as present or absent across areas to generate geographic matrices. Overall, 24 of the 30 endemic species had a continental island (either Australia, or New Zealand, or both) in their geographic range, and only six taxa were found exclusively associated with the subtropical islands (Lord Howe, Norfolk, and/or Rangitāhua, Table 5).

Table 6. The areas (biogeographic regions) defined to accommodate taxa across the 14 clades used for biogeographic analyses in 'BioGeoBEARS'.

Area	Code	Locations included
Australia Temperate	AUST	New South Wales (North boundary: Bermagui), Victoria, Tasmania, South Australia, lower Western Australia
Australia Subtropical	AUSST	South Queensland, New South Wales (South boundary: Bermagui)
Lord Howe	LH	Lord Howe Island
Norfolk	N	Norfolk Island
Rangitāhua	R	Rangitāhua (Kermadec Islands)
New Zealand Subtropical	NZST	North Island limited by East Cape in the East and Cape Egmont in the West
New Zealand Temperate	NZT	Remaining North Island and South Island
West and South-Central Pacific	WCP	West Pacific, South Pacific from New Caledonia to French Polynesia
Northwest Pacific	NWP	Japan, Korea, China
Hawaii	H	Hawaii
Rapa Nui/Pitcairn	RNP	Rapa Nui (Easter Island), Pitcairn
Eastern Pacific	EP	Tropical East and Central Pacific (California, Mexico, Galápagos), Southeast Pacific (Juan Fernández, Desventuradas, Peru, Chile)
Indian	I	Indian Ocean
Atlantic	A	Atlantic Ocean

3.3.3. Biogeographic analysis

Ancestral range estimates were inferred with 'BioGeoBEARS' (Matzke, 2013) in R v.3.6.3 using RStudio v.1.2.5033. The package includes three commonly used models in historical biogeography that differ in their assumptions on cladogenetic processes: the likelihood-based Dispersal-Extinction-Cladogenesis (DEC) model (Ree and Smith, 2008) as implemented in LAGRANGE; the likelihood interpretation of the Dispersal-Vicariance Analysis (DIVA) (Ronquist, 1997), called DIVALIKE; and the likelihood interpretation of

the BAYAREA model (Landis et al., 2013), called BAYAREALIKE. Besides the anagenetic parameters for range expansion ("d") and extinction ("e") estimated by default for all standard models, we tested the three parameters "j" (jump-dispersal weight), "x" (geographic distance), and "n" (distance based on climate zone) during the ancestral range estimations by setting them from fixed (default value of 0, equivalent to standard models) to free parameters. For each clade, we tested the three standard models, and, in each case, seven more complex models based on the combination of tested parameters, for a total of 336 biogeographic models across the 14 clades. All runs used the optimization routine 'optimx' under the 'speedup' option set on FALSE, which avoids shortcuts during the full maximum-likelihood search. We assessed optimization issues for each run, making sure that the most complex models resulted in equal or higher log-likelihood values compared to nested models. When 'optimx' yielded lower log-likelihood, we replaced it with the optimizer 'GenSA', which performs better for models with a high number of parameters. As 'GenSA' did not automatically improve log-likelihood for all four and five parameter-based models during our initial runs, we proceeded with the replacement only when 'optimx' performed poorly.

Our BioGeoBEARS analyses included time constraints to account for geological events likely to have affected dispersal among areas. We considered emergence timings of oceanic islands at 2.5 Ma for Rapa Nui (Clouard and Bonneville, 2005), 2.58 Ma for Rangitāhua (Brook, 1998), 3.05 Ma for Norfolk (Jones and McDougall, 1973), 6 Ma for Juan Fernández (Burridge et al., 2006), and 6.9 Ma for Lord Howe (McDougall et al., 1981), and for the Central American land barrier at 3.1 Ma (Cowman and Bellwood, 2013). For each clade, we partitioned the evolutionary time scale in time slices using the ages of the geological events that influenced the geographic distribution of taxa included in the phylogeny. For clades with taxa found in the East Pacific, we included Juan Fernández as a time constraint only when it was the sole location covered within our East Pacific area. Conversely, when additional locations were covered within the East

Pacific, we did not include Juan Fernández as a time constraint, which was the case for the *Girella* and *Chironemus-Aplodactylus* clades. Across all clades, we applied constraints on dispersal within each time slice using the 'areas_allowed' option which removes the possibility of dispersal (value of 0) to oceanic islands, when these were not yet emerged while moving backward in time, and between areas in the Pacific and the Atlantic separated by the closure of the Panama Isthmus.

For clades with Atlantic representatives, we set a value of 0 among Atlantic and Pacific areas in time slices where the Isthmus of Panama was closed (i.e. younger than 3.1 Ma), whereas the values were set to 1 (areas allowed) for older time slices. We allowed connectivity between Atlantic and specific Pacific areas in younger time slices depending on the geographic distribution of particular taxa. For *Nemadactylus*, taxa are found in cold southern waters of the Atlantic and the Pacific, for which reason we allowed the connection between the Atlantic and temperate Australia to simulate the connectivity of these waters along the West Wind Drift (Waters, 2008). For *Girella*, given that the sole Atlantic member is closely related to congeners found in the Northwest Pacific (Beldade et al., 2021, Samayoa et al., 2022), we allowed connectivity among both areas. For *Upeneus*, the Atlantic and the Pacific were connected through the Indian Ocean where most taxa occur.

3.3.4. Geographic distances and climate zones

The estimation of "x" and "n" required the generation of distance matrices. For "x", we measured great-circle distances among pairs of areas using the 'sf' package (Pebesma, 2018) for R. The shortest geographic distance was measured along oceanic routes between approximate midpoints of areas (i.e. the center of an area or archipelago, the mid-point of a coastline, and/or oceanic islands). For each clade, distances were kept constant across time slices except between areas of the Atlantic and the Pacific which were separated by the Panama Isthmus until 3.1 Ma. For areas of the Atlantic and Pacific separated 3.1 Ma, distances were calculated westwards, whereas for areas separated

by more than 3.1 Ma, measurements were performed eastwards if they were the shortest distances among areas across the open channel. For “n”, we allocated distances on a scale from 1 to 3: a value of 1 was set between areas within the same climate (subtropical, tropical, or temperate); a value of 2 was set for adjacent climates (temperate/subtropical and subtropical/tropical); and a value of 3 was set for non-adjacent climates (tropical/temperate). Distances in both geographic and climate matrices were divided by the highest value to obtain relative distances. When distance parameters are set free, the parameters “d” and “j” are multiplied by distance to a power (e.g., “x” and “n”) (Matzke, 2013, Van Dam and Matzke, 2016): when “x” (or “n”) equals 0, distance has no effect, corresponding to the default setting; when “x” (or “n”) is negative, dispersal rate decreases when distance increases. To test the effect of distances, we therefore set the limits for “x” and “n” between -2.5 (default minimum for “x”) and 0.0.

3.3.5. Best-fitting model selection

Model selection procedures included AIC, its sample size corrected version (AICc), and log-likelihood ratio tests (LRT). The calculation of AICc requires that the sample size of each clade (i.e. the number of included taxa) is over k+1, k being the number of free parameters. Given that the maximum number of free parameters to estimate was five (“d”, “e”, “j”, “x”, “n”) in the more complex models, AICc was calculated for clades with more than six taxa, which was not the case for *Optivus*, *Arripis*, *Atypichthys-Microcanthus*, and *Scorpis*. Finally, we determined the parameters that significantly improved model fit by performing LRTs between nested models and their more complex counterparts, using a threshold of 0.05 for the p-value. For each clade, we performed 57 LRTs, yielding a total of 798 tests across all clades.

3.4. Results

3.4.1. Optimization of parameter estimates

We compared values for log-likelihood across 336 models and performed 798 LRT (Tables S1.1S-28S) to estimate the ancestral range of our 30 endemic species. In 60 of the 798 LRTs, the more complex models yielded lower log-likelihood than their respective nested model. In 38 of the 60 LRTs, the complex models involved four or five free parameters, and replacing 'optimx' with 'GenSA' increased log-likelihood for 17% (17/99) and 63% (21/23) of four- and five-parameter models, respectively (Table S1.29S). In 22 of the 60 LRTs, the average log-likelihood difference was 0.0024 and changing the optimizer did not increase log-likelihood. As more complex models were expected to yield either higher or the same log-likelihood, and given the small difference detected for the 22 tests, we considered in these cases that the more complex models displayed the same log-likelihood value.

Among the parameters estimated across the 336 models, jump-dispersal estimates ("j") reached their maximum value in 23 models using the default BioGeoBEARS settings, an indication of optimization issues. Maximum "j" estimates were mainly reported for BAYAREALIKE (18/23 cases; max=0.9999), followed by DIVALIKE (5/23 cases; max=1.9999), with no reports for DEC models. High "j" values were consistently yielded under different 'BioGeoBEARS' settings: trials with three optimizers; unconstrained analyses; setting the re-scaling option 'rescale_params' on TRUE when free parameters are in different scales; and modifying limits for "d", "e", and "j". Optimization issues were minimized by: rescaling distances; checking log-likelihood differences between complex and nested models; using 'GenSA' when appropriate; and verifying that convergence was achieved after optimization. Since we tried all available optimizers in the package, we believe we have reached the best estimates possible under the current 'BioGeoBEARS' configuration, and given the available data for our focal genera. Estimates appeared unrelated to sample size since our largest clade

(*Upeneus*, 29 taxa) showed low "j" values similar to one of the smallest clades (*Parma*, 8 taxa).

For *Optivus*, values over 1 for range expansion ("d") were recovered in three of the eight BAYAREALIKE models, and for extinction ("e"), values over 1 were recovered in seven of the eight BAYAREALIKE models (Table S1.1S). Since values of e <1 indicate less than one anagenetic event (either range expansion or extinction) per million years (Matzke, 2013), the high values in *Optivus* suggest more frequent anagenetic events for this clade. However, this clade also exhibited the lowest taxonomic coverage in our dataset (Table 5), requiring caution in interpreting estimates for anagenetic processes.

3.4.2. Ancestral range estimations

Inferred biogeographic origins and colonization routes for endemic taxa revealed that most originated in Australia (Fig. 3; Fig. 3.1S-28S). Thirteen endemic lineages originated from Temperate Australia (*Optivus agastos*, *O. elongatus*, *Arripis trutta*, *A. xylabion*, *Scorpis violacea*, *Atypichthys latus*, *Kathetostoma binigrasella*, *Lepidoperca inornata*, *Parma alboscapularis*, *P. kermadecensis*, *Hypoplectrodes* sp. C, *Chironemus marmoratus*, and *Goniistius vestitus*), while seven originated from Subtropical Australia (*Microcanthus joyceae*, *Nemadactylus douglasii*, *Hypoplectrodes* sp. A, *Aplodactylus etheridgii*, *Morwong ephippium*, *M. fuscus*, and *Chromis kennensis*). Our analyses also showed that two endemic lineages originated from the East Pacific (*Girella cyanea* and *G. fimbriata*), two in the West and Central Pacific (*Chromis nitida* and *Upeneus francisi*), and one in Hawaii (*Goniistius francisi*). Five lineages had unresolved origins (*Nemadactylus* n.sp., *Chironemus microlepis*, *Chromis abyssicola*, *C. dispila*, and *C. hypsilepis*). Furthermore, endemic species restricted to the subtropical islands (Table 5) did not appear to have a common origin.

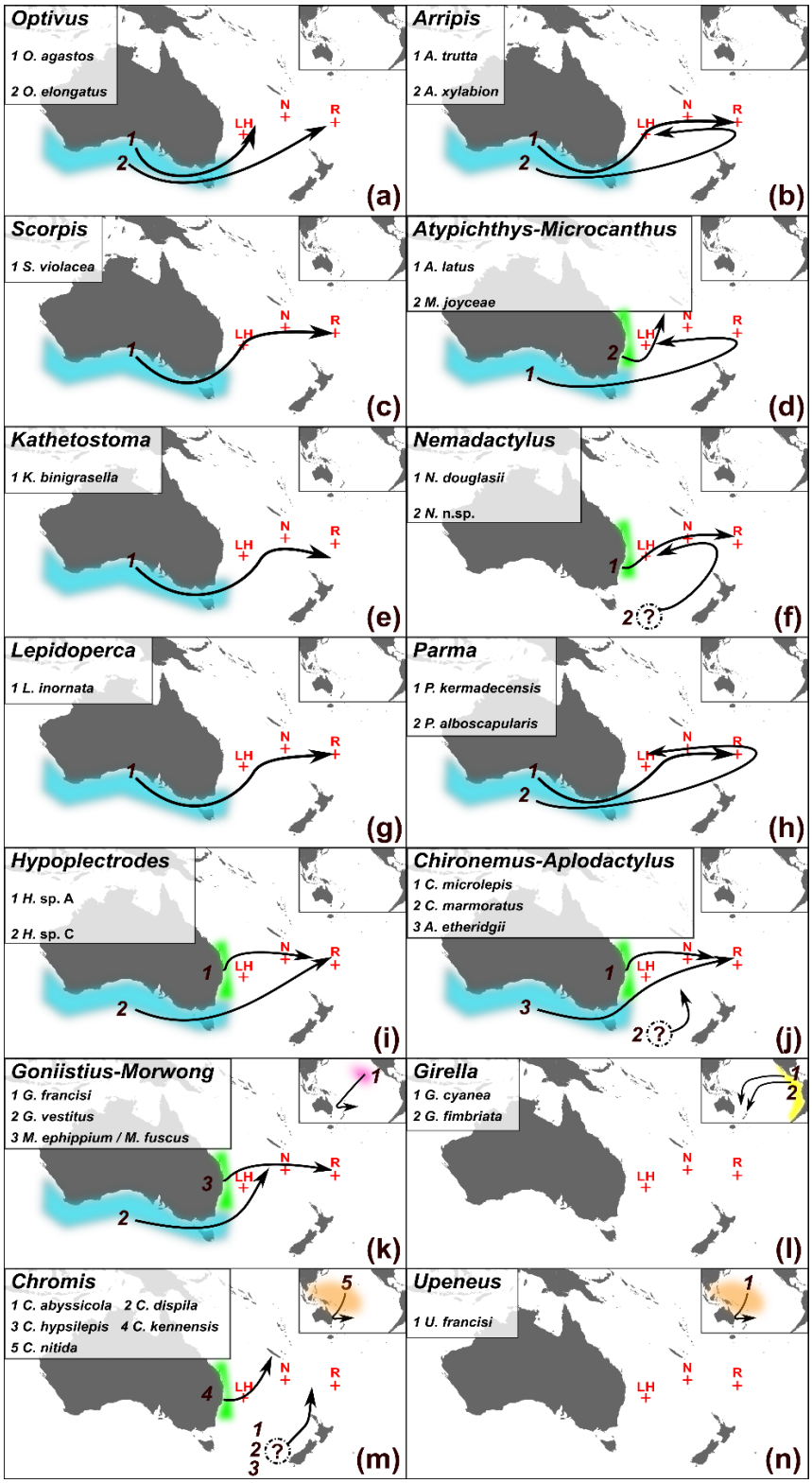

Fig. 3. Presumed biogeographic origin and colonization pathways for 30 marine fishes endemic to the subtropical Southwest Pacific islands based on the best-fitting models in 'BioGeoBEARS' (Mollweide projection). Colors indicate biogeographic regions included in the analysis: blue is Temperate Australia, green is Subtropical Australia, pink is Hawaii, yellow is East Pacific, and orange is West/Central Pacific. Circles with a question mark indicate an unresolved origin. Red crosses indicate the position of the Southwest Pacific islands of Lord Howe (LH), Norfolk (N), and Rangitāhua (R). (a) *Optivus*; (b) *Arripis*; (c) *Scorpis*; (d) *Atypichthys-Microcanthus*); (e) *Kathetostoma*; (f) *Nemadactylus*; (g) *Lepidoperca*; (h) *Parma*; (i) *Hypoplectrodes*; (j) *Chironemus-Aplodactylus*; (k) *Goniistius-Morwong*); (l) *Girella*; (m) *Chromis*; (n) *Upeneus*.

DEC was the most common biogeographic model supported by our data (7/14), with the geographic distance parameter ("x") significantly improving the model in six cases, the climate parameter ("n") in three cases, and jump-dispersal ("j") in two cases (Table 7; Tables S1.1S-27S). DIVALIKE was the second-best standard model supported by our data (5/14), with geographic distance ("x") and jump-dispersal ("j") significantly improving the model in two cases each, with no significant improvement by any parameter in two cases. BAYAREALIKE was the best-supported model in 2-of-14 clades, always in combination with jump-dispersal ("j"), with geographic distance ("x") and climate ("n") significantly improving one model each.

Table 7. Best-fitting biogeographic model per clade, contrasted with the number of taxa sampled and the model selection method. Models based on Matzke (2013): DEC, Dispersal-Extinction-Cladogenesis model; DIVALIKE, likelihood implementation of the Dispersal-Variance Analysis model; BAYAREALIKE, likelihood implementation of the BAYAREALIKE model; +j, model with significant jump-dispersal parameter "j"; +x, model with significant geographic distance parameter "x"; +n, model with significant environmental distance parameter "n", based on climate zone.

Name of Clade	Number of taxa	Best-fitting model
Optivus	3	DEC+x
Arripis	4	DEC+x+n
Scorpis	4	DEC+x
Atypichthys - Microcanthus	6	DEC+x
Kathetostoma	7	DIVALIKE+x
Nemadactylus	8	DEC+n
Lepidoperca	8	DIVALIKE
Parma	8	DIVALIKE
Hypoplectrodes	9	DIVALIKE+j
Chironemus - Aplodactylus	11	BAYAREALIKE+j+x
Goniistius - Morwong	11	DIVALIKE+j+x
Girella	17	DEC+j+x
Chromis	19	DEC+j+x+n
Upeneus	29	BAYAREALIKE+j+n

Overall, jump-dispersal was included in 6-of-14 best-fitting models (Table 7). Ancestral range estimates show that 8-of-30 endemic species emerged through jump-dispersal (Fig. 3.1S-28S): *Aplodactylus etheridgii*, *Chironemus microlepis*, *Chromis nitida*, *Girella cyanea*, *G. fimbriata*, *Goniistius francisi*, *Hypoplectrodes* sp. C, and *Upeneus francisi*. When contrasting this result with the divergence timing of the endemic lineages, we found that both old and young endemics have emerged from founder-event speciation (Fig. 4), unrelating this mode of speciation with the time of divergence. Of the eight endemic taxa that likely diverged from a founder-event, five are restricted to the subtropical islands (Fig. 4).

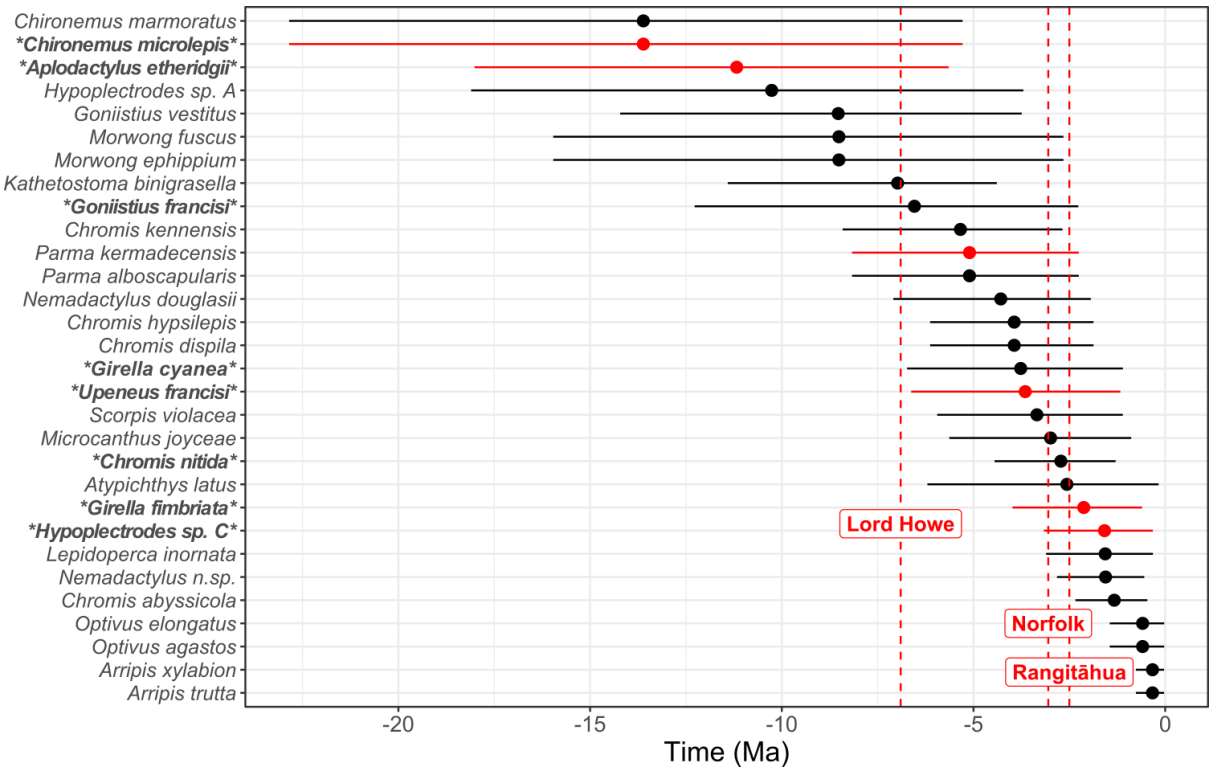

Fig. 4. Divergence time estimates in million years (Ma) for 30 marine fish taxa endemic to the Southwest Pacific, based on Samayoa et al. (2022). Mean divergence age (dots) and 95% posterior distribution (horizontal bars) are represented. Red bars indicate endemic taxa restricted to the subtropical islands of Lord Howe, Norfolk, and/or Rangitāhua, and vertical dotted lines show the estimated age of the islands: Lord Howe (6.9 Ma); Norfolk (3.05 Ma); and Rangitāhua (2.58 Ma). Asterisk-framed taxa in bold indicate endemics with strong support for jump-dispersal speciation according to best-fitting biogeographic models.

3.5. Discussion

Our analyses of the historical biogeography of marine fishes endemic to subtropical islands of the Southwest Pacific highlight vicariance and jump-dispersal as significant actors shaping endemism in the region, with geographic distance and climatic zones significantly limiting dispersal in particular marine fish groups. We present hypotheses on the origin of endemic lineages and subsequent colonization routes, where eastward colonization from mainland Australia is the dominant pattern, followed by rare southward pathways from tropical areas, and westward routes from the East Pacific. Finally, by acknowledging caveats in our analysis, we highlight our study's contributions to understanding the historical biogeography of marine fish endemism in the Southwest Pacific.

3.5.1. Biogeographic processes: vicariance and jump-dispersal

Our results indicate that vicariance is a prevalent driver of allopatric speciation in the Southwest Pacific. DEC was selected for most clades (seven, Table 7), implying that range evolution in these cases has been driven by cladogenetic processes (i.e. peripatry and within-area vicariance) where bifurcating lineages are distributed in one area only (Ree and Smith, 2008), although careful interpretation is required for four clades due to their small sample sizes (*Optivus*, *Arripis*, *Scorpis*, and *Atypichthys-Microcanthus*). Interestingly, for *Microcanthus*, a previous assessment of the historical biogeography of Microcanthidae retrieved DIVALIKE as the best-fitting model (Tea et al., 2019). Despite fewer sister taxa sampled in the previous investigation, both results show vicariance as a significant driver of range evolution in microcanthids. Models based on DIVALIKE were selected for five additional clades (Table 7), indicating in these cases that classic vicariance has been significant in their range evolution (Ronquist and Sanmartín, 2011). These results indicate that the formation of isolated volcanic islands by intense geological activity in the region (Francis, 1993) has likely facilitated the speciation of more range-restricted lineages over time. However, for the two BAYAREALIKE-based

models (Table 7), the simulations did not include cladogenetic processes (i.e. peripatry and vicariance), implying that vicariance is not the only determinant of range evolution in fishes of the Southwest Pacific (*Chironemus-Aplodactylus* and *Upeneus*).

Marine island biogeography theory predicts that recently emerged oceanic islands are colonized by organisms with high dispersal capacities, followed by an increase in speciation and endemism richness (Dawson, 2016). In our analyses, six of the best-fitting biogeographic models included jump-dispersal (Table 7), highlighting its relevance as a cladogenetic process in the emergence of endemic species restricted to these subtropical, oceanic islands (5/8), while its role seems to have been minor for endemic species present in both continental and oceanic islands (3/24). For two clades (*Chironemus-Aplodactylus* and *Upeneus*), range evolution was best explained by BAYAREALIKE+j-based models, indicating that jump-dispersal is the likely cladogenetic process driving range evolution in these groups. A similar result was detected in surgeonfishes and parrotfishes (Siqueira et al., 2019), kyphosids (Knudsen et al., 2019), and in two taxa endemic to Rapa Nui (*Myripristis tiki* and *Chrysiptera rapanui* in Delrieu-Trottin et al., 2019). For four clades (*Hypoplectrodes*, *Goniistius-Morwong*, *Girella*, and *Chromis*), best-fitting models were based on DEC/DIVALIKE plus “j”, indicating that vicariance and jump-dispersal both drive range evolution in these cases. For *Chromis*, we found that DEC+j+x+n best fitted our data, indicating that jump-dispersal, geographic distance, and climatic differences are important, and in accordance with Delrieu-Trottin et al. (2019) who found DEC+j as the best model for *Chromis* taxa, even though taxonomic sampling differed and only the “j” parameter was tested in their case. In our study, the best-fitting models for *Hypoplectrodes* and *Goniistius-Morwong* were DIVALIKE+j and DIVALIKE+j+x respectively. Similarly, DIVALIKE+j was recovered as the best model for *Goniistius plessisi* and four other endemics to Rapa Nui (Delrieu-Trottin et al., 2019), and for *Apogon* taxa in the Tropical Eastern Pacific (Piñeros et al., 2019), suggesting overall that the spatial patterns in these marine fish groups were

driven by a combination of vicariant events and long-distance colonizations. In seven clades (Table 7), vicariance is found to be significant while jump-dispersal is not, a similar evolutionary scenario inferred for rabbitfishes (Siqueira et al., 2019).

Overall, biogeographic results demonstrate that jump-dispersal is significant in most but not all of our models, and instead show that vicariance and jump-dispersal act with different weights depending on taxonomic and spatio-temporal scales (Sanmartín, 2012), a conclusion that has been reported in marine crustaceans (Liu et al., 2018) and mollusks (Cunha et al., 2019), as well as in freshwater stingrays (Fontenelle et al., 2021).

3.5.2. Effect of geographic distance and climate zone differences on dispersal

Geographic distance is known to limit dispersal in the sea (Cowen and Sponaugle, 2009), and in our study geographic distance significantly influenced patterns of endemism driven by dispersal in 64% of the 14 clades examined (Table 7), which encompasses more than two-thirds of the endemics studied here (22/30, Table 5). These taxa vary considerably in their ecology, evolutionary history, and biology, including various: diet types, such as herbivory (e.g., *Girella fimbriata*), omnivory (e.g., *Girella cyanea*), and zooplanktivory (e.g., *Scorpis violacea*) (Knudsen et al., 2019); patterns of lineage origination (Fig. 3); and divergence timings (Fig. 4). Scarce data is available regarding the early life history of five endemics (*Chromis abyssicola*, *C. dispila*, *C. hypsilepis*, *C. kennensis*, *C. nitida*, and *Girella fimbriata*) in Fishbase (Froese and Pauly, 2021). However, the four *Chromis* taxa lay demersal eggs, supporting other studies that suggest that the dispersal of taxa with benthic eggs is more affected by geographic distance than in those with pelagic eggs (Riginos et al., 2011). Interestingly, in four clades (*Chironemus-Aplodactylus*, *Goniistius-Morwong*, *Girella*, and *Chromis*), range evolution is driven by both geographic distance constraints and jump-dispersal events. This result suggests long-distance dispersal events can occur even in marine fishes where colonization mainly occurs among geographically proximal locations (Benestan et al., 2021).

We hypothesized that lineages from climatically similar locations would be more successful in colonizing the subtropical islands of the Southwest Pacific, and would then speciate to become endemic species. We found that climatic zone differences significantly affected dispersal in four clades (Table 7). These groups comprise endemic lineages that display relatively recent diversification timings (5.34 Ma for *Chromis kennensis* to 0.33 Ma for *Arripis trutta*/*A. xylabion*; Fig. 4), and include the temperate taxa within *Arripis* and *Nemadactylus* and the only two cases of tropical origination among our dataset (*Chromis* and *Upeneus*; Fig. 3 *m*-*n*). Our results suggest that climate has been a relevant factor in marine fish speciation within the last 5 Ma, a period characterized by rapid glacial/interglacial periods with latitudinal shifts in subtropical and temperate oceanic boundaries in the Southwest Pacific (McClymont et al., 2016, Nelson and Cooke, 2001). This geological setting is known to have influenced the biogeography of *Arripis* taxa which are highly sensitive to climate changes (Moore and Chaplin, 2014), and the longitudinal distribution of *Nemadactylus* members across Australia (Burridge, 2000a). For endemic species within *Chromis* and *Upeneus*, biogeographic patterns could be partially explained by poleward shifts of subtropical marine boundaries in the Southwest Pacific during interglacial periods (McClymont et al., 2016), facilitating rare colonization of higher latitude islands from taxonomic groups mainly inhabiting tropical waters.

3.5.3. Origin and colonization routes of the Southwest Pacific islands

Similar to other taxa (Goldberg et al., 2008), our historical biogeographic scenarios (Fig. 3) revealed mainland Australia as the inferred origin for 66% (20/30) of endemic lineages, representing the major source of marine fish endemism in the Southwest Pacific. Of the 20 lineages, 13 originate in Temperate Australia and 7 in Subtropical Australia. These results support the qualitative inferences from Samayoa et al. (2022) where 53% of Southwest Pacific endemics were most closely related to Australian fauna. Our data also show that colonization routes departing from Temperate Australia involve an

intermediate subtropical range, and that all routes leaving Australia follow an eastward pathway likely facilitated by the predominant eastward oceanic circulation of the region (Trnski and de Lange, 2015). Lineages originating in Australia involve diversification timings between 13.61 Ma (*Chironemus microlepis*) and 0.33 Ma (*Arripis trutta*/*A. xylabion*), implying multiple independent colonization events over a long temporal scale.

Low-latitude, tropical regions are generally more biodiverse than high-latitude regions, and tend to export marine fish biodiversity to subtropical and temperate regions (Bowen et al., 2013). Our results suggest that three of the endemic lineages of the Southwest Pacific likely originated in tropical areas (Fig. 3). For *Chromis nitida*, results point to an origin in the West/Central Pacific, with an intermediate range in Subtropical Australia, and eventual expansion to Lord Howe (Fig. 3.25S). For *Goniistius francisi*, ancestral range estimation (Fig. 3.21S) shows an origin in Hawaii, the migration to New Caledonia 6.54 Ma, and the eventual colonization of the Southwest Pacific islands. For *Upeneus francisi*, our data highlight its origin in the West/Central Pacific, a migration to Lord Howe 3.65 Ma, and an expansion to Norfolk and Rangitāhua (Fig. 3.27S). In all three cases, jump-dispersal is a significant driver of range evolution (Table 7). Colonization from warmer tropical regions is similarly implicated over recent timescales in Rangitāhua (Liggins et al., 2020), and temperate New Zealand (Middleton et al., 2021, Middleton et al., in review), and has been described in Eastern and Western Australia (Stuart-Smith et al., 2018, Wernberg et al., 2016). These immigration and colonization events are becoming more frequent as the subtropical and even temperate regions warm over contemporary timescales due to climate change (Hastings et al., 2020).

Molecular evidence has also highlighted the connection between marine fish fauna on both sides of the Pacific (Burridge et al., 2006, Delrieu-Trottin et al., 2018, Liggins et al., 2022), a pattern revealed by our study in two recently diversified lineages within *Girella*, where colonization is inferred to originate in the East Pacific (Fig. 3; Fig. 3.23S), and driven by vicariant and jump-dispersal events (Table 7). For five lineages,

we were unable to determine their origin and colonization pathways. In two cases, the ancestral ranges before divergence are considerably wide: for *Nemadactylus* n. sp., the ancestral range includes Australia, New Zealand, and the Atlantic (Fig. 3.11S); and for *Chironemus microlepis*, the ancestor is estimated to have occurred in Australia mainland and Subtropical New Zealand, a range from which it would have colonized Lord Howe (Fig. 3.19S). The other three lineages belong to *Chromis*, and all display unresolved origins at the most proximate ancestral nodes (Fig. 3.26S).

Oceanic islands are key actors in actinopterygian evolution in the Indo-Pacific (Bowen et al., 2013), and in our study, Lord Howe, Norfolk, and Rangitāhua are included in ancestral range estimations after their emergence (dashed lines in Fig. 3.1S-28S), highlighting their role in range evolution for endemic lineages (Samayoa et al., 2022). Lord Howe appears as the first stepping-stone in the northern pathway of *Optivus agastos* (Fig. 3*a*; Fig. 3.1S), and the eastward routes of *Scorpis violacea* (Fig. 3*c*; Fig. 3.5S), and *Upeneus francisi* (Fig. 3*n*; Fig. 3.27S). Its oldest emergence and closest proximity to Australia among the three island groups (Francis, 1993) might have facilitated its leading role in shaping endemism patterns in the region. Our analyses also highlight the role of Subtropical New Zealand as an intermediate stepping-stone for seven endemic lineages: in three cases (*Optivus elongatus*, *Kathetostoma binigrasella*, and *Lepidoperca inornata*), the area appears as a stepping-stone before colonization of Rangitāhua in the north; however, in four cases (*Atypichthys latus*, *Arripis xylabion*, *Nemadactylus* n.sp., and *Parma alboscapularis*), analyses indicate a westward pathway from New Zealand mainland towards Lord Howe, a rare route inferred for plants (Birch and Keeley, 2013) and freshwater gastropods (Zielske et al., 2017). A westward route seems counter-intuitive for the region's marine fishes as it implies active dispersal against the predominant eastward oceanic currents, but it might also enlighten the evolutionary descendance of *Chrysiptera notialis* (Southwest Pacific) from *C. galba* (Central Pacific) (Liggins et al., 2022).

3.6. Conclusions

In our study, we investigated the historical biogeography of 30 marine fish taxa endemic to subtropical islands of the Southwest Pacific, characterized by a dominant eastward colonization from mainland Australia and rare routes from northern tropical and eastern Pacific areas, involving independent colonization events across a wide temporal scale. Vicariance and jump-dispersal were not mutually exclusive processes in the evolution of endemism in the region, and both geographic distance and climate zone differences were relevant but not dominant factors determining dispersal. Our inferences are limited by small sample sizes in four clades, and by the necessity of grouping small marine areas into larger regions (e.g., clumping small islands into “East Pacific” obscuring the exact origination of endemic *Girella* lineages) to ensure that our analyses were computationally feasible. Consequently, processes operating at smaller spatial scales may be overlooked. Integrating inter-disciplinary evidence from biological and oceanographic sources to better understand dispersal processes (Cowen and Sponaugle, 2009) could potentially clarify the modes of speciation and dispersal routes unveiled by our analyses. Finally, our study reveals how biogeographic processes and factors affecting dispersal at sea act at distinct taxonomic and spatio-temporal scales, requiring the need to define a spatio-temporal framework in future studies aiming at understanding the origin and evolution of endemism in marine fishes.

3.7. Authors’ contributions

APS and **LL** conceived the study; **APS**, **EDT**, and **LL** designed sampling; **APS** and **JDA** analyzed the data; **APS** wrote the original draft; **APS**, **EDT**, **JDA**, and **LL** reviewed and edited the manuscript; **LL** supervised the investigation and provided funding.

3.8. Acknowledgments

We thank Nicholas J. Matzke for providing constructive insights on BioGeoBEARS, as well as Adam N. H. Smith (Massey University) and José I. Carvajal for the early feedback on this study. This research was a continuation of the collaboration between Massey

University and Te Papa Tongarewa founded by Marti J. Anderson and Clive D. Roberts and funded by a Royal Society of New Zealand Te Apārangi Marsden Grant (15-MAU-132). We wish to thank and acknowledge mana whenua (the traditional owners) of Rangitāhua, the Māori iwi of Ngāti Kuri for their support, and the New Zealand Department of Conservation for sampling permission (Authorisation number: 47976 MAR). Expeditions to Rangitāhua were made possible by the crew of the RV Braveheart, Stoney Creek Shipping Company. These expeditions were supported by Natural History New Zealand and the New Zealand on Air Platinum Fund, the Auckland Museum Institute, Auckland Museum, C&L Gregory Trust, the Pew Charitable Trusts, the School of Natural Sciences Massey University, and the National Institute of Water and Atmospheric Research Ltd Core Funded Coasts & Oceans Programme 2: Biological Resources subcontract for fundamental knowledge of marine fish biodiversity with the Museum of New Zealand Te Papa Tongarewa, Museum of New Zealand Te Papa Tongarewa Collection Development fund: AP's 4788 and 4862. Ongoing biodiversity research of Rangitāhua is supported by a New Zealand Ministry of Business, Innovation, and Employment Endeavour Research Fund ''Te Mana o Rangitāhua'' (69495-ENDRP-AWMMU2001). André P. Samayoa is supported by a Massey University Doctoral Scholarship. Libby Liggins is supported by a Rutherford Discovery Fellowship (RDF-20-MAU-001).

3.9. Supplementary material

The BioGeoBEARS files used in this study can be found online at https://doi.org/10.17632/dydncy77b5.2.

Table 3.1S. Parameter estimates, log-likelihood values (LnL), and model selection score for each of the 24 models assessed for the clade *Optivus* (sample size=3). The model selection score selected was AIC as the sample size of the genus was too small to calculate AICc scores for models with two or more free parameters. Bold italicized row indicates the best-fitting model based on AIC and LRT results.

Biogeographic model	Free parameters	*d*	*e*	*j*	*x*	*n*	LnL	AIC
DEC	2	0.1242	1.00E-12	0	0	0	-11.39	26.79
DEC+J	3	0.1013	1.00E-12	2.1230	0	0	-10.27	26.55
DEC+X	***3***	***0.0187***	***1.00E-12***	***0***	***-2.5***	***0***	***-6.39***	***18.78***
DEC+N	3	0.0896	1.00E-12	0	0	-0.5872	-11.34	28.68
DEC+J+X	4	0.0176	1.00E-12	0.0757	-2.5	0	-6.36	20.71
DEC+J+N	4	0.1013	1.00E-12	2.1165	0	0.0000	-10.27	28.55
DEC+X+N	4	0.0187	1.00E-12	0	-2.5	-0.0001	-6.39	20.78
DEC+J+X+N	5	0.0187	1.00E-12	0.0856	-2.5	0.0987	-6.36	22.71
DIVALIKE	2	0.1284	2.00E-09	0	0	0	-10.49	24.99
DIVALIKE+J	3	0.1088	1.00E-12	1.0609	0	0	-10.33	26.66
DIVALIKE+X	3	0.0197	2.57E-08	0	-2.5	0	-6.83	19.66
DIVALIKE+N	3	0.1029	2.57E-08	0	0	-0.4040	-10.47	26.94
DIVALIKE+J+X	4	0.0197	1.00E-12	1.00E-05	-2.5	0	-6.83	21.66
DIVALIKE+J+N	4	0.1088	2.57E-08	1.0654	0	0.0000	-10.33	28.66
DIVALIKE+X+N	4	0.0197	1.00E-12	0	-2.5	0.0000	-6.83	21.66
DIVALIKE+J+X+N	5	0.0197	1.00E-12	1.00E-05	-2.5	0.0000	-6.83	23.66
BAYAREALIKE	2	1.0530	1.7261	0	0	0	-10.85	25.70
BAYAREALIKE+J	3	1.0353	1.7049	1.00E-05	0	0	-10.85	27.70
BAYAREALIKE+X	3	0.3293	1.9443	0	-1.2814	0	-10.22	26.45
BAYAREALIKE+N	3	1.0538	1.7278	0	0	0.0000	-10.85	27.70
BAYAREALIKE+J+X	4	0.3242	1.9254	1.00E-05	-1.2844	0	-10.22	28.45
BAYAREALIKE+J+N	4	0.1142	0.0501	0.9999	0	0.0000	-10.77	29.55
BAYAREALIKE+X+N	4	0.3256	1.9330	0	-1.2848	0.0000	-10.22	28.45
BAYAREALIKE+J+X+N	5	0.3251	1.9252	1.00E-05	-1.28197	0.0000	-10.22	30.45

Table 3.2S. Likelihood-Ratio test results for the clade *Optivus*. P-values with an asterisk indicate rejection of null hypothesis (no significative improvement when adding parameters) at p<0.05.

Nested model	More complex model	LnL Null	LnL Alt	DF Null	DF Alt	DF	D Statistic	p-value
DEC	DEC+J	-11.3927	-10.273	2	3	1	2.23936	0.134537
DEC	DEC+X	-11.3927	-6.39046	2	3	1	10.0044	0.001562 *
DEC	DEC+N	-11.3927	-11.3396	2	3	1	0.10612	0.744605
DEC	DEC+J+X	-11.3927	-6.35687	2	4	2	10.07158	0.006501 *
DEC	DEC+J+N	-11.3927	-10.273	2	4	2	2.23934	0.326387
DEC	DEC+X+N	-11.3927	-6.39045	2	4	2	10.00441	0.006723 *
DEC	DEC+J+X+N	-11.3927	-6.35686	2	5	3	10.07159	0.017967 *
DEC+J	DEC+J+X	-10.273	-6.35687	3	4	1	7.832216	0.005132 *
DEC+J	DEC+J+N	-10.273	-10.273	3	4	1	0	1
DEC+J	DEC+J+X+N	-10.273	-6.35686	3	5	2	7.832234	0.019918 *
DEC+X	DEC+J+X	-6.39046	-6.35687	3	4	1	0.067174	0.795497
DEC+X	DEC+X+N	-6.39046	-6.39045	3	4	1	1E-05	0.997477
DEC+X	DEC+J+X+N	-6.39046	-6.35686	3	5	2	0.067192	0.966962
DEC+N	DEC+J+N	-11.3396	-10.273	3	4	1	2.13322	0.144138
DEC+N	DEC+X+N	-11.3396	-6.39045	3	4	1	9.898292	0.001654 *
DEC+N	DEC+J+X+N	-11.3396	-6.35686	3	5	2	9.965474	0.006855 *
DEC+J+X	DEC+J+X+N	-6.35687	-6.35686	4	5	1	1.8E-05	0.996615
DEC+J+N	DEC+J+X+N	-10.273	-6.35686	4	5	1	7.832254	0.005132 *
DEC+X+N	DEC+J+X+N	-6.39045	-6.35686	4	5	1	0.067182	0.795485
DIVALIKE	DIVALIKE+J	-10.4949	-10.3281	2	3	1	0.33364	0.563524
DIVALIKE	DIVALIKE+X	-10.4949	-6.8318	2	3	1	7.326206	0.006796 *
DIVALIKE	DIVALIKE+N	-10.4949	-10.4704	2	3	1	0.04906	0.824707
DIVALIKE	DIVALIKE+J+X	-10.4949	-6.83203	2	4	2	7.325748	0.025659 *
DIVALIKE	DIVALIKE+J+N	-10.4949	-10.3281	2	4	2	0.33366	0.846343
DIVALIKE	DIVALIKE+X+N	-10.4949	-6.8318	2	4	2	7.326206	0.025653 *
DIVALIKE	DIVALIKE+J+X+N	-10.4949	-6.83203	2	5	3	7.325746	0.062209
DIVALIKE+J	DIVALIKE+J+X	-10.3281	-6.83203	3	4	1	6.992108	0.008187 *
DIVALIKE+J	DIVALIKE+J+N	-10.3281	-10.3281	3	4	1	2E-05	0.996432
DIVALIKE+J	DIVALIKE+J+X+N	-10.3281	-6.83203	3	5	2	6.992106	0.030317 *
DIVALIKE+X	DIVALIKE+J+X	-6.8318	-6.83203	3	4	1	0	1
DIVALIKE+X	DIVALIKE+X+N	-6.8318	-6.8318	3	4	1	0	1
DIVALIKE+X	DIVALIKE+J+X+N	-6.8318	-6.83203	3	5	2	0	1
DIVALIKE+N	DIVALIKE+J+N	-10.4704	-10.3281	3	4	1	0.2846	0.593702
DIVALIKE+N	DIVALIKE+X+N	-10.4704	-6.8318	3	4	1	7.277146	0.006984 *
DIVALIKE+N	DIVALIKE+J+X+N	-10.4704	-6.83203	3	5	2	7.276686	0.026296 *
DIVALIKE+J+X	DIVALIKE+J+X+N	-6.83203	-6.83203	4	5	1	0	1
DIVALIKE+J+N	DIVALIKE+J+X+N	-10.3281	-6.83203	4	5	1	6.992086	0.008187 *
DIVALIKE+X+N	DIVALIKE+J+X+N	-6.8318	-6.83203	4	5	1	0	1
BAYAREALIKE	BAYAREALIKE+J	-10.8509	-10.8511	2	3	1	0	1
BAYAREALIKE	BAYAREALIKE+X	-10.8509	-10.2239	2	3	1	1.25392	0.262805
BAYAREALIKE	BAYAREALIKE+N	-10.8509	-10.8509	2	3	1	0	1
BAYAREALIKE	BAYAREALIKE+J+X	-10.8509	-10.2239	2	4	2	1.25392	0.534213
BAYAREALIKE	BAYAREALIKE+J+N	-10.8509	-10.3291	2	4	2	1.04352	0.593475
BAYAREALIKE	BAYAREALIKE+X+N	-10.8509	-10.2239	2	4	2	1.25402	0.534187
BAYAREALIKE	BAYAREALIKE+J+X+N	-10.8509	-10.2239	2	5	3	1.25392	0.740103
BAYAREALIKE+J	BAYAREALIKE+J+X	-10.8511	-10.2239	3	4	1	1.25432	0.262729
BAYAREALIKE+J	BAYAREALIKE+J+N	-10.8511	-10.3291	3	4	1	1.04392	0.306912
BAYAREALIKE+J	BAYAREALIKE+J+X+N	-10.8511	-10.2239	3	5	2	1.25432	0.534107
BAYAREALIKE+X	BAYAREALIKE+J+X	-10.2239	-10.2239	3	4	1	0	1
BAYAREALIKE+X	BAYAREALIKE+X+N	-10.2239	-10.2239	3	4	1	1E-04	0.992021
BAYAREALIKE+X	BAYAREALIKE+J+X+N	-10.2239	-10.2239	3	5	2	0	1
BAYAREALIKE+N	BAYAREALIKE+J+N	-10.8509	-10.3291	3	4	1	1.04354	0.307
BAYAREALIKE+N	BAYAREALIKE+X+N	-10.8509	-10.2239	3	4	1	1.25404	0.262782
BAYAREALIKE+N	BAYAREALIKE+J+X+N	-10.8509	-10.2239	3	5	2	1.25394	0.534208
BAYAREALIKE+J+X	BAYAREALIKE+J+X+N	-10.2239	-10.2239	4	5	1	0	1
BAYAREALIKE+J+N	BAYAREALIKE+J+X+N	-10.3291	-10.2239	4	5	1	0.2104	0.646454
BAYAREALIKE+X+N	BAYAREALIKE+J+X+N	-10.2239	-10.2239	4	5	1	0	1

Table 3.3S. Parameter estimates, log-likelihood values (LnL), and model selection score for each of the 24 models assessed for the clade *Arripis* (sample size=4). The model selection score selected was AIC as the sample size of the genus was too small to calculate AICc scores for models with three or more free parameters. Bold italicized row indicates the best-fitting model based on AIC and LRT results.

Biogeographic model	Free parameters	*d*	*e*	*j*	*x*	*n*	LnL	AIC
DEC	2	0.1080	1.00E-12	0	0	0	-17.68	39.36
DEC+J	3	0.1080	2.16E-08	1.00E-05	0	0	-17.68	41.36
DEC+X	3	0.0171	1.00E-12	0	-2.5	0	-9.63	25.27
DEC+N	3	0.0601	0.0555	0	0	-2.5	-13.96	33.92
DEC+J+X	4	0.0171	1.00E-12	1.00E-05	-2.5	0	-9.63	27.27
DEC+J+N	4	0.0601	0.0555	0.0001	0	-2.5	-13.96	35.92
DEC+X+N	***4***	***0.0055***	***1.00E-12***	***0***	***-2.5***	***-2.5***	***-8.12***	***24.24***
DEC+J+X+N	5	0.0055	1.00E-12	1.00E-05	-2.5	-2.5	-8.12	26.24
DIVALIKE	2	0.1283	4.85E-08	0	0	0	-20.78	45.56
DIVALIKE+J	3	0.3501	0.4698	1.9999	0	0	-18.42	42.84
DIVALIKE+X	3	0.0196	1.00E-12	0	-2.5	0	-13.46	32.92
DIVALIKE+N	3	0.0798	0.1181	0	0	-2.5	-16.90	39.80
DIVALIKE+J+X	4	0.0198	1.00E-12	0.0055	-2.5	0	-13.44	34.87
DIVALIKE+J+N	4	0.0833	0.2106	1.8222	0	-2.5	-15.46	38.93
DIVALIKE+X+N	4	0.0073	1.00E-12	0	-2.4984	-2.3896	-12.62	33.25
DIVALIKE+J+X+N	5	0.0044	1.00E-12	1.7422	-2.5	-2.5	-11.10	32.19
BAYAREALIKE	2	0.3879	0.7740	0	0	0	-19.17	42.33
BAYAREALIKE+J	3	0.1401	0.2525	0.2137	0	0	-16.10	38.21
BAYAREALIKE+X	3	0.2259	0.7677	0	-0.5282	0	-19.05	44.10
BAYAREALIKE+N	3	0.1228	0.6070	0	0	-2.1678	-19.05	44.11
BAYAREALIKE+J+X	4	0.0167	0.1229	0.9999	-2.5	0	-14.38	36.76
BAYAREALIKE+J+N	4	0.0581	0.2359	0.1829	0	-2.5	-14.93	37.87
BAYAREALIKE+X+N	4	0.2160	0.7555	0	-0.4965	-0.1662	-19.04	46.09
BAYAREALIKE+J+X+N	5	0.0056	0.1149	0.9999	-2.5	-2.5	-12.89	35.78

Table 3.4S. Likelihood-Ratio test results for the clade *Arripis*. P-values with an asterisk indicate rejection of null hypothesis (no significative improvement when adding parameters) at p<0.05.

Nested model	More complex model	LnL Null	LnL Alt	DF Null	DF Alt	DF	D Statistic	p-value
DEC	DEC+J	-17.6802	-17.6802	2	3	1	0	1
DEC	DEC+X	-17.6802	-9.63293	2	3	1	16.09445	6.03E-05 *
DEC	DEC+N	-17.6802	-13.9591	2	3	1	7.44218	0.006371 *
DEC	DEC+J+X	-17.6802	-9.63298	2	4	2	16.09437	0.00032 *
DEC	DEC+J+N	-17.6802	-13.9591	2	4	2	7.44216	0.024208 *
DEC	DEC+X+N	-17.6802	-8.12061	2	4	2	19.1191	7.05E-05 *
DEC	DEC+J+X+N	-17.6802	-8.12068	2	5	3	19.11895	0.000258 *
DEC+J	DEC+J+X	-17.6802	-9.63298	3	4	1	16.09437	6.03E-05 *
DEC+J	DEC+J+N	-17.6802	-13.9591	3	4	1	7.44216	0.006371 *
DEC+J	DEC+J+X+N	-17.6802	-8.12068	3	5	2	19.11895	7.05E-05 *
DEC+X	DEC+J+X	-9.63293	-9.63298	3	4	1	0	1
DEC+X	DEC+X+N	-9.63293	-8.12061	3	4	1	3.024644	0.082008
DEC+X	DEC+J+X+N	-9.63293	-8.12068	3	5	2	3.0245	0.220413
DEC+N	DEC+J+N	-13.9591	-13.9591	3	4	1	0	1
DEC+N	DEC+X+N	-13.9591	-8.12061	3	4	1	11.67692	0.000633 *
DEC+N	DEC+J+X+N	-13.9591	-8.12068	3	5	2	11.67677	0.002914 *
DEC+J+X	DEC+J+X+N	-9.63298	-8.12068	4	5	1	3.024584	0.082011
DEC+J+N	DEC+J+X+N	-13.9591	-8.12068	4	5	1	11.67679	0.000633 *
DEC+X+N	DEC+J+X+N	-8.12061	-8.12068	4	5	1	0	1
DIVALIKE	DIVALIKE+J	-20.7801	-18.4191	2	3	1	4.7221	0.029777 *
DIVALIKE	DIVALIKE+X	-20.7801	-13.4576	2	3	1	14.64502	0.00013 *
DIVALIKE	DIVALIKE+N	-20.7801	-16.9015	2	3	1	7.7573	0.00535 *
DIVALIKE	DIVALIKE+J+X	-20.7801	-13.4372	2	4	2	14.68582	0.000647 *
DIVALIKE	DIVALIKE+J+N	-20.7801	-15.4634	2	4	2	10.63348	0.004909 *
DIVALIKE	DIVALIKE+X+N	-20.7801	-12.6229	2	4	2	16.31454	0.000287 *
DIVALIKE	DIVALIKE+J+X+N	-20.7801	-11.0953	2	5	3	19.36968	0.000229 *
DIVALIKE+J	DIVALIKE+J+X	-18.4191	-13.4372	3	4	1	9.96372	0.001597 *
DIVALIKE+J	DIVALIKE+J+N	-18.4191	-15.4634	3	4	1	5.91138	0.015043 *
DIVALIKE+J	DIVALIKE+J+X+N	-18.4191	-11.0953	3	5	2	14.64758	0.00066 *
DIVALIKE+X	DIVALIKE+J+X	-13.4576	-13.4372	3	4	1	0.0408	0.839924
DIVALIKE+X	DIVALIKE+X+N	-13.4576	-12.6229	3	4	1	1.66952	0.196323
DIVALIKE+X	DIVALIKE+J+X+N	-13.4576	-11.0953	3	5	2	4.72466	0.0942
DIVALIKE+N	DIVALIKE+J+N	-16.9015	-15.4634	3	4	1	2.87618	0.089899
DIVALIKE+N	DIVALIKE+X+N	-16.9015	-12.6229	3	4	1	8.55724	0.003442 *
DIVALIKE+N	DIVALIKE+J+X+N	-16.9015	-11.0953	3	5	2	11.61238	0.003009 *
DIVALIKE+J+X	DIVALIKE+J+X+N	-13.4372	-11.0953	4	5	1	4.68386	0.030447 *
DIVALIKE+J+N	DIVALIKE+J+X+N	-15.4634	-11.0953	4	5	1	8.7362	0.00312 *
DIVALIKE+X+N	DIVALIKE+J+X+N	-12.6229	-11.0953	4	5	1	3.05514	0.080482
BAYAREALIKE	BAYAREALIKE+J	-19.1669	-16.1028	2	3	1	6.12816	0.013305 *
BAYAREALIKE	BAYAREALIKE+X	-19.1669	-19.0488	2	3	1	0.23632	0.626877
BAYAREALIKE	BAYAREALIKE+N	-19.1669	-19.0549	2	3	1	0.22404	0.635979
BAYAREALIKE	BAYAREALIKE+J+X	-19.1669	-14.3813	2	4	2	9.57124	0.008349 *
BAYAREALIKE	BAYAREALIKE+J+N	-19.1669	-14.9331	2	4	2	8.4677	0.014496 *
BAYAREALIKE	BAYAREALIKE+X+N	-19.1669	-19.0444	2	4	2	0.2451	0.884662
BAYAREALIKE	BAYAREALIKE+J+X+N	-19.1669	-12.8907	2	5	3	12.55246	0.005712
BAYAREALIKE+J	BAYAREALIKE+J+X	-16.1028	-14.3813	3	4	1	3.44308	0.063517
BAYAREALIKE+J	BAYAREALIKE+J+N	-16.1028	-14.9331	3	4	1	2.33954	0.126127
BAYAREALIKE+J	BAYAREALIKE+J+X+N	-16.1028	-12.8907	3	5	2	6.4243	0.04027 *
BAYAREALIKE+X	BAYAREALIKE+J+X	-19.0488	-14.3813	3	4	1	9.33492	0.002248 *
BAYAREALIKE+X	BAYAREALIKE+X+N	-19.0488	-19.0444	3	4	1	0.00878	0.925346
BAYAREALIKE+X	BAYAREALIKE+J+X+N	-19.0488	-12.8907	3	5	2	12.31614	0.002116 *
BAYAREALIKE+N	BAYAREALIKE+J+N	-19.0549	-14.9331	3	4	1	8.24366	0.004089 *
BAYAREALIKE+N	BAYAREALIKE+X+N	-19.0549	-19.0444	3	4	1	0.02106	0.884616
BAYAREALIKE+N	BAYAREALIKE+J+X+N	-19.0549	-12.8907	3	5	2	12.32842	0.002103 *
BAYAREALIKE+J+X	BAYAREALIKE+J+X+N	-14.3813	-12.8907	4	5	1	2.98122	0.084236
BAYAREALIKE+J+N	BAYAREALIKE+J+X+N	-14.9331	-12.8907	4	5	1	4.08476	0.043272 *
BAYAREALIKE+X+N	BAYAREALIKE+J+X+N	-19.0444	-12.8907	4	5	1	12.30736	0.000451 *

Table 3.5S. Parameter estimates, log-likelihood values (LnL), and model selection score for each of the 24 models assessed for the clade *Scorpis* (sample size=4). The model selection score selected was AIC as the sample size of the genus was too small to calculate AICc scores for models with three or more free parameters. Bold italicized row indicates the best-fitting model based on AIC and LRT results.

Biogeographic model	Free parameters	*d*	*e*	*j*	*x*	*n*	LnL	AIC
DEC	2	0.0540	0.0394	0	0	0	-15.79	35.58
DEC+J	3	0.0535	0.0406	0.8324	0	0	-15.73	37.47
DEC+X	***3***	***0.0044***	***1.00E-12***	***0***	***-2.0185***	***0***	***-12.15***	***30.30***
DEC+N	3	0.0197	0.0292	0	0	-2.5	-14.39	34.78
DEC+J+X	4	0.0044	1.00E-12	0.0001	-2.0185	0	-12.15	32.30
DEC+J+N	4	0.0198	0.0324	0.9070	0	-2.5	-14.36	36.73
DEC+X+N	4	0.0044	1.00E-12	0	-2.0185	0.0000	-12.15	32.30
DEC+J+X+N	5	0.0044	1.00E-12	0.0001	-2.0185	0.0000	-12.15	34.30
DIVALIKE	2	0.0647	0.0486	0	0	0	-16.21	36.43
DIVALIKE+J	3	0.0537	0.0453	1.9999	0	0	-15.72	37.43
DIVALIKE+X	3	0.0066	1.00E-12	0	-1.8940	0	-12.94	31.88
DIVALIKE+N	3	0.0239	0.0375	0	0	-2.5	-14.78	35.56
DIVALIKE+J+X	4	0.0033	1.00E-12	1.9999	-2.4562	0	-12.02	32.03
DIVALIKE+J+N	4	0.0217	0.0400	1.9999	0	-2.5	-14.31	36.63
DIVALIKE+X+N	4	0.0066	1.00E-12	0	-1.8940	0.0000	-12.94	33.88
DIVALIKE+J+X+N	5	0.0033	1.00E-12	1.9999	-2.4562	0.0000	-12.02	34.03
BAYAREALIKE	2	0.0495	0.0708	0	0	0	-15.46	34.92
BAYAREALIKE+J	3	0.0307	0.0315	0.2075	0	0	-14.54	35.07
BAYAREALIKE+X	3	0.0204	0.0663	0	-0.9029	0	-14.96	35.92
BAYAREALIKE+N	3	0.0278	0.0677	0	0	-1.6380	-14.71	35.42
BAYAREALIKE+J+X	4	0.0112	3.08E-02	0.1497	-1.1860	0	-13.74	35.48
BAYAREALIKE+J+N	4	0.0118	0.0293	0.0814	0	-2.5	-13.53	35.07
BAYAREALIKE+X+N	4	0.0189	0.0659	0	-0.0002	-2.5	-14.45	36.90
BAYAREALIKE+J+X+N	5	0.0029	1.00E-12	0.9999	-2.4999	-0.4407	-12.42	34.84

Table 3.6S. Likelihood-Ratio test results for the clade *Scorpis*. P-values with an asterisk indicate rejection of null hypothesis (no significative improvement when adding parameters) at p<0.05.

Nested model	More complex model	LnL Null	LnL Alt	DF Null	DF Alt	DF	D Statistic	p-value
DEC	DEC+J	-15.7904	-15.7333	2	3	1	0.11428	0.735323
DEC	DEC+X	-15.7904	-12.1524	2	3	1	7.27598	0.006988 *
DEC	DEC+N	-15.7904	-14.3893	2	3	1	2.80224	0.094133
DEC	DEC+J+X	-15.7904	-12.1525	2	4	2	7.27586	0.026307 *
DEC	DEC+J+N	-15.7904	-14.3636	2	4	2	2.8536	0.240076
DEC	DEC+X+N	-15.7904	-12.1524	2	4	2	7.27598	0.026305 *
DEC	DEC+J+X+N	-15.7904	-12.1525	2	5	3	7.27586	0.063606 *
DEC+J	DEC+J+X	-15.7333	-12.1525	3	4	1	7.16158	0.007448 *
DEC+J	DEC+J+N	-15.7333	-14.3636	3	4	1	2.73932	0.097906
DEC+J	DEC+J+X+N	-15.7333	-12.1525	3	5	2	7.16158	0.027854 *
DEC+X	DEC+J+X	-12.1524	-12.1525	3	4	1	0	1
DEC+X	DEC+X+N	-12.1524	-12.1524	3	4	1	0	1
DEC+X	DEC+J+X+N	-12.1524	-12.1525	3	5	2	0	1
DEC+N	DEC+J+N	-14.3893	-14.3636	3	4	1	0.05136	0.820713
DEC+N	DEC+X+N	-14.3893	-12.1524	3	4	1	4.47374	0.03442 *
DEC+N	DEC+J+X+N	-14.3893	-12.1525	3	5	2	4.47362	0.106799
DEC+J+X	DEC+J+X+N	-12.1525	-12.1525	4	5	1	0	1
DEC+J+N	DEC+J+X+N	-14.3636	-12.1525	4	5	1	4.42226	0.035473 *
DEC+X+N	DEC+J+X+N	-12.1524	-12.1525	4	5	1	0	1
DIVALIKE	DIVALIKE+J	-16.2145	-15.7161	2	3	1	0.99694	0.318052
DIVALIKE	DIVALIKE+X	-16.2145	-12.9387	2	3	1	6.55162	0.010479 *
DIVALIKE	DIVALIKE+N	-16.2145	-14.7813	2	3	1	2.86648	0.090442
DIVALIKE	DIVALIKE+J+X	-16.2145	-12.0172	2	4	2	8.39468	0.015036 *
DIVALIKE	DIVALIKE+J+N	-16.2145	-14.3136	2	4	2	3.8019	0.149427
DIVALIKE	DIVALIKE+X+N	-16.2145	-12.9387	2	4	2	6.55162	0.037786 *
DIVALIKE	DIVALIKE+J+X+N	-16.2145	-12.0172	2	5	3	8.39468	0.038522 *
DIVALIKE+J	DIVALIKE+J+X	-15.7161	-12.0172	3	4	1	7.39774	0.006531 *
DIVALIKE+J	DIVALIKE+J+N	-15.7161	-14.3136	3	4	1	2.80496	0.093973
DIVALIKE+J	DIVALIKE+J+X+N	-15.7161	-12.0172	3	5	2	7.39774	0.024751 *
DIVALIKE+X	DIVALIKE+J+X	-12.9387	-12.0172	3	4	1	1.84306	0.174593
DIVALIKE+X	DIVALIKE+X+N	-12.9387	-12.9387	3	4	1	0	1
DIVALIKE+X	DIVALIKE+J+X+N	-12.9387	-12.0172	3	5	2	1.84306	0.39791
DIVALIKE+N	DIVALIKE+J+N	-14.7813	-14.3136	3	4	1	0.93542	0.333458
DIVALIKE+N	DIVALIKE+X+N	-14.7813	-12.9387	3	4	1	3.68514	0.054899
DIVALIKE+N	DIVALIKE+J+X+N	-14.7813	-12.0172	3	5	2	5.5282	0.063033
DIVALIKE+J+X	DIVALIKE+J+X+N	-12.0172	-12.0172	4	5	1	0	1
DIVALIKE+J+N	DIVALIKE+J+X+N	-14.3136	-12.0172	4	5	1	4.59278	0.032107 *
DIVALIKE+X+N	DIVALIKE+J+X+N	-12.9387	-12.0172	4	5	1	1.84306	0.174593
BAYAREALIKE	BAYAREALIKE+J	-15.4592	-14.537	2	3	1	1.84432	0.174445
BAYAREALIKE	BAYAREALIKE+X	-15.4592	-14.9613	2	3	1	0.99578	0.318334
BAYAREALIKE	BAYAREALIKE+N	-15.4592	-14.7098	2	3	1	1.49868	0.220875
BAYAREALIKE	BAYAREALIKE+J+X	-15.4592	-13.7404	2	4	2	3.4375	0.17929
BAYAREALIKE	BAYAREALIKE+J+N	-15.4592	-13.5349	2	4	2	3.84856	0.145981
BAYAREALIKE	BAYAREALIKE+X+N	-15.4592	-14.4517	2	4	2	2.01488	0.365153
BAYAREALIKE	BAYAREALIKE+J+X+N	-15.4592	-12.4183	2	5	3	6.0817	0.107702
BAYAREALIKE+J	BAYAREALIKE+J+X	-14.537	-13.7404	3	4	1	1.59318	0.206872
BAYAREALIKE+J	BAYAREALIKE+J+N	-14.537	-13.5349	3	4	1	2.00424	0.15686
BAYAREALIKE+J	BAYAREALIKE+J+X+N	-14.537	-12.4183	3	5	2	4.23738	0.120189
BAYAREALIKE+X	BAYAREALIKE+J+X	-14.9613	-13.7404	3	4	1	2.44172	0.118147
BAYAREALIKE+X	BAYAREALIKE+X+N	-14.9613	-14.4517	3	4	1	1.0191	0.312733
BAYAREALIKE+X	BAYAREALIKE+J+X+N	-14.9613	-12.4183	3	5	2	5.08592	0.078633
BAYAREALIKE+N	BAYAREALIKE+J+N	-14.7098	-13.5349	3	4	1	2.34988	0.125293
BAYAREALIKE+N	BAYAREALIKE+X+N	-14.7098	-14.4517	3	4	1	0.5162	0.472467
BAYAREALIKE+N	BAYAREALIKE+J+X+N	-14.7098	-12.4183	3	5	2	4.58302	0.101114
BAYAREALIKE+J+X	BAYAREALIKE+J+X+N	-13.7404	-12.4183	4	5	1	2.6442	0.103928
BAYAREALIKE+J+N	BAYAREALIKE+J+X+N	-13.5349	-12.4183	4	5	1	2.23314	0.135079
BAYAREALIKE+X+N	BAYAREALIKE+J+X+N	-14.4517	-12.4183	4	5	1	4.06682	0.043734 *

Table 3.7S. Parameter estimates, log-likelihood values (LnL), and model selection score for each of the 24 models assessed for the clade *Atypichthys-Microcanthus* (sample size=6). The model selection score selected was AIC as the sample size of the genus was too small to calculate AICc scores for models with five free parameters. Bold italicized row indicates the best-fitting model based on AIC and LRT results.

Biogeographic model	Free parameters	*d*	*e*	*j*	*x*	*n*	LnL	AIC
DEC	2	0.0232	9.54E-09	0	0	0	-29.53	63.06
DEC+J	3	0.0232	1.00E-12	1.00E-05	0	0	-29.53	65.06
DEC+X	***3***	***0.0011***	***1.00E-12***	***0***	***-2.1854***	***0***	***-17.17***	***40.34***
DEC+N	3	0.0040	9.24E-09	0	0	-2.5	-26.19	58.38
DEC+J+X	4	0.0008	1.00E-12	0.0023	-2.3736	0	-16.61	41.22
DEC+J+N	4	0.0040	9.24E-09	0.0001	0	-2.5	-26.19	60.38
DEC+X+N	4	0.0003	1.00E-12	0	-2.5	-0.7383	-16.61	41.23
DEC+J+X+N	5	0.0004	1.00E-12	0.0017	-2.4772	-0.6715	-16.24	42.49
DIVALIKE	2	0.0262	1.00E-12	0	0	0	-28.02	60.03
DIVALIKE+J	3	0.0262	1.00E-12	1.00E-05	0	0	-28.02	62.03
DIVALIKE+X	3	0.0012	1.00E-12	0	-2.2280	0	-18.09	42.18
DIVALIKE+N	3	0.0046	1.00E-12	0	0	-2.4933	-24.87	55.75
DIVALIKE+J+X	4	0.0008	1.00E-12	0.0002	-2.4103	0	-18.05	44.09
DIVALIKE+J+N	4	0.0045	1.00E-12	0.0017	0	-2.4933	-24.86	57.72
DIVALIKE+X+N	4	0.0008	1.00E-12	0	-2.3847	-0.1686	-18.02	44.03
DIVALIKE+J+X+N	5	0.0011	1.00E-12	0.0004	-2.0685	-0.4653	-17.96	45.91
BAYAREALIKE	2	0.1062	0.2466	0	0	0	-31.10	66.20
BAYAREALIKE+J	3	0.0488	0.0909	0.9999	0	0	-30.58	67.15
BAYAREALIKE+X	3	0.0049	0.1112	0	-1.6053	0	-27.90	61.80
BAYAREALIKE+N	3	0.0333	0.2058	0	0	-1.2061	-30.90	67.80
BAYAREALIKE+J+X	4	0.0008	0.0231	0.5920	-2.5	0	-19.65	47.29
BAYAREALIKE+J+N	4	0.0159	0.0729	0.9126	0	-1.4653	-29.44	66.88
BAYAREALIKE+X+N	4	0.0027	0.1056	0	-1.4816	-1.1136	-27.22	62.45
BAYAREALIKE+J+X+N	5	0.0008	0.0231	0.9997	-2.5	-0.0402	-19.60	49.21

Table 3.8S. Likelihood-Ratio test results for the clade *Atypichthys-Microcanthus*. P-values with an asterisk indicate rejection of null hypothesis (no significative improvement when adding parameters) at p<0.05.

Nested model	More complex model	LnL Null	LnL Alt	DF Null	DF Alt	DF	D Statistic	p-value
DEC	DEC+J	-29.5305	-29.5306	2	3	1	0	1
DEC	DEC+X	-29.5305	-17.1715	2	3	1	24.71804	6.64E-07 *
DEC	DEC+N	-29.5305	-26.1902	2	3	1	6.68052	0.009747 *
DEC	DEC+J+X	-29.5305	-16.6079	2	4	2	25.84512	2.44E-06 *
DEC	DEC+J+N	-29.5305	-26.1895	2	4	2	6.68202	0.035401 *
DEC	DEC+X+N	-29.5305	-16.613	2	4	2	25.835	2.45E-06 *
DEC	DEC+J+X+N	-29.5305	-16.2435	2	5	3	26.57392	7.23E-06 *
DEC+J	DEC+J+X	-29.5306	-16.6079	3	4	1	25.84532	3.7E-07 *
DEC+J	DEC+J+N	-29.5306	-26.1895	3	4	1	6.68222	0.009738 *
DEC+J	DEC+J+X+N	-29.5306	-16.2435	3	5	2	26.57412	1.7E-06 *
DEC+X	DEC+J+X	-17.1715	-16.6079	3	4	1	1.12708	0.288399
DEC+X	DEC+X+N	-17.1715	-16.613	3	4	1	1.11696	0.290574
DEC+X	DEC+J+X+N	-17.1715	-16.2435	3	5	2	1.85588	0.395367
DEC+N	DEC+J+N	-26.1902	-26.1895	3	4	1	0.0015	0.969106
DEC+N	DEC+X+N	-26.1902	-16.613	3	4	1	19.15448	1.21E-05 *
DEC+N	DEC+J+X+N	-26.1902	-16.2435	3	5	2	19.8934	4.79E-05 *
DEC+J+X	DEC+J+X+N	-16.6079	-16.2435	4	5	1	0.7288	0.393272
DEC+J+N	DEC+J+X+N	-26.1895	-16.2435	4	5	1	19.8919	8.19E-06 *
DEC+X+N	DEC+J+X+N	-16.613	-16.2435	4	5	1	0.73892	0.390007
DIVALIKE	DIVALIKE+J	-28.0167	-28.0167	2	3	1	0	1
DIVALIKE	DIVALIKE+X	-28.0167	-18.089	2	3	1	19.8554	8.35E-06 *
DIVALIKE	DIVALIKE+N	-28.0167	-24.874	2	3	1	6.2853	0.012174 *
DIVALIKE	DIVALIKE+J+X	-28.0167	-18.0463	2	4	2	19.94074	4.68E-05 *
DIVALIKE	DIVALIKE+J+N	-28.0167	-24.8587	2	4	2	6.31582	0.042515 *
DIVALIKE	DIVALIKE+X+N	-28.0167	-18.0166	2	4	2	20.00006	4.54E-05 *
DIVALIKE	DIVALIKE+J+X+N	-28.0167	-17.9569	2	5	3	20.11948	0.00016 *
DIVALIKE+J	DIVALIKE+J+X	-28.0167	-18.0463	3	4	1	19.94092	7.99E-06 *
DIVALIKE+J	DIVALIKE+J+N	-28.0167	-24.8587	3	4	1	6.316	0.011965 *
DIVALIKE+J	DIVALIKE+J+X+N	-28.0167	-17.9569	3	5	2	20.11966	4.28E-05 *
DIVALIKE+X	DIVALIKE+J+X	-18.089	-18.0463	3	4	1	0.08534	0.770187
DIVALIKE+X	DIVALIKE+X+N	-18.089	-18.0166	3	4	1	0.14466	0.703692
DIVALIKE+X	DIVALIKE+J+X+N	-18.089	-17.9569	3	5	2	0.26408	0.876306
DIVALIKE+N	DIVALIKE+J+N	-24.874	-24.8587	3	4	1	0.03052	0.861316
DIVALIKE+N	DIVALIKE+X+N	-24.874	-18.0166	3	4	1	13.71476	0.000213 *
DIVALIKE+N	DIVALIKE+J+X+N	-24.874	-17.9569	3	5	2	13.83418	0.000991 *
DIVALIKE+J+X	DIVALIKE+J+X+N	-18.0463	-17.9569	4	5	1	0.17874	0.672458
DIVALIKE+J+N	DIVALIKE+J+X+N	-24.8587	-17.9569	4	5	1	13.80366	0.000203 *
DIVALIKE+X+N	DIVALIKE+J+X+N	-18.0166	-17.9569	4	5	1	0.11942	0.729664
BAYAREALIKE	BAYAREALIKE+J	-31.1017	-30.5762	2	3	1	1.0511	0.305254
BAYAREALIKE	BAYAREALIKE+X	-31.1017	-27.9006	2	3	1	6.4022	0.011398 *
BAYAREALIKE	BAYAREALIKE+N	-31.1017	-30.8986	2	3	1	0.40614	0.523935
BAYAREALIKE	BAYAREALIKE+J+X	-31.1017	-19.6465	2	4	2	22.91048	1.06E-05 *
BAYAREALIKE	BAYAREALIKE+J+N	-31.1017	-29.4408	2	4	2	3.32192	0.189957
BAYAREALIKE	BAYAREALIKE+X+N	-31.1017	-27.2241	2	4	2	7.75514	0.020701 *
BAYAREALIKE	BAYAREALIKE+J+X+N	-31.1017	-19.6029	2	5	3	22.99764	4.04E-05 *
BAYAREALIKE+J	BAYAREALIKE+J+X	-30.5762	-19.6465	3	4	1	21.85938	2.93E-06 *
BAYAREALIKE+J	BAYAREALIKE+J+N	-30.5762	-29.4408	3	4	1	2.27082	0.13183
BAYAREALIKE+J	BAYAREALIKE+J+X+N	-30.5762	-19.6029	3	5	2	21.94654	1.72E-05 *
BAYAREALIKE+X	BAYAREALIKE+J+X	-27.9006	-19.6465	3	4	1	16.50828	4.84E-05 *
BAYAREALIKE+X	BAYAREALIKE+X+N	-27.9006	-27.2241	3	4	1	1.35294	0.244765
BAYAREALIKE+X	BAYAREALIKE+J+X+N	-27.9006	-19.6029	3	5	2	16.59544	0.000249 *
BAYAREALIKE+N	BAYAREALIKE+J+N	-30.8986	-29.4408	3	4	1	2.91578	0.087717
BAYAREALIKE+N	BAYAREALIKE+X+N	-30.8986	-27.2241	3	4	1	7.349	0.00671 *
BAYAREALIKE+N	BAYAREALIKE+J+X+N	-30.8986	-19.6029	3	5	2	22.5915	1.24E-05 *
BAYAREALIKE+J+X	BAYAREALIKE+J+X+N	-19.6465	-19.6029	4	5	1	0.08716	0.767819
BAYAREALIKE+J+N	BAYAREALIKE+J+X+N	-29.4408	-19.6029	4	5	1	19.67572	9.18E-06 *
BAYAREALIKE+X+N	BAYAREALIKE+J+X+N	-27.2241	-19.6029	4	5	1	15.2425	9.46E-05 *

Table 3.9S. Parameter estimates, log-likelihood values (LnL), and model selection score for each of the 24 models assessed for the clade *Kathetostoma* (sample size=7). Bold italicized row indicates the best-fitting model based on AICc and LRT results.

Biogeographic model	Free parameters	*d*	*e*	*j*	*x*	*n*	LnL	AICc
DEC	2	0.0353	0.0398	0	0	0	-26.57	60.14
DEC+J	3	0.0170	0.0069	0.6365	0	0	-24.67	63.34
DEC+X	3	0.0013	0.0029	0	-1.3776	0	-22.01	58.02
DEC+N	3	0.0353	0.0398	0	0	0.0000	-26.57	67.14
DEC+J+X	4	0.0008	1.00E-12	0.0724	-1.4549	0	-18.28	64.56
DEC+J+N	4	0.0169	0.0068	0.6607	0	0.0000	-24.67	77.33
DEC+X+N	4	0.0007	1.00E-12	0	-1.6019	0.0000	-21.94	71.89
DEC+J+X+N	5	0.0008	1.00E-12	0.0724	-1.4549	0.0000	-18.28	106.56
DIVALIKE	2	0.0302	0.0188	0	0	0	-25.58	58.15
DIVALIKE+J	3	0.0171	2.33E-07	0.2037	0	0	-24.30	62.59
DIVALIKE+X	***3***	***0.0015***	***1.00E-12***	***0***	***-1.3653***	***0***	***-19.91***	***53.82***
DIVALIKE+N	3	0.0302	0.0188	0	0	0.0000	-25.58	65.15
DIVALIKE+J+X	4	0.0008	1.00E-12	0.0199	-1.5052	0	-17.62	63.24
DIVALIKE+J+N	4	0.0171	1.00E-12	0.2032	0	0.0000	-24.30	76.59
DIVALIKE+X+N	4	0.0015	1.00E-12	0	-1.3653	0.0000	-19.91	67.82
DIVALIKE+J+X+N	5	0.0004	1.00E-12	0.0115	-1.7999	0.0000	-17.51	105.03
BAYAREALIKE	2	0.0518	0.1137	0	0	0	-27.00	61.01
BAYAREALIKE+J	3	0.0072	1.00E-12	0.2029	0	0	-22.86	59.71
BAYAREALIKE+X	3	0.0053	0.1062	0	-1.0986	0	-23.97	61.94
BAYAREALIKE+N	3	0.0510	0.1137	0	0	-0.0299	-27.00	68.00
BAYAREALIKE+J+X	4	0.0009	1.00E-12	0.0495	-1.1495	0	-18.25	64.51
BAYAREALIKE+J+N	4	0.0072	1.00E-12	0.2031	0	0.0000	-22.86	73.71
BAYAREALIKE+X+N	4	0.0049	0.1058	0	-1.1306	0.0000	-23.96	75.92
BAYAREALIKE+J+X+N	5	0.0006	1.00E-12	0.0357	-1.3619	0.0000	-18.02	106.05

Table 3.10S. Likelihood-Ratio test results for the clade *Kathetostoma*. P-values with an asterisk indicate rejection of null hypothesis (no significative improvement when adding parameters) at p<0.05.

Nested model	More complex model	LnL Null	LnL Alt	DF Null	DF Alt	DF	D Statistic	p-value
DEC	DEC+J	-26.57	-24.6676	2	3	1	3.80476	0.051107
DEC	DEC+X	-26.57	-22.0104	2	3	1	9.11918	0.002529 *
DEC	DEC+N	-26.57	-26.57	2	3	1	0	1
DEC	DEC+J+X	-26.57	-18.2812	2	4	2	16.57764	0.000251 *
DEC	DEC+J+N	-26.57	-24.6671	2	4	2	3.80576	0.149138
DEC	DEC+X+N	-26.57	-21.9443	2	4	2	9.25136	0.009797 *
DEC	DEC+J+X+N	-26.57	-18.2812	2	5	3	16.57764	0.000863 *
DEC+J	DEC+J+X	-24.6676	-18.2812	3	4	1	12.77288	0.000352 *
DEC+J	DEC+J+N	-24.6676	-24.6671	3	4	1	0.001	0.974773
DEC+J	DEC+J+X+N	-24.6676	-18.2812	3	5	2	12.77288	0.001684 *
DEC+X	DEC+J+X	-22.0104	-18.2812	3	4	1	7.45846	0.006314 *
DEC+X	DEC+X+N	-22.0104	-21.9443	3	4	1	0.13218	0.716182
DEC+X	DEC+J+X+N	-22.0104	-18.2812	3	5	2	7.45846	0.024011 *
DEC+N	DEC+J+N	-26.57	-24.6671	3	4	1	3.80576	0.051077
DEC+N	DEC+X+N	-26.57	-21.9443	3	4	1	9.25136	0.002353 *
DEC+N	DEC+J+X+N	-26.57	-18.2812	3	5	2	16.57764	0.000251 *
DEC+J+X	DEC+J+X+N	-18.2812	-18.2812	4	5	1	0	1
DEC+J+N	DEC+J+X+N	-24.6671	-18.2812	4	5	1	12.77188	0.000352 *
DEC+X+N	DEC+J+X+N	-21.9443	-18.2812	4	5	1	7.32628	0.006795 *
DIVALIKE	DIVALIKE+J	-25.5767	-24.2965	2	3	1	2.56042	0.109569
DIVALIKE	DIVALIKE+X	-25.5767	-19.9108	2	3	1	11.3318	0.000762 *
DIVALIKE	DIVALIKE+N	-25.5767	-25.5767	2	3	1	0	1
DIVALIKE	DIVALIKE+J+X	-25.5767	-17.6197	2	4	2	15.91386	0.00035 *
DIVALIKE	DIVALIKE+J+N	-25.5767	-24.2965	2	4	2	2.56042	0.277979
DIVALIKE	DIVALIKE+X+N	-25.5767	-19.9108	2	4	2	11.3318	0.003462 *
DIVALIKE	DIVALIKE+J+X+N	-25.5767	-17.5127	2	5	3	16.12798	0.001067 *
DIVALIKE+J	DIVALIKE+J+X	-24.2965	-17.6197	3	4	1	13.35344	0.000258 *
DIVALIKE+J	DIVALIKE+J+N	-24.2965	-24.2965	3	4	1	0	1
DIVALIKE+J	DIVALIKE+J+X+N	-24.2965	-17.5127	3	5	2	13.56756	0.001132 *
DIVALIKE+X	DIVALIKE+J+X	-19.9108	-17.6197	3	4	1	4.58206	0.032308 *
DIVALIKE+X	DIVALIKE+X+N	-19.9108	-19.9108	3	4	1	0	1
DIVALIKE+X	DIVALIKE+J+X+N	-19.9108	-17.5127	3	5	2	4.79618	0.090891
DIVALIKE+N	DIVALIKE+J+N	-25.5767	-24.2965	3	4	1	2.56042	0.109569
DIVALIKE+N	DIVALIKE+X+N	-25.5767	-19.9108	3	4	1	11.3318	0.000762 *
DIVALIKE+N	DIVALIKE+J+X+N	-25.5767	-17.5127	3	5	2	16.12798	0.000315 *
DIVALIKE+J+X	DIVALIKE+J+X+N	-17.6197	-17.5127	4	5	1	0.21412	0.643557
DIVALIKE+J+N	DIVALIKE+J+X+N	-24.2965	-17.5127	4	5	1	13.56756	0.00023 *
DIVALIKE+X+N	DIVALIKE+J+X+N	-19.9108	-17.5127	4	5	1	4.79618	0.028523 *
BAYAREALIKE	BAYAREALIKE+J	-27.0036	-22.8573	2	3	1	8.29256	0.003981 *
BAYAREALIKE	BAYAREALIKE+X	-27.0036	-23.9683	2	3	1	6.0705	0.013746 *
BAYAREALIKE	BAYAREALIKE+N	-27.0036	-27.0007	2	3	1	0.00568	0.939924
BAYAREALIKE	BAYAREALIKE+J+X	-27.0036	-18.2531	2	4	2	17.50096	0.000158 *
BAYAREALIKE	BAYAREALIKE+J+N	-27.0036	-22.8573	2	4	2	8.29256	0.015823 *
BAYAREALIKE	BAYAREALIKE+X+N	-27.0036	-23.962	2	4	2	6.0831	0.047761 *
BAYAREALIKE	BAYAREALIKE+J+X+N	-27.0036	-18.0225	2	5	3	17.9621	0.000448 *
BAYAREALIKE+J	BAYAREALIKE+J+X	-22.8573	-18.2531	3	4	1	9.2084	0.002409 *
BAYAREALIKE+J	BAYAREALIKE+J+N	-22.8573	-22.8573	3	4	1	0	1
BAYAREALIKE+J	BAYAREALIKE+J+X+N	-22.8573	-18.0225	3	5	2	9.66954	0.007949 *
BAYAREALIKE+X	BAYAREALIKE+J+X	-23.9683	-18.2531	3	4	1	11.43046	0.000722 *
BAYAREALIKE+X	BAYAREALIKE+X+N	-23.9683	-23.962	3	4	1	0.0126	0.910625
BAYAREALIKE+X	BAYAREALIKE+J+X+N	-23.9683	-18.0225	3	5	2	11.8916	0.002617 *
BAYAREALIKE+N	BAYAREALIKE+J+N	-27.0007	-22.8573	3	4	1	8.28688	0.003993 *
BAYAREALIKE+N	BAYAREALIKE+X+N	-27.0007	-23.962	3	4	1	6.07742	0.013692 *
BAYAREALIKE+N	BAYAREALIKE+J+X+N	-27.0007	-18.0225	3	5	2	17.95642	0.000126 *
BAYAREALIKE+J+X	BAYAREALIKE+J+X+N	-18.2531	-18.0225	4	5	1	0.46114	0.497092
BAYAREALIKE+J+N	BAYAREALIKE+J+X+N	-22.8573	-18.0225	4	5	1	9.66954	0.001873 *
BAYAREALIKE+X+N	BAYAREALIKE+J+X+N	-23.962	-18.0225	4	5	1	11.879	0.000568 *

Table 3.11S. Parameter estimates, log-likelihood values (LnL), and model selection score for each of the 24 models assessed for the clade *Nemadactylus* (sample size=8). Bold italicized row indicates the best-fitting model based on AICc and LRT results.

Biogeographic model	Free parameters	*d*	*e*	*j*	*x*	*n*	LnL	AICc
DEC	2	0.0456	0.0000	0	0	0	-37.59	81.58
DEC+J	3	0.0385	1.00E-12	1.5951	0	0	-35.11	82.23
DEC+X	3	0.0085	1.00E-12	0	-0.7329	0	-35.57	83.15
DEC+N	***3***	***0.0187***	***1.00E-12***	***0***	***0***	***-2.5***	***-34.26***	***80.52***
DEC+J+X	4	0.0099	1.00E-12	0.4246	-0.6174	0	-33.55	88.44
DEC+J+N	4	0.0171	1.00E-12	0.6117	0	-2.5	-31.85	85.04
DEC+X+N	4	0.0078	1.00E-12	0	-0.3851	-2.5	-33.40	88.13
DEC+J+X+N	5	0.0078	1.00E-12	0.2630	-0.3532	-2.5	-31.09	102.19
DIVALIKE	2	0.0503	1.00E-12	0	0	0	-40.34	87.08
DIVALIKE+J	3	0.0369	1.00E-12	1.0843	0	0	-35.63	83.26
DIVALIKE+X	3	0.0216	1.00E-12	0	-0.4037	0	-39.62	91.25
DIVALIKE+N	3	0.0208	1.00E-12	0	0	-2.5	-37.01	86.03
DIVALIKE+J+X	4	0.0143	1.00E-12	0.6939	-0.4312	0	-34.45	90.23
DIVALIKE+J+N	4	0.0160	1.00E-12	0.4764	0	-2.5	-32.68	86.69
DIVALIKE+X+N	4	0.0144	1.00E-12	0	-0.1817	-2.5	-36.81	94.94
DIVALIKE+J+X+N	5	0.0089	1.00E-12	0.3143	-0.2636	-2.5	-32.16	104.32
BAYAREALIKE	2	0.3657	0.7260	0	0	0	-50.70	107.79
BAYAREALIKE+J	3	0.0451	0.0567	0.9999	0	0	-36.28	84.56
BAYAREALIKE+X	3	0.1825	0.6777	0	-0.3026	0	-50.24	112.49
BAYAREALIKE+N	3	0.3693	0.7293	0	0	0.0000	-50.70	113.39
BAYAREALIKE+J+X	4	0.0177	0.0463	0.9999	-0.4016	0	-35.23	91.80
BAYAREALIKE+J+N	4	0.0158	0.0317	0.9999	0	-2.4999	-34.19	89.71
BAYAREALIKE+X+N	4	0.1822	0.6771	0	-0.3029	0.0000	-50.24	121.82
BAYAREALIKE+J+X+N	5	0.0091	0.0310	0.9999	-0.2792	-2.3808	-33.68	107.36

Table 3.12S. Likelihood-Ratio test results for the clade *Nemadactylus*. P-values with an asterisk indicate rejection of null hypothesis (no significative improvement when adding parameters) at p<0.05.

Nested model	More complex model	LnL Null	LnL Alt	DF Null	DF Alt	DF	D Statistic	p-value
DEC	DEC+J	-37.5901	-35.11467	2	3	1	4.95086	0.026077693 *
DEC	DEC+X	-37.5901	-35.57414	2	3	1	4.03192	0.044647102 *
DEC	DEC+N	-37.5901	-34.25932	2	3	1	6.66156	0.009851464 *
DEC	DEC+J+X	-37.5901	-33.55278	2	4	2	8.07464	0.017644697 *
DEC	DEC+J+N	-37.5901	-31.85416	2	4	2	11.47188	0.003227847 *
DEC	DEC+X+N	-37.5901	-33.40069	2	4	2	8.37882	0.015155224 *
DEC	DEC+J+X+N	-37.5901	-31.0941	2	5	3	12.992	0.004653938 *
DEC+J	DEC+J+X	-35.11467	-33.55278	3	4	1	3.12378	0.077157606
DEC+J	DEC+J+N	-35.11467	-31.85416	3	4	1	6.52102	0.010660684 *
DEC+J	DEC+J+X+N	-35.11467	-31.0941	3	5	2	8.04114	0.017942735 *
DEC+X	DEC+J+X	-35.57414	-33.55278	3	4	1	4.04272	0.044362266 *
DEC+X	DEC+X+N	-35.57414	-33.40069	3	4	1	4.3469	0.037076376 *
DEC+X	DEC+J+X+N	-35.57414	-31.0941	3	5	2	8.96008	0.01133296 *
DEC+N	DEC+J+N	-34.25932	-31.85416	3	4	1	4.81032	0.028289792 *
DEC+N	DEC+X+N	-34.25932	-33.40069	3	4	1	1.71726	0.190046125
DEC+N	DEC+J+X+N	-34.25932	-31.0941	3	5	2	6.33044	0.042204856 *
DEC+J+X	DEC+J+X+N	-33.55278	-31.0941	4	5	1	4.91736	0.026588116 *
DEC+J+N	DEC+J+X+N	-31.85416	-31.0941	4	5	1	1.52012	0.217601335
DEC+X+N	DEC+J+X+N	-33.40069	-31.0941	4	5	1	4.61318	0.031727146 *
DIVALIKE	DIVALIKE+J	-40.33964	-35.62817	2	3	1	9.42294	0.002142877 *
DIVALIKE	DIVALIKE+X	-40.33964	-39.62359	2	3	1	1.4321	0.231422023
DIVALIKE	DIVALIKE+N	-40.33964	-37.01401	2	3	1	6.65126	0.009908573 *
DIVALIKE	DIVALIKE+J+X	-40.33964	-34.44601	2	4	2	11.78726	0.002756951 *
DIVALIKE	DIVALIKE+J+N	-40.33964	-32.67665	2	4	2	15.32598	0.0004699 *
DIVALIKE	DIVALIKE+X+N	-40.33964	-36.8056	2	4	2	7.06808	0.029186763 *
DIVALIKE	DIVALIKE+J+X+N	-40.33964	-32.15921	2	5	3	16.36086	0.00095627 *
DIVALIKE+J	DIVALIKE+J+X	-35.62817	-34.44601	3	4	1	2.36432	0.124137996
DIVALIKE+J	DIVALIKE+J+N	-35.62817	-32.67665	3	4	1	5.90304	0.015114775 *
DIVALIKE+J	DIVALIKE+J+X+N	-35.62817	-32.15921	3	5	2	6.93792	0.031149409 *
DIVALIKE+X	DIVALIKE+J+X	-39.62359	-34.44601	3	4	1	10.35516	0.001291133 *
DIVALIKE+X	DIVALIKE+X+N	-39.62359	-36.8056	3	4	1	5.63598	0.017595507 *
DIVALIKE+X	DIVALIKE+J+X+N	-39.62359	-32.15921	3	5	2	14.92876	0.00057314 *
DIVALIKE+N	DIVALIKE+J+N	-37.01401	-32.67665	3	4	1	8.67472	0.003226544 *
DIVALIKE+N	DIVALIKE+X+N	-37.01401	-36.8056	3	4	1	0.41682	0.518528083
DIVALIKE+N	DIVALIKE+J+X+N	-37.01401	-32.15921	3	5	2	9.7096	0.007790891 *
DIVALIKE+J+X	DIVALIKE+J+X+N	-34.44601	-32.15921	4	5	1	4.5736	0.032468266 *
DIVALIKE+J+N	DIVALIKE+J+X+N	-32.67665	-32.15921	4	5	1	1.03488	0.309015246
DIVALIKE+X+N	DIVALIKE+J+X+N	-36.8056	-32.15921	4	5	1	9.29278	0.002300588 *
BAYAREALIKE	BAYAREALIKE+J	-50.69599	-36.27845	2	3	1	28.83508	7.88107E-08 *
BAYAREALIKE	BAYAREALIKE+X	-50.69599	-50.24485	2	3	1	0.90228	0.342171094
BAYAREALIKE	BAYAREALIKE+N	-50.69599	-50.69591	2	3	1	0.00016	0.989907739
BAYAREALIKE	BAYAREALIKE+J+X	-50.69599	-35.23302	2	4	2	30.92594	1.92538E-07 *
BAYAREALIKE	BAYAREALIKE+J+N	-50.69599	-34.18966	2	4	2	33.01266	6.78253E-08 *
BAYAREALIKE	BAYAREALIKE+X+N	-50.69599	-50.24485	2	4	2	0.90228	0.63690167
BAYAREALIKE	BAYAREALIKE+J+X+N	-50.69599	-33.67983	2	5	3	34.03232	1.95031E-07 *
BAYAREALIKE+J	BAYAREALIKE+J+X	-36.27845	-35.23302	3	4	1	2.09086	0.148182633
BAYAREALIKE+J	BAYAREALIKE+J+N	-36.27845	-34.18966	3	4	1	4.17758	0.040962151 *
BAYAREALIKE+J	BAYAREALIKE+J+X+N	-36.27845	-33.67983	3	5	2	5.19724	0.074376147
BAYAREALIKE+X	BAYAREALIKE+J+X	-50.24485	-35.23302	3	4	1	30.02366	4.26807E-08 *
BAYAREALIKE+X	BAYAREALIKE+X+N	-50.24485	-50.24485	3	4	1	0	1
BAYAREALIKE+X	BAYAREALIKE+J+X+N	-50.24485	-33.67983	3	5	2	33.13004	6.39592E-08 *
BAYAREALIKE+N	BAYAREALIKE+J+N	-50.69591	-34.18966	3	4	1	33.0125	9.15683E-09 *
BAYAREALIKE+N	BAYAREALIKE+X+N	-50.69591	-50.24485	3	4	1	0.90212	0.342213897
BAYAREALIKE+N	BAYAREALIKE+J+X+N	-50.69591	-33.67983	3	5	2	34.03216	4.0739E-08 *
BAYAREALIKE+J+X	BAYAREALIKE+J+X+N	-35.23302	-33.67983	4	5	1	3.10638	0.077986113
BAYAREALIKE+J+N	BAYAREALIKE+J+X+N	-34.18966	-33.67983	4	5	1	1.01966	0.312599672
BAYAREALIKE+X+N	BAYAREALIKE+J+X+N	-50.24485	-33.67983	4	5	1	33.13004	8.61967E-09 *

Table 3.13S. Parameter estimates, log-likelihood values (LnL), and model selection score for each of the 24 models assessed for the clade *Lepidoperca* (sample size=8). Bold italicized row indicates the best-fitting model based on AICc and LRT results.

Biogeographic model	Free parameters	*d*	*e*	*j*	*x*	*n*	LnL	AICc
DEC	2	0.0542	5.02E-08	0	0	0	-25.04	56.48
DEC+J	3	0.0394	1.00E-12	0.6657	0	0	-22.68	57.36
DEC+X	3	0.1700	1.00E-12	0	-1.3240	0	-23.79	59.58
DEC+N	3	0.0370	0.0264	0	0	-1.7756	-24.00	60.00
DEC+J+X	4	0.1303	1.00E-12	1.1585	-1.4034	0	-21.57	64.48
DEC+J+N	4	0.0197	1.00E-12	0.5991	0	-1.9337	-21.23	63.80
DEC+X+N	4	0.0974	1.00E-12	0	-1.4409	-1.7968	-22.71	66.76
DEC+J+X+N	5	0.0580	1.00E-12	1.1098	-1.3852	-2.1002	-20.11	80.21
DIVALIKE	***2***	***0.0622***	***1.00E-12***	***0***	***0***	***0***	***-23.57***	***53.54***
DIVALIKE+J	3	0.0486	1.00E-12	0.2215	0	0	-22.54	57.08
DIVALIKE+X	3	0.1718	1.00E-12	0	-1.1616	0	-22.41	56.83
DIVALIKE+N	3	0.0397	1.00E-12	0	0	-1.4952	-22.61	57.22
DIVALIKE+J+X	4	0.1492	1.00E-12	0.4387	-1.3090	0	-21.38	64.10
DIVALIKE+J+N	4	0.0252	1.00E-12	0.2010	0	-1.8226	-21.24	63.81
DIVALIKE+X+N	4	0.1045	1.00E-12	0	-1.1407	-1.4978	-21.55	64.43
DIVALIKE+J+X+N	5	0.0735	1.00E-12	0.3997	-1.2554	-1.8076	-20.23	80.47
BAYAREALIKE	2	0.1161	0.1981	0	0	0	-26.83	60.05
BAYAREALIKE+J	3	0.0421	0.0233	0.9999	0	0	-24.28	60.56
BAYAREALIKE+X	3	0.3421	0.2068	0	-1.2191	0	-26.02	64.03
BAYAREALIKE+N	3	0.0653	0.2063	0	0	-1.9607	-25.83	63.66
BAYAREALIKE+J+X	4	0.1908	1.00E-12	0.7398	-1.9462	0	-23.19	67.72
BAYAREALIKE+J+N	4	0.0207	0.0251	0.9999	0	-2.0703	-22.57	66.46
BAYAREALIKE+X+N	4	0.1699	0.2042	0	-1.1163	-1.8261	-25.26	71.85
BAYAREALIKE+J+X+N	5	0.0489	0.0173	0.9999	-1.2320	-2.3711	-21.58	83.17

Table 3.14S. Likelihood-Ratio test results for the clade *Lepidoperca*. P-values with an asterisk indicate rejection of null hypothesis (no significative improvement when adding parameters) at p<0.05.

Nested model	More complex model	LnL Null	LnL Alt	DF Null	DF Alt	DF	D Statistic	p-value
DEC	DEC+J	-25.0404	-22.6799	2	3	1	4.72094	0.029797 *
DEC	DEC+X	-25.0404	-23.7882	2	3	1	2.50448	0.113523
DEC	DEC+N	-25.0404	-24.0008	2	3	1	2.07926	0.149313
DEC	DEC+J+X	-25.0404	-21.5715	2	4	2	6.93782	0.031151 *
DEC	DEC+J+N	-25.0404	-21.2332	2	4	2	7.61434	0.022211 *
DEC	DEC+X+N	-25.0404	-22.7144	2	4	2	4.65192	0.09769
DEC	DEC+J+X+N	-25.0404	-20.1052	2	5	3	9.87034	0.019701 *
DEC+J	DEC+J+X	-22.6799	-21.5715	3	4	1	2.21688	0.136509
DEC+J	DEC+J+N	-22.6799	-21.2332	3	4	1	2.8934	0.088943
DEC+J	DEC+J+X+N	-22.6799	-20.1052	3	5	2	5.1494	0.076177
DEC+X	DEC+J+X	-23.7882	-21.5715	3	4	1	4.43334	0.035243 *
DEC+X	DEC+X+N	-23.7882	-22.7144	3	4	1	2.14744	0.142808
DEC+X	DEC+J+X+N	-23.7882	-20.1052	3	5	2	7.36586	0.025149 *
DEC+N	DEC+J+N	-24.0008	-21.2332	3	4	1	5.53508	0.018639 *
DEC+N	DEC+X+N	-24.0008	-22.7144	3	4	1	2.57266	0.108725
DEC+N	DEC+J+X+N	-24.0008	-20.1052	3	5	2	7.79108	0.020332 *
DEC+J+X	DEC+J+X+N	-21.5715	-20.1052	4	5	1	2.93252	0.086812
DEC+J+N	DEC+J+X+N	-21.2332	-20.1052	4	5	1	2.256	0.133097
DEC+X+N	DEC+J+X+N	-22.7144	-20.1052	4	5	1	5.21842	0.022349 *
DIVALIKE	DIVALIKE+J	-23.5725	-22.5403	2	3	1	2.0644	0.150774
DIVALIKE	DIVALIKE+X	-23.5725	-22.4146	2	3	1	2.31574	0.12807
DIVALIKE	DIVALIKE+N	-23.5725	-22.61	2	3	1	1.92488	0.16532
DIVALIKE	DIVALIKE+J+X	-23.5725	-21.3842	2	4	2	4.37656	0.112109
DIVALIKE	DIVALIKE+J+N	-23.5725	-21.2396	2	4	2	4.66582	0.097013
DIVALIKE	DIVALIKE+X+N	-23.5725	-21.5481	2	4	2	4.0488	0.132073
DIVALIKE	DIVALIKE+J+X+N	-23.5725	-20.2326	2	5	3	6.67978	0.082836
DIVALIKE+J	DIVALIKE+J+X	-22.5403	-21.3842	3	4	1	2.31216	0.128366
DIVALIKE+J	DIVALIKE+J+N	-22.5403	-21.2396	3	4	1	2.60142	0.106768
DIVALIKE+J	DIVALIKE+J+X+N	-22.5403	-20.2326	3	5	2	4.61538	0.099491
DIVALIKE+X	DIVALIKE+J+X	-22.4146	-21.3842	3	4	1	2.06082	0.151129
DIVALIKE+X	DIVALIKE+X+N	-22.4146	-21.5481	3	4	1	1.73306	0.188021
DIVALIKE+X	DIVALIKE+J+X+N	-22.4146	-20.2326	3	5	2	4.36404	0.112813
DIVALIKE+N	DIVALIKE+J+N	-22.61	-21.2396	3	4	1	2.74094	0.097807
DIVALIKE+N	DIVALIKE+X+N	-22.61	-21.5481	3	4	1	2.12392	0.145015
DIVALIKE+N	DIVALIKE+J+X+N	-22.61	-20.2326	3	5	2	4.7549	0.092787
DIVALIKE+J+X	DIVALIKE+J+X+N	-21.3842	-20.2326	4	5	1	2.30322	0.129106
DIVALIKE+J+N	DIVALIKE+J+X+N	-21.2396	-20.2326	4	5	1	2.01396	0.155858
DIVALIKE+X+N	DIVALIKE+J+X+N	-21.5481	-20.2326	4	5	1	2.63098	0.104797
BAYAREALIKE	BAYAREALIKE+J	-26.8258	-24.2801	2	3	1	5.09148	0.024044 *
BAYAREALIKE	BAYAREALIKE+X	-26.8258	-26.0159	2	3	1	1.61976	0.203125
BAYAREALIKE	BAYAREALIKE+N	-26.8258	-25.8296	2	3	1	1.99242	0.158088
BAYAREALIKE	BAYAREALIKE+J+X	-26.8258	-23.1943	2	4	2	7.26304	0.026476 *
BAYAREALIKE	BAYAREALIKE+J+N	-26.8258	-22.5657	2	4	2	8.52022	0.014121 *
BAYAREALIKE	BAYAREALIKE+X+N	-26.8258	-25.2567	2	4	2	3.13822	0.20823
BAYAREALIKE	BAYAREALIKE+J+X+N	-26.8258	-21.5832	2	5	3	10.48528	0.014861 *
BAYAREALIKE+J	BAYAREALIKE+J+X	-24.2801	-23.1943	3	4	1	2.17156	0.140584
BAYAREALIKE+J	BAYAREALIKE+J+N	-24.2801	-22.5657	3	4	1	3.42874	0.064071
BAYAREALIKE+J	BAYAREALIKE+J+X+N	-24.2801	-21.5832	3	5	2	5.3938	0.067414
BAYAREALIKE+X	BAYAREALIKE+J+X	-26.0159	-23.1943	3	4	1	5.64328	0.017522 *
BAYAREALIKE+X	BAYAREALIKE+X+N	-26.0159	-25.2567	3	4	1	1.51846	0.217853
BAYAREALIKE+X	BAYAREALIKE+J+X+N	-26.0159	-21.5832	3	5	2	8.86552	0.011882 *
BAYAREALIKE+N	BAYAREALIKE+J+N	-25.8296	-22.5657	3	4	1	6.5278	0.01062 *
BAYAREALIKE+N	BAYAREALIKE+X+N	-25.8296	-25.2567	3	4	1	1.1458	0.28443
BAYAREALIKE+N	BAYAREALIKE+J+X+N	-25.8296	-21.5832	3	5	2	8.49286	0.014315 *
BAYAREALIKE+J+X	BAYAREALIKE+J+X+N	-23.1943	-21.5832	4	5	1	3.22224	0.072644
BAYAREALIKE+J+N	BAYAREALIKE+J+X+N	-22.5657	-21.5832	4	5	1	1.96506	0.160973
BAYAREALIKE+X+N	BAYAREALIKE+J+X+N	-25.2567	-21.5832	4	5	1	7.34706	0.006717 *

Table 3.15S. Parameter estimates, log-likelihood values (LnL), and model selection score for each of the 24 models assessed for the clade *Parma* (sample size=8). Bold italicized row indicates the best-fitting model based on AICc and LRT results.

Biogeographic model	Free parameters	*d*	*e*	*j*	*x*	*n*	LnL	AICc
DEC	2	0.0287	0.0308	0	0	0	-26.87	60.14
DEC+J	3	0.0221	0.0212	0.0980	0	0	-26.01	64.02
DEC+X	3	0.0181	0.0287	0	-0.5523	0	-26.55	65.10
DEC+N	3	0.0190	0.0292	0	0	-1.2126	-26.41	64.81
DEC+J+X	4	0.0100	0.0195	0.0774	-0.8560	0	-25.23	71.80
DEC+J+N	4	0.0104	0.0217	0.1127	0	-1.9463	-24.90	71.14
DEC+X+N	4	0.0175	0.0286	0	-0.1570	-1.0431	-26.40	74.14
DEC+J+X+N	5	0.0093	0.0212	0.1045	-0.1875	-1.7583	-24.89	89.79
DIVALIKE	***2***	***0.0277***	***0.0224***	***0***	***0***	***0***	***-26.29***	***58.98***
DIVALIKE+J	3	0.0232	0.0182	0.0691	0	0	-25.73	63.45
DIVALIKE+X	3	0.0199	0.0225	0	-0.4476	0	-26.06	64.11
DIVALIKE+N	3	0.0224	0.0243	0	0	-0.8492	-26.05	64.10
DIVALIKE+J+X	4	0.0114	0.0176	0.0647	-0.7900	0	-25.04	71.42
DIVALIKE+J+N	4	0.0114	0.0203	0.1037	0	-1.8845	-24.77	70.87
DIVALIKE+X+N	4	0.0209	0.0240	0	-0.1335	-0.7242	-26.03	73.40
DIVALIKE+J+X+N	5	0.0114	0.0203	0.1037	0.0000	-1.8845	-24.77	89.53
BAYAREALIKE	2	0.0322	0.0671	0	0	0	-28.02	62.44
BAYAREALIKE+J	3	0.0218	0.0343	0.1225	0	0	-26.78	65.56
BAYAREALIKE+X	3	0.0218	0.0669	0	-0.4697	0	-27.79	67.57
BAYAREALIKE+N	3	0.0159	0.0697	0	0	-1.7165	-27.50	66.99
BAYAREALIKE+J+X	4	0.0094	0.0305	0.0904	-0.9015	0	-25.89	73.12
BAYAREALIKE+J+N	4	0.0087	0.0321	0.1333	0	-2.3446	-25.40	72.13
BAYAREALIKE+X+N	4	0.0159	0.0696	0	0.0000	-1.7166	-27.50	76.32
BAYAREALIKE+J+X+N	5	0.0087	0.0321	0.1333	0.0000	-2.3446	-25.40	90.80

Table 3.16S. Likelihood-Ratio test results for the clade *Parma*. P-values with an asterisk indicate rejection of null hypothesis (no significative improvement when adding parameters) at p<0.05.

Nested model	More complex model	LnL Null	LnL Alt	DF Null	DF Alt	DF	D Statistic	p-value
DEC	DEC+J	-26.8678	-26.0109	2	3	1	1.71392	0.190478
DEC	DEC+X	-26.8678	-26.5514	2	3	1	0.6329	0.426294
DEC	DEC+N	-26.8678	-26.4058	2	3	1	0.92406	0.336411
DEC	DEC+J+X	-26.8678	-25.2334	2	4	2	3.26892	0.195058
DEC	DEC+J+N	-26.8678	-24.9025	2	4	2	3.93058	0.140115
DEC	DEC+X+N	-26.8678	-26.4032	2	4	2	0.9293	0.628355
DEC	DEC+J+X+N	-26.8678	-24.8944	2	5	3	3.94688	0.267258
DEC+J	DEC+J+X	-26.0109	-25.2334	3	4	1	1.555	0.212399
DEC+J	DEC+J+N	-26.0109	-24.9025	3	4	1	2.21666	0.136528
DEC+J	DEC+J+X+N	-26.0109	-24.8944	3	5	2	2.23296	0.32743
DEC+X	DEC+J+X	-26.5514	-25.2334	3	4	1	2.63602	0.104465
DEC+X	DEC+X+N	-26.5514	-26.4032	3	4	1	0.2964	0.586148
DEC+X	DEC+J+X+N	-26.5514	-24.8944	3	5	2	3.31398	0.190712
DEC+N	DEC+J+N	-26.4058	-24.9025	3	4	1	3.00652	0.08293
DEC+N	DEC+X+N	-26.4058	-26.4032	3	4	1	0.00524	0.942293
DEC+N	DEC+J+X+N	-26.4058	-24.8944	3	5	2	3.02282	0.220599
DEC+J+X	DEC+J+X+N	-25.2334	-24.8944	4	5	1	0.67796	0.41029
DEC+J+N	DEC+J+X+N	-24.9025	-24.8944	4	5	1	0.0163	0.898409
DEC+X+N	DEC+J+X+N	-26.4032	-24.8944	4	5	1	3.01758	0.082366
DIVALIKE	DIVALIKE+J	-26.2881	-25.7253	2	3	1	1.12562	0.288712
DIVALIKE	DIVALIKE+X	-26.2881	-26.0561	2	3	1	0.46408	0.495723
DIVALIKE	DIVALIKE+N	-26.2881	-26.0488	2	3	1	0.47858	0.489066
DIVALIKE	DIVALIKE+J+X	-26.2881	-25.0417	2	4	2	2.49286	0.287529
DIVALIKE	DIVALIKE+J+N	-26.2881	-24.766	2	4	2	3.04428	0.218244
DIVALIKE	DIVALIKE+X+N	-26.2881	-26.0333	2	4	2	0.50962	0.775064
DIVALIKE	DIVALIKE+J+X+N	-26.2881	-24.766	2	5	3	3.04428	0.384848
DIVALIKE+J	DIVALIKE+J+X	-25.7253	-25.0417	3	4	1	1.36724	0.242287
DIVALIKE+J	DIVALIKE+J+N	-25.7253	-24.766	3	4	1	1.91866	0.166004
DIVALIKE+J	DIVALIKE+J+X+N	-25.7253	-24.766	3	5	2	1.91866	0.38315
DIVALIKE+X	DIVALIKE+J+X	-26.0561	-25.0417	3	4	1	2.02878	0.154344
DIVALIKE+X	DIVALIKE+X+N	-26.0561	-26.0333	3	4	1	0.04554	0.831014
DIVALIKE+X	DIVALIKE+J+X+N	-26.0561	-24.766	3	5	2	2.5802	0.275243
DIVALIKE+N	DIVALIKE+J+N	-26.0488	-24.766	3	4	1	2.5657	0.109204
DIVALIKE+N	DIVALIKE+X+N	-26.0488	-26.0333	3	4	1	0.03104	0.860151
DIVALIKE+N	DIVALIKE+J+X+N	-26.0488	-24.766	3	5	2	2.5657	0.277246
DIVALIKE+J+X	DIVALIKE+J+X+N	-25.0417	-24.766	4	5	1	0.55142	0.457738
DIVALIKE+J+N	DIVALIKE+J+X+N	-24.766	-24.766	4	5	1	0	1
DIVALIKE+X+N	DIVALIKE+J+X+N	-26.0333	-24.766	4	5	1	2.53466	0.111371
BAYAREALIKE	BAYAREALIKE+J	-28.0204	-26.779	2	3	1	2.48286	0.115093
BAYAREALIKE	BAYAREALIKE+X	-28.0204	-27.7874	2	3	1	0.4661	0.494787
BAYAREALIKE	BAYAREALIKE+N	-28.0204	-27.4953	2	3	1	1.05026	0.305447
BAYAREALIKE	BAYAREALIKE+J+X	-28.0204	-25.8912	2	4	2	4.25848	0.118928
BAYAREALIKE	BAYAREALIKE+J+N	-28.0204	-25.4004	2	4	2	5.24	0.072803
BAYAREALIKE	BAYAREALIKE+X+N	-28.0204	-27.4953	2	4	2	1.05026	0.591478
BAYAREALIKE	BAYAREALIKE+J+X+N	-28.0204	-25.4004	2	5	3	5.24	0.155043
BAYAREALIKE+J	BAYAREALIKE+J+X	-26.779	-25.8912	3	4	1	1.77562	0.182688
BAYAREALIKE+J	BAYAREALIKE+J+N	-26.779	-25.4004	3	4	1	2.75714	0.096821
BAYAREALIKE+J	BAYAREALIKE+J+X+N	-26.779	-25.4004	3	5	2	2.75714	0.251939
BAYAREALIKE+X	BAYAREALIKE+J+X	-27.7874	-25.8912	3	4	1	3.79238	0.051486
BAYAREALIKE+X	BAYAREALIKE+X+N	-27.7874	-27.4953	3	4	1	0.58416	0.444686
BAYAREALIKE+X	BAYAREALIKE+J+X+N	-27.7874	-25.4004	3	5	2	4.7739	0.09191
BAYAREALIKE+N	BAYAREALIKE+J+N	-27.4953	-25.4004	3	4	1	4.18974	0.040669 *
BAYAREALIKE+N	BAYAREALIKE+X+N	-27.4953	-27.4953	3	4	1	0	1
BAYAREALIKE+N	BAYAREALIKE+J+X+N	-27.4953	-25.4004	3	5	2	4.18974	0.123086
BAYAREALIKE+J+X	BAYAREALIKE+J+X+N	-25.8912	-25.4004	4	5	1	0.98152	0.321824
BAYAREALIKE+J+N	BAYAREALIKE+J+X+N	-25.4004	-25.4004	4	5	1	0	1
BAYAREALIKE+X+N	BAYAREALIKE+J+X+N	-27.4953	-25.4004	4	5	1	4.18974	0.040669 *

Table 3.17S. Parameter estimates, log-likelihood values (LnL), and model selection score for each of the 24 models assessed for the clade *Hypoplectrodes* (sample size=9). Bold italicized row indicates the best-fitting model based on AICc and LRT results.

Biogeographic model	Free parameters	*d*	*e*	*j*	*x*	*n*	LnL	AICc
DEC	2	0.0379	0.0314	0	0	0	-40.02	86.04
DEC+J	3	0.0223	1.00E-12	0.9972	0	0	-32.23	75.27
DEC+X	3	0.0201	0.0350	0	-0.4100	0	-39.45	89.70
DEC+N	3	0.0335	0.0276	0	0	-0.2814	-39.99	90.77
DEC+J+X	4	0.0080	1.00E-12	0.4685	-0.6293	0	-31.23	80.46
DEC+J+N	4	0.0183	7.59E-09	0.8503	0	-0.5306	-32.08	82.16
DEC+X+N	4	0.0197	0.0330	0	-0.3982	-0.0877	-39.45	96.91
DEC+J+X+N	5	0.0082	1.00E-12	0.6263	-0.5512	-0.2774	-31.20	92.40
DIVALIKE	2	0.0365	1.00E-12	0	0	0	-36.29	78.58
DIVALIKE+J	***3***	***0.0240***	***1.00E-12***	***0.4704***	***0***	***0***	***-31.71***	***74.21***
DIVALIKE+X	3	0.0216	1.00E-12	0	-0.3372	0	-35.89	82.59
DIVALIKE+N	3	0.0316	1.00E-12	0	0	-0.3953	-36.20	83.21
DIVALIKE+J+X	4	0.0091	1.00E-12	0.3195	-0.5833	0	-30.81	79.62
DIVALIKE+J+N	4	0.0196	1.00E-12	0.4120	0	-0.5347	-31.55	81.09
DIVALIKE+X+N	4	0.0199	1.00E-12	0	-0.3457	-0.1828	-35.88	89.75
DIVALIKE+J+X+N	5	0.0088	1.00E-12	0.3075	-0.5414	-0.2744	-30.78	91.55
BAYAREALIKE	2	0.0553	0.1894	0	0	0	-44.06	94.13
BAYAREALIKE+J	3	0.0213	3.79E-08	0.9999	0	0	-32.72	76.24
BAYAREALIKE+X	3	0.0274	0.1991	0	-0.4768	0	-43.37	97.54
BAYAREALIKE+N	3	0.0514	0.1887	0	0	-0.1860	-44.10	99.01
BAYAREALIKE+J+X	4	0.0066	1.00E-12	0.8592	-0.7141	0	-31.59	81.19
BAYAREALIKE+J+N	4	0.0175	1.00E-12	0.9999	0	-0.5265	-32.58	83.15
BAYAREALIKE+X+N	4	0.0273	0.1991	0	-0.4792	0.0000	-43.37	104.74
BAYAREALIKE+J+X+N	5	0.0071	1.00E-12	0.9999	-0.6312	-0.2141	-31.55	93.11

Table 3.18S. Likelihood-Ratio test results for the clade *Hypoplectrodes*. P-values with an asterisk indicate rejection of null hypothesis (no significative improvement when adding parameters) at $p<0.05$.

Nested model	More complex model	LnL Null	LnL Alt	DF Null	DF Alt	DF	D Statistic	p-value
DEC	DEC+J	-40.0204	-32.2335	2	3	1	15.5739	7.93E-05 *
DEC	DEC+X	-40.0204	-39.4504	2	3	1	1.14	0.285652
DEC	DEC+N	-40.0204	-39.9867	2	3	1	0.06736	0.79522
DEC	DEC+J+X	-40.0204	-31.2314	2	4	2	17.578	0.000152 *
DEC	DEC+J+N	-40.0204	-32.0798	2	4	2	15.88126	0.000356 *
DEC	DEC+X+N	-40.0204	-39.4529	2	4	2	1.13506	0.566924
DEC	DEC+J+X+N	-40.0204	-31.2012	2	5	3	17.63854	0.000522 *
DEC+J	DEC+J+X	-32.2335	-31.2314	3	4	1	2.0041	0.156874
DEC+J	DEC+J+N	-32.2335	-32.0798	3	4	1	0.30736	0.579305
DEC+J	DEC+J+X+N	-32.2335	-31.2012	3	5	2	2.06464	0.35618
DEC+X	DEC+J+X	-39.4504	-31.2314	3	4	1	16.438	5.03E-05 *
DEC+X	DEC+X+N	-39.4504	-39.4529	3	4	1	0	1
DEC+X	DEC+J+X+N	-39.4504	-31.2012	3	5	2	16.49854	0.000261 *
DEC+N	DEC+J+N	-39.9867	-32.0798	3	4	1	15.8139	6.99E-05 *
DEC+N	DEC+X+N	-39.9867	-39.4529	3	4	1	1.0677	0.301466
DEC+N	DEC+J+X+N	-39.9867	-31.2012	3	5	2	17.57118	0.000153 *
DEC+J+X	DEC+J+X+N	-31.2314	-31.2012	4	5	1	0.06054	0.805644
DEC+J+N	DEC+J+X+N	-32.0798	-31.2012	4	5	1	1.75728	0.184964
DEC+X+N	DEC+J+X+N	-39.4529	-31.2012	4	5	1	16.50348	4.86E-05 *
DIVALIKE	DIVALIKE+J	-36.2889	-31.7058	2	3	1	9.16626	0.002465 *
DIVALIKE	DIVALIKE+X	-36.2889	-35.8948	2	3	1	0.7883	0.374615
DIVALIKE	DIVALIKE+N	-36.2889	-36.2041	2	3	1	0.16974	0.680343
DIVALIKE	DIVALIKE+J+X	-36.2889	-30.8123	2	4	2	10.9533	0.004183 *
DIVALIKE	DIVALIKE+J+N	-36.2889	-31.5455	2	4	2	9.48684	0.008709 *
DIVALIKE	DIVALIKE+X+N	-36.2889	-35.8751	2	4	2	0.82778	0.661074
DIVALIKE	DIVALIKE+J+X+N	-36.2889	-30.7757	2	5	3	11.0265	0.011583 *
DIVALIKE+J	DIVALIKE+J+X	-31.7058	-30.8123	3	4	1	1.78704	0.181287
DIVALIKE+J	DIVALIKE+J+N	-31.7058	-31.5455	3	4	1	0.32058	0.571259
DIVALIKE+J	DIVALIKE+J+X+N	-31.7058	-30.7757	3	5	2	1.86024	0.394506
DIVALIKE+X	DIVALIKE+J+X	-35.8948	-30.8123	3	4	1	10.165	0.001431 *
DIVALIKE+X	DIVALIKE+X+N	-35.8948	-35.8751	3	4	1	0.03948	0.842501
DIVALIKE+X	DIVALIKE+J+X+N	-35.8948	-30.7757	3	5	2	10.2382	0.005981 *
DIVALIKE+N	DIVALIKE+J+N	-36.2041	-31.5455	3	4	1	9.3171	0.00227 *
DIVALIKE+N	DIVALIKE+X+N	-36.2041	-35.8751	3	4	1	0.65804	0.417253
DIVALIKE+N	DIVALIKE+J+X+N	-36.2041	-30.7757	3	5	2	10.85676	0.00439 *
DIVALIKE+J+X	DIVALIKE+J+X+N	-30.8123	-30.7757	4	5	1	0.0732	0.786733
DIVALIKE+J+N	DIVALIKE+J+X+N	-31.5455	-30.7757	4	5	1	1.53966	0.214668
DIVALIKE+X+N	DIVALIKE+J+X+N	-35.8751	-30.7757	4	5	1	10.19872	0.001405 *
BAYAREALIKE	BAYAREALIKE+J	-44.0641	-32.7224	2	3	1	22.68332	1.91E-06 *
BAYAREALIKE	BAYAREALIKE+X	-44.0641	-43.3701	2	3	1	1.38802	0.23874
BAYAREALIKE	BAYAREALIKE+N	-44.0641	-44.1048	2	3	1	0	1
BAYAREALIKE	BAYAREALIKE+J+X	-44.0641	-31.5941	2	4	2	24.94004	3.84E-06 *
BAYAREALIKE	BAYAREALIKE+J+N	-44.0641	-32.5761	2	4	2	22.97594	1.03E-05 *
BAYAREALIKE	BAYAREALIKE+X+N	-44.0641	-43.3701	2	4	2	1.38806	0.499559
BAYAREALIKE	BAYAREALIKE+J+X+N	-44.0641	-31.553	2	5	3	25.0222	1.53E-05 *
BAYAREALIKE+J	BAYAREALIKE+J+X	-32.7224	-31.5941	3	4	1	2.25672	0.133036
BAYAREALIKE+J	BAYAREALIKE+J+N	-32.7224	-32.5761	3	4	1	0.29262	0.588546
BAYAREALIKE+J	BAYAREALIKE+J+X+N	-32.7224	-31.553	3	5	2	2.33888	0.310541
BAYAREALIKE+X	BAYAREALIKE+J+X	-43.3701	-31.5941	3	4	1	23.55202	1.22E-06 *
BAYAREALIKE+X	BAYAREALIKE+X+N	-43.3701	-43.3701	3	4	1	4E-05	0.994954
BAYAREALIKE+X	BAYAREALIKE+J+X+N	-43.3701	-31.553	3	5	2	23.63418	7.38E-06 *
BAYAREALIKE+N	BAYAREALIKE+J+N	-44.1048	-32.5761	3	4	1	23.0574	1.57E-06 *
BAYAREALIKE+N	BAYAREALIKE+X+N	-44.1048	-43.3701	3	4	1	1.46952	0.225421
BAYAREALIKE+N	BAYAREALIKE+J+X+N	-44.1048	-31.553	3	5	2	25.10366	3.54E-06 *
BAYAREALIKE+J+X	BAYAREALIKE+J+X+N	-31.5941	-31.553	4	5	1	0.08216	0.774391
BAYAREALIKE+J+N	BAYAREALIKE+J+X+N	-32.5761	-31.553	4	5	1	2.04626	0.152581
BAYAREALIKE+X+N	BAYAREALIKE+J+X+N	-43.3701	-31.553	4	5	1	23.63414	1.17E-06 *

Table 3.19S. Parameter estimates, log-likelihood values (LnL), and model selection score for each of the 24 models assessed for the clade *Chironemus-Aplodactylus* (sample size=11). Bold italicized row indicates the best-fitting model based on AICc and LRT results.

Biogeographic model	Free parameters	*d*	*e*	*j*	*x*	*n*	LnL	AICc
DEC	2	0.0188	0.0295	0	0	0	-53.36	112.22
DEC+J	3	0.0160	0.0249	0.8565	0	0	-52.12	113.67
DEC+X	3	0.0050	0.0225	0	-0.9609	0	-49.92	109.28
DEC+N	3	0.0145	0.0297	0	0	-0.8259	-52.84	115.12
DEC+J+X	4	0.0029	0.0187	0.3442	-1.1672	0	-47.60	109.87
DEC+J+N	4	0.0094	0.0268	1.3932	0	-1.4836	-51.17	117.00
DEC+X+N	4	0.0040	0.0217	0	-0.9748	-0.5266	-49.52	113.71
DEC+J+X+N	5	0.0029	0.0201	0.4410	-1.0989	-0.3700	-47.33	116.67
DIVALIKE	2	0.0193	0.0243	0	0	0	-53.06	111.63
DIVALIKE+J	3	0.0165	0.0228	0.3466	0	0	-51.99	113.41
DIVALIKE+X	3	0.0059	0.0204	0	-0.8919	0	-49.54	108.50
DIVALIKE+N	3	0.0140	0.0247	0	0	-0.9949	-52.54	114.51
DIVALIKE+J+X	4	0.0016	0.0222	1.4867	-1.5909	0	-45.98	106.64
DIVALIKE+J+N	4	0.0106	0.0263	0.9415	0	-1.2006	-51.13	116.92
DIVALIKE+X+N	4	0.0047	0.0201	0	-0.8732	-0.7189	-49.06	112.78
DIVALIKE+J+X+N	5	0.0016	0.0222	1.4867	-1.5909	0.0000	-45.98	113.97
BAYAREALIKE	2	0.0292	0.0823	0	0	0	-52.98	111.46
BAYAREALIKE+J	3	0.0283	0.0799	0.0088	0	0	-52.98	115.39
BAYAREALIKE+X	3	0.0085	0.0738	0	-0.8137	0	-50.66	110.74
BAYAREALIKE+N	3	0.0165	0.0790	0	0	-1.3963	-52.23	113.88
BAYAREALIKE+J+X	***4***	***0.0016***	***0.0229***	***0.9999***	***-1.6099***	***0***	***-45.53***	***105.73***
BAYAREALIKE+J+N	4	0.0096	0.0304	0.9999	0	-1.5120	-51.15	116.97
BAYAREALIKE+X+N	4	0.0052	0.0688	0	-0.8317	-1.0764	-49.87	114.42
BAYAREALIKE+J+X+N	5	0.0013	0.0225	0.9999	-1.7115	-0.0207	-45.51	113.01

Table 3.20S. Likelihood-Ratio test results for the clade *Chironemus-Aplodactylus*. P-values with an asterisk indicate rejection of null hypothesis (no significative improvement when adding parameters) at p<0.05.

Nested model	More complex model	LnL Null	LnL Alt	DF Null	DF Alt	DF	D Statistic	p-value
DEC	DEC+J	-53.3576	-52.12	2	3	1	2.47522	0.115653
DEC	DEC+X	-53.3576	-49.9245	2	3	1	6.86624	0.008784 *
DEC	DEC+N	-53.3576	-52.8439	2	3	1	1.02742	0.310765
DEC	DEC+J+X	-53.3576	-47.6036	2	4	2	11.50808	0.00317 *
DEC	DEC+J+N	-53.3576	-51.1673	2	4	2	4.38058	0.111884
DEC	DEC+X+N	-53.3576	-49.5225	2	4	2	7.67016	0.0216 *
DEC	DEC+J+X+N	-53.3576	-47.3342	2	5	3	12.04676	0.007225 *
DEC+J	DEC+J+X	-52.12	-47.6036	3	4	1	9.03286	0.002652 *
DEC+J	DEC+J+N	-52.12	-51.1673	3	4	1	1.90536	0.16748
DEC+J	DEC+J+X+N	-52.12	-47.3342	3	5	2	9.57154	0.008348 *
DEC+X	DEC+J+X	-49.9245	-47.6036	3	4	1	4.64184	0.031202 *
DEC+X	DEC+X+N	-49.9245	-49.5225	3	4	1	0.80392	0.369924
DEC+X	DEC+J+X+N	-49.9245	-47.3342	3	5	2	5.18052	0.075001
DEC+N	DEC+J+N	-52.8439	-51.1673	3	4	1	3.35316	0.067076
DEC+N	DEC+X+N	-52.8439	-49.5225	3	4	1	6.64274	0.009956 *
DEC+N	DEC+J+X+N	-52.8439	-47.3342	3	5	2	11.01934	0.004047 *
DEC+J+X	DEC+J+X+N	-47.6036	-47.3342	4	5	1	0.53868	0.46298
DEC+J+N	DEC+J+X+N	-51.1673	-47.3342	4	5	1	7.66618	0.005627 *
DEC+X+N	DEC+J+X+N	-49.5225	-47.3342	4	5	1	4.3766	0.036436 *
DIVALIKE	DIVALIKE+J	-53.0646	-51.993	2	3	1	2.1432	0.143203
DIVALIKE	DIVALIKE+X	-53.0646	-49.5371	2	3	1	7.05486	0.007905 *
DIVALIKE	DIVALIKE+N	-53.0646	-52.5428	2	3	1	1.04348	0.307013
DIVALIKE	DIVALIKE+J+X	-53.0646	-45.9845	2	4	2	14.16008	0.000842 *
DIVALIKE	DIVALIKE+J+N	-53.0646	-51.1285	2	4	2	3.8721	0.144273
DIVALIKE	DIVALIKE+X+N	-53.0646	-49.0553	2	4	2	8.01848	0.018147 *
DIVALIKE	DIVALIKE+J+X+N	-53.0646	-45.9845	2	5	3	14.16008	0.002695 *
DIVALIKE+J	DIVALIKE+J+X	-51.993	-45.9845	3	4	1	12.01688	0.000527 *
DIVALIKE+J	DIVALIKE+J+N	-51.993	-51.1285	3	4	1	1.7289	0.188551
DIVALIKE+J	DIVALIKE+J+X+N	-51.993	-45.9845	3	5	2	12.01688	0.002458 *
DIVALIKE+X	DIVALIKE+J+X	-49.5371	-45.9845	3	4	1	7.10522	0.007686 *
DIVALIKE+X	DIVALIKE+X+N	-49.5371	-49.0553	3	4	1	0.96362	0.326277
DIVALIKE+X	DIVALIKE+J+X+N	-49.5371	-45.9845	3	5	2	7.10522	0.02865 *
DIVALIKE+N	DIVALIKE+J+N	-52.5428	-51.1285	3	4	1	2.82862	0.092598
DIVALIKE+N	DIVALIKE+X+N	-52.5428	-49.0553	3	4	1	6.975	0.008266 *
DIVALIKE+N	DIVALIKE+J+X+N	-52.5428	-45.9845	3	5	2	13.1166	0.001418 *
DIVALIKE+J+X	DIVALIKE+J+X+N	-45.9845	-45.9845	4	5	1	0	1
DIVALIKE+J+N	DIVALIKE+J+X+N	-51.1285	-45.9845	4	5	1	10.28798	0.001339 *
DIVALIKE+X+N	DIVALIKE+J+X+N	-49.0553	-45.9845	4	5	1	6.1416	0.013204 *
BAYAREALIKE	BAYAREALIKE+J	-52.9793	-52.9796	2	3	1	0	1
BAYAREALIKE	BAYAREALIKE+X	-52.9793	-50.6573	2	3	1	4.64402	0.031162 *
BAYAREALIKE	BAYAREALIKE+N	-52.9793	-52.2257	2	3	1	1.50712	0.219579
BAYAREALIKE	BAYAREALIKE+J+X	-52.9793	-45.5296	2	4	2	14.89934	0.000582 *
BAYAREALIKE	BAYAREALIKE+J+N	-52.9793	-51.1524	2	4	2	3.65372	0.160918
BAYAREALIKE	BAYAREALIKE+X+N	-52.9793	-49.8743	2	4	2	6.21	0.044825 *
BAYAREALIKE	BAYAREALIKE+J+X+N	-52.9793	-45.5067	2	5	3	14.94512	0.001864 *
BAYAREALIKE+J	BAYAREALIKE+J+X	-52.9796	-45.5296	3	4	1	14.9	0.000113 *
BAYAREALIKE+J	BAYAREALIKE+J+N	-52.9796	-51.1524	3	4	1	3.65438	0.055922
BAYAREALIKE+J	BAYAREALIKE+J+X+N	-52.9796	-45.5067	3	5	2	14.94578	0.000568 *
BAYAREALIKE+X	BAYAREALIKE+J+X	-50.6573	-45.5296	3	4	1	10.25532	0.001363 *
BAYAREALIKE+X	BAYAREALIKE+X+N	-50.6573	-49.8743	3	4	1	1.56598	0.210792
BAYAREALIKE+X	BAYAREALIKE+J+X+N	-50.6573	-45.5067	3	5	2	10.3011	0.005796 *
BAYAREALIKE+N	BAYAREALIKE+J+N	-52.2257	-51.1524	3	4	1	2.1466	0.142886
BAYAREALIKE+N	BAYAREALIKE+X+N	-52.2257	-49.8743	3	4	1	4.70288	0.030112 *
BAYAREALIKE+N	BAYAREALIKE+J+X+N	-52.2257	-45.5067	3	5	2	13.438	0.001208 *
BAYAREALIKE+J+X	BAYAREALIKE+J+X+N	-45.5296	-45.5067	4	5	1	0.04578	0.830576
BAYAREALIKE+J+N	BAYAREALIKE+J+X+N	-51.1524	-45.5067	4	5	1	11.2914	0.000779 *
BAYAREALIKE+X+N	BAYAREALIKE+J+X+N	-49.8743	-45.5067	4	5	1	8.73512	0.003121 *

Table 3.21S. Parameter estimates, log-likelihood values (LnL), and model selection score for each of the 24 models assessed for the clade *Goniistius-Morwong* (sample size=11). Bold italicized row indicates the best-fitting model based on AICc and LRT results.

Biogeographic model	Free parameters	*d*	*e*	*j*	*x*	*n*	LnL	AICc
DEC	2	0.0247	0.0600	0	0	0	-57.34	120.19
DEC+J	3	0.0182	0.0338	0.1638	0	0	-56.05	121.52
DEC+X	3	0.0094	0.0512	0	-0.8473	0	-49.02	107.47
DEC+N	3	0.0224	0.0603	0	0	-0.1428	-57.25	123.93
DEC+J+X	4	0.0031	0.0604	0.1982	-1.4396	0	-44.71	104.09
DEC+J+N	4	0.0168	0.0340	0.1438	0	-0.1175	-55.94	126.56
DEC+X+N	4	0.0029	0.0506	0	-1.4064	-0.4316	-46.80	108.26
DEC+J+X+N	5	0.0011	0.0212	0.0558	-1.7730	-0.2562	-42.40	106.79
DIVALIKE	2	0.0222	0.0350	0	0	0	-56.06	117.63
DIVALIKE+J	3	0.0181	0.0241	0.0936	0	0	-55.25	119.93
DIVALIKE+X	3	0.0119	0.0281	0	-0.5902	0	-49.43	108.29
DIVALIKE+N	3	0.0184	0.0350	0	0	-0.2604	-55.93	121.29
DIVALIKE+J+X	***4***	***0.0017***	***0.0191***	***0.0536***	***-1.6833***	***0***	***-42.11***	***98.89***
DIVALIKE+J+N	4	0.0170	0.0244	0.0857	0	-0.1314	-55.16	124.98
DIVALIKE+X+N	4	0.0081	0.0808	0	-1.0747	-0.0099	-47.43	109.52
DIVALIKE+J+X+N	5	0.0010	0.0184	0.0476	-1.9300	-0.0517	-41.92	105.84
BAYAREALIKE	2	0.0287	0.1261	0	0	0	-57.23	119.96
BAYAREALIKE+J	3	0.0241	0.0975	0.0582	0	0	-56.90	123.23
BAYAREALIKE+X	3	0.0224	0.1336	0	-0.3124	0	-53.97	117.37
BAYAREALIKE+N	3	0.0275	0.1280	0	0	0.0696	-57.18	123.79
BAYAREALIKE+J+X	4	0.0094	0.0662	0.1258	-0.6714	0	-49.61	113.88
BAYAREALIKE+J+N	4	0.0146	0.0913	0.0461	0	-0.5886	-56.57	127.81
BAYAREALIKE+X+N	4	0.0025	0.1131	0	-1.5704	-0.3708	-46.90	108.47
BAYAREALIKE+J+X+N	5	0.0012	0.0314	0.0825	-1.8152	-0.1731	-43.48	108.95

Table 3.22S. Likelihood-Ratio test results for the clade *Goniistius-Morwong*. P-values with an asterisk indicate rejection of null hypothesis (no significative improvement when adding parameters) at p<0.05.

Nested model	More complex model	LnL Null	LnL Alt	DF Null	DF Alt	DF	D Statistic	p-value
DEC	DEC+J	-57.3426	-56.045	2	3	1	2.59522	0.107187
DEC	DEC+X	-57.3426	-49.0194	2	3	1	16.64656	4.5E-05*
DEC	DEC+N	-57.3426	-57.2505	2	3	1	0.18428	0.667721
DEC	DEC+J+X	-57.3426	-44.7132	2	4	2	25.25878	3.27E-06*
DEC	DEC+J+N	-57.3426	-55.9448	2	4	2	2.7957	0.247128
DEC	DEC+X+N	-57.3426	-46.7976	2	4	2	21.09014	2.63E-05*
DEC	DEC+J+X+N	-57.3426	-42.3964	2	5	3	29.8924	1.45E-06*
DEC+J	DEC+J+X	-56.045	-44.7132	3	4	1	22.66356	1.93E-06*
DEC+J	DEC+J+N	-56.045	-55.9448	3	4	1	0.20048	0.654334
DEC+J	DEC+J+X+N	-56.045	-42.3964	3	5	2	27.29718	1.18E-06*
DEC+X	DEC+J+X	-49.0194	-44.7132	3	4	1	8.61222	0.003339*
DEC+X	DEC+X+N	-49.0194	-46.7976	3	4	1	4.44358	0.035033*
DEC+X	DEC+J+X+N	-49.0194	-42.3964	3	5	2	13.24584	0.00133*
DEC+N	DEC+J+N	-57.2505	-55.9448	3	4	1	2.61142	0.106097
DEC+N	DEC+X+N	-57.2505	-46.7976	3	4	1	20.90586	4.82E-06*
DEC+N	DEC+J+X+N	-57.2505	-42.3964	3	5	2	29.70812	3.54E-07*
DEC+J+X	DEC+J+X+N	-44.7132	-42.3964	4	5	1	4.63362	0.031351*
DEC+J+N	DEC+J+X+N	-55.9448	-42.3964	4	5	1	27.0967	1.94E-07*
DEC+X+N	DEC+J+X+N	-46.7976	-42.3964	4	5	1	8.80226	0.003009*
DIVALIKE	DIVALIKE+J	-56.0629	-55.2492	2	3	1	1.62736	0.202069
DIVALIKE	DIVALIKE+X	-56.0629	-49.4326	2	3	1	13.26064	0.000271*
DIVALIKE	DIVALIKE+N	-56.0629	-55.9292	2	3	1	0.2675	0.605014
DIVALIKE	DIVALIKE+J+X	-56.0629	-42.1099	2	4	2	27.906	8.72E-07*
DIVALIKE	DIVALIKE+J+N	-56.0629	-55.1564	2	4	2	1.8131	0.403915
DIVALIKE	DIVALIKE+X+N	-56.0629	-47.425	2	4	2	17.27576	0.000177*
DIVALIKE	DIVALIKE+J+X+N	-56.0629	-41.9186	2	5	3	28.2887	3.16E-06*
DIVALIKE+J	DIVALIKE+J+X	-55.2492	-42.1099	3	4	1	26.27864	2.96E-07*
DIVALIKE+J	DIVALIKE+J+N	-55.2492	-55.1564	3	4	1	0.18574	0.666486
DIVALIKE+J	DIVALIKE+J+X+N	-55.2492	-41.9186	3	5	2	26.66134	1.62E-06*
DIVALIKE+X	DIVALIKE+J+X	-49.4326	-42.1099	3	4	1	14.64536	0.00013*
DIVALIKE+X	DIVALIKE+X+N	-49.4326	-47.425	3	4	1	4.01512	0.045094*
DIVALIKE+X	DIVALIKE+J+X+N	-49.4326	-41.9186	3	5	2	15.02806	0.000545*
DIVALIKE+N	DIVALIKE+J+N	-55.9292	-55.1564	3	4	1	1.5456	0.213786
DIVALIKE+N	DIVALIKE+X+N	-55.9292	-47.425	3	4	1	17.00826	3.72E-05*
DIVALIKE+N	DIVALIKE+J+X+N	-55.9292	-41.9186	3	5	2	28.0212	8.23E-07*
DIVALIKE+J+X	DIVALIKE+J+X+N	-42.1099	-41.9186	4	5	1	0.3827	0.536162
DIVALIKE+J+N	DIVALIKE+J+X+N	-55.1564	-41.9186	4	5	1	26.4756	2.67E-07*
DIVALIKE+X+N	DIVALIKE+J+X+N	-47.425	-41.9186	4	5	1	11.01294	0.000905*
BAYAREALIKE	BAYAREALIKE+J	-57.2312	-56.9029	2	3	1	0.65652	0.417791
BAYAREALIKE	BAYAREALIKE+X	-57.2312	-53.9704	2	3	1	6.52162	0.010657*
BAYAREALIKE	BAYAREALIKE+N	-57.2312	-57.1783	2	3	1	0.10568	0.745117
BAYAREALIKE	BAYAREALIKE+J+X	-57.2312	-49.6078	2	4	2	15.24668	0.000489*
BAYAREALIKE	BAYAREALIKE+J+N	-57.2312	-56.574	2	4	2	1.3144	0.518301
BAYAREALIKE	BAYAREALIKE+X+N	-57.2312	-46.8993	2	4	2	20.6638	3.26E-05*
BAYAREALIKE	BAYAREALIKE+J+X+N	-57.2312	-43.4759	2	5	3	27.51064	4.6E-06*
BAYAREALIKE+J	BAYAREALIKE+J+X	-56.9029	-49.6078	3	4	1	14.59016	0.000134*
BAYAREALIKE+J	BAYAREALIKE+J+N	-56.9029	-56.574	3	4	1	0.65788	0.417309
BAYAREALIKE+J	BAYAREALIKE+J+X+N	-56.9029	-43.4759	3	5	2	26.85412	1.47E-06*
BAYAREALIKE+X	BAYAREALIKE+J+X	-53.9704	-49.6078	3	4	1	8.72506	0.003139*
BAYAREALIKE+X	BAYAREALIKE+X+N	-53.9704	-46.8993	3	4	1	14.14218	0.00017*
BAYAREALIKE+X	BAYAREALIKE+J+X+N	-53.9704	-43.4759	3	5	2	20.98902	2.77E-05*
BAYAREALIKE+N	BAYAREALIKE+J+N	-57.1783	-56.574	3	4	1	1.20872	0.271586
BAYAREALIKE+N	BAYAREALIKE+X+N	-57.1783	-46.8993	3	4	1	20.55812	5.78E-06*
BAYAREALIKE+N	BAYAREALIKE+J+X+N	-57.1783	-43.4759	3	5	2	27.40496	1.12E-06*
BAYAREALIKE+J+X	BAYAREALIKE+J+X+N	-49.6078	-43.4759	4	5	1	12.26396	0.000462*
BAYAREALIKE+J+N	BAYAREALIKE+J+X+N	-56.574	-43.4759	4	5	1	26.19624	3.08E-07*
BAYAREALIKE+X+N	BAYAREALIKE+J+X+N	-46.8993	-43.4759	4	5	1	6.84684	0.00888*

Table 3.23S. Parameter estimates, log-likelihood values (LnL), and model selection score for each of the 24 models assessed for the clade *Girella* (sample size=17). Bold italicized row indicates the best-fitting model based on AICc and LRT results.

Biogeographic model	Free parameters	*d*	*e*	*j*	*x*	*n*	LnL	AICc
DEC	2	0.0160	0.0380	0	0	0	-62.80	130.45
DEC+J	3	0.0096	0.0142	0.0698	0	0	-57.50	122.84
DEC+X	3	0.0026	0.0204	0	-1.0594	0	-58.00	123.84
DEC+N	3	0.0128	0.0366	0	0	-0.3443	-62.61	133.07
DEC+J+X	***4***	***0.0013***	***0.0095***	***0.0214***	***-1.1936***	***0***	***-50.56***	***112.45***
DEC+J+N	4	0.0064	0.0139	0.0498	0	-0.6046	-57.18	125.68
DEC+X+N	4	0.0028	0.0210	0	-1.0308	0.0000	-57.99	127.32
DEC+J+X+N	5	0.0012	0.0095	0.0209	-1.2136	0.0000	-50.55	116.55
DIVALIKE	2	0.0178	0.0340	0	0	0	-62.72	130.29
DIVALIKE+J	3	0.0102	0.0130	0.0664	0	0	-57.15	122.14
DIVALIKE+X	3	0.0058	0.0254	0	-0.7464	0	-59.08	126.01
DIVALIKE+N	3	0.0147	0.0332	0	0	-0.3049	-62.65	133.14
DIVALIKE+J+X	4	0.0025	0.0102	0.0300	-0.8874	0	-51.25	113.83
DIVALIKE+J+N	4	0.0071	0.0128	0.0507	0	-0.5450	-56.86	125.05
DIVALIKE+X+N	4	0.0053	0.0250	0	-0.7956	0.0000	-59.07	129.47
DIVALIKE+J+X+N	5	0.0017	0.0099	0.0252	-1.0934	0.0000	-50.94	117.34
BAYAREALIKE	2	0.0168	0.1125	0	0	0	-65.14	135.13
BAYAREALIKE+J	3	0.0078	0.0349	0.0827	0	0	-58.38	124.61
BAYAREALIKE+X	3	0.0031	0.0986	0	-1.0037	0	-61.54	130.92
BAYAREALIKE+N	3	0.0162	0.1125	0	0	-0.0580	-65.09	138.03
BAYAREALIKE+J+X	4	0.0012	0.0100	0.0272	-1.2100	0	-52.15	115.64
BAYAREALIKE+J+N	4	0.0053	0.0362	0.0595	0	-0.5762	-57.96	127.26
BAYAREALIKE+X+N	4	0.0033	0.0990	0	-0.9818	0.0000	-61.54	134.42
BAYAREALIKE+J+X+N	5	0.0012	0.0097	0.0274	-1.2177	0.0000	-52.15	119.75

Table 3.24S. Likelihood-Ratio test results for the clade *Girella*. P-values with an asterisk indicate rejection of null hypothesis (no significative improvement when adding parameters) at p<0.05.

Nested model	More complex model	LnL Null	LnL Alt	DF Null	DF Alt	DF	D Statistic	p-value
DEC	DEC+J	-62.7952	-57.4955	2	3	1	10.59942	0.001131 *
DEC	DEC+X	-62.7952	-57.9962	2	3	1	9.598	0.001948 *
DEC	DEC+N	-62.7952	-62.6103	2	3	1	0.36974	0.543146
DEC	DEC+J+X	-62.7952	-50.5582	2	4	2	24.47408	4.85E-06 *
DEC	DEC+J+N	-62.7952	-57.1751	2	4	2	11.2401	0.003624 *
DEC	DEC+X+N	-62.7952	-57.995	2	4	2	9.60042	0.008228
DEC	DEC+J+X+N	-62.7952	-50.5458	2	5	3	24.4988	1.97E-05 *
DEC+J	DEC+J+X	-57.4955	-50.5582	3	4	1	13.87466	0.000195 *
DEC+J	DEC+J+N	-57.4955	-57.1751	3	4	1	0.64068	0.423465
DEC+J	DEC+J+X+N	-57.4955	-50.5458	3	5	2	13.89938	0.000959 *
DEC+X	DEC+J+X	-57.9962	-50.5582	3	4	1	14.87608	0.000115 *
DEC+X	DEC+X+N	-57.9962	-57.995	3	4	1	0.00242	0.960765
DEC+X	DEC+J+X+N	-57.9962	-50.5458	3	5	2	14.9008	0.000581 *
DEC+N	DEC+J+N	-62.6103	-57.1751	3	4	1	10.87036	0.000977 *
DEC+N	DEC+X+N	-62.6103	-57.995	3	4	1	9.23068	0.00238 *
DEC+N	DEC+J+X+N	-62.6103	-50.5458	3	5	2	24.12906	5.76E-06 *
DEC+J+X	DEC+J+X+N	-50.5582	-50.5458	4	5	1	0.02472	0.875067
DEC+J+N	DEC+J+X+N	-57.1751	-50.5458	4	5	1	13.2587	0.000271 *
DEC+X+N	DEC+J+X+N	-57.995	-50.5458	4	5	1	14.89838	0.000113 *
DIVALIKE	DIVALIKE+J	-62.7176	-57.1475	2	3	1	11.1402	0.000845 *
DIVALIKE	DIVALIKE+X	-62.7176	-59.0836	2	3	1	7.2679	0.00702 *
DIVALIKE	DIVALIKE+N	-62.7176	-62.6457	2	3	1	0.1438	0.704532
DIVALIKE	DIVALIKE+J+X	-62.7176	-51.2459	2	4	2	22.9433	1.04E-05 *
DIVALIKE	DIVALIKE+J+N	-62.7176	-56.8572	2	4	2	11.72064	0.00285 *
DIVALIKE	DIVALIKE+X+N	-62.7176	-59.0663	2	4	2	7.30258	0.025958 *
DIVALIKE	DIVALIKE+J+X+N	-62.7176	-50.9436	2	5	3	23.54788	3.1E-05 *
DIVALIKE+J	DIVALIKE+J+X	-57.1475	-51.2459	3	4	1	11.8031	0.000591 *
DIVALIKE+J	DIVALIKE+J+N	-57.1475	-56.8572	3	4	1	0.58044	0.44614
DIVALIKE+J	DIVALIKE+J+X+N	-57.1475	-50.9436	3	5	2	12.40768	0.002022 *
DIVALIKE+X	DIVALIKE+J+X	-59.0836	-51.2459	3	4	1	15.6754	7.52E-05 *
DIVALIKE+X	DIVALIKE+X+N	-59.0836	-59.0663	3	4	1	0.03468	0.852268
DIVALIKE+X	DIVALIKE+J+X+N	-59.0836	-50.9436	3	5	2	16.27998	0.000292 *
DIVALIKE+N	DIVALIKE+J+N	-62.6457	-56.8572	3	4	1	11.57684	0.000668 *
DIVALIKE+N	DIVALIKE+X+N	-62.6457	-59.0663	3	4	1	7.15878	0.00746 *
DIVALIKE+N	DIVALIKE+J+X+N	-62.6457	-50.9436	3	5	2	23.40408	8.28E-06 *
DIVALIKE+J+X	DIVALIKE+J+X+N	-51.2459	-50.9436	4	5	1	0.60458	0.436836
DIVALIKE+J+N	DIVALIKE+J+X+N	-56.8572	-50.9436	4	5	1	11.82724	0.000584 *
DIVALIKE+X+N	DIVALIKE+J+X+N	-59.0663	-50.9436	4	5	1	16.2453	5.56E-05 *
BAYAREALIKE	BAYAREALIKE+J	-65.1361	-58.38	2	3	1	13.51236	0.000237 *
BAYAREALIKE	BAYAREALIKE+X	-65.1361	-61.5373	2	3	1	7.1977	0.0073 *
BAYAREALIKE	BAYAREALIKE+N	-65.1361	-65.0941	2	3	1	0.08416	0.771737
BAYAREALIKE	BAYAREALIKE+J+X	-65.1361	-52.1543	2	4	2	25.96362	2.3E-06 *
BAYAREALIKE	BAYAREALIKE+J+N	-65.1361	-57.9615	2	4	2	14.3493	0.000766 *
BAYAREALIKE	BAYAREALIKE+X+N	-65.1361	-61.5444	2	4	2	7.18354	0.02755 *
BAYAREALIKE	BAYAREALIKE+J+X+N	-65.1361	-52.1482	2	5	3	25.97578	9.65E-06 *
BAYAREALIKE+J	BAYAREALIKE+J+X	-58.38	-52.1543	3	4	1	12.45126	0.000418 *
BAYAREALIKE+J	BAYAREALIKE+J+N	-58.38	-57.9615	3	4	1	0.83694	0.360273
BAYAREALIKE+J	BAYAREALIKE+J+X+N	-58.38	-52.1482	3	5	2	12.46342	0.001966 *
BAYAREALIKE+X	BAYAREALIKE+J+X	-61.5373	-52.1543	3	4	1	18.76592	1.48E-05 *
BAYAREALIKE+X	BAYAREALIKE+X+N	-61.5373	-61.5444	3	4	1	0	1
BAYAREALIKE+X	BAYAREALIKE+J+X+N	-61.5373	-52.1482	3	5	2	18.77808	8.36E-05 *
BAYAREALIKE+N	BAYAREALIKE+J+N	-65.0941	-57.9615	3	4	1	14.26514	0.000159 *
BAYAREALIKE+N	BAYAREALIKE+X+N	-65.0941	-61.5444	3	4	1	7.09938	0.007711 *
BAYAREALIKE+N	BAYAREALIKE+J+X+N	-65.0941	-52.1482	3	5	2	25.89162	2.39E-06 *
BAYAREALIKE+J+X	BAYAREALIKE+J+X+N	-52.1543	-52.1482	4	5	1	0.01216	0.912193
BAYAREALIKE+J+N	BAYAREALIKE+J+X+N	-57.9615	-52.1482	4	5	1	11.62648	0.00065 *
BAYAREALIKE+X+N	BAYAREALIKE+J+X+N	-61.5444	-52.1482	4	5	1	18.79224	1.46E-05 *

Table 3.25S. Parameter estimates, log-likelihood values (LnL), and model selection score for each of the 24 models assessed for the clade *Chromis* (sample size=19). Bold italicized row indicates the best-fitting model based on AICc and LRT results.

Biogeographic model	Free parameters	*d*	*e*	*j*	*x*	*n*	LnL	AICc
DEC	2	0.0223	0.0502	0	0	0	-85.05	174.85
DEC+J	3	0.0150	0.0206	0.1307	0	0	-80.03	167.66
DEC+X	3	0.0051	0.0448	0	-0.8775	0	-79.79	167.17
DEC+N	3	0.0058	0.0393	0	0	-1.6487	-80.60	168.81
DEC+J+X	4	0.0015	0.0161	0.0390	-1.2953	0	-71.71	154.28
DEC+J+N	4	0.0034	0.0180	0.0364	0	-1.8110	-75.30	161.46
DEC+X+N	4	0.0016	0.0369	0	-0.8702606	-1.4679	-75.68	162.21
DEC+J+X+N	***5***	***0.0010***	***0.0155***	***0.0217***	***-1.1390***	***-0.9588***	***-68.53***	***151.67***
DIVALIKE	2	0.0211	0.0186	0	0	0	-81.19	167.12
DIVALIKE+J	3	0.0167	0.0167	0.0643	0	0	-79.26	166.12
DIVALIKE+X	3	0.0133	0.0189	0	-0.3225	0	-77.92	163.44
DIVALIKE+N	3	0.0122	0.0191	0	0	-0.7569	-78.22	164.05
DIVALIKE+J+X	4	0.0106	0.0171	0.0279	-0.3057	0	-76.02	162.90
DIVALIKE+J+N	4	0.0127	0.0200	0.0762	0	-0.3573	-77.87	166.59
DIVALIKE+X+N	4	0.0093	0.0183	0	-0.5372	-0.0120	-76.42	163.71
DIVALIKE+J+X+N	5	0.0003	0.0065	0.0392	-1.4658	-0.7789	-73.25	161.11
BAYAREALIKE	2	0.0300	0.2308	0	0	0	-93.72	192.18
BAYAREALIKE+J	3	0.0138	0.0400	0.1386	0	0	-82.22	172.04
BAYAREALIKE+X	3	0.0070	0.2237	0	-0.8570	0	-89.14	185.88
BAYAREALIKE+N	3	0.0068	0.2168	0	0	-1.7517	-90.57	188.75
BAYAREALIKE+J+X	4	0.0017	0.0294	0.0468	-1.24062	0	-74.55	159.95
BAYAREALIKE+J+N	4	0.0036	0.0367	0.0514	0	-1.6795	-78.10	167.05
BAYAREALIKE+X+N	4	0.0028	0.2159	0	-0.7966	-1.2623	-86.77	184.39
BAYAREALIKE+J+X+N	5	0.0011	0.0292	0.0297	-1.146759	-0.7867	-71.88	158.38

Table 3.26S. Likelihood-Ratio test results for the clade *Chromis*. P-values with an asterisk indicate rejection of null hypothesis (no significative improvement when adding parameters) at p<0.05.

Nested model	More complex model	LnL Null	LnL Alt	DF Null	DF Alt	DF	D Statistic	p-value
DEC	DEC+J	-85.049	-80.0313	2	3	1	10.03528	0.001536 *
DEC	DEC+X	-85.049	-79.7864	2	3	1	10.52508	0.001178 *
DEC	DEC+N	-85.049	-80.6036	2	3	1	8.89074	0.002866 *
DEC	DEC+J+X	-85.049	-71.7105	2	4	2	26.677	1.61E-06 *
DEC	DEC+J+N	-85.049	-75.3009	2	4	2	19.49614	5.84E-05 *
DEC	DEC+X+N	-85.049	-75.6771	2	4	2	18.7437	8.51E-05 *
DEC	DEC+J+X+N	-85.049	-68.5281	2	5	3	33.04168	3.16E-07 *
DEC+J	DEC+J+X	-80.0313	-71.7105	3	4	1	16.64172	4.51E-05 *
DEC+J	DEC+J+N	-80.0313	-75.3009	3	4	1	9.46086	0.002099 *
DEC+J	DEC+J+X+N	-80.0313	-68.5281	3	5	2	23.0064	1.01E-05 *
DEC+X	DEC+J+X	-79.7864	-71.7105	3	4	1	16.15192	5.85E-05 *
DEC+X	DEC+X+N	-79.7864	-75.6771	3	4	1	8.21862	0.004146 *
DEC+X	DEC+J+X+N	-79.7864	-68.5281	3	5	2	22.5166	1.29E-05 *
DEC+N	DEC+J+N	-80.6036	-75.3009	3	4	1	10.6054	0.001128 *
DEC+N	DEC+X+N	-80.6036	-75.6771	3	4	1	9.85296	0.001696 *
DEC+N	DEC+J+X+N	-80.6036	-68.5281	3	5	2	24.15094	5.7E-06 *
DEC+J+X	DEC+J+X+N	-71.7105	-68.5281	4	5	1	6.36468	0.011641 *
DEC+J+N	DEC+J+X+N	-75.3009	-68.5281	4	5	1	13.54554	0.000233 *
DEC+X+N	DEC+J+X+N	-75.6771	-68.5281	4	5	1	14.29798	0.000156 *
DIVALIKE	DIVALIKE+J	-81.1869	-79.2607	2	3	1	3.85234	0.049677 *
DIVALIKE	DIVALIKE+X	-81.1869	-77.9222	2	3	1	6.52944	0.01061 *
DIVALIKE	DIVALIKE+N	-81.1869	-78.2243	2	3	1	5.9253	0.014925 *
DIVALIKE	DIVALIKE+J+X	-81.1869	-76.0205	2	4	2	10.3329	0.005705 *
DIVALIKE	DIVALIKE+J+N	-81.1869	-77.8689	2	4	2	6.63598	0.036226 *
DIVALIKE	DIVALIKE+X+N	-81.1869	-76.4242	2	4	2	9.52544	0.008542 *
DIVALIKE	DIVALIKE+J+X+N	-81.1869	-73.2465	2	5	3	15.88092	0.0012 *
DIVALIKE+J	DIVALIKE+J+X	-79.2607	-76.0205	3	4	1	6.48056	0.010906 *
DIVALIKE+J	DIVALIKE+J+N	-79.2607	-77.8689	3	4	1	2.78364	0.095232
DIVALIKE+J	DIVALIKE+J+X+N	-79.2607	-73.2465	3	5	2	12.02858	0.002444 *
DIVALIKE+X	DIVALIKE+J+X	-77.9222	-76.0205	3	4	1	3.80346	0.051147
DIVALIKE+X	DIVALIKE+X+N	-77.9222	-76.4242	3	4	1	2.996	0.08347
DIVALIKE+X	DIVALIKE+J+X+N	-77.9222	-73.2465	3	5	2	9.35148	0.009319 *
DIVALIKE+N	DIVALIKE+J+N	-78.2243	-77.8689	3	4	1	0.71068	0.399218
DIVALIKE+N	DIVALIKE+X+N	-78.2243	-76.4242	3	4	1	3.60014	0.057775
DIVALIKE+N	DIVALIKE+J+X+N	-78.2243	-73.2465	3	5	2	9.95562	0.006889 *
DIVALIKE+J+X	DIVALIKE+J+X+N	-76.0205	-73.2465	4	5	1	5.54802	0.018502 *
DIVALIKE+J+N	DIVALIKE+J+X+N	-77.8689	-73.2465	4	5	1	9.24494	0.002361 *
DIVALIKE+X+N	DIVALIKE+J+X+N	-76.4242	-73.2465	4	5	1	6.35548	0.011702 *
BAYAREALIKE	BAYAREALIKE+J	-93.7161	-82.2223	2	3	1	22.98758	1.63E-06 *
BAYAREALIKE	BAYAREALIKE+X	-93.7161	-89.141	2	3	1	9.15018	0.002487 *
BAYAREALIKE	BAYAREALIKE+N	-93.7161	-90.5746	2	3	1	6.28296	0.01219 *
BAYAREALIKE	BAYAREALIKE+J+X	-93.7161	-74.5453	2	4	2	38.34162	4.72E-09 *
BAYAREALIKE	BAYAREALIKE+J+N	-93.7161	-78.095	2	4	2	31.24212	1.64E-07 *
BAYAREALIKE	BAYAREALIKE+X+N	-93.7161	-86.7675	2	4	2	13.89718	0.00096 *
BAYAREALIKE	BAYAREALIKE+J+X+N	-93.7161	-71.8847	2	5	3	43.66276	1.78E-09 *
BAYAREALIKE+J	BAYAREALIKE+J+X	-82.2223	-74.5453	3	4	1	15.35404	8.91E-05 *
BAYAREALIKE+J	BAYAREALIKE+J+N	-82.2223	-78.095	3	4	1	8.25454	0.004065 *
BAYAREALIKE+J	BAYAREALIKE+J+X+N	-82.2223	-71.8847	3	5	2	20.67518	3.24E-05 *
BAYAREALIKE+X	BAYAREALIKE+J+X	-89.141	-74.5453	3	4	1	29.19144	6.56E-08 *
BAYAREALIKE+X	BAYAREALIKE+X+N	-89.141	-86.7675	3	4	1	4.747	0.029349 *
BAYAREALIKE+X	BAYAREALIKE+J+X+N	-89.141	-71.8847	3	5	2	34.51258	3.2E-08 *
BAYAREALIKE+N	BAYAREALIKE+J+N	-90.5746	-78.095	3	4	1	24.95916	5.86E-07 *
BAYAREALIKE+N	BAYAREALIKE+X+N	-90.5746	-86.7675	3	4	1	7.61422	0.005791 *
BAYAREALIKE+N	BAYAREALIKE+J+X+N	-90.5746	-71.8847	3	5	2	37.3798	7.64E-09 *
BAYAREALIKE+J+X	BAYAREALIKE+J+X+N	-74.5453	-71.8847	4	5	1	5.32114	0.021068 *
BAYAREALIKE+J+N	BAYAREALIKE+J+X+N	-78.095	-71.8847	4	5	1	12.42064	0.000425 *
BAYAREALIKE+X+N	BAYAREALIKE+J+X+N	-86.7675	-71.8847	4	5	1	29.76558	4.88E-08 *

Table 3.27S. Parameter estimates, log-likelihood values (LnL), and model selection score for each of the 24 models assessed for the clade *Upeneus* (sample size=29). Bold italicized row indicates the best-fitting model based on AICc and LRT results.

Biogeographic model	Free parameters	*d*	*e*	*j*	*x*	*n*	LnL	AICc
DEC	2	0.0194	0.0126	0	0	0	-100.19	204.84
DEC+J	3	0.0154	3.88E-09	0.0142	0	0	-99.22	205.39
DEC+X	3	0.0169	0.0111	0	-0.0905	0	-100.12	207.19
DEC+N	3	0.0125	0.0207	0	0	-2.5	-87.58	182.13
DEC+J+X	4	0.0126	1.00E-12	0.0113	-0.1551	0	-98.98	207.62
DEC+J+N	4	0.0106	0.0138	0.0115	0	-2.5	-86.71	183.08
DEC+X+N	4	0.0099	0.0196	0	-0.1643	-2.5	-87.37	184.41
DEC+J+X+N	5	0.0052	1.00E-12	0.0090	-0.3552	-2.5	-86.41	185.43
DIVALIKE	2	0.0252	0.0188	0	0	0	-111.60	227.66
DIVALIKE+J	3	0.0211	0.0088	0.0078	0	0	-111.35	229.65
DIVALIKE+X	3	0.0201	0.0149	0	-0.1523	0	-111.41	229.77
DIVALIKE+N	3	0.0150	0.0219	0	0	-2.5	-95.26	197.49
DIVALIKE+J+X	4	0.0137	1.00E-12	0.0084	-0.2639	0	-110.60	230.87
DIVALIKE+J+N	4	0.0132	0.0169	0.0065	0	-2.5	-94.81	199.29
DIVALIKE+X+N	4	0.0126	0.0212	0	-0.1331	-2.5	-95.13	199.93
DIVALIKE+J+X+N	5	0.0103	0.0154	0.0059	-0.1689	-2.5	-94.60	201.81
BAYAREALIKE	2	0.0112	0.0612	0	0	0	-93.30	191.06
BAYAREALIKE+J	3	0.0081	0.0453	0.0076	0	0	-91.37	189.70
BAYAREALIKE+X	3	0.0057	0.0577	0	-0.3857	0	-92.59	192.14
BAYAREALIKE+N	3	0.0121	0.0769	0	0	-2.5	-87.55	182.06
BAYAREALIKE+J+X	4	0.0037	0.0428	0.0041	-0.4508	0	-90.41	190.50
BAYAREALIKE+J+N	***4***	***0.0081***	***0.0508***	***0.0086***	***0***	***-2.5***	***-85.78***	***181.23***
BAYAREALIKE+X+N	4	0.0085	0.0729	0	-0.2254	-2.5	-87.27	184.20
BAYAREALIKE+J+X+N	5	0.0048	0.0470	0.0058	-0.3244	-2.5	-85.22	183.06

Table 3.28S. Likelihood-Ratio test results for the clade *Upeneus*. P-values with an asterisk indicate rejection of null hypothesis (no significative improvement when adding parameters) at $p<0.05$.

Nested model	More complex model	LnL Null	LnL Alt	DF Null	DF Alt	DF	D Statistic	p-value
DEC	DEC+J	-100.189	-99.2158	2	3	1	1.9458	0.16304
DEC	DEC+X	-100.189	-100.116	2	3	1	0.1452	0.703165
DEC	DEC+N	-100.189	-87.5839	2	3	1	25.20964	5.14E-07 *
DEC	DEC+J+X	-100.189	-98.9752	2	4	2	2.42692	0.297167
DEC	DEC+J+N	-100.189	-86.7068	2	4	2	26.9639	1.4E-06 *
DEC	DEC+X+N	-100.189	-87.3726	2	4	2	25.63226	2.72E-06 *
DEC	DEC+J+X+N	-100.189	-86.4084	2	5	3	27.5607	4.49E-06 *
DEC+J	DEC+J+X	-99.2158	-98.9752	3	4	1	0.48112	0.487915
DEC+J	DEC+J+N	-99.2158	-86.7068	3	4	1	25.0181	5.68E-07 *
DEC+J	DEC+J+X+N	-99.2158	-86.4084	3	5	2	25.6149	2.74E-06 *
DEC+X	DEC+J+X	-100.116	-98.9752	3	4	1	2.28172	0.130907
DEC+X	DEC+X+N	-100.116	-87.3726	3	4	1	25.48706	4.45E-07 *
DEC+X	DEC+J+X+N	-100.116	-86.4084	3	5	2	27.4155	1.11E-06 *
DEC+N	DEC+J+N	-87.5839	-86.7068	3	4	1	1.75426	0.185342
DEC+N	DEC+X+N	-87.5839	-87.3726	3	4	1	0.42262	0.515633
DEC+N	DEC+J+X+N	-87.5839	-86.4084	3	5	2	2.35106	0.308655
DEC+J+X	DEC+J+X+N	-98.9752	-86.4084	4	5	1	25.13378	5.35E-07 *
DEC+J+N	DEC+J+X+N	-86.7068	-86.4084	4	5	1	0.5968	0.439802
DEC+X+N	DEC+J+X+N	-87.3726	-86.4084	4	5	1	1.92844	0.164929
DIVALIKE	DIVALIKE+J	-111.599	-111.346	2	3	1	0.505	0.477311
DIVALIKE	DIVALIKE+X	-111.599	-111.407	2	3	1	0.3846	0.535152
DIVALIKE	DIVALIKE+N	-111.599	-95.2649	2	3	1	32.66798	1.09E-08 *
DIVALIKE	DIVALIKE+J+X	-111.599	-110.602	2	4	2	1.9938	0.369022
DIVALIKE	DIVALIKE+J+N	-111.599	-94.8125	2	4	2	33.57288	5.13E-08 *
DIVALIKE	DIVALIKE+X+N	-111.599	-95.1292	2	4	2	32.9394	7.04E-08 *
DIVALIKE	DIVALIKE+J+X+N	-111.599	-94.6011	2	5	3	33.99554	1.99E-07 *
DIVALIKE+J	DIVALIKE+J+X	-111.346	-110.602	3	4	1	1.4888	0.222403
DIVALIKE+J	DIVALIKE+J+N	-111.346	-94.8125	3	4	1	33.06788	8.9E-09 *
DIVALIKE+J	DIVALIKE+J+X+N	-111.346	-94.6011	3	5	2	33.49054	5.34E-08 *
DIVALIKE+X	DIVALIKE+J+X	-111.407	-110.602	3	4	1	1.6092	0.204604
DIVALIKE+X	DIVALIKE+X+N	-111.407	-95.1292	3	4	1	32.5548	1.16E-08 *
DIVALIKE+X	DIVALIKE+J+X+N	-111.407	-94.6011	3	5	2	33.61094	5.03E-08 *
DIVALIKE+N	DIVALIKE+J+N	-95.2649	-94.8125	3	4	1	0.9049	0.341471
DIVALIKE+N	DIVALIKE+X+N	-95.2649	-95.1292	3	4	1	0.27142	0.602381
DIVALIKE+N	DIVALIKE+J+X+N	-95.2649	-94.6011	3	5	2	1.32756	0.514901
DIVALIKE+J+X	DIVALIKE+J+X+N	-110.602	-94.6011	4	5	1	32.00174	1.54E-08 *
DIVALIKE+J+N	DIVALIKE+J+X+N	-94.8125	-94.6011	4	5	1	0.42266	0.515613
DIVALIKE+X+N	DIVALIKE+J+X+N	-95.1292	-94.6011	4	5	1	1.05614	0.304097
BAYAREALIKE	BAYAREALIKE+J	-93.2968	-91.3715	2	3	1	3.85064	0.049727 *
BAYAREALIKE	BAYAREALIKE+X	-93.2968	-92.5899	2	3	1	1.41382	0.234423
BAYAREALIKE	BAYAREALIKE+N	-93.2968	-87.5489	2	3	1	11.49578	0.000698 *
BAYAREALIKE	BAYAREALIKE+J+X	-93.2968	-90.415	2	4	2	5.76364	0.056033
BAYAREALIKE	BAYAREALIKE+J+N	-93.2968	-85.7837	2	4	2	15.02624	0.000546 *
BAYAREALIKE	BAYAREALIKE+X+N	-93.2968	-87.2671	2	4	2	12.05928	0.002406 *
BAYAREALIKE	BAYAREALIKE+J+X+N	-93.2968	-85.2244	2	5	3	16.14476	0.001059 *
BAYAREALIKE+J	BAYAREALIKE+J+X	-91.3715	-90.415	3	4	1	1.913	0.16663
BAYAREALIKE+J	BAYAREALIKE+J+N	-91.3715	-85.7837	3	4	1	11.1756	0.000829 *
BAYAREALIKE+J	BAYAREALIKE+J+X+N	-91.3715	-85.2244	3	5	2	12.29412	0.00214 *
BAYAREALIKE+X	BAYAREALIKE+J+X	-92.5899	-90.415	3	4	1	4.34982	0.037013 *
BAYAREALIKE+X	BAYAREALIKE+X+N	-92.5899	-87.2671	3	4	1	10.64546	0.001103 *
BAYAREALIKE+X	BAYAREALIKE+J+X+N	-92.5899	-85.2244	3	5	2	14.73094	0.000633 *
BAYAREALIKE+N	BAYAREALIKE+J+N	-87.5489	-85.7837	3	4	1	3.53046	0.060251
BAYAREALIKE+N	BAYAREALIKE+X+N	-87.5489	-87.2671	3	4	1	0.5635	0.452853
BAYAREALIKE+N	BAYAREALIKE+J+X+N	-87.5489	-85.2244	3	5	2	4.64898	0.097833
BAYAREALIKE+J+X	BAYAREALIKE+J+X+N	-90.415	-85.2244	4	5	1	10.38112	0.001273 *
BAYAREALIKE+J+N	BAYAREALIKE+J+X+N	-85.7837	-85.2244	4	5	1	1.11852	0.290237
BAYAREALIKE+X+N	BAYAREALIKE+J+X+N	-87.2671	-85.2244	4	5	1	4.08548	0.043253 *

Table 3.29S. Biogeographic models that required the 'optimx' (o) and 'GenSA' optimizers across the 14 clades examined. Opt.: *Optivus*; Arr.: *Arripis*; Sco.: *Scorpis*; AM: *Atypichthys* and *Microcanthus*; Kat.: *Kathetostoma*; Nem.: *Nemadactylus*; Lep.: *Lepidoperca*; Par.: *Parma*; Hyp.: *Hypoplectrodes*; ChA: *Chironemus* and *Aplodactylus*; GM: *Goniistius* and *Morwong*; Gir.: Girella; Chr.: Chromis; Upe.: Upeneus.

Model	Opt.	Arr.	Sco.	AM	Kat.	Nem.	Lep.	Par.	Hyp.	ChA	GM	Gir.	Chr.	Upe.
DEC	o	o	o	o	o	o	o	o	o	o	o	o	o	o
DEC+J	o	o	o	o	o	o	o	o	o	o	o	o	o	o
DEC+X	o	o	o	o	o	o	o	o	o	o	o	o	o	o
DEC+N	o	o	o	o	o	o	o	o	o	o	o	o	o	o
DEC+J+X	o	o	GenSA	o	o	o	o	o	o	o	GenSA	o	o	o
DEC+J+N	o	GenSA	o	GenSA	o	o	o	o	o	o	o	o	o	o
DEC+X+N	o	o	GenSA	GenSA	GenSA	o	o	o	o	GenSA	o	o	o	o
DEC+J+X+N	o	GenSA	GenSA	o	GenSA	GenSA	o	o	o	GenSA		o	o	GenSA
DIVALIKE	o	o	o	o	o	o	o	o	o	o	o	o	o	o
DIVALIKE+J	o	o	o	o	o	o	o	o	o	o	o	o	o	o
DIVALIKE+X	o	o	o	o	o	o	o	o	o	o	o	o	o	o
DIVALIKE+N	o	o	o	o	o	o	o	o	o	o	o	o	o	o
DIVALIKE+J+X	o	o	o	GenSA	o	o	o	o	o	o	o	o	o	o
DIVALIKE+J+N	o	o	o	GenSA	o	o	o	o	o	o	o	o	o	o
DIVALIKE+X+N	o	o	GenSA	GenSA	GenSA	o	o	o	o	o	o	o	o	o
DIVALIKE+J+X+N	GenSA	GenSA	GenSA	GenSA	GenSA	o	o	GenSA	o	GenSA	GenSA	o	GenSA	GenSA
BAYAREALIKE	o	o	o	o	o	o	o	o	o	o	o	o	o	o
BAYAREALIKE+J	o	o	o	o	o	o	o	o	o	o	o	o	o	o
BAYAREALIKE+X	o	o	o	o	o	o	o	o	o	o	o	o	o	o
BAYAREALIKE+N	o	o	o	o	o	o	o	o	o	o	o	o	o	o
BAYAREALIKE+J+X	o	o	o	o	o	o	o	o	o	o	o	o	o	o
BAYAREALIKE+J+N	GenSA	o	o	o	o	o	o	o	o	o	o	o	o	GenSA
BAYAREALIKE+X+N	o	o	o	o	o	o	o	GenSA	o	o	o	GenSA	o	o
BAYAREALIKE+J+X+N	o	o	GenSA	GenSA	o	o	o	GenSA	o	GenSA	o	o	o	GenSA

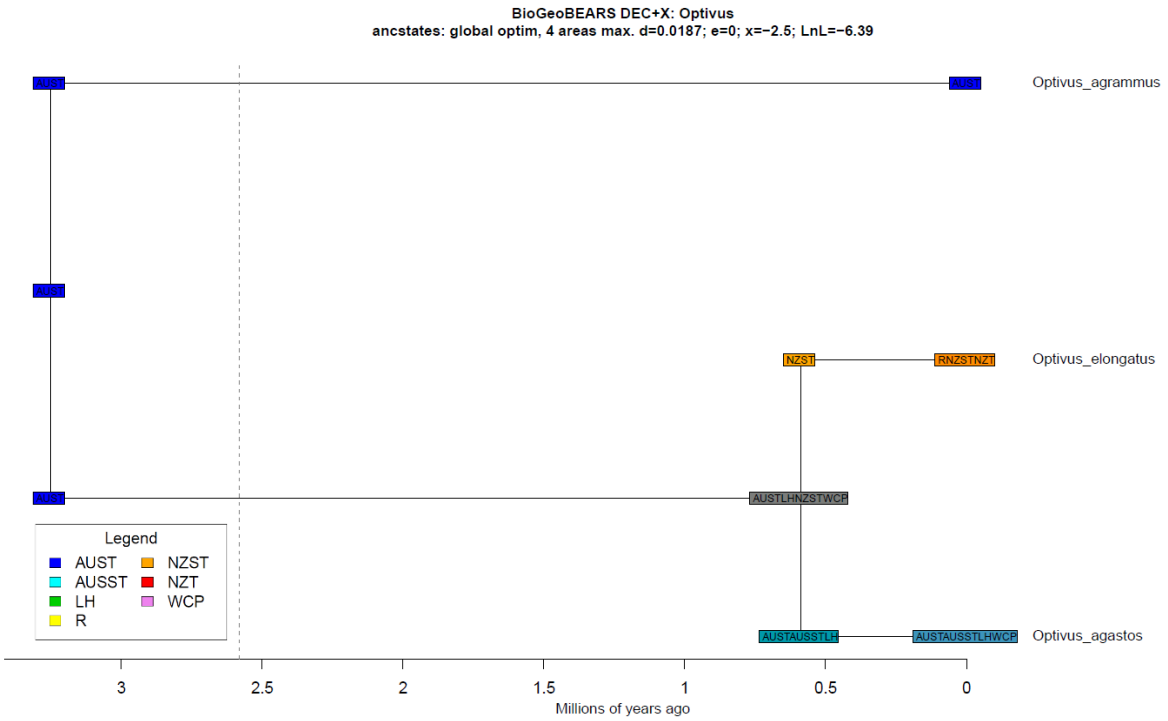

Figure 3.1S. Most likely ancestral ranges for *Optivus* based on the best-fitting model (DEC+X) as inferred in 'BioGeoBEARS'. Ranges with more than one area display the mixture of colors from the base areas they include (cf. legend): AUST, Australia Temperate; AUSST, Australia Subtropical; LH, Lord Howe; R, Rangitāhua; NZST, New Zealand Subtropical; NZT, New Zealand Temperate; WCP, West/Central Pacific. Dashed line represents a time constraint.

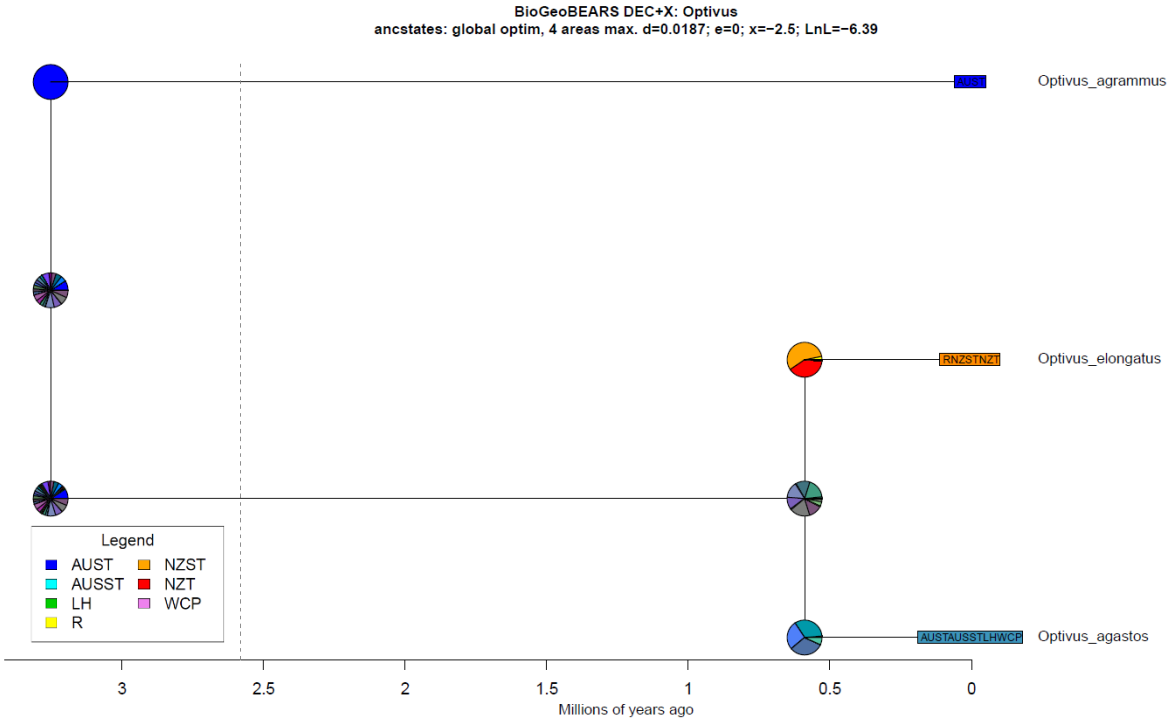

Figure 3.2S. Pie charts showing the probabilities of each ancestral range per node at the *Optivus* tree based on the DEC+X model. Each range color within a pie is a mixture of base area colors (cf. legend): AUST, Australia Temperate; AUSST, Australia Subtropical; LH, Lord Howe; R, Rangitāhua; NZST, New Zealand Subtropical; NZT, New Zealand Temperate; WCP, West/Central Pacific. Dashed line represents a time constraint.

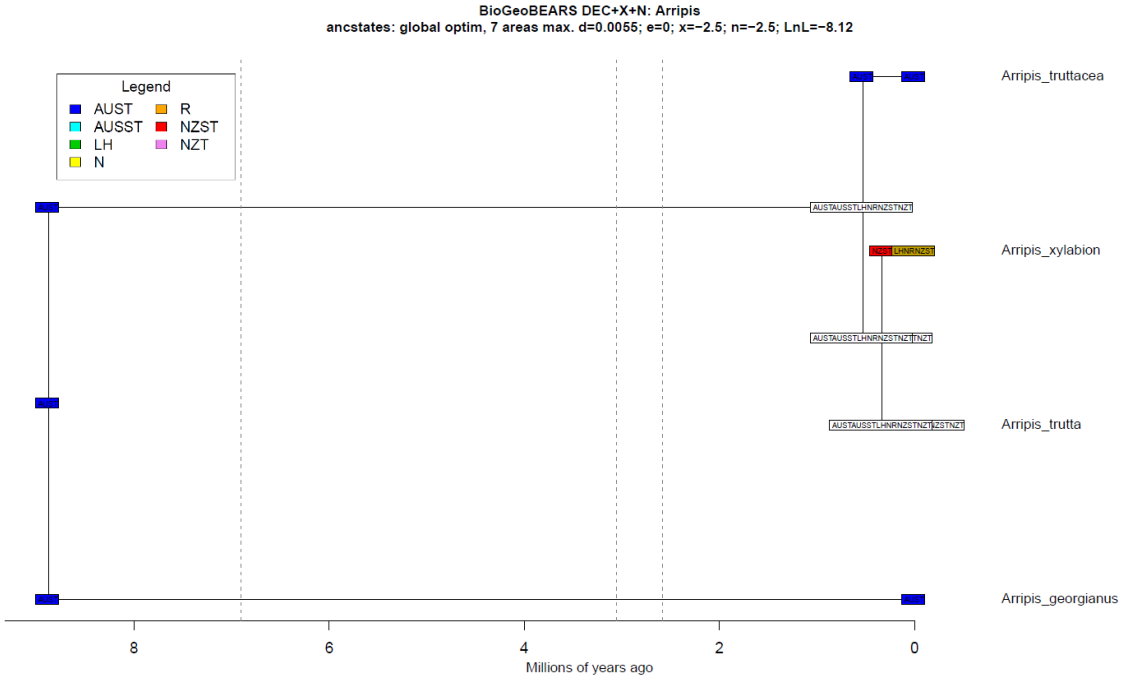

Figure 3.3S. Most likely ancestral ranges for *Arripis* based on the best-fitting model (DEC+X+N) as inferred in 'BioGeoBEARS'. Ranges with more than one area display the mixture of colors from the base areas they include (cf. legend): AUST, Australia Temperate; AUSST, Australia Subtropical; LH, Lord Howe; N, Norfolk; R, Rangitāhua; NZST, New Zealand Subtropical; NZT, New Zealand Temperate. Dashed lines represent time constraints.

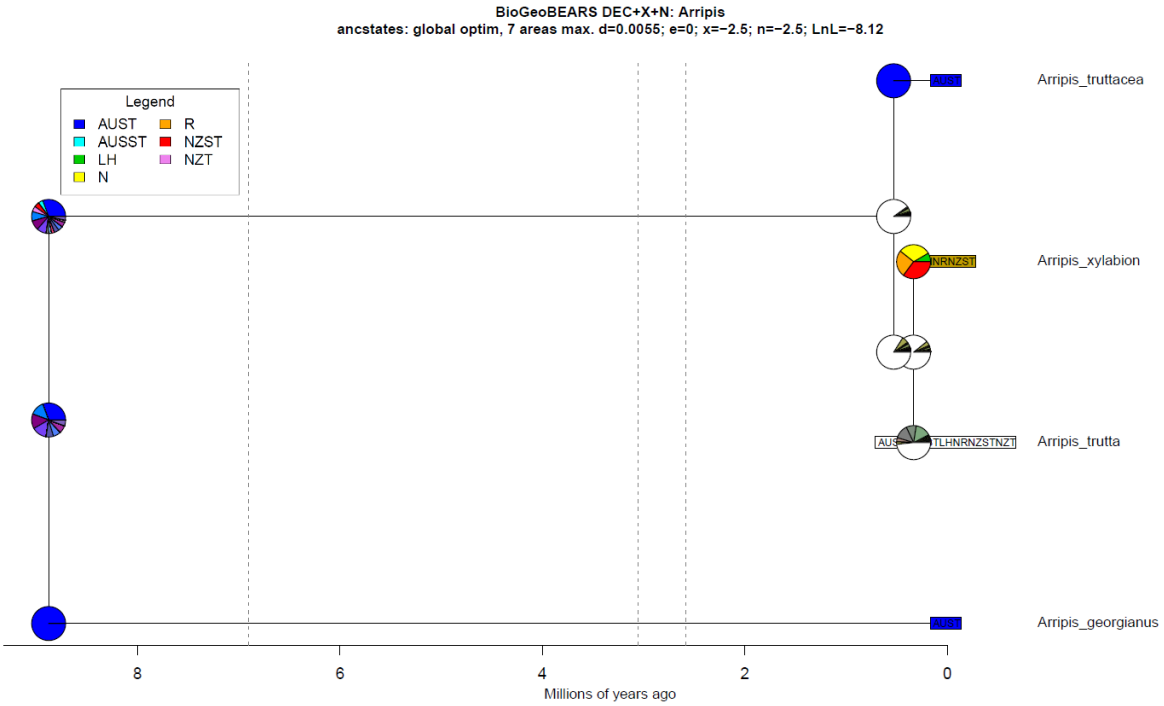

Figure 3.4S. Pie charts showing the probabilities of each ancestral range per node at the *Arripis* tree based on the DEC+X+N model. Each range color within a pie is a mixture of base area colors (cf. legend): AUST, Australia Temperate; AUSST, Australia Subtropical; LH, Lord Howe; N, Norfolk; R, Rangitāhua; NZST, New Zealand Subtropical; NZT, New Zealand Temperate. Dashed lines represent time constraints.

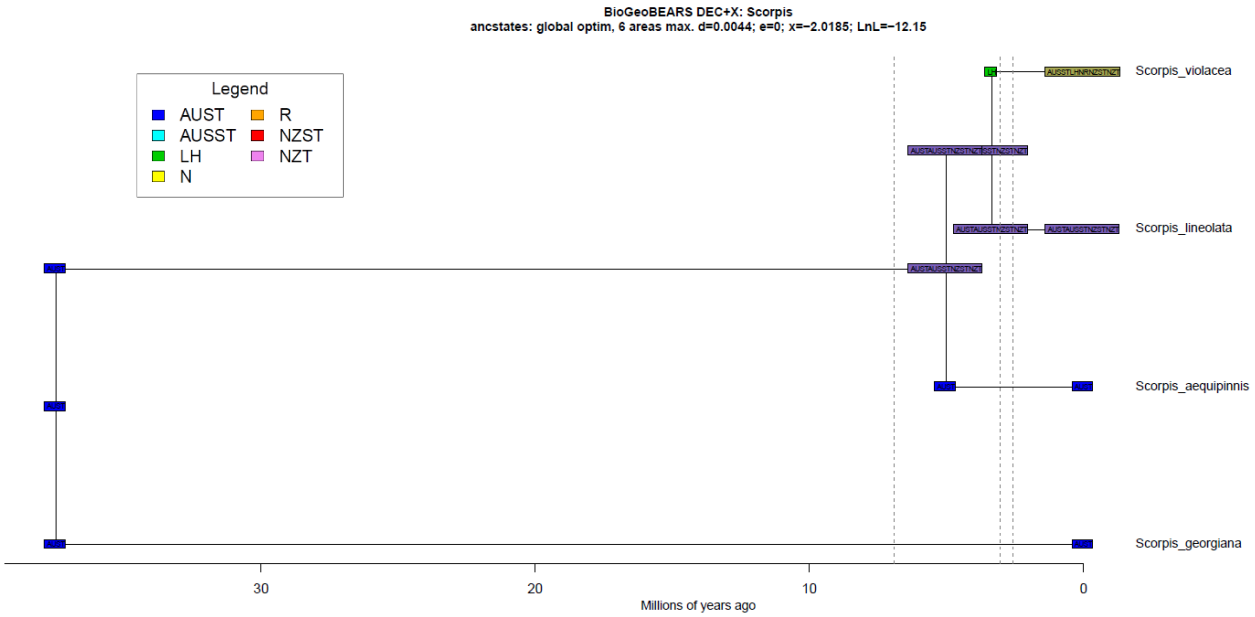

Figure 3.5S. Most likely ancestral ranges for *Scorpis* based on the best-fitting model (DEC+X) as inferred in 'BioGeoBEARS'. Ranges with more than one area display the mixture of colors from the base areas they include (cf. legend): AUST, Australia Temperate; AUSST, Australia Subtropical; LH, Lord Howe; N, Norfolk; R, Rangitāhua; NZST, New Zealand Subtropical; NZT, New Zealand Temperate. Dashed lines represent time constraints.

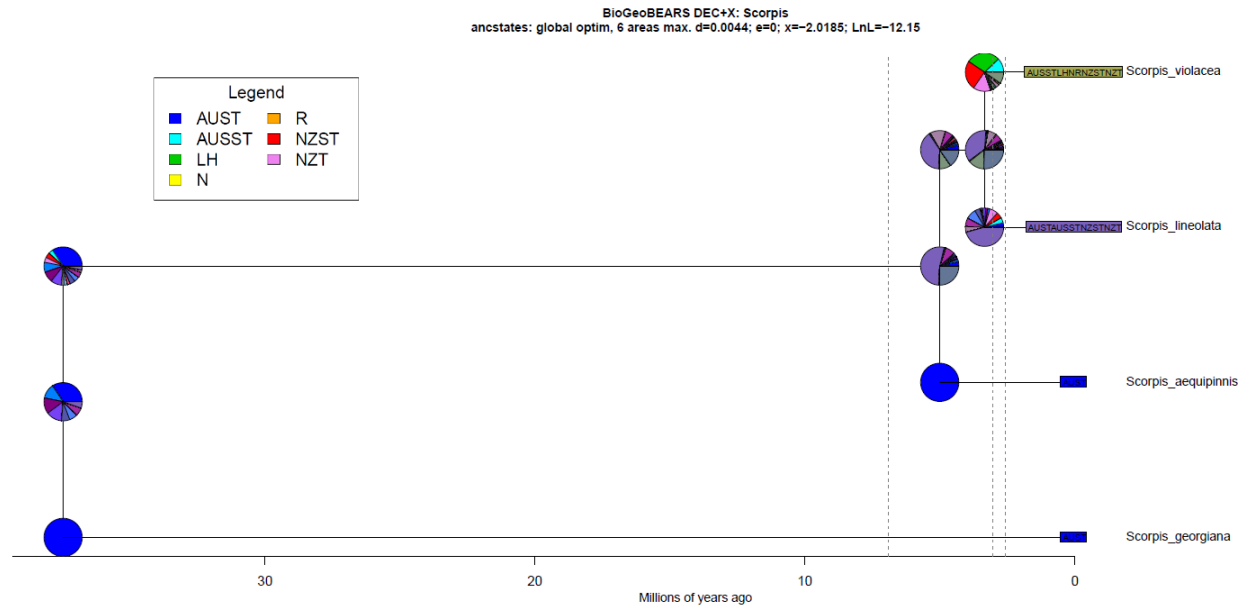

Figure 3.6S. Pie charts showing the probabilities of each ancestral range per node at the *Scorpis* tree based on the DEC+X model. Each range color within a pie is a mixture of base area colors (cf. legend): AUST, Australia Temperate; AUSST, Australia Subtropical; LH, Lord Howe; N, Norfolk; R, Rangitāhua; NZST, New Zealand Subtropical; NZT, New Zealand Temperate. Dashed lines represent time constraints.

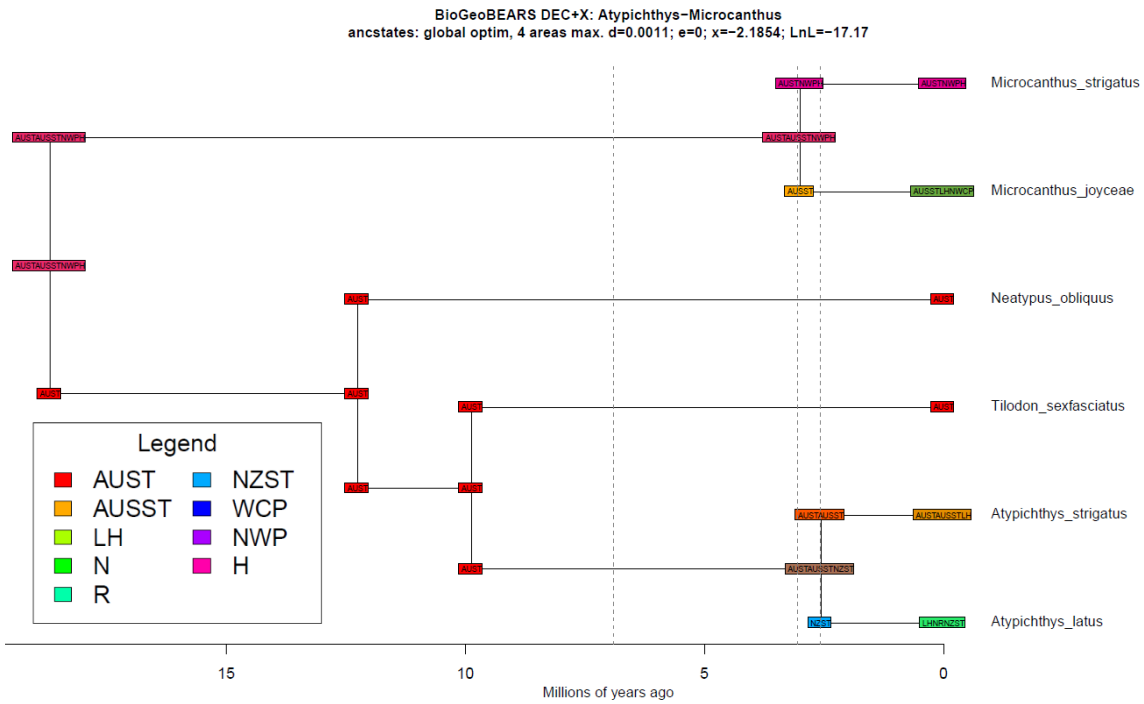

Figure 3.7S. Most likely ancestral ranges for *Atypichthys* and *Microcanthus* based on the best-fitting model (DEC+X) as inferred in 'BioGeoBEARS'. Ranges with more than one area display the mixture of colors from the base areas they include (cf. legend): AUST, Australia Temperate; AUSST, Australia Subtropical; LH, Lord Howe; N, Norfolk; R, Rangitāhua; NZST, New Zealand Subtropical; WCP, West/Central Pacific; NWP, Northwest Pacific; H: Hawaii. Dashed lines represent time constraints.

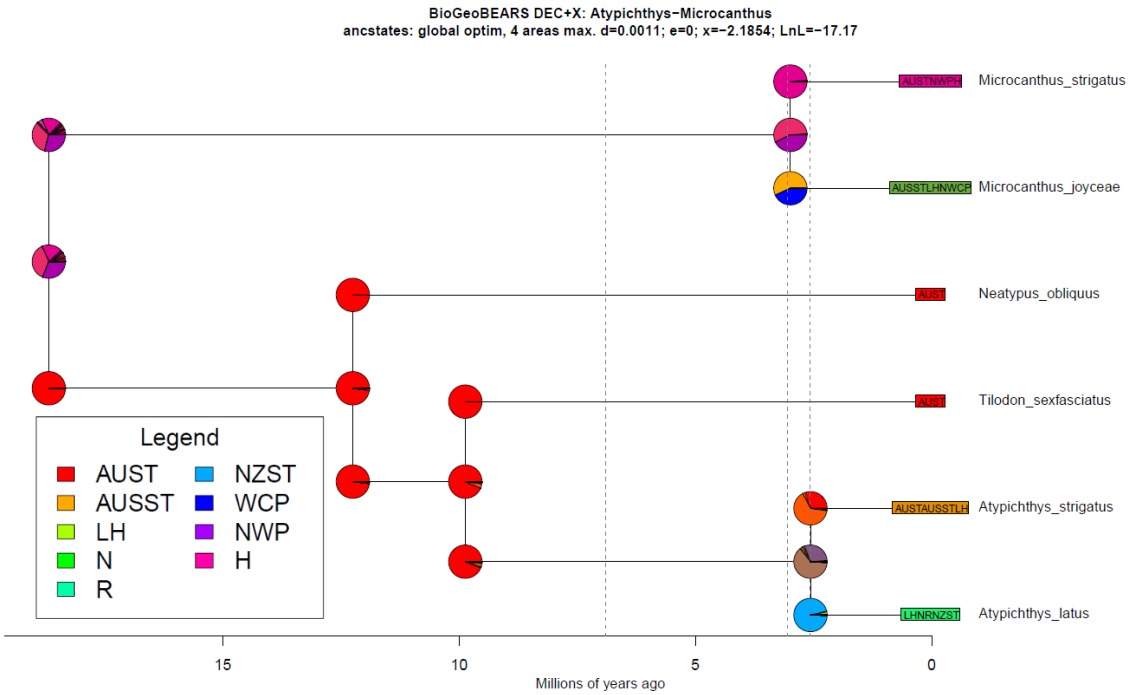

Figure 3.8S. Pie charts showing the probabilities of each ancestral range per node for *Atypichthys* and *Microcanthus* based on the DEC+X model. Each range color within a pie is a mixture of base area colors (cf. legend): AUST, Australia Temperate; AUSST, Australia Subtropical; LH, Lord Howe; N, Norfolk; R, Rangitāhua; NZST, New Zealand Subtropical; WCP, West/Central Pacific; NWP, Northwest Pacific; H: Hawaii. Dashed lines represent time constraints.

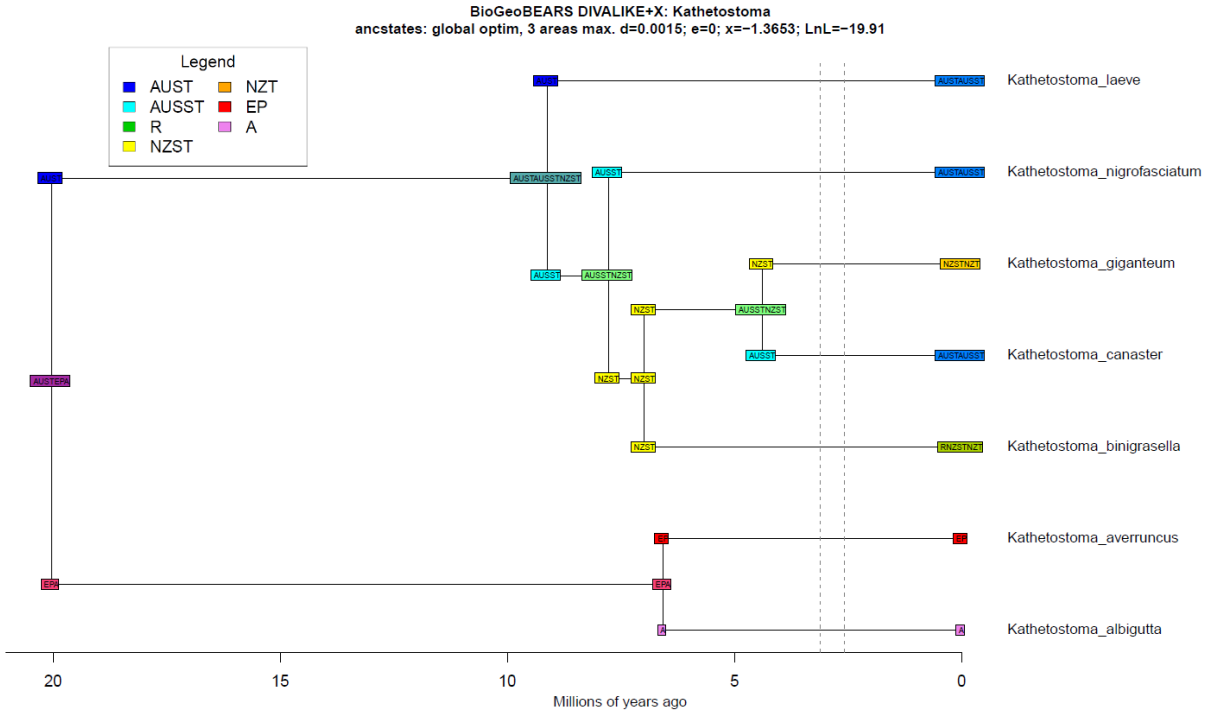

Figure 3.9S. Most likely ancestral ranges for *Kathetostoma* based on the best-fitting model (DIVALIKE+X) as inferred in 'BioGeoBEARS'. Ranges with more than one area display the mixture of colors from the base areas they include (cf. legend): AUST, Australia Temperate; AUSST, Australia Subtropical; R, Rangitāhua; NZST, New Zealand Subtropical; NZT, New Zealand Temperate; EP, East Pacific; A, Atlantic Ocean. Dashed lines represent time constraints.

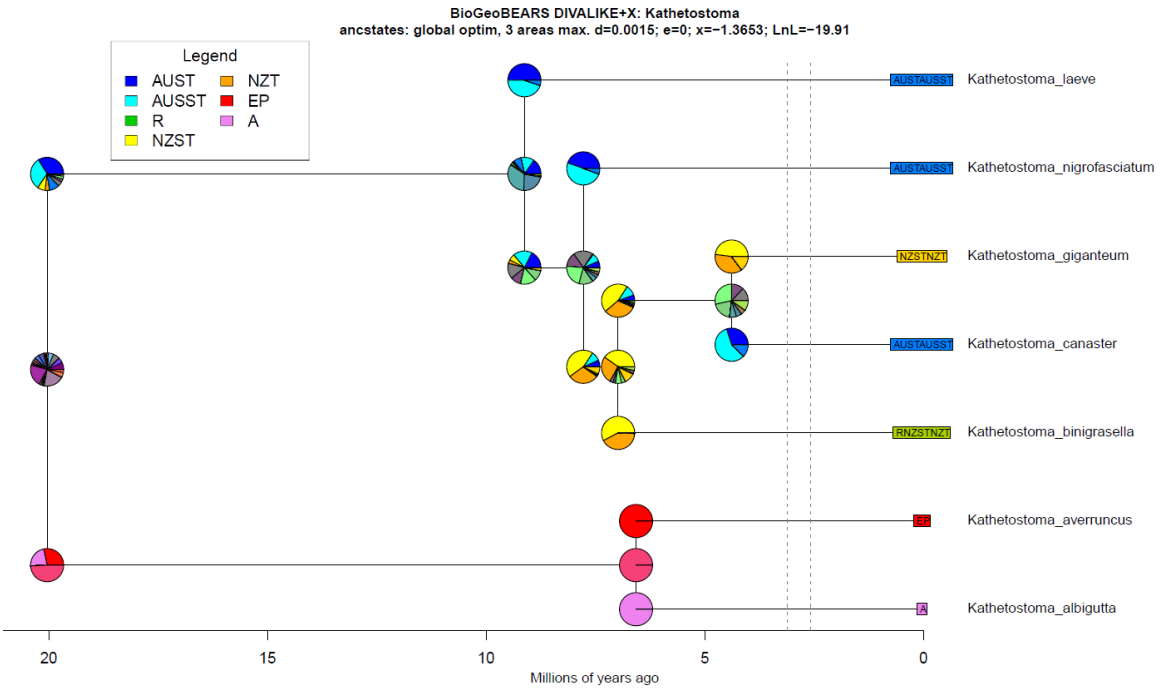

Figure 3.10S. Pie charts showing the probabilities of each ancestral range per node at the *Kathetostoma* tree based on the DIVALIKE+X model. Each range color within a pie is a mixture of base area colors (cf. legend): AUST, Australia Temperate; AUSST, Australia Subtropical; R, Rangitāhua; NZST, New Zealand Subtropical; NZT, New Zealand Temperate; EP, East Pacific; A, Atlantic Ocean. Dashed lines represent time constraints.

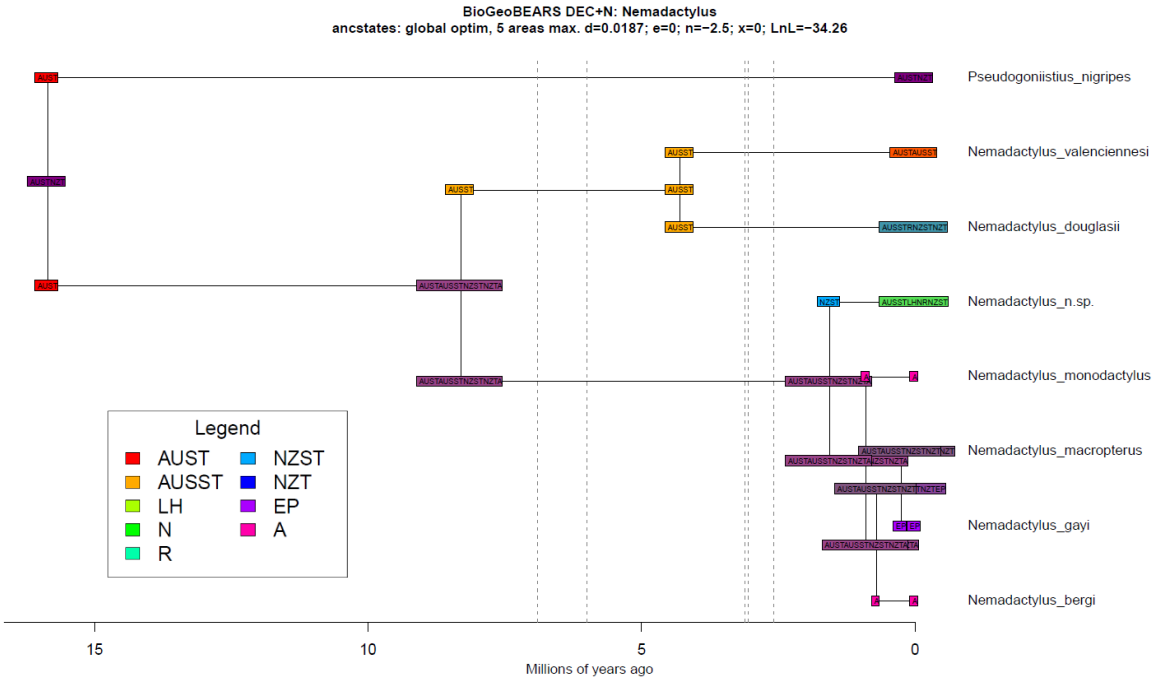

Figure 3.11S. Most likely ancestral ranges for *Nemadactylus* based on the best-fitting model (DEC+N) as inferred in 'BioGeoBEARS'. Ranges with more than one area display the mixture of colors from the base areas they include (cf. legend): AUST, Australia Temperate; AUSST, Australia Subtropical; LH, Lord Howe; N, Norfolk; R, Rangitāhua; NZST, New Zealand Subtropical; NZT, New Zealand Temperate; EP, East Pacific; A, Atlantic Ocean. Dashed lines represent time constraints.

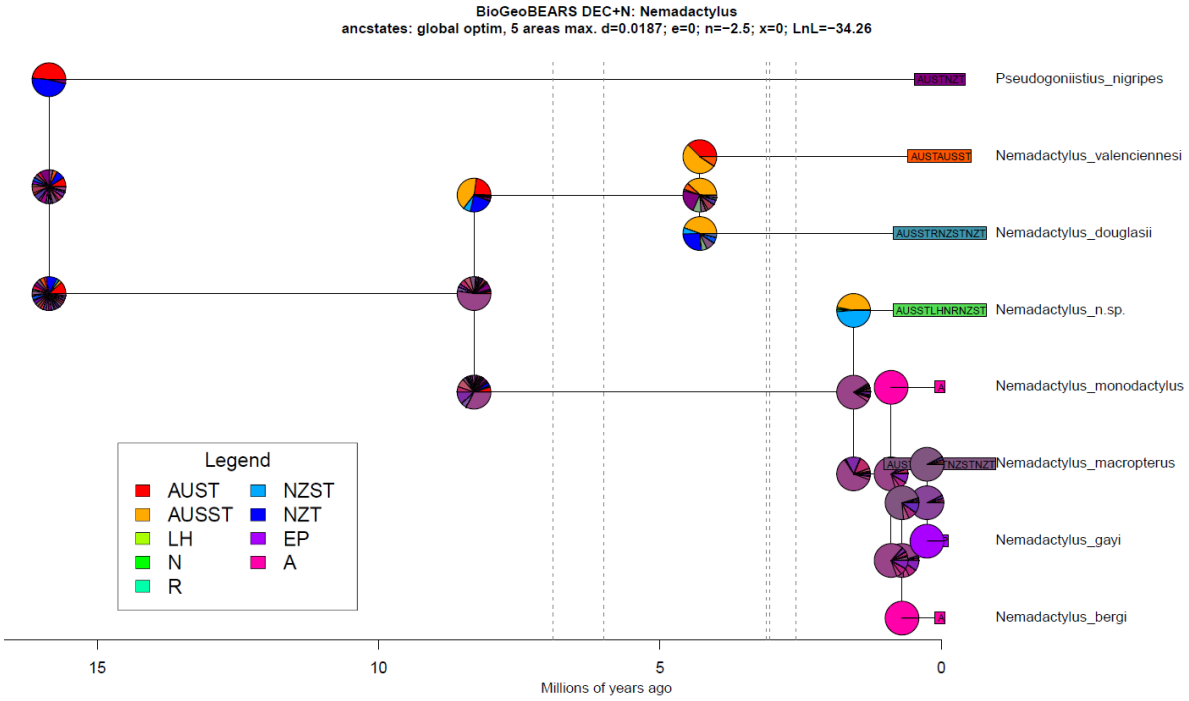

Figure 3.12S. Pie charts showing the probabilities of each ancestral range per node at the *Nemadactylus* tree based on the DEC+N model. Each range color within a pie is a mixture of base area colors (cf. legend): AUST, Australia Temperate; AUSST, Australia Subtropical; LH, Lord Howe; N, Norfolk; R, Rangitāhua; NZST, New Zealand Subtropical; NZT, New Zealand Temperate; EP, East Pacific; A, Atlantic Ocean. Dashed lines represent time constraints.

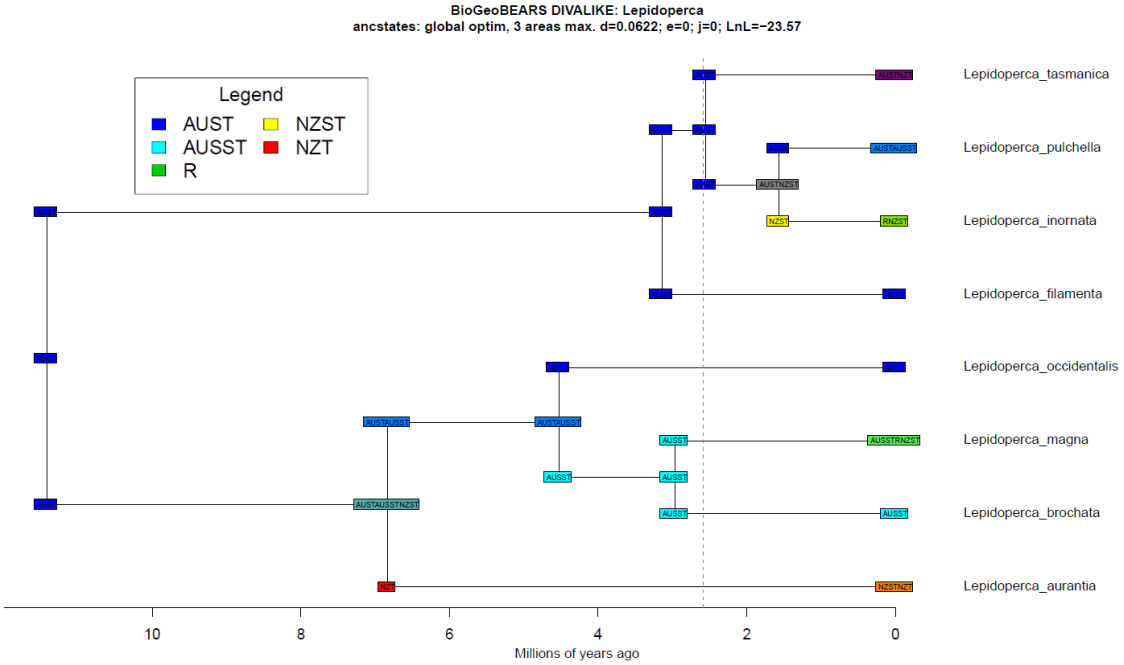

Figure 3.13S. Most likely ancestral ranges for *Lepidoperca* based on the best-fitting model (DIVALIKE) as inferred in 'BioGeoBEARS'. Ranges with more than one area display the mixture of colors from the base areas they include (cf. legend): AUST, Australia Temperate; AUSST, Australia Subtropical; R, Rangitāhua; NZST, New Zealand Subtropical; NZT, New Zealand Temperate. Dashed line represents a time constraint.

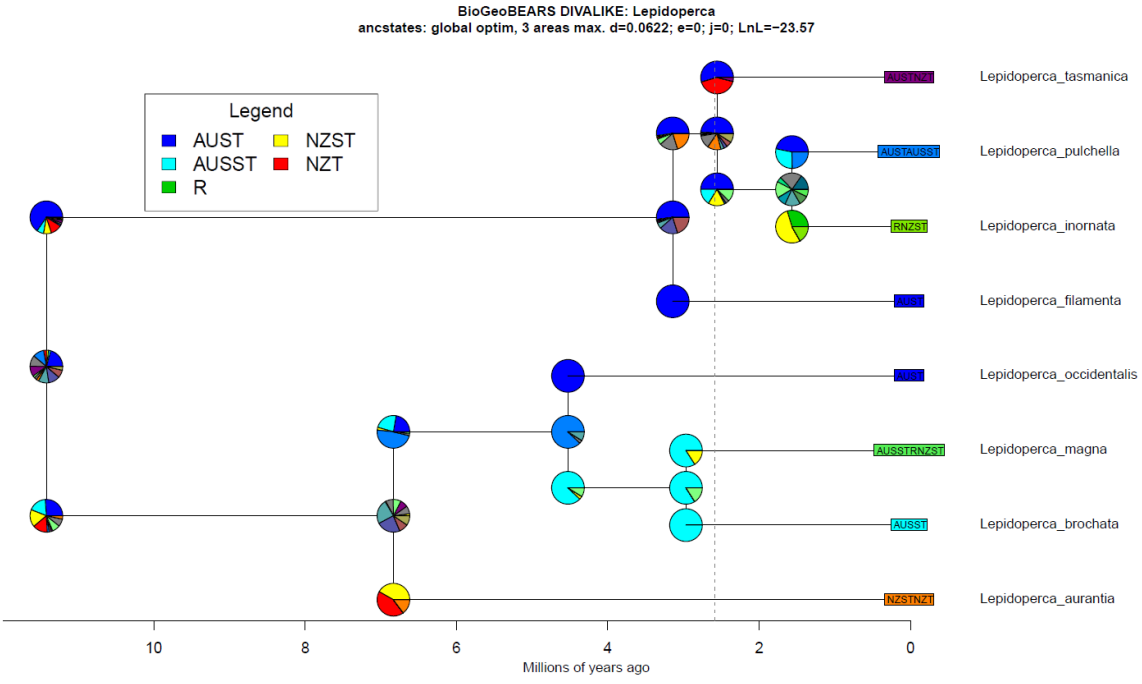

Figure 3.14S. Pie charts showing the probabilities of each ancestral range per node at the *Lepidoperca* tree based on the DIVALIKE model. Each range color within a pie is a mixture of base area colors (cf. legend): AUST, Australia Temperate; AUSST, Australia Subtropical; R, Rangitāhua; NZST, New Zealand Subtropical; NZT, New Zealand Temperate. Dashed line represents a time constraint.

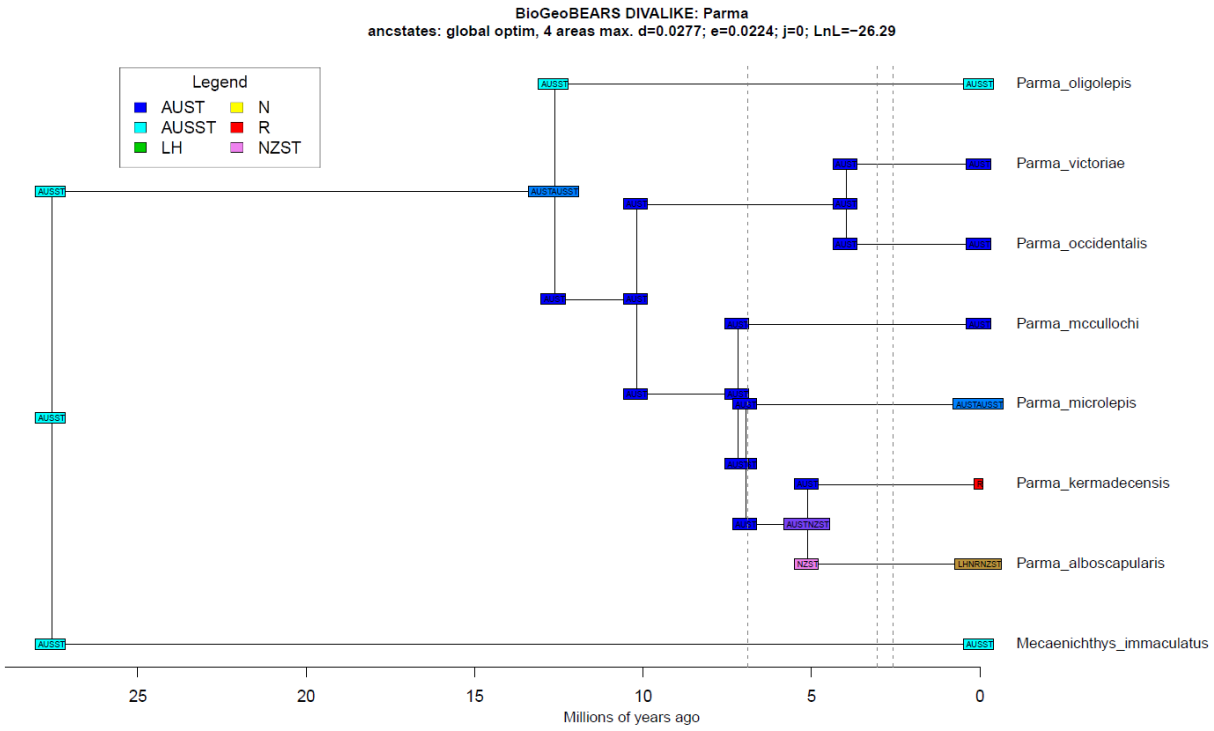

Figure 3.15S. Most likely ancestral ranges for *Parma* based on the best-fitting model (DIVALIKE) as inferred in 'BioGeoBEARS'. Ranges with more than one area display the mixture of colors from the base areas they include (cf. legend): AUST, Australia Temperate; AUSST, Australia Subtropical; LH, Lord Howe; N, Norfolk; R, Rangitāhua; NZST, New Zealand Subtropical. Dashed lines represent time constraints.

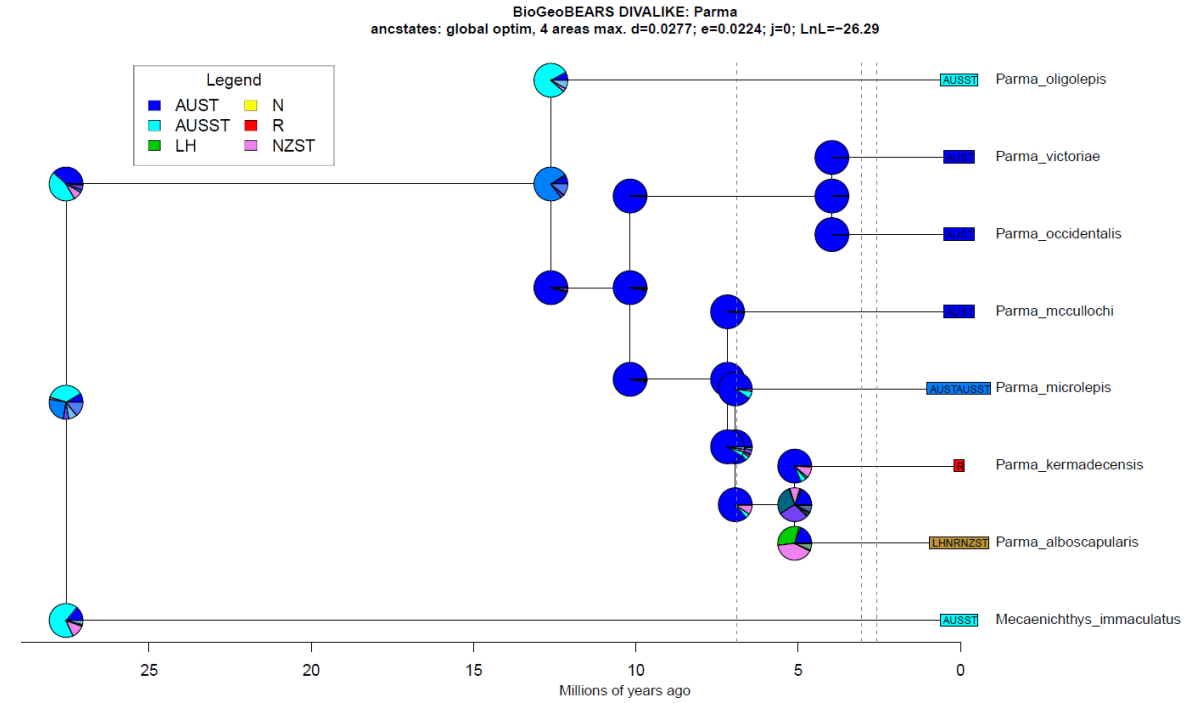

Figure 3.16S. Pie charts showing the probabilities of each ancestral range per node at the *Parma* tree based on the DIVALIKE model. Each range color within a pie is a mixture of base area colors (cf. legend): AUST, Australia Temperate; AUSST, Australia Subtropical; LH, Lord Howe; N, Norfolk; R, Rangitāhua; NZST, New Zealand Subtropical. Dashed lines represent time constraints.

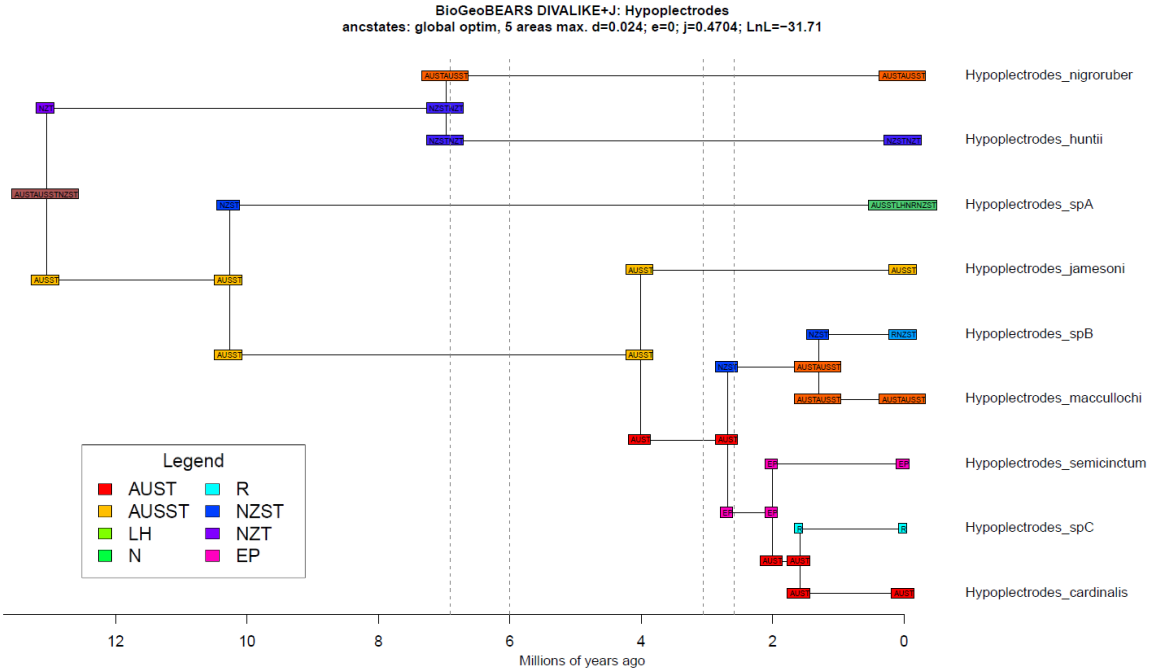

Figure 3.17S. Most likely ancestral ranges for *Hypoplectrodes* based on the best-fitting model (DIVALIKE+J) as inferred in 'BioGeoBEARS'. Ranges with more than one area display the mixture of colors from the base areas they include (cf. legend): AUST, Australia Temperate; AUSST, Australia Subtropical; LH, Lord Howe; N, Norfolk; R, Rangitāhua; NZST, New Zealand Subtropical; NZT, New Zealand Temperate; EP, East Pacific. Dashed lines represent time constraints.

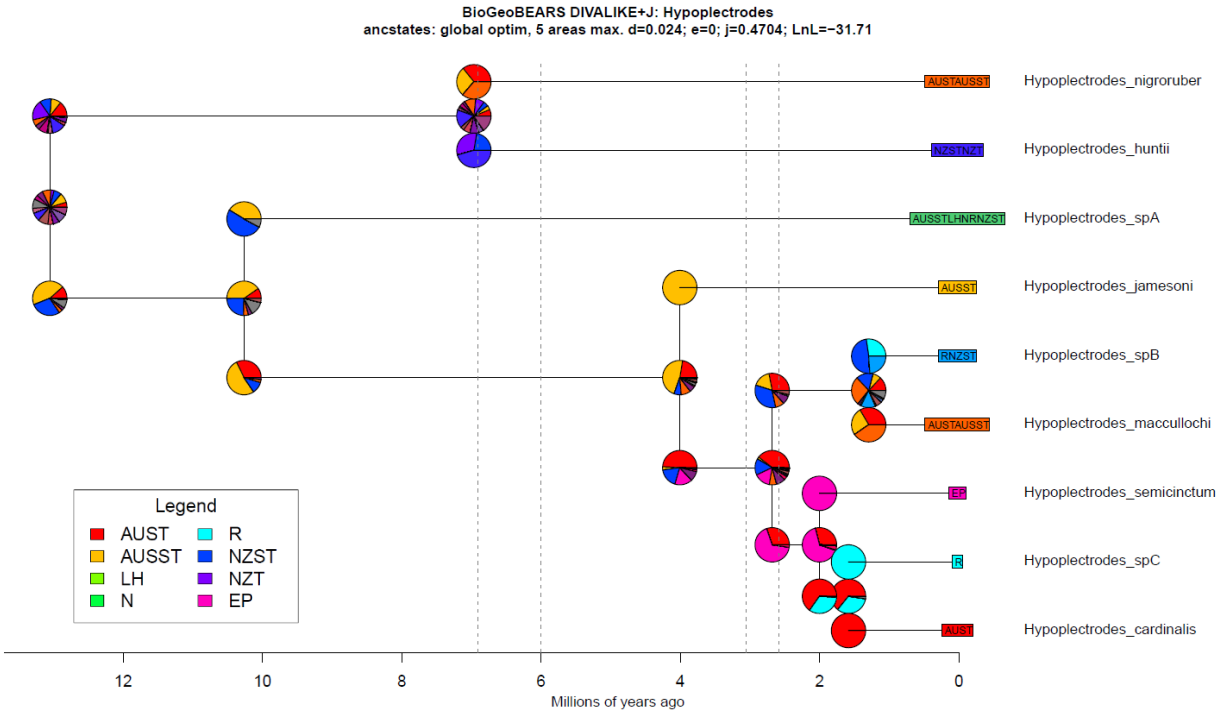

Figure 3.18S. Pie charts showing the probabilities of each ancestral range per node at the *Hypoplectrodes* tree based on the DIVALIKE+J model. Each range color within a pie is a mixture of base area colors (cf. legend): AUST, Australia Temperate; AUSST, Australia Subtropical; LH, Lord Howe; N, Norfolk; R, Rangitāhua; NZST, New Zealand Subtropical; NZT, New Zealand Temperate; EP, East Pacific. Dashed lines represent time constraints.

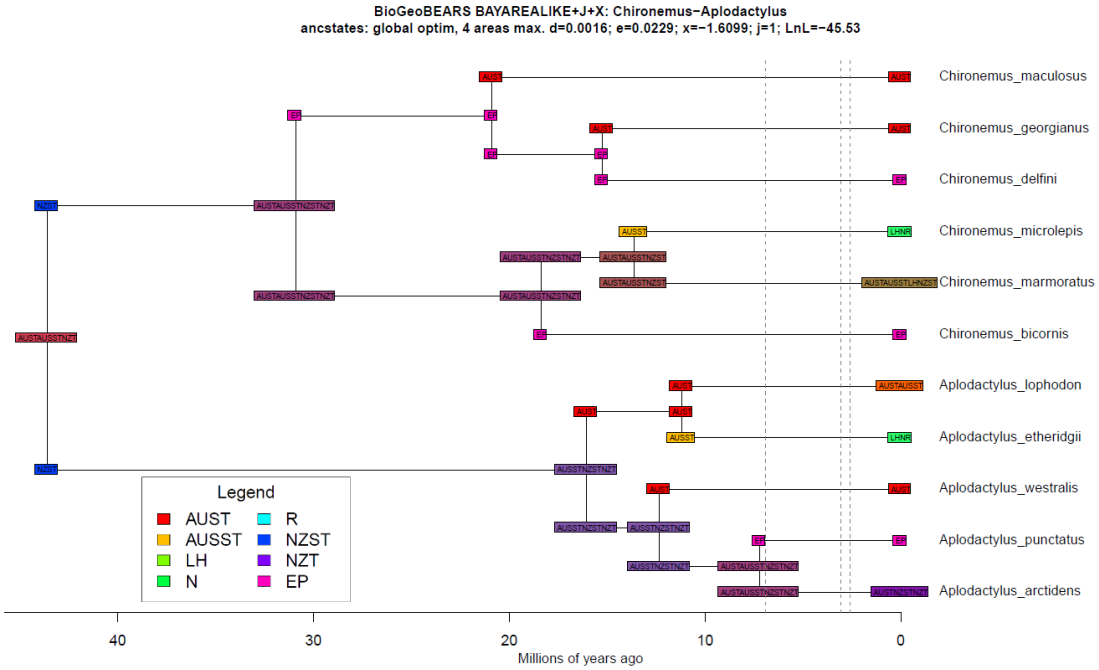

Figure 3.19S. Most likely ancestral ranges for *Chironemus* and *Aplodactylus* based on the best-fitting model (BAYAREALIKE+J+X) as inferred in 'BioGeoBEARS'. Ranges with more than one area display the mixture of colors from the base areas they include (cf. legend): AUST, Australia Temperate; AUSST, Australia Subtropical; LH, Lord Howe; N, Norfolk; R, Rangitāhua; NZST, New Zealand Subtropical; NZT, New Zealand Temperate; EP, East Pacific. Dashed lines represent time constraints.

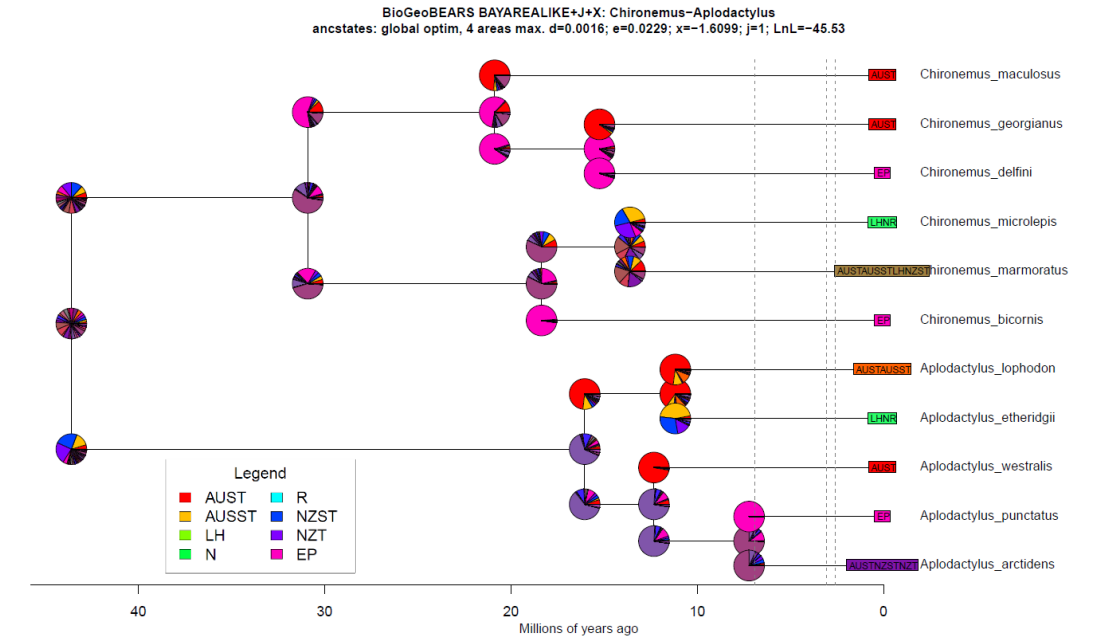

Figure 3.20S. Pie charts showing the probabilities of each ancestral range per node for *Chironemus* and *Aplodactylus* based on the BAYAREALIKE+J+X model. Each range color within a pie is a mixture of base area colors (cf. legend): AUST, Australia Temperate; AUSST, Australia Subtropical; LH, Lord Howe; N, Norfolk; R, Rangitāhua; NZST, New Zealand Subtropical; NZT, New Zealand Temperate; EP, East Pacific. Dashed lines represent time constraints.

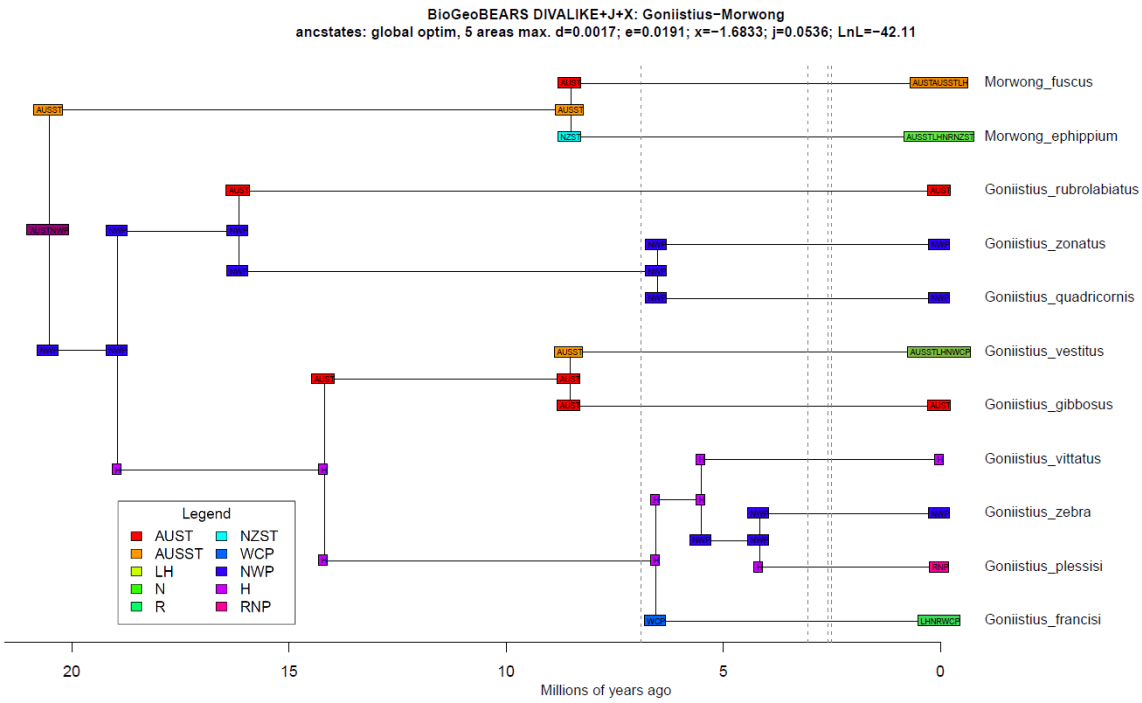

Figure 3.21S. Most likely ancestral ranges for *Goniistius* and *Morwong* based on the best-fitting model (DIVALIKE+J+X) as inferred in 'BioGeoBEARS'. Ranges with more than one area display the mixture of colors from the base areas they include (cf. legend): AUST, Australia Temperate; AUSST, Australia Subtropical; LH, Lord Howe; N, Norfolk; R, Rangitāhua; NZST, New Zealand Subtropical; WCP, West/Central Pacific; NWP, Northwest Pacific; H, Hawaii; RNP, Rapa Nui/Pitcairn. Dashed lines represent time constraints.

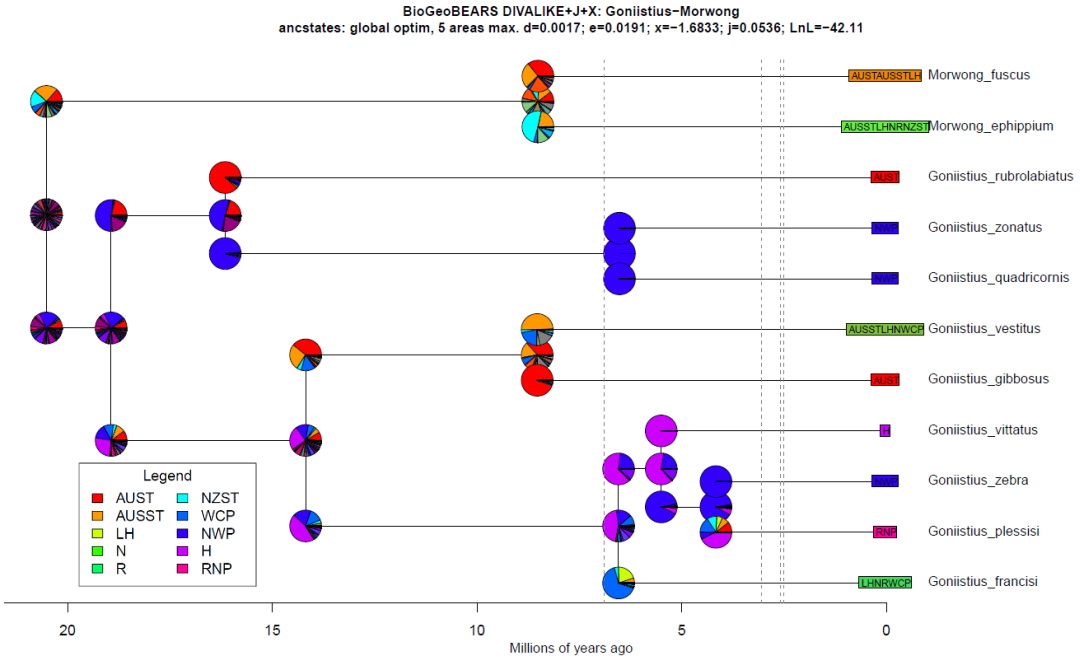

Figure 3.22S. Pie charts showing the probabilities of each ancestral range per node for *Goniistius* and *Morwong* based on the DIVALIKE+J+X model. Each range color within a pie is a mixture of base area colors (cf. legend): AUST, Australia Temperate; AUSST, Australia Subtropical; LH, Lord Howe; N, Norfolk; R, Rangitāhua; NZST, New Zealand Subtropical; WCP, West/Central Pacific; NWP, Northwest Pacific; H, Hawaii; RNP, Rapa Nui/Pitcairn. Dashed lines represent time constraints.

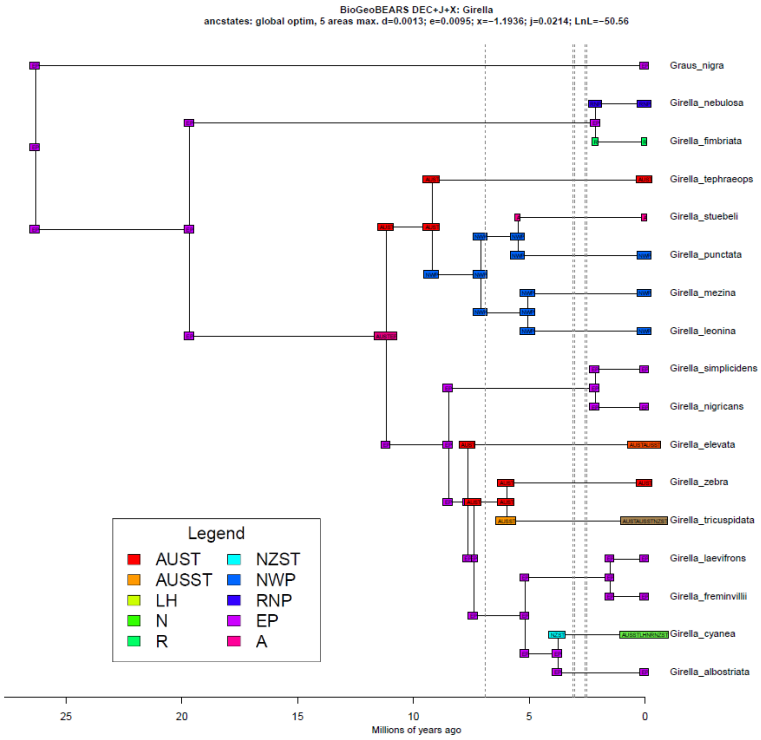

Figure 3.23S. Most likely ancestral ranges for *Girella* based on the best-fitting model (DEC+J) as inferred in 'BioGeoBEARS'. Ranges with more than one area display the mixture of colors from the base areas they include (cf. legend): AUST, Australia Temperate; AUSST, Australia Subtropical; LH, Lord Howe; N, Norfolk; R, Rangitāhua; NZST, New Zealand Subtropical; NWP, Northwest Pacific; RNP, Rapa Nui/Pitcairn; EP, East Pacific; A, Atlantic Ocean. Dashed lines represent time constraints.

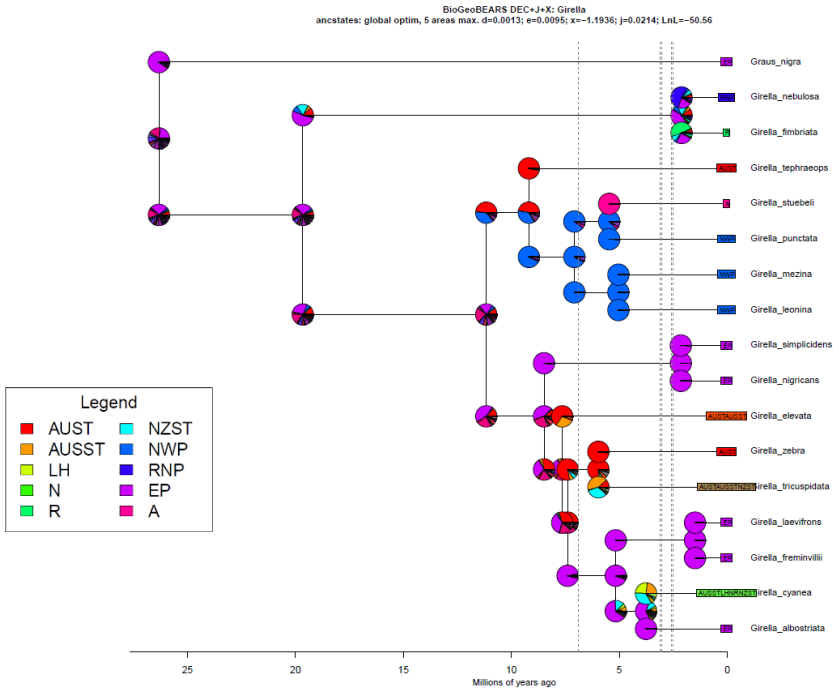

Figure 3.24S. Pie charts showing the probabilities of each ancestral range per node at the *Girella* tree based on the DEC+J model. Each range color within a pie is a mixture of base area colors (cf. legend): AUST, Australia Temperate; AUSST, Australia Subtropical; LH, Lord Howe; N, Norfolk; R, Rangitāhua; NZST, New Zealand Subtropical; NWP, Northwest Pacific; RNP, Rapa Nui/Pitcairn; EP, East Pacific; A, Atlantic Ocean. Dashed lines represent time constraints.

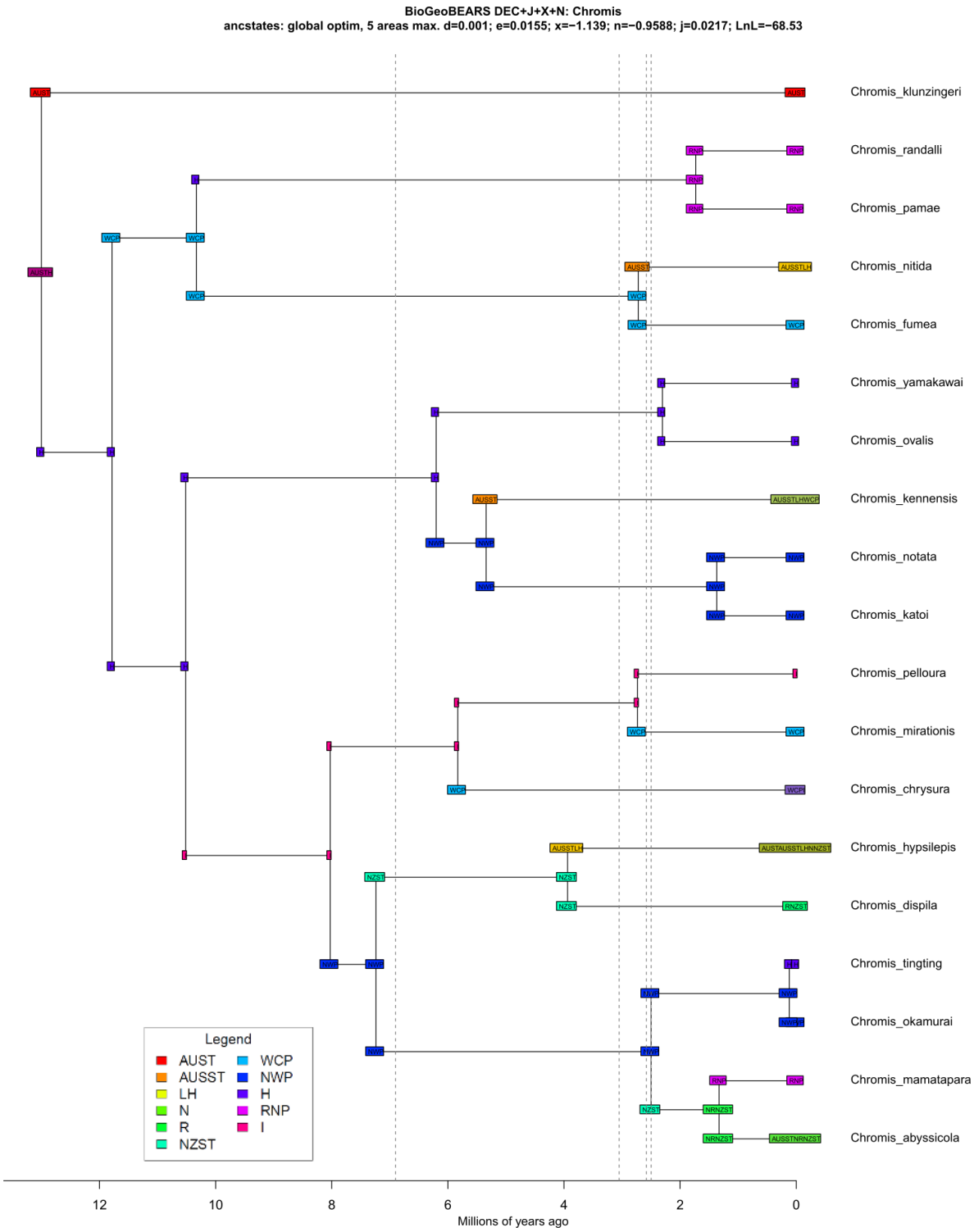

Figure 3.25S. Most likely ancestral ranges for *Chromis* based on the best-fitting model (DEC+J+X+N) as inferred in 'BioGeoBEARS'. Ranges with more than one area display the mixture of colors from the base areas they include (cf. legend): AUST, Australia Temperate; AUSST, Australia Subtropical; LH, Lord Howe; N, Norfolk; R, Rangitāhua; NZST, New Zealand Subtropical; WCP, West/Central Pacific; NWP, Northwest Pacific; H, Hawaii; RNP, Rapa Nui/Pitcairn; I, Indian Ocean. Dashed lines represent time constraints.

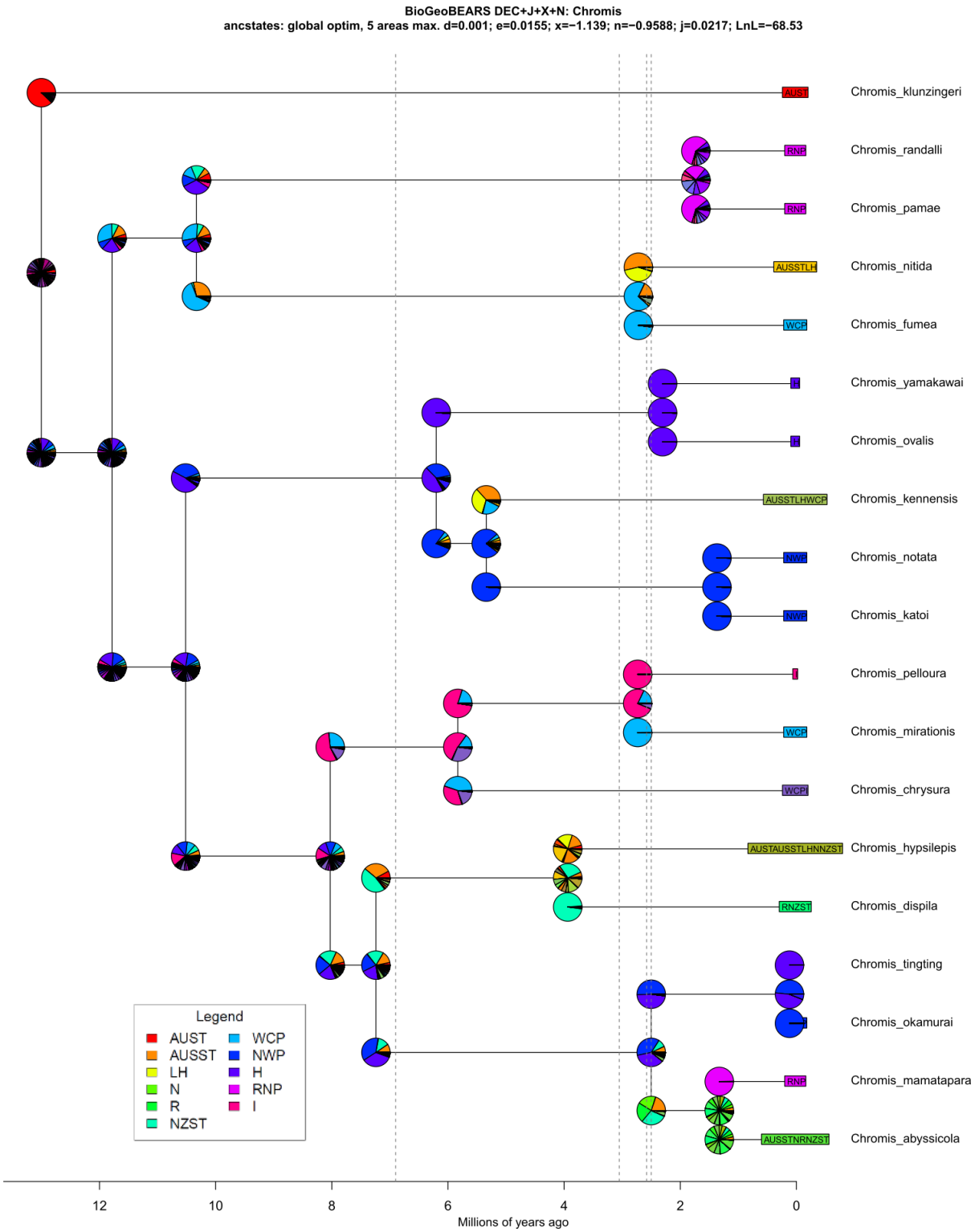

Figure 3.26S. Pie charts showing the probabilities of each ancestral range per node at the *Chromis* tree based on the DEC+J+X+N model. Each range color within a pie is a mixture of base area colors (cf. legend): AUST, Australia Temperate; AUSST, Australia Subtropical; LH, Lord Howe; N, Norfolk; R, Rangitāhua; NZST, New Zealand Subtropical; WCP, West/Central Pacific; NWP, Northwest Pacific; H, Hawaii; RNP, Rapa Nui/Pitcairn; I, Indian Ocean. Dashed lines represent time constraints.

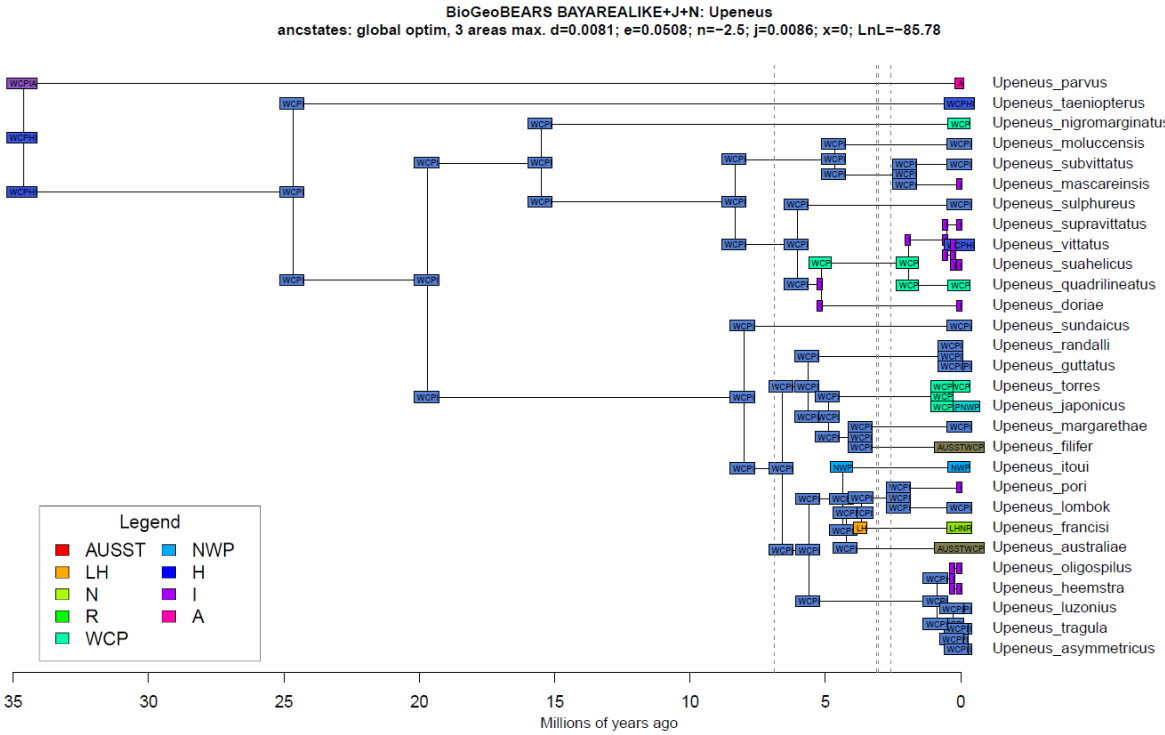

Figure 3.27S. Most likely ancestral ranges for *Upeneus* based on the best-fitting model (BAYAREALIKE+J+N) as inferred in 'BioGeoBEARS'. Ranges with more than one area display the mixture of colors from the base areas they include (cf. legend): AUSST, Australia Subtropical; LH, Lord Howe; N, Norfolk; R, Rangitāhua; WCP, West/Central Pacific; NWP, Northwest Pacific; H, Hawaii; I, Indian Ocean; A, Atlantic Ocean. Dashed lines represent time constraints.

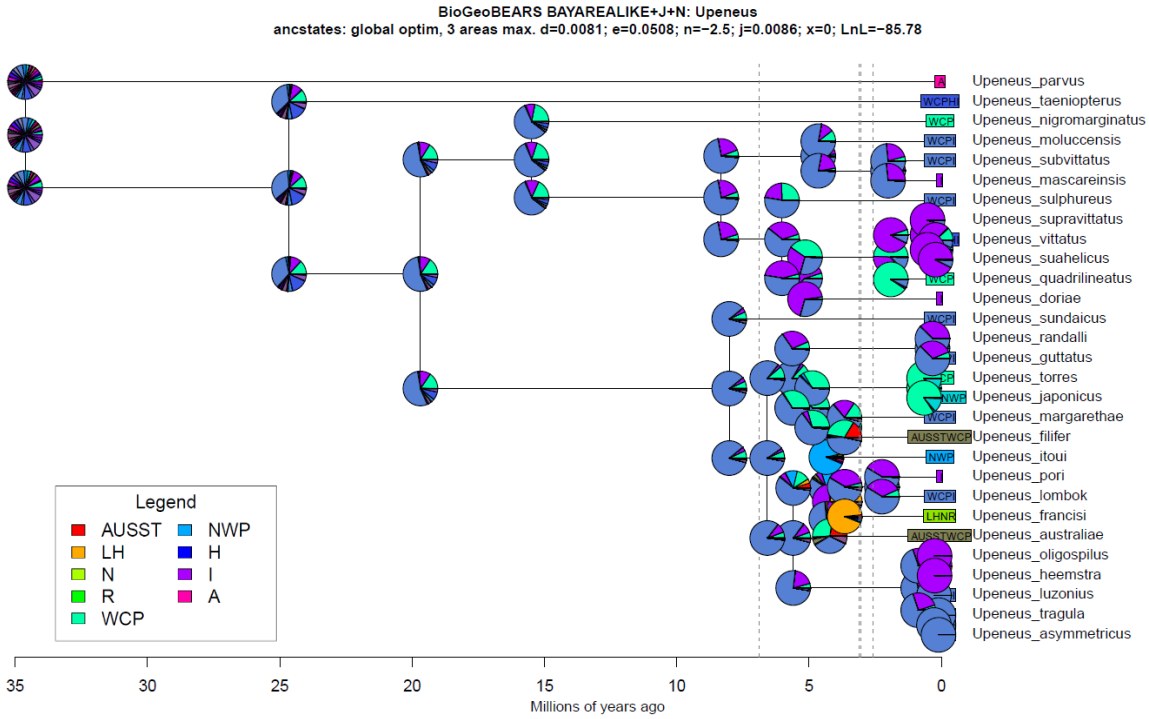

Figure 3.28S. Pie charts showing the probabilities of each ancestral range per node at the *Upeneus* tree based on the BAYAREALIKE+J+N model. Each range color within a pie is a mixture of base area colors (cf. legend): AUSST, Australia Subtropical; LH, Lord Howe; N, Norfolk; R, Rangitāhua; WCP, West/Central Pacific; NWP, Northwest Pacific; H, Hawaii; I, Indian Ocean; A, Atlantic Ocean. Dashed lines represent time constraints.

4. Centers of species richness, neoendemism, and paleoendemism for marine fishes occur in different regions of New Zealand

MASSEY UNIVERSITY
TE KUNENGA KI PŪREHUROA
UNIVERSITY OF NEW ZEALAND

GRADUATE RESEARCH SCHOOL

STATEMENT OF CONTRIBUTION
DOCTORATE WITH PUBLICATIONS/MANUSCRIPTS

We, the student and the student's main supervisor, certify that all co-authors have consented to their work being included in the thesis and they have accepted the student's contribution as indicated below in the Statement of Originality.

Student name:	André Philippe SAMAYOA
Name and title of main supervisor:	Dr. Libby Liggins
In which chapter is the manuscript/published work?	Chapter 4
What percentage of the manuscript/published work was contributed by the student?	80%

Describe the contribution that the student has made to the manuscript/published work:
Study conception, sampling design, data curation, data analysis, results interpretation, original manuscript draft, manuscript review

Please select one of the following three options:

- ○ The manuscript/published work is published or in press
  Please provide the full reference of the research output:
- ○ The manuscript is currently under review for publication
  Please provide the name of the journal:
- ◉ It is intended that the manuscript will be published, but it has not yet been submitted to a journal

Student's signature:	André Philippe SAMAYOA Digitally signed by André Philippe SAMAYOA Date: 2022.10.26 15:06:15 +02'00'	Main supervisor's signature:	Libby Liggins Digitally signed by Libby Liggins Date: 2022.10.27 10:36:25 +13'00'

This form should be placed at the beginning of each relevant thesis chapter.

4.1. Abstract

High species diversity and endemism are important to spatial conservation, but do not always occur in the same places. Furthermore, high endemism can result from two different evolutionary processes – the generation of novel lineages (neoendemism) versus the survival of relict lineages (paleoendemism). Here, we examined the biodiversity patterns of marine fishes in Aotearoa New Zealand, and surrounding regions, using taxonomic and phylogenetic measures of richness and endemism. Although we detected an overall decrease in all indices with increasing latitude, areas of high biodiversity richness and endemism were different. Richness peaked around Northland, likely the result of the northerly input of warm water. We also identified centers of endemism in New Zealand, where neoendemism was prevalent in subtropical volcanic islands, and paleoendemism in two coastal areas of the main islands, the Hauraki Gulf and the Banks Peninsula. We hypothesize that northern neoendemism is driven by the isolation of recently emerged oceanic islands, and that southern paleoendemism arose from relatively stable environmental conditions over time, particularly in the Hauraki Gulf. Our investigation is a significant step to understand the processes shaping marine fish biodiversity and endemism patterns in a geologically active region of the Pacific.

4.2. Introduction

Understanding the patterns and processes of biodiversity richness and endemism are important to conservation (Bowen et al., 2013). Centers of endemism can reveal originating processes (Bellwood and Meyer, 2009), distinguish whether an endemic species is at the beginning or end of its evolutionary trajectory, and identify geographic areas as either ‘cradles’ or ‘museums’ for marine biodiversity (Cowman et al., 2017). The study of biodiversity and endemism has traditionally relied on measures at the species level (Gaston, 1996), including: species richness, the count of species; and weighted endemism, the count of species weighted by their range size (Crisp et al., 2001). Species richness indicates locations with high/low taxonomic richness, whereas weighted

endemism reveals locations with a predominance of species with small ranges, providing a measure of relative endemism. However, such taxonomic measures can be sensitive to variation in nomenclature and taxon designation across groups (Lee and Mishler, 2014), and do not capture the different evolutionary histories of constituent species, which may include young species among closely related taxa, and old species that are relicts of a formerly widespread lineage. In contrast, phylogenetic metrics consider the evolutionary history of taxonomic lineages (Tucker et al., 2017), and can reveal the evolutionary mechanisms that have shaped biodiversity patterns over time, otherwise uncaptured by taxonomic metrics (Cadotte and Davies, 2010).

Among phylogenetic metrics, measures of richness and endemism include phylogenetic diversity (Faith, 1992), the sum of branch lengths within a phylogenetic tree spanning all occurring taxa at a given location, and phylogenetic endemism (Rosauer et al., 2009), the sum of branch lengths spanning taxa present in an assemblage, weighted by the range of the clade that includes those taxa. Both metrics often display similar geographic patterns to species richness, however, where patterns of phylogenetic and taxonomic measures differ can highlight where local evolutionary and ecological processes are uncaptured by taxonomic indices alone (Pavoine and Bonsall, 2011). Significant departures in these patterns can be revealed by contrasting the observed phylogenetic biodiversity with values obtained from a “null” model, where phylogenetic measures are iteratively recalculated by shuffling local taxa, but keeping species richness constant (Thornhill et al., 2016). Locations with higher PD than taxonomic diversity indicate an overrepresentation of a low number of long branches (i.e. few older lineages than expected by species richness alone); in contrast, locations with lower PD than taxonomic diversity have a high number of short branches (i.e. many closely related young lineages, suggesting recent radiation). The contrast between the spatial patterns of PD and species richness has enhanced our understanding of the evolutionary mechanisms shaping the global biogeography of major taxonomic groups (Forest et al.,

2007, Fritz and Rahbek, 2012, Safi et al., 2011, Voskamp et al., 2017). Similarly, the randomization of PE, performed through a statistical approach called “categorical analysis of neo- and paleoendemism” (CANAPE) (Mishler et al., 2014), can quantitatively delineate endemism centers that generate new biodiversity (neoendemism) and/or accumulate rare old lineages (paleoendemism). CANAPE has been effective in the identification of endemism centers undervalued with taxonomic measures in flora (e.g., Dagallier et al., 2020, Heenan et al., 2017, Mishler et al., 2020, Schmidt-Lebuhn et al., 2015) and fauna (e.g., Azevedo et al., 2020, Camacho et al., 2021, Earl et al., 2021, Garcia–R et al., 2019, López-Aguirre et al., 2018). These examples show the utility of examining the spatial patterns of phylogenetic diversity and endemism to identify locations of evolutionary value (Pavoine and Bonsall, 2011).

Aotearoa New Zealand hosts a unique marine fauna (Costello et al., 2017). It is an island nation comprising two main and seven major offshore groups of islands, most of them being the aerial section of the largely submerged Zealandia continent of Gondwanan origin (Trewick et al., 2017). Consequently, an extensive continental shelf surrounds New Zealand representing a highly heterogeneous habitat for marine biodiversity (Gordon et al., 2010). New Zealand stretches a longitudinally narrow but latitudinally long area, from the northernmost Rangitāhua (Kermadec Islands) (29°S) to the southernmost Campbell Island (52°S) (Gordon et al., 2010). The country crosses three distinct climate zones (warm subtropical, temperate, and cold subantarctic) resulting in a unique faunal composition, particularly in marine fishes (Briggs and Bowen, 2012). The taxonomic richness of coastal fishes decreases with latitude (Beaumont et al., 2009), and around 19% of New Zealand’s fish fauna is endemic (Gordon et al., 2010), predominantly occurring in Rangitāhua (Trnski and de Lange, 2015), a young volcanic archipelago of distinct geological origin than the remainder of the Gondwanan islands (Brook, 1998). Molecular evidence shows that marine fishes endemic to remote oceanic volcanic islands of the Southwest Pacific, including Rangitāhua, are neoendemics

(Samayoa et al., 2022), suggesting that northern New Zealand exports biodiversity novelties, while endemism in other regions remains unexplored. New Zealand's marine fish fauna is among the most comprehensively inventoried at a global scale (Mora et al., 2008, Roberts et al., 2020), and phylogenetic relationships have been inferred for over 71% of taxa (Eme et al., 2019), providing the opportunity to critically examine which regions of New Zealand are centers of neoendemism and paleoendemism, and to infer the processes shaping contemporary biogeographic patterns.

Recently, novel biogeographic insights have emerged from integrative analyses of marine fish biodiversity along broad-scale environmental gradients in New Zealand (Myers et al., 2021, Zintzen et al., 2017). A recent phylogenetic investigation (Eme et al., 2020) divided New Zealand's marine environment into three depth zones according to a multivariate analysis of phylogenetic diversity measures: the shallow 0-500 m, with high taxonomic and phylogenetic diversity; the species-poor intermediate 500-900 m, displaying a wide range of distantly related lineages; and the deep 900-1,200 m characterized by older taxa. Depth was the main driver of patterns in phylogenetic measures, despite evidence of a latitude gradient in these measures. The study highlighted how speciation in the shallows was likely driven by different factors from deeper depth, such as high energy, habitat diversity, and isolation events due to past sea-level fluctuation. Our study builds on this baseline by using the most updated molecular phylogeny for New Zealand's marine fishes to calculate phylogenetic and taxonomic measures of richness and endemism for the 0-500 m assemblage, and to apply randomization tests to search for mechanisms driving the biogeography of New Zealand's marine fishes.

Our study aims to examine patterns of biodiversity richness and endemism of New Zealand's marine fishes occurring at 0-500 m using a phylogenetic approach. In particular, we aimed to (1) describe the spatial patterns of richness and endemism based on taxonomic and phylogenetic metrics, (2) identify locations with high biodiversity

richness and endemism, (3) identify locations where phylogenetic measures provide novel insights into the evolutionary origins of biodiversity, by contrasting taxonomic and phylogenetic patterns, and (4) propose hypotheses for the processes underlying the observed patterns. Considering the decreasing gradient of species richness in New Zealand's marine fishes with increasing latitude, and the generally positive relationship between species richness and phylogenetic metrics, we anticipated detecting a similar gradient with phylogenetic measures where values tend to decrease with latitude. We also expected to find phylogenetic evidence that the remote northern subtropical oceanic islands act mainly as centers of neoendemism for marine fishes. Our study represents a significant step into describing patterns of phylogenetic richness and endemism in marine fishes, and a continuing working framework to infer processes responsible for generating and maintaining the biodiversity of marine ray-finned fishes in New Zealand.

4.3. Materials and methods

4.3.1. Taxonomic checklist

We focused on marine fishes inhabiting 0-500 m depths around New Zealand. We extracted occurrence data from the Ocean Biogeographic Information System (OBIS; www.obis.org) using the 'robis' package (Provoost and Bosch, 2020) in R v.4.2.0 (R Core Team, 2022) using RStudio v.2022.02.3.492 (RStudio Team, 2022) limiting our searches to a geographic area between 25°S-55°S and 160°E-170°W to include all main and offshore islands of New Zealand (Fig. 5) bounded in the north by Rangitāhua, the south by Campbell Island, the east by Chatham Islands, and the west by Auckland Island. Because we limited our study area based on topographic criteria and not political boundaries, the Australian territory of Norfolk Island (29°S, 167°E) is included in our biogeographic analyses, and consequently mentioned in our inferences. The OBIS search was filtered by depth and limited to actinopterygians, accepted species (as per WoRMS, WoRMS Editorial Board, 2022), and marine and brackish taxa (excluding freshwater taxa), resulting in a list of 417 taxa. Although depth information is not

consistently reported in occurrence repositories, and the gathered data is likely biased by varying sampling effort across areas, more occurrence data is available for coastal areas than for offshore locations within OBIS (Webb et al., 2010), and these data are the best available for understanding species distributions for New Zealand's actinopterygians.

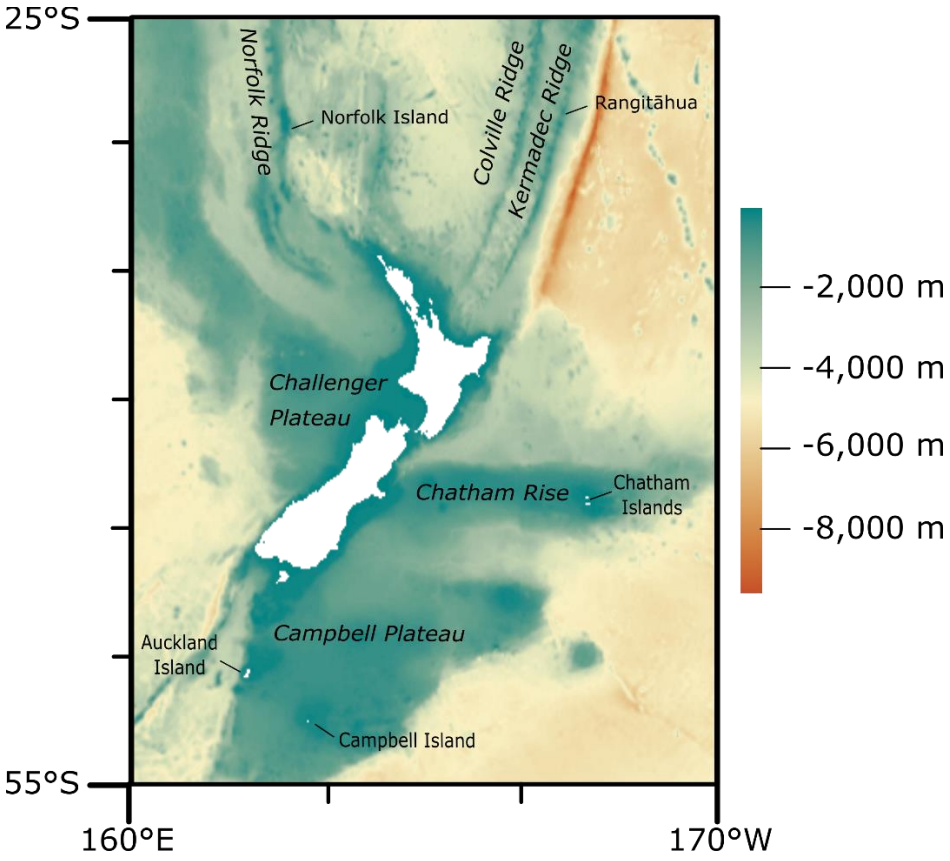

Fig. 5. Study area in our investigation, bounded by latitudes 25°S and 55°S, and longitudes 160°E and 170°W. The area is shown as a bathymetric map to indicate the main underwater topographic features (italicized) and bounding offshore islands, emerged landmasses appearing in white. All islands are territories of New Zealand, except Norfolk Island which belongs to Australia.

To refine our taxa list according to regional expertise, we cross-referenced our OBIS checklist with the taxa included in the Fishes of New Zealand (Roberts et al., 2020, Roberts et al., 2015), which provides a comprehensive list of New Zealand fishes. Specifically, we retained taxa in our list from OBIS only when these were included in the New Zealand checklist, reducing the taxa list to 237. In this process, we detected that not all listed taxa in the Fishes of New Zealand are reported in OBIS. For these unlisted taxa, we individually verified their nomenclature, habitat, and depth distribution by cross-

referencing data with the Eschmeyer's Catalog of Fishes (Fricke et al., 2022) and Fishbase (Froese and Pauly, 2022). Of these, we excluded taxa for which there were nomenclature discrepancies among data sources at the time of research (access in May 2022), taxa that mainly inhabit deep waters (500-4,000 m) even though there are records at 500 m or shallower, and undescribed taxa. Our resulting taxonomic list consisted of 541 marine fish taxa.

4.3.2. Geographic distribution data

We searched native distribution maps for the 541 taxa using AquaMaps (Kaschner et al., 2011), a web-based tool that generates distribution models by integrating occurrence data from OBIS and environmental variables (sea surface temperature, salinity, primary productivity, and ice coverage) to estimate probabilities of occurrence in half degree cells. We opted for these models since they yield distribution maps for marine taxa otherwise difficult to infer by direct survey efforts: marine systems are not as thoroughly and easily sampled as land environments (Hughes et al., 2021), with a further bias towards easily accessible marine areas (e.g. coastal areas) leaving many open-water locations unsampled (Hortal et al., 2015). AquaMaps allows the inference of ranges in these difficult-to-reach areas of the ocean, and has been used for the assessment of biodiversity patterns in marine fishes (Lin et al., 2021, Rabosky et al., 2018) and other marine taxa (Brito-Morales et al., 2020, Coll et al., 2010), and for marine protection planning (Klein et al., 2015, Selig et al., 2014, Visalli et al., 2020).

In our study, we retained 408 taxa that had non-zero probabilities of occurrence in cells within our study area, excluding: 86 taxa with no available map; 30 with an available map but no data within our study area; 8 for which their depth range was below 500 m after contrasting depth data among web-based repositories; 6 with a map based on poorly sampled datasets as flagged by AquaMaps; and three with invalid nomenclature (according to AquaMaps and Fishbase) to which no map could be matched. After downloading distribution data for each of the 408 taxa, we used the

'raster' package (Hijmans and van Etten 2012) for R to rasterize occurrence data and fit it to our bounding box. We downloaded depth contour data for New Zealand as a raster layer from the Global Marine Environment Databases (GMED; www. https://gmed.auckland.ac.nz), limiting it to 0-500 m with the 'marmap' package (Pante and Simon-Bouhet 2013) for R. Depth data was added to our rasterized distribution maps to retain cells within the 0-500 m depth contour and to remove those that fell on land using functions of the 'raster' package. The 408 raster layers were converted to binary presence/absence layers using the 'raster' package according to varying thresholds of occurrence probabilities.

4.3.3. Occurrence probability thresholds

AquaMaps provides occurrence data as probabilities ranging 0-1, where 0 represents areas outside a taxon's range, and 1 is the best-suited environment. To select the best value for downstream analysis, there is no standard procedure, although Kaschner et al. (2011) suggested to cross-validate inferred maps with externally curated distribution information to facilitate the process, an approach the authors applied to marine mammals, suggesting a value of 0.6 as an appropriate threshold to select suitable habitats (Louis et al., 2020, Skovrind et al., 2021). For marine fishes, no standard procedure is currently available for threshold selection, with examples of studies using all non-zero probability cells (Lin et al., 2021) and a threshold value of 0.5 (Rabosky et al., 2018). In our study, we generated five range maps per species based on different occurrence probability thresholds (0.01, 0.25, 0.50, 0.75, and 1.00), and performed biogeographic analyses across these datasets to ensure results and interpretations did not substantially differ according to the threshold used. Resulting maps and plots based on the five thresholds are included as Supplementary Material (Fig. 4.1S-4.16S). Small differences were observed in the range-based metrics (weighted and phylogenetic endemism) across datasets, where values in some northern locations decreased when the threshold increased (Fig. 4.4S-4.5S), likely an artifact of higher range constriction at

higher probability thresholds (Selig et al., 2014, Venegas-Li et al., 2019). Despite these minor differences, biogeographic patterns remained generally constant across the datasets. Hence, we present our main findings based on a threshold of 0.75, a conservative value that confines taxa close to their core range, while acknowledging that organisms can occur in habitats slightly less suitable.

4.3.4. Molecular phylogeny

We used the most comprehensive time-calibrated phylogeny for marine fishes in New Zealand (Eme et al., 2020) which includes 803 taxa. Of our 408 taxa with available distribution data, 313 were included in the phylogeny. Therefore, our subsequent biogeographic analyses included 77% of marine fishes inferred to inhabit depths of 0-500 m in New Zealand.

4.3.5. Taxonomic and phylogenetic metrics

Taxonomic diversity was assessed with species richness (SR) and weighted endemism (WE) (Crisp et al., 2001). Phylogenetic metrics included phylogenetic diversity (PD) (Faith, 1992), phylogenetic endemism (PE) (Rosauer et al., 2009), and their relative versions, relative phylogenetic diversity (RPD) and relative phylogenetic endemism (RPE), defined as the ratio of the observed PD/PE in the actual phylogenetic tree and the estimated PD/PE from a tree with equal branch lengths that retains the original topology (Mishler et al., 2014). For these relative measures, values over 1 suggest an overrepresentation of long branches for RPD and rare long branches for RPE, and values under 1 indicate an overrepresentation of short branches for RPD and rare short lineages for RPE. All metrics were calculated in Biodiverse v. 3.99_03 (Laffan et al., 2010) using the rasterized data derived from AquaMaps.

4.3.6. Statistical analysis

To detect locations where the observed values of phylogenetic metrics (PD, RPD, PE, and RPE) differed from what might be expected based on SR alone, we performed

randomization tests as in Mishler et al. (2014): taxa occurrences within each grid cell were randomly reassigned across the grid without replacement, keeping constant the SR within each cell and the number of cells per taxon during each randomization. Values calculated for each randomization were used to create a null distribution per cell for each metric. The significance of each observed value per cell was evaluated using a two-tailed test with α=0.05 by contrasting it with the null distribution. Significance levels were classified according to their values: significantly very high (>0.99), significantly high (>0.975), significantly low (<0.025), significantly very low (<0.01), and not significant otherwise. A set of 999 randomizations were run across the four metrics using the *rand_structured* algorithm in Biodiverse v. 3.99_03.

To identify centers of endemism, we used the randomization results of PE and RPE to perform the two-step categorical analysis of neo- and paleoendemism (CANAPE) (Mishler et al., 2014) which determines the contribution of rare (i.e. endemic) short and long branches to PE. The first step identified cells that were significantly high (one-tailed test, α=0.05) for the numerator of RPE (observed PE in the actual phylogeny) and/or the denominator (expected PE based on a phylogeny where all branch lengths are equal). Cells that passed one of these tests were, in the second step, placed into one of the following four non-overlapping groups: center of neoendemism when RPE is significantly low (two-tailed test, α=0.05); center of paleoendemism when RPE is significantly high (two-tailed test, α=0.05); center of mixed endemism (i.e. a mix of both rare short and long branches) when both the numerator and denominator are significantly high (taken alone), but RPE is not; and centers of super-endemism when the mixed endemism cells displayed high significance at α=0.01. All our rasters resulting from the individual plots per metric, randomization output, and CANAPE were set to WSG84 with 130,682 grid cells of 0.083° x 0.083° resolution.

4.4. Results

4.4.1. Spatial patterns of biodiversity metrics

Patterns in taxonomic (SR) and phylogenetic (PD, RPD) richness metrics within New Zealand's 0-500 m depth layer generally declined with increasing latitude (Fig. 6), with an initial poleward increase from low latitudes to a peak at 35°S and a subsequent progressive decrease (Fig. 4.12S-4.16S). The highest values occurred around the North Island and Norfolk Island (Australia) south of the Norfolk Ridge, and the lowest in three southern patches of the Campbell Plateau. Within intermediate values, mid to high estimates were found in areas from the southwest of the North Island down to the north and west coast of the South Island, and in the furthest eastern shallow areas of the Chatham Rise. Mid to low values were found in other areas of the Chatham Rise and all the eastern and southern coasts of the South Island.

Trends in taxonomic (WE) and phylogenetic (PE, RPE) endemism values were similar, decreasing from a distinctive peak at the lowest latitudes (Fig. 7, Fig. 4.12S-4.16S). Most of our study area displayed low values for WE and PE, with slightly higher values along the northeast coast of the North Island, and a notable maximum along the south of the Norfolk Ridge. For RPE, most of our study area was generally characterized by values under 1, except in northern patches with values slightly over 1.

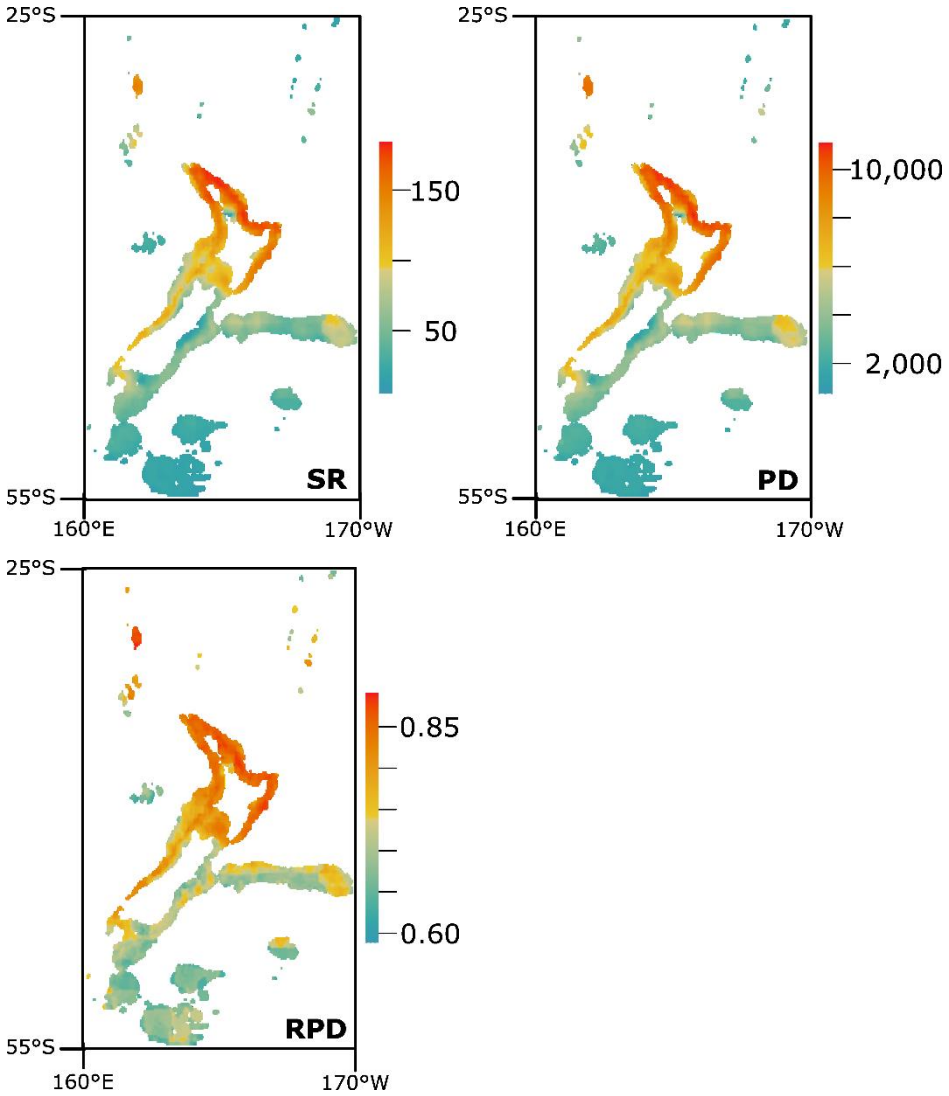

Fig. 6. Spatial patterns of taxonomic and phylogenetic richness indices for marine fishes occurring at 0-500 m around New Zealand. SR: species richness; PD: phylogenetic diversity; RPD: relative phylogenetic diversity.

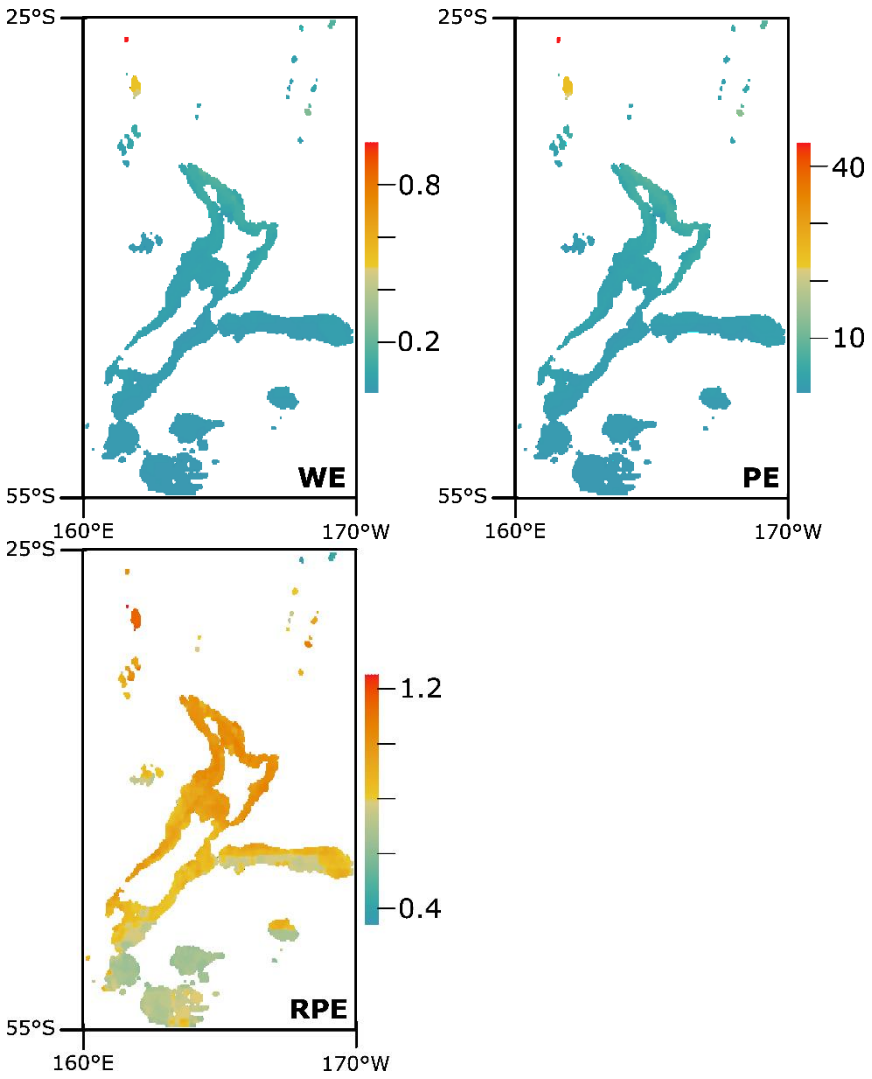

Fig. 7. Spatial patterns of taxonomic and phylogenetic endemism indices for marine fishes occurring at 0-500 m depth around New Zealand. WE: weighted endemism; PE: phylogenetic endemism; RPE: relative phylogenetic endemism.

4.4.2. Areas with higher- or lower-than-expected phylogenetic diversity

Within our study area, randomization tests highlighted locations where phylogenetic indices departed from expectations based on SR alone (Fig. 8). Significantly high phylogenetic indices appeared within the northern half of the study area which includes the North Island, the south of the Norfolk Ridge, and locations along the Colville and Kermadec Ridges. Conversely, significantly low phylogenetic indices were found within the southern half of the study area which includes locations around the South Island, the Chatham Rise, and all subantarctic shallow patches.

4.4.3. Centers of endemism

CANAPE identified all northern outlying islands and shallow banks as centers of endemism (Fig. 9), a common pattern across all our five datasets based on different probability of occurrence thresholds (Fig. 4.11S). The majority of northern locations were centers of neoendemism, followed by a lower number of centers of paleoendemism, and a minor number of locations with mixed endemism. Two particular locations appeared as centers of endemism along the main islands: the first location was the Hauraki Gulf in the North Island (also identified in four of the five threshold datasets, except the one based in all non-zero occurrence probability cells; Fig. 4.11Sa); the second location was the Banks Peninsula in the South Island, in particular Pegasus Bay in the north and Canterbury Bight in the south of the peninsula (a consistent result across four of the five datasets, except the one based on all-1s occurrence probability cells; Fig. 4.11Se). Both endemism centers were characterized by an equal incidence of neo- and paleoendemism, followed by a lower number of mixed centers.

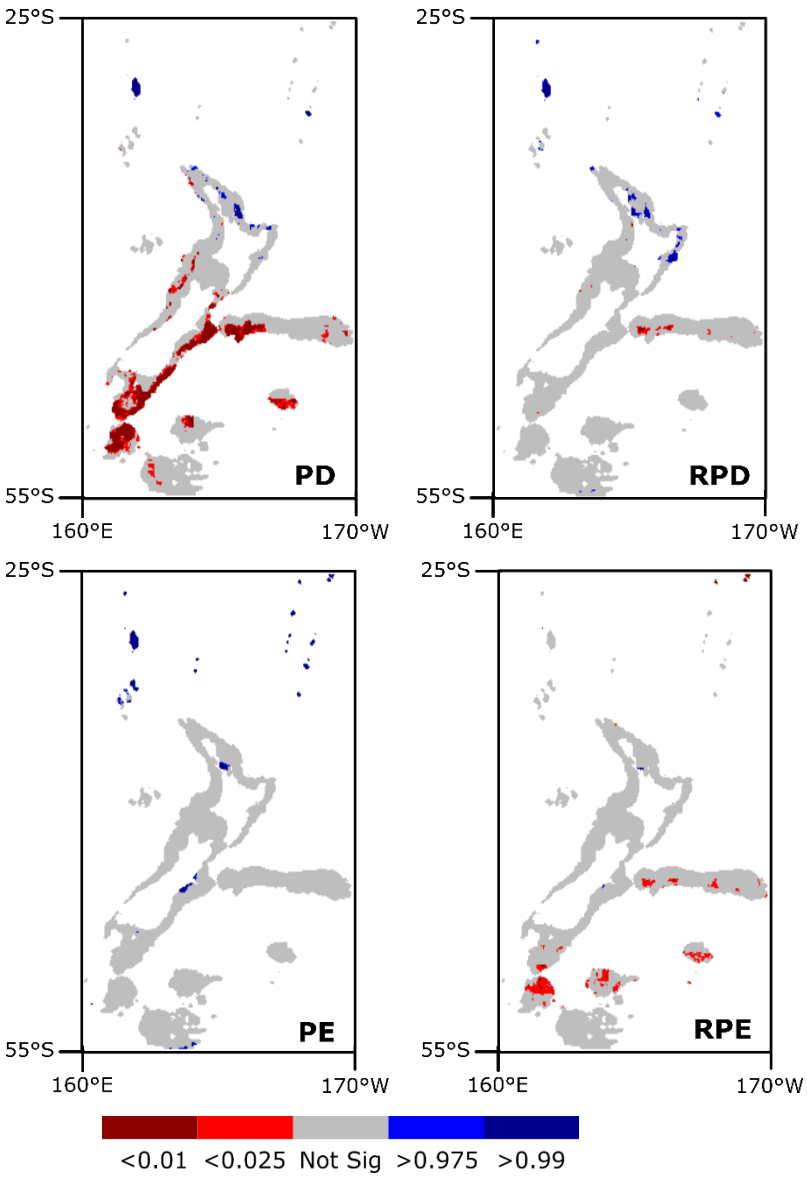

Fig. 8. Plots of significance levels for phylogenetic diversity (PD), relative phylogenetic diversity (RPD), phylogenetic endemism (PE), and relative phylogenetic endemism (RPE) after 999 randomization iterations as calculated for marine fishes occurring within 0-500 m around New Zealand's main and outlying islands. Red cells indicate significantly lower values than expected based on species richness (two-tailed test; dark red <0.01, bright red p<0.025); blue cells indicate significantly higher values than expected based on species richness (two-tailed test; bright blue p>0.975, dark blue p>0.99); and grey cells indicate cells within the study area where values are not significant.

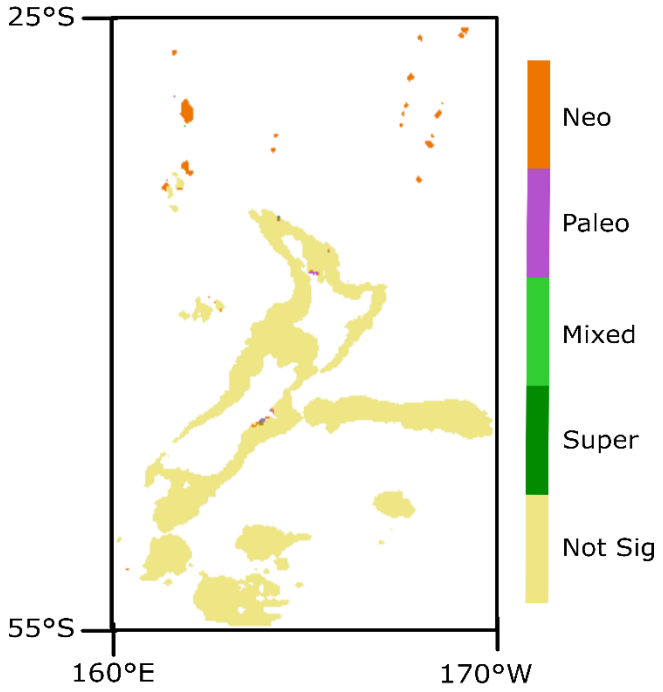

Fig. 9. Plot of cells identified as significant endemism centers from the "categorical analysis of neo- and paleoendemism" (CANAPE) which is based on the randomization results of phylogenetic endemism (PE) and relative phylogenetic endemism (RPE) for New Zealand's marine fishes. Orange indicates centers of neoendemism with significant overrepresentation of rare short branches. Purple indicates centers of paleoendemism with significant overrepresentation of rare long branches. Green indicates locations with overrepresentation of both rare short and rare long branches, significant at α=0.05 (light green, centers of mixed endemism) and at α=0.01 (dark green, centers of super-endemism). Golden yellow shows cells that did not pass the first step in CANAPE.

4.5. Discussion

Regions of high marine fish biodiversity and endemism, and the processes shaping such biogeographic patterns, are highly valuable to understand how biodiversity is generated and persists in the sea (Cowman et al., 2017). In our study, we identified regions of high richness and endemism for New Zealand´s marine fishes within 0-500 m using taxonomic and phylogenetic indices, showing that centers of biodiversity richness and endemism are different. We identified locations where evolutionary processes shape biodiversity in ways that cannot be captured by species richness alone. Our study highlights the northernmost subtropical oceanic islands as major centers of neoendemism in the region, and, unexpectedly, two coastal areas of paleoendemism

located in the Hauraki Gulf in the North Island, and the Banks Peninsula in the South Island. Our investigation represents a significant step in understanding the contribution of different geographic locations in New Zealand to the actinopterygian biodiversity in the region.

4.5.1. Contrasting patterns of biodiversity richness and endemism

Biodiversity patterns along latitude have been intensely documented at global, regional, and local scales in terrestrial, marine, and freshwater systems (Gaston, 2007). For New Zealand, our study shows a general decrease in taxonomic and phylogenetic measures of marine fish biodiversity and endemism with increasing latitude, confirming previous taxonomic evidence (Beaumont et al., 2009, Eme et al., 2020, Myers et al., 2021). This pattern seems restricted to shallow depths given the decreasing effect of latitude on marine fish biodiversity along New Zealand's greater depths (Leathwick et al., 2006, Zintzen et al., 2017). However, detailed results show differences in the latitudinal trends for taxonomic richness and endemism (Fig. 4.12S-4.16S), whereby the highest values are displayed around 35°S, and at the lowest latitudes of our study area, respectively. Our results highlight a geographic mismatch between richness hotspots and endemism centers in New Zealand's marine fishes, a similar scenario reported for marine fishes in the Pacific (Cowman et al., 2017) and avian fauna (Orme et al., 2005), suggesting that processes generating richness and endemism patterns are different.

For richness, we detected similar trends between taxonomic and phylogenetic indices with latitude (Fig. 6), an expected result given the correlation between both biodiversity measures (Faith, 2013). In both cases, we observed a non-linear relationship between metrics and latitude (Fig. 4.12S-4.16S) with a slight poleward increase peaking at 35°S (i.e. Northland within the North Island) after which values progressively decrease, a similar trend reported in New Zealand's marine fishes for species richness (Myers et al., 2021), and species richness and PD (Eme et al., 2020). Latitudinal gradients in environmental variables might be shaping the observed pattern (Willig et al., 2013), a

hypothesis supported by the similar peak in marine fish biodiversity at 30°-35°S along the Chilean coast (20°-55°S) in a comparable latitudinal climate setting to New Zealand in the Southern Hemisphere (Navarrete et al., 2014). Peaks in biodiversity at mid/temperate latitudes (25°S-30°S) reported for marine fishes in the Southern Hemisphere may also be explained by an overlap in the ranges of temperate and tropical taxa, and poleward shifts of species due to warming conditions (Chaudhary et al., 2016). Within New Zealand, our results are congruent with occurrence data showing that the north-eastern coast of the North Island displays the highest richness of tropical and subtropical fishes (Middleton et al., in review), an area considered a hotspot for range extensions (Middleton et al., 2021) likely facilitated by the East Auckland Current that connects the northeast coast of North Island with warmer waters in the northwest (Chiswell and Rickard, 2011).

Although taxonomic and phylogenetic measures followed similar patterns in our study, we also identified locations where both biodiversity indices significantly departed from their close association (Fig. 8), enabling inferences about the evolutionary and ecological processes shaping the observed patterns (Pavoine and Bonsall, 2011). Significantly high PD and RPD occurred at locations in the northeast and east of the North Island, and in subtropical oceanic islands, indicating that these locations host an unusually high number of long branches. The suggestion that the identified places have accumulated old lineages is concordant with the older persistence of tropical environments due to their stability over geological time (Miller et al., 2018) allowing the establishment of old lineages. Although this hypothesis seems incongruent with phylogenetic data from Samayoa et al. (2022), showing that the subtropical islands of the Southwest Pacific are ‘cradles’ for marine fish biodiversity, it is worth noting that these inferences relied on temperate and subtropical taxa endemic to the region. Given that the present study also includes widespread and tropical species, our findings translate phylogenetic signals left by historical events in the genetic composition of older tropical

taxa. Significantly low PD and RPD is reported for locations within the southern half of the study area, with RPD locations restricted to the Chatham Rise shallows, representing a fraction of the geographic area covered by PD (Fig. 8). While PD mismatches are a good indicator of evolutionary processes, RPD performs better than PD in detecting the overrepresentation of long and short branches as it is based on the comparison to a null tree with equal branch lengths (Mishler et al., 2014). In this sense, we believe that the Chatham Rise is the main New Zealand location hosting a significant number of short branches, an indication of recent diversification. This pattern is supported by the high environmental heterogeneity in the Chathams, mainly caused by the mixture of two surface currents of distinct oceanographic characteristics, a condition that facilitates the generation of a high number of potential niches to be filled by species (Zintzen et al., 2017).

4.5.2. Centers of neo- and paleoendemism for marine fishes of New Zealand

The identification of endemism centers is key to understanding the evolutionary processes generating biodiversity (Bellwood and Meyer, 2009), and to determining if a location has generated new unique taxa (neoendemism) or accumulated rare old evolutionary lineages (paleoendemism) (Cowman et al., 2017). In our study, we provide for the first time the quantitative delineation of endemism centers for New Zealand's marine fishes using phylogenetic indices (Fig. 9). The shallow areas along the Norfolk, Colville, and Kermadec Ridges are centers of neoendemism, including the subtropical islands of Norfolk Island (Australia) and Rangitāhua (New Zealand), whereas little significant paleoendemism is detected for the remainder of New Zealand. Interestingly, this marine biogeographic pattern is the opposite of what has been found in New Zealand's land environments. Terrestrial neoendemism was high in the South Island, due to younger alpine habitats, and paleoendemism was found in the North Island, due to its role as a refugium during past interglacial periods (Heenan et al., 2017). These opposing patterns exemplify how different processes shape distinct island biogeographic

patterns between marine and terrestrial environments within the same region (Hachich et al., 2015).

The identification of subtropical centers of neoendemism is concordant with Samayoa et al. (2022) who found that the subtropical islands of Lord Howe, Norfolk, and Rangitāhua act as ‘cradles’ of biodiversity. These results are supported by the peak in endemism measures at low latitudes (Fig. 7, Fig. 4.12S-4.16S), and the high endemism richness of coastal fishes in Rangitāhua (Trnski et al., 2015). Oceanic islands in other Pacific regions are also endemism centers, including Hawaii (Randall, 2007), the Marquesas Islands (Delrieu-Trottin et al., 2015), Juan Fernández and Desventuradas (Friedlander et al., 2016), and Easter Island (Rapa Nui) which particularly promotes neoendemism (Delrieu-Trottin et al., 2019). Our results exemplify the general role of subtropical oceanic islands of recent geological emergence as features that promote novelty in marine biodiversity (Bowen et al., 2013). Potential factors limiting island colonization, and eventually allopatric speciation, include: geography (e.g., distance) and geology (e.g., volcanism, sea level fluctuation) (Pinheiro et al., 2017); feeding behavior and locomotion (Liggins et al., 2022); and climate differences (Samayoa et al., in review).

Endemism tends to concentrate in oceanic islands where geographic isolation facilitates the diversification of range-restricted taxa (Anderson, 1994), although some continental coastlines can also generate biodiversity (Bowen et al., 2013). We detected two isolated clusters of paleoendemism centers, one along the eastern coastline of the North Island (Hauraki Gulf), and the other on the mid-eastern coast of the South Island (Banks Peninsula) (Fig. 9). Our results suggest that these two locations represented refugia for the remnant populations of previously widespread taxa, likely resulting from mild environmental conditions (Harrison and Noss, 2007) in an otherwise old Gondwanan coastal environment where the topographic continuum has minimized isolation processes (Pyron and Burbrink, 2010). The Hauraki Gulf / Tikapa Moana is under protection by the Hauraki Gulf Marine Park Act 2000 for its “quality and diversity

of biology and landscape that makes it outstanding within New Zealand", and receives low wave energy due to its sheltered configuration (Aguirre et al., 2016). The Gulf is a relatively stable environment for local marine biodiversity, serving as a refugium for rare old lineages (Harrison and Noss, 2017), and resulting in a "museum" for paleoendemism. In the South Island, there are two no-take marine reserves around the Banks Peninsula (Akaroa and Pōhatu) but they are very small. Given that local taxonomic inventories are underestimated by accessibility difficulties, alternative approaches to surveying the area would clarify biodiversity patterns in the area (Brough et al., 2018).

4.6. Conclusions

In this study, we examined the geographic distribution of biodiversity richness and endemism in New Zealand's marine fishes employing phylogenetic measures. Despite using data repositories that are characterized by inherent knowledge gaps (Hortal et al., 2015), our study highlights latitudinal gradients in taxonomic and phylogenetic indices, as previously reported for New Zealand's marine fish fauna. Moreover, we identified hotspots of biodiversity richness and endemism, and we determined that they are in different places within New Zealand. We also identified centers of endemism in subtropical volcanic islands, acting as exporters of novel biodiversity, and in two previously unacknowledged coastal locations, acting as refugia for rare old biodiversity along the North and South Islands. Our study exemplifies the value of incorporating phylogenetic information into biogeographic research. Our study proposes robust inferences about the evolutionary mechanisms that have given rise to contemporary spatial patterns of marine fish biodiversity in New Zealand, significantly contributing to our understanding of the actinopterygian biogeography in the region.

4.7. Authors' contributions

APS, **JDA**, **ANHS**, and **LL** conceived the study; **APS**, **JDA**, and **LL** designed the sampling methods; **APS** conceived the analytical approach; **APS** analyzed and

interpreted the data; **APS** wrote the original draft; **APS**, **ANHS**, and **LL** reviewed and edited the manuscript; **LL** supervised the study.

4.8. Acknowledgments

We thank Prof. Shawn Laffan for providing technical clarifications on Biodiverse, and for integrating our feedback into the subsequent software release. André P. Samayoa is supported by a Massey University Doctoral Scholarship. Libby Liggins and J. David Aguirre are supported by Rutherford Discovery Fellowships (RDF-20-MAU-001 and RDF-19-MAU-006).

4.9. Supplementary material

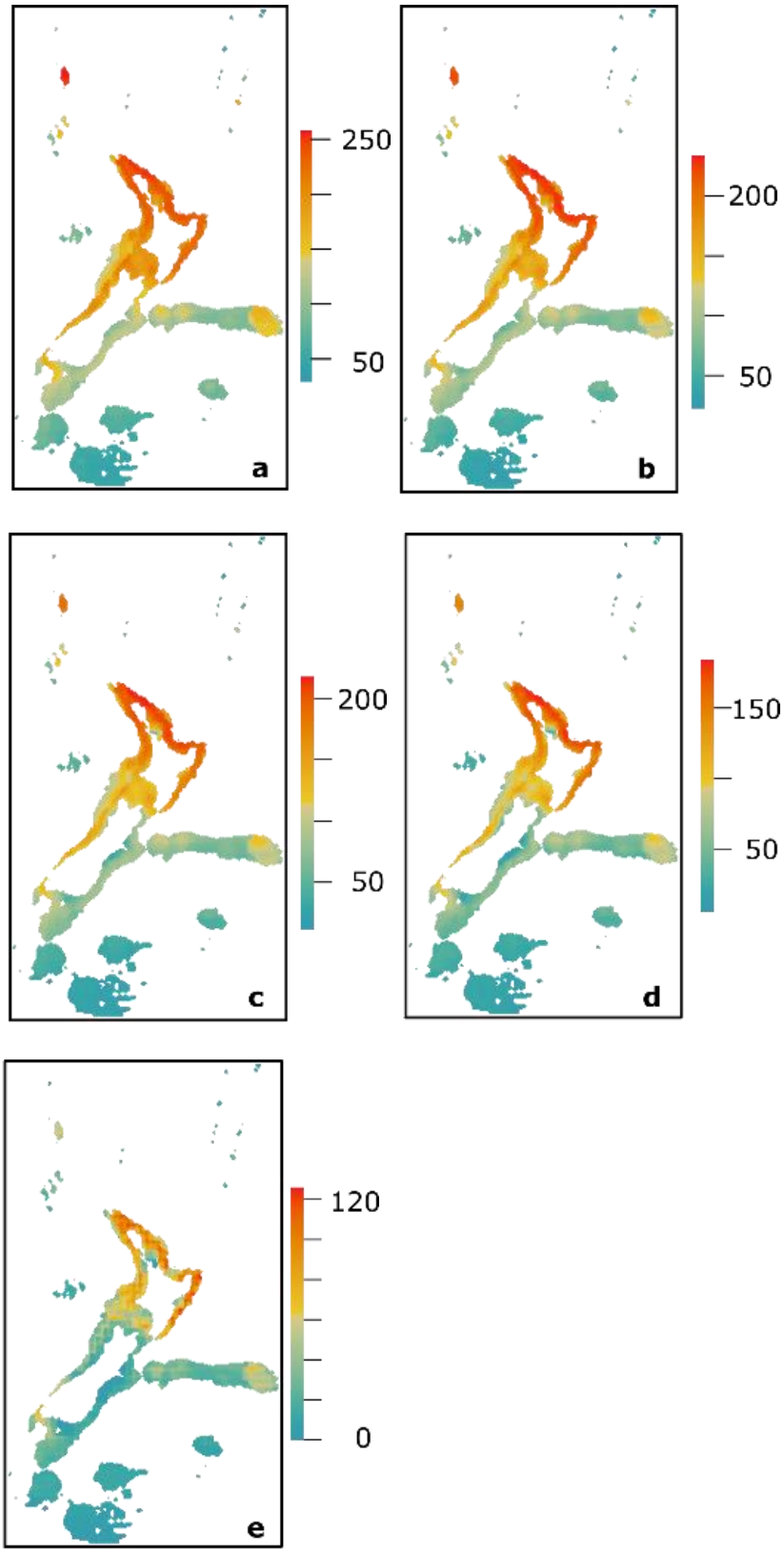

Figure 4.1S. Map of species richness (SR) for marine fishes occurring at 0-500 m around New Zealand using five occurrence probability thresholds yielded by AquaMaps. a: 0.01; b: 0.25; c: 0.50; d; 0.75; e: 1.00.

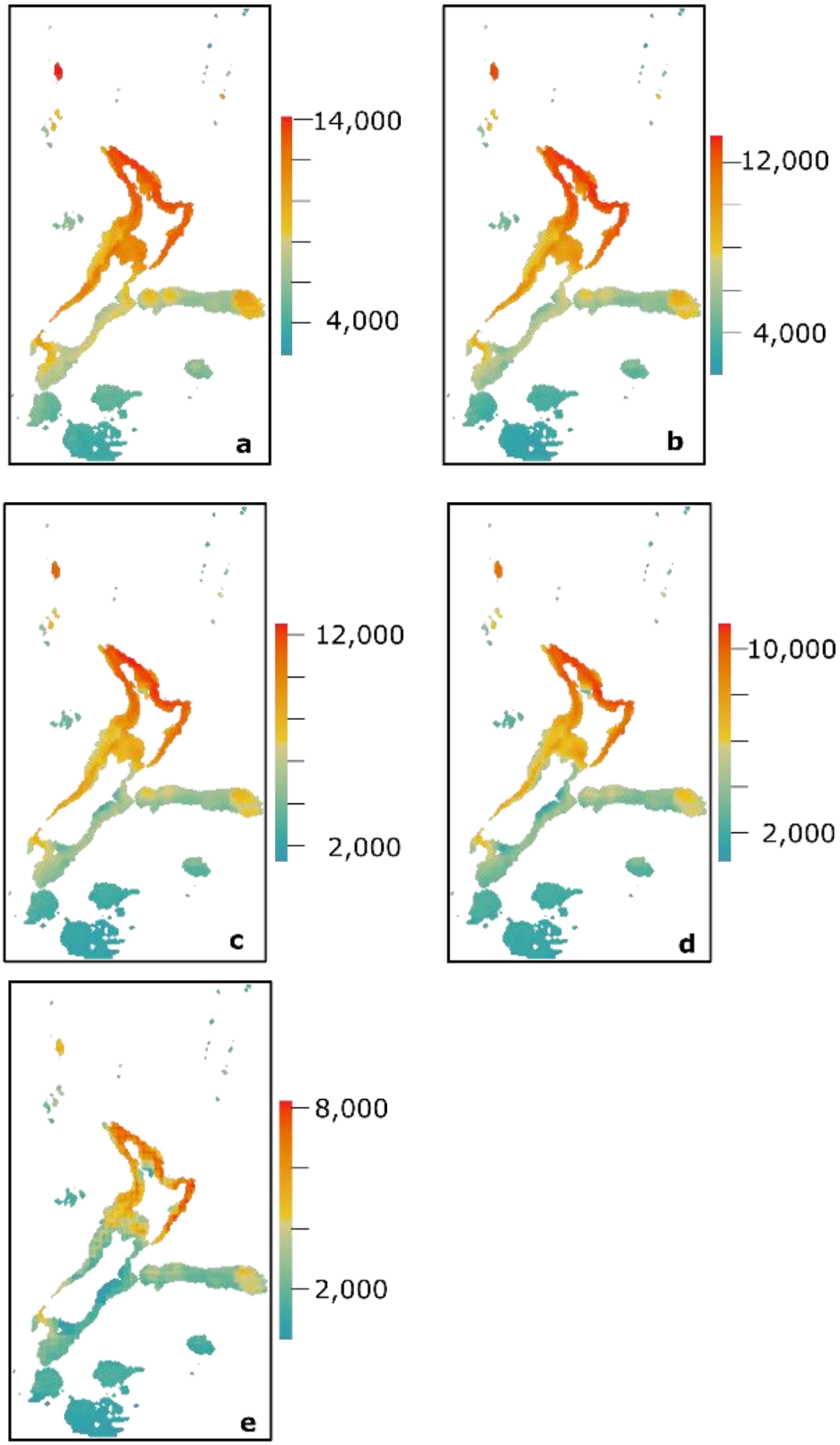

Figure 4.2S. Map of phylogenetic diversity (PD) for marine fishes occurring at 0-500 m around New Zealand using five occurrence probability thresholds yielded by AquaMaps. a: 0.01; b: 0.25; c: 0.50; d; 0.75; e: 1.00.

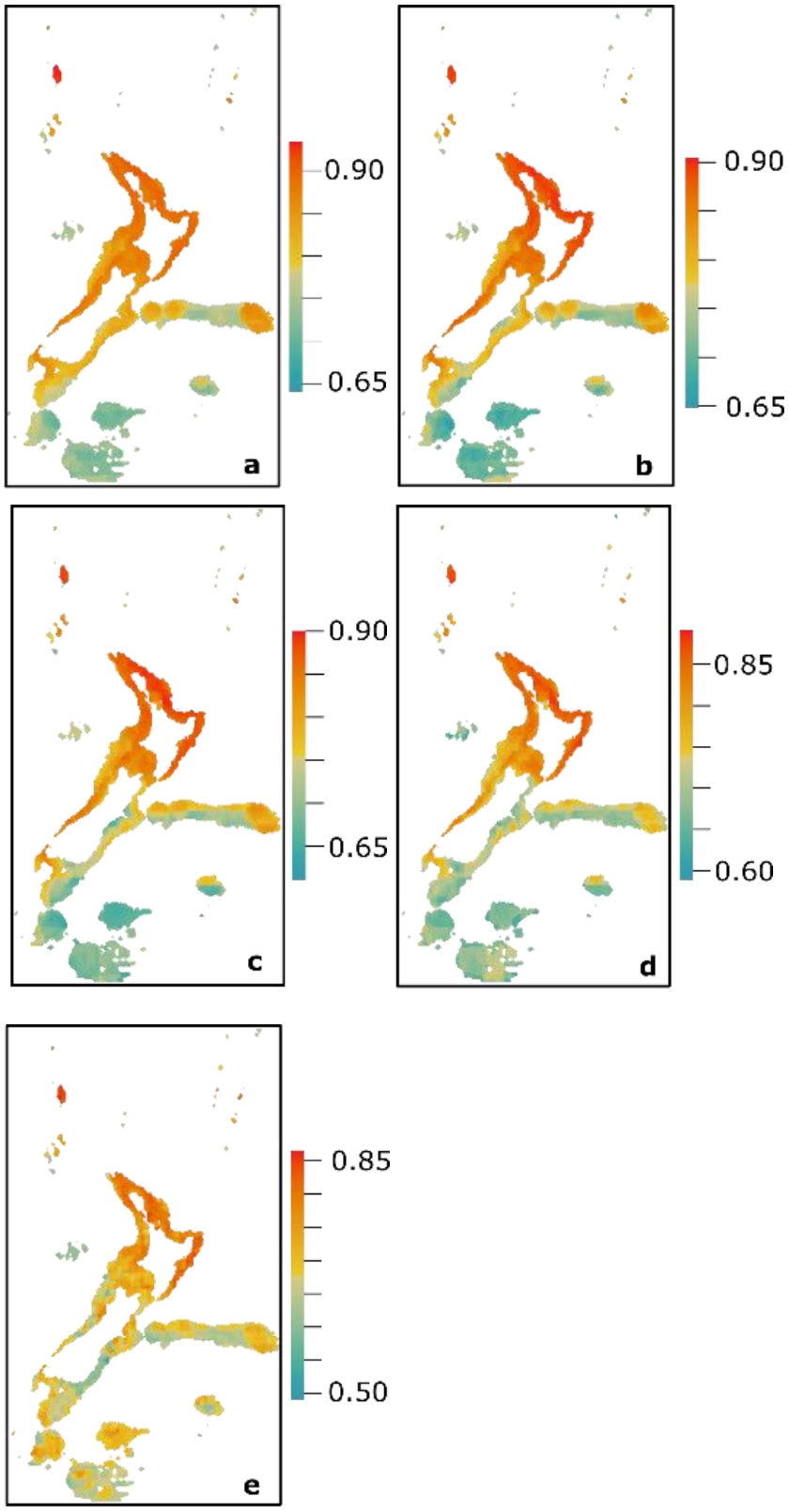

Figure 4.3S. Map of relative phylogenetic diversity (RPD) for marine fishes occurring at 0-500 m around New Zealand using five occurrence probability thresholds yielded by AquaMaps. a: 0.01; b: 0.25; c: 0.50; d; 0.75; e: 1.00.

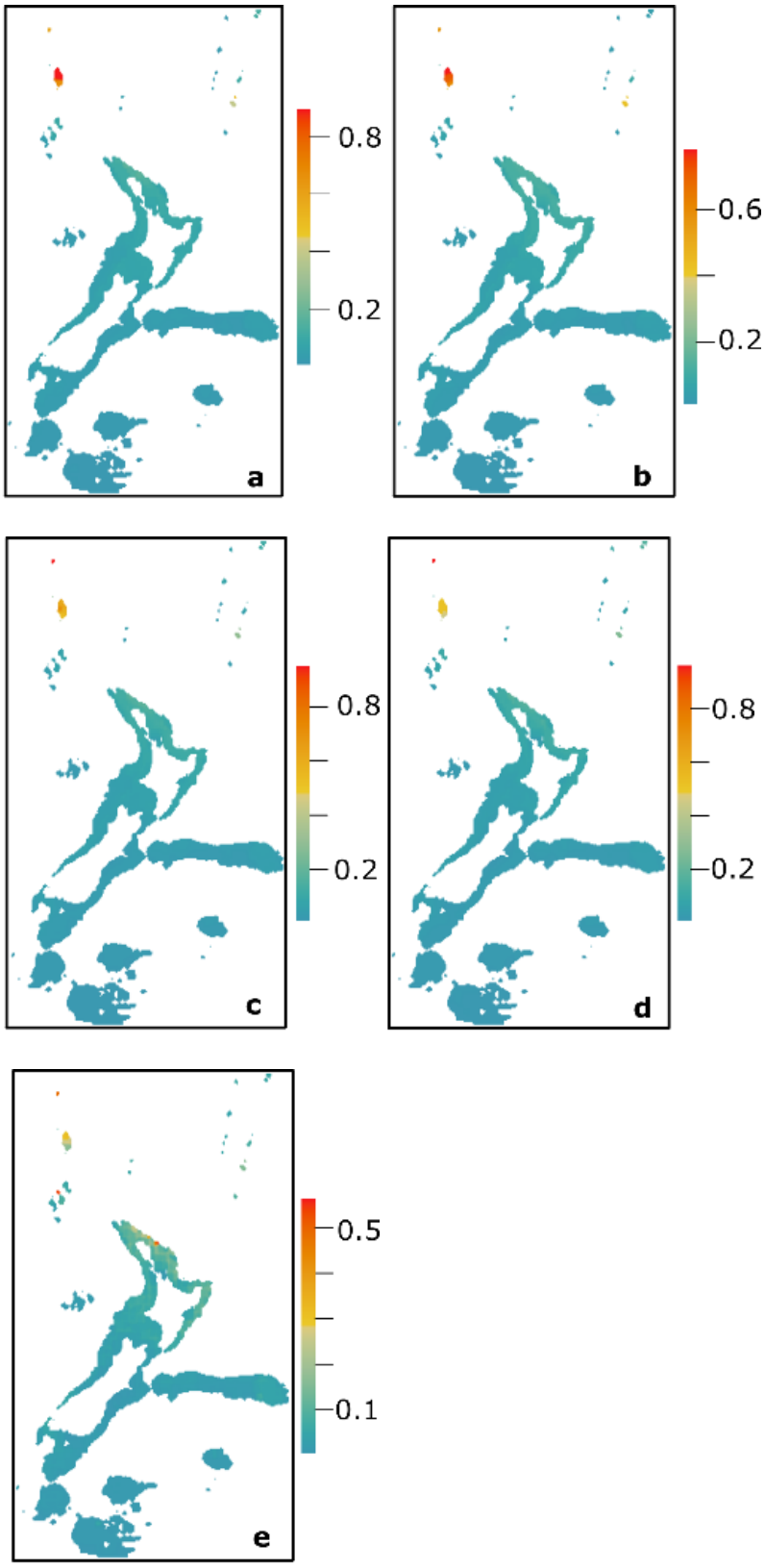

Figure 4.4S. Map of weighted endemism (WE) for marine fishes occurring at 0-500 m around New Zealand using five occurrence probability thresholds yielded by AquaMaps. a: 0.01; b: 0.25; c: 0.50; d; 0.75; e: 1.00.

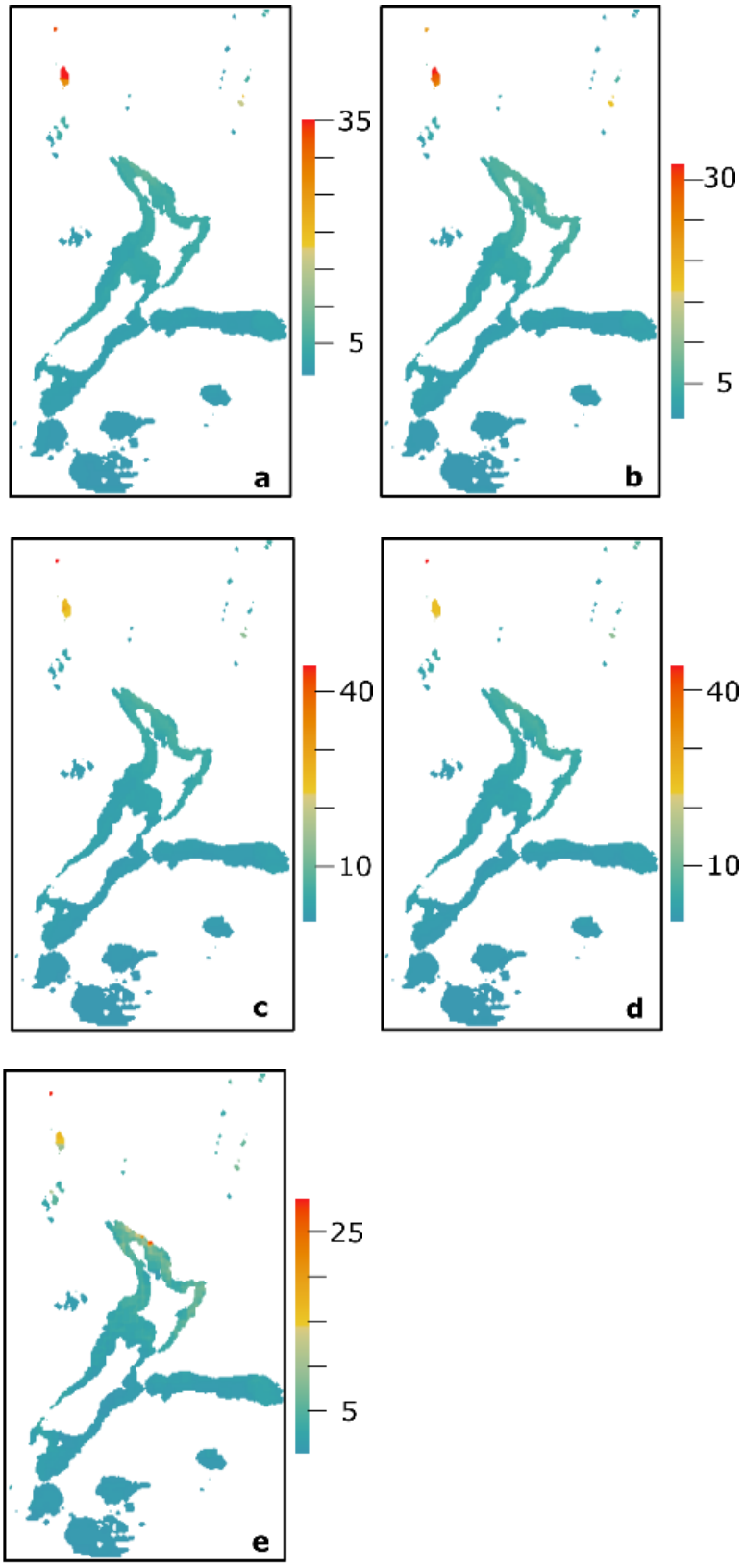

Figure 4.5S. Map of phylogenetic endemism (PE) for marine fishes occurring at 0-500 m around New Zealand using five occurrence probability thresholds yielded by AquaMaps. a: 0.01; b: 0.25; c: 0.50; d; 0.75; e: 1.00.

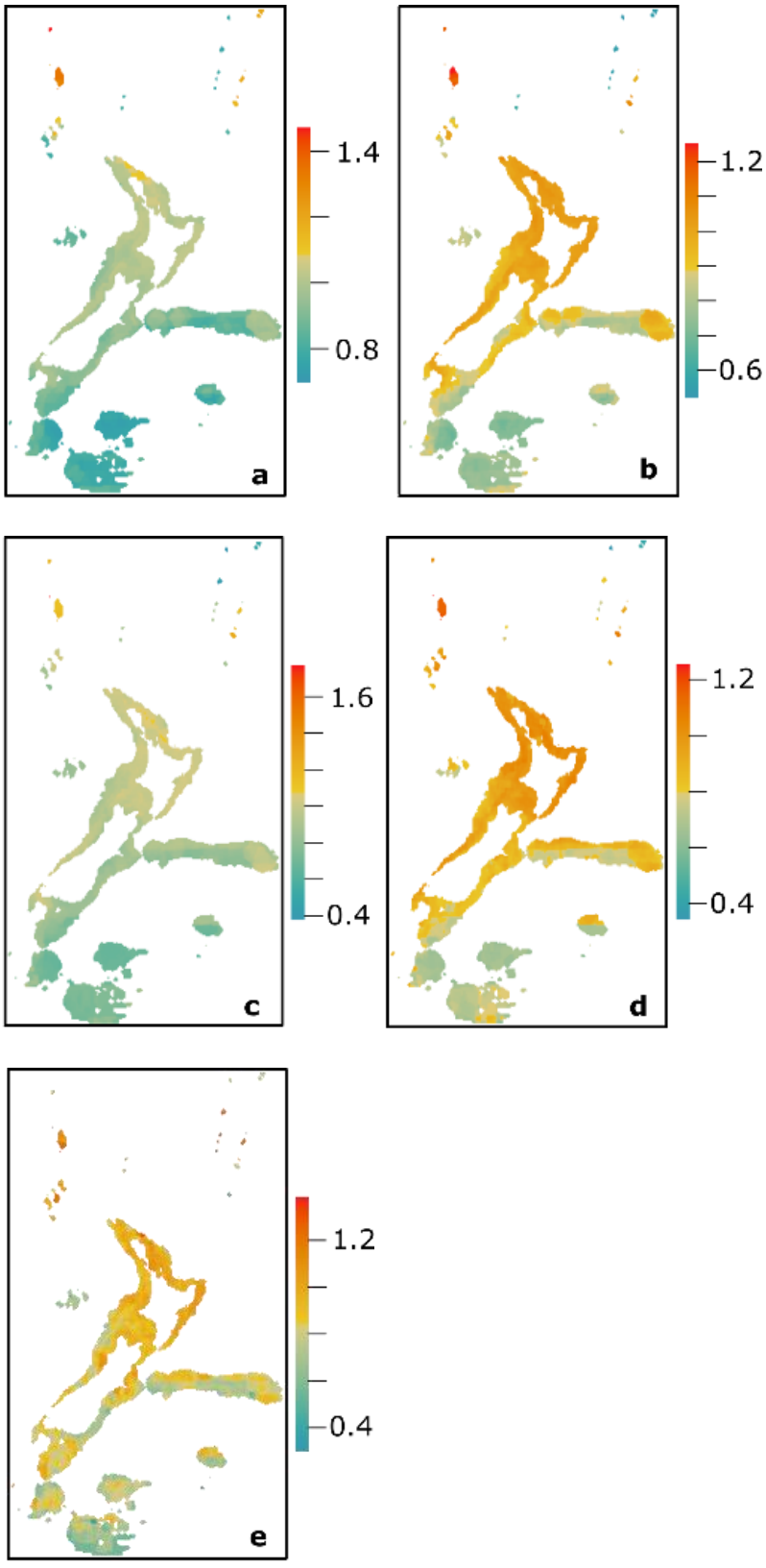

Figure 4.6S. Map of relative phylogenetic endemism (RPE) for marine fishes occurring at 0-500 m around New Zealand using five occurrence probability thresholds yielded by AquaMaps. a: 0.01; b: 0.25; c: 0.50; d; 0.75; e: 1.00.

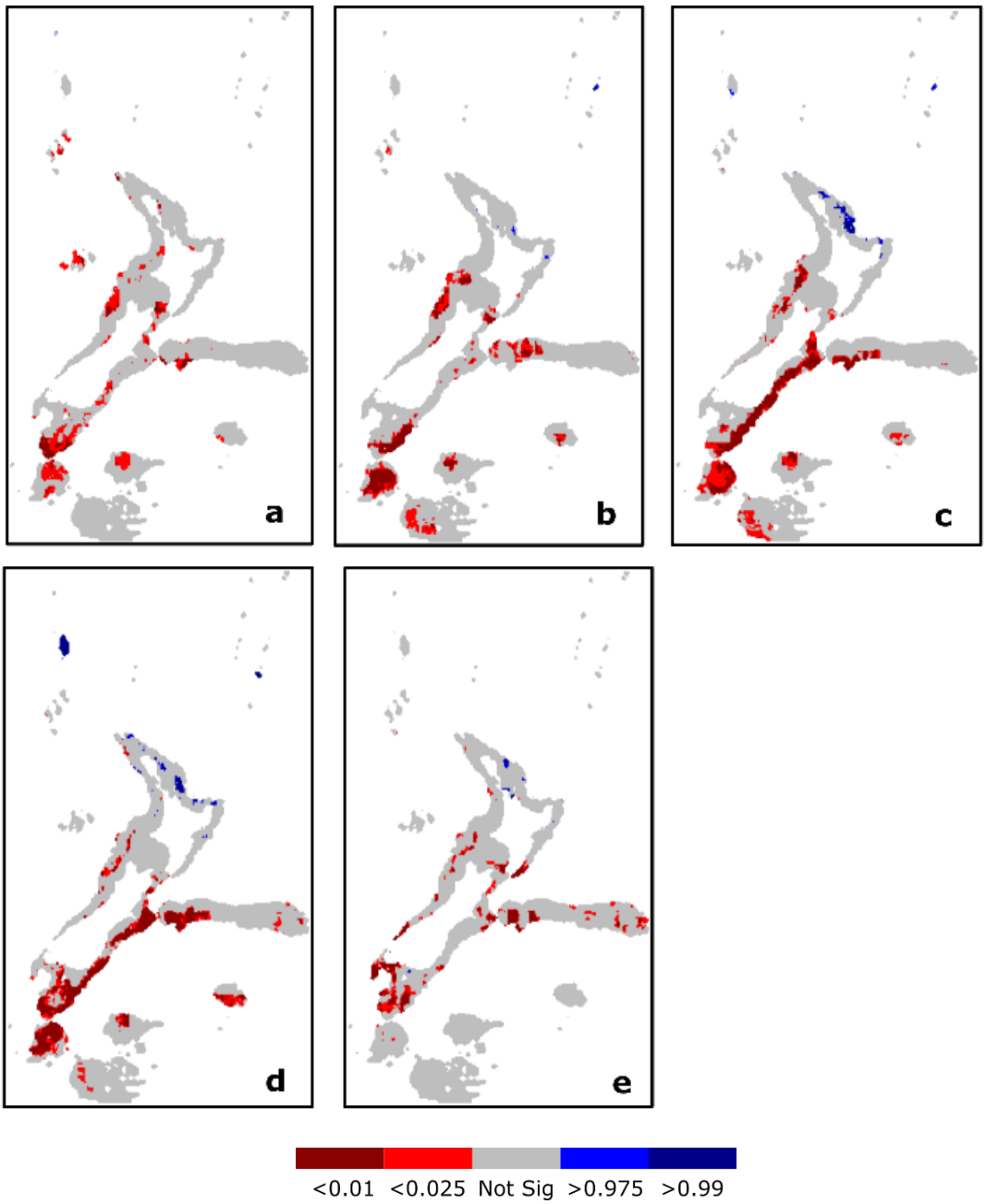

Figure 4.7S. Map of significance levels for phylogenetic diversity (PD) after 999 randomization iterations. Maps based on five occurrence probability thresholds yielded by AquaMaps (a: 0.01, b: 0.25, c: 0.50, d: 0.75, and e: 1.00). Red cells are where observed values are significantly lower than expected based on species richness (two-tailed test; dark red <0.01, bright red p<0.025); blue cells are where observed values are significantly higher than expected based on species richness (two-tailed test; bright blue p>0.975, dark blue p>0.99).; and grey cells are where observed values are not significant.

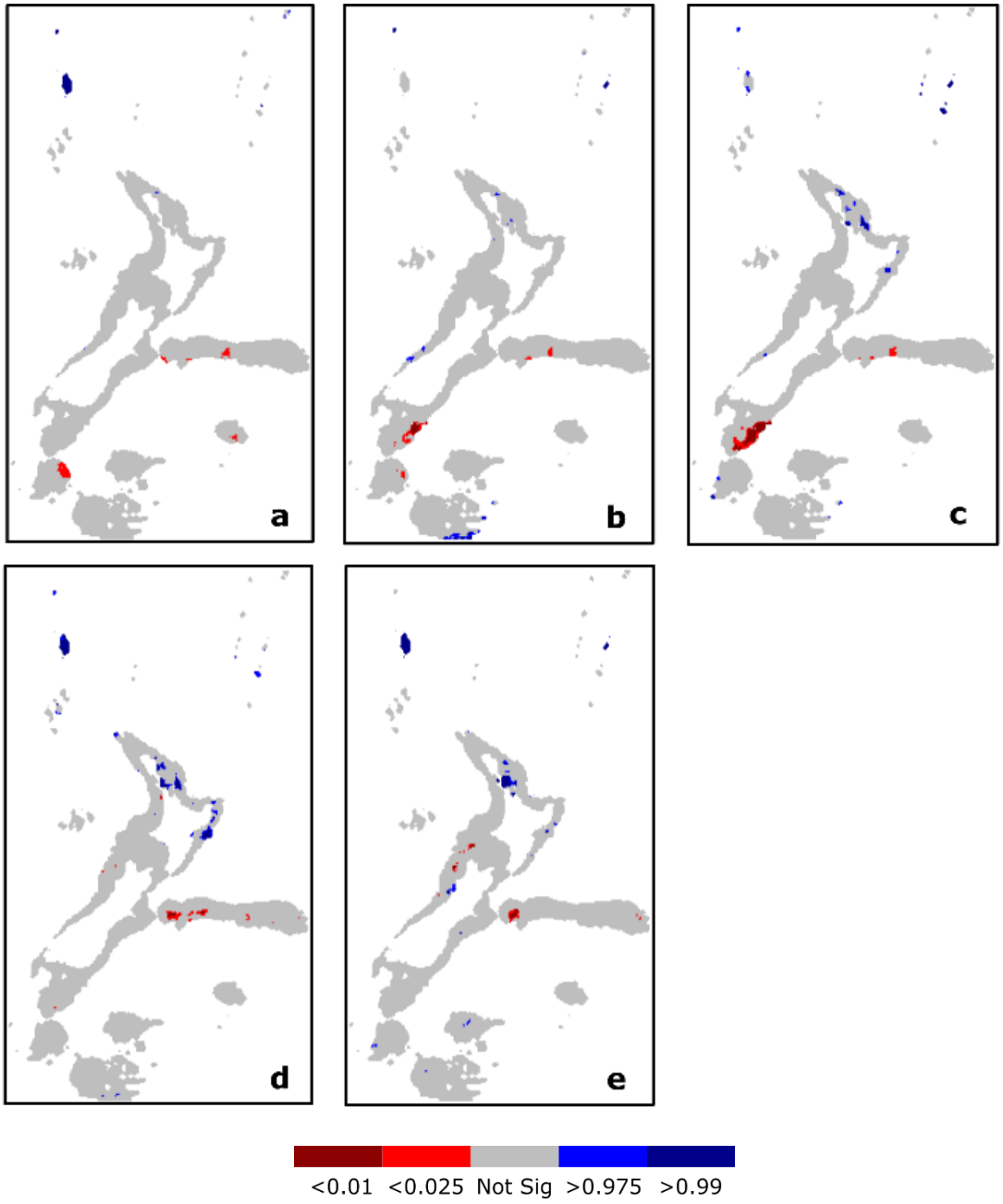

Figure 4.8S. Map of significance levels for relative phylogenetic diversity (RPD) after 999 randomization iterations. Maps based on five occurrence probability thresholds yielded by AquaMaps (a: 0.01, b: 0.25, c: 0.50, d: 0.75, and e: 1.00). Red cells are where observed values are significantly lower than expected based on species richness (two-tailed test; dark red <0.01, bright red p<0.025); blue cells are where observed values are significantly higher than expected based on species richness (two-tailed test; bright blue p>0.975, dark blue p>0.99).; and grey cells are where observed values are not significant.

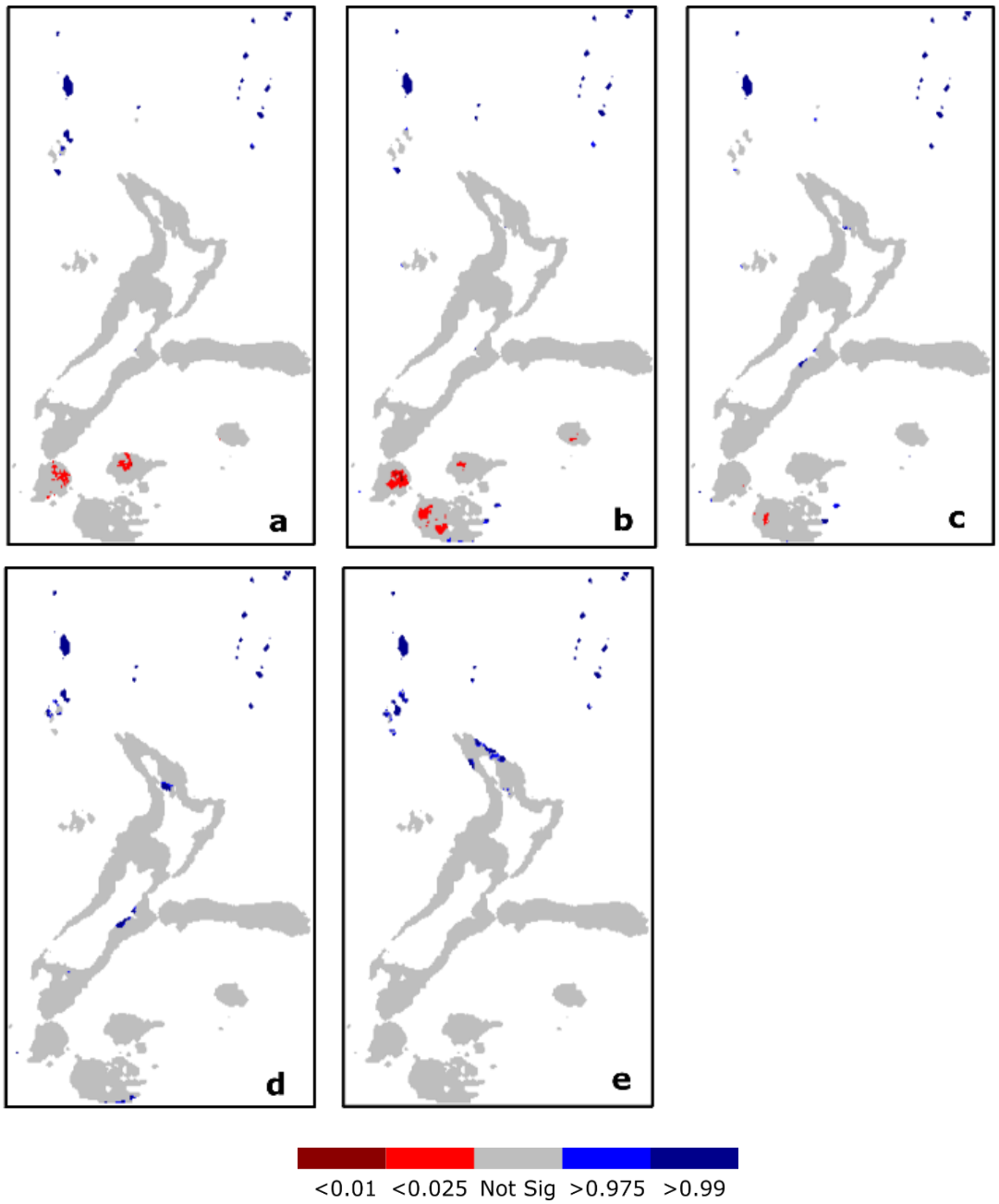

Figure 4.9S. Map of significance levels for phylogenetic endemism (PE) after 999 randomization iterations. Maps based on five occurrence probability thresholds yielded by AquaMaps (a: 0.01, b: 0.25, c: 0.50, d: 0.75, and e: 1.00). Red cells are where observed values are significantly lower than expected based on species richness (two-tailed test; dark red <0.01, bright red p<0.025); blue cells are where observed values are significantly higher than expected based on species richness (two-tailed test; bright blue p>0.975, dark blue p>0.99).; and grey cells are where observed values are not significant.

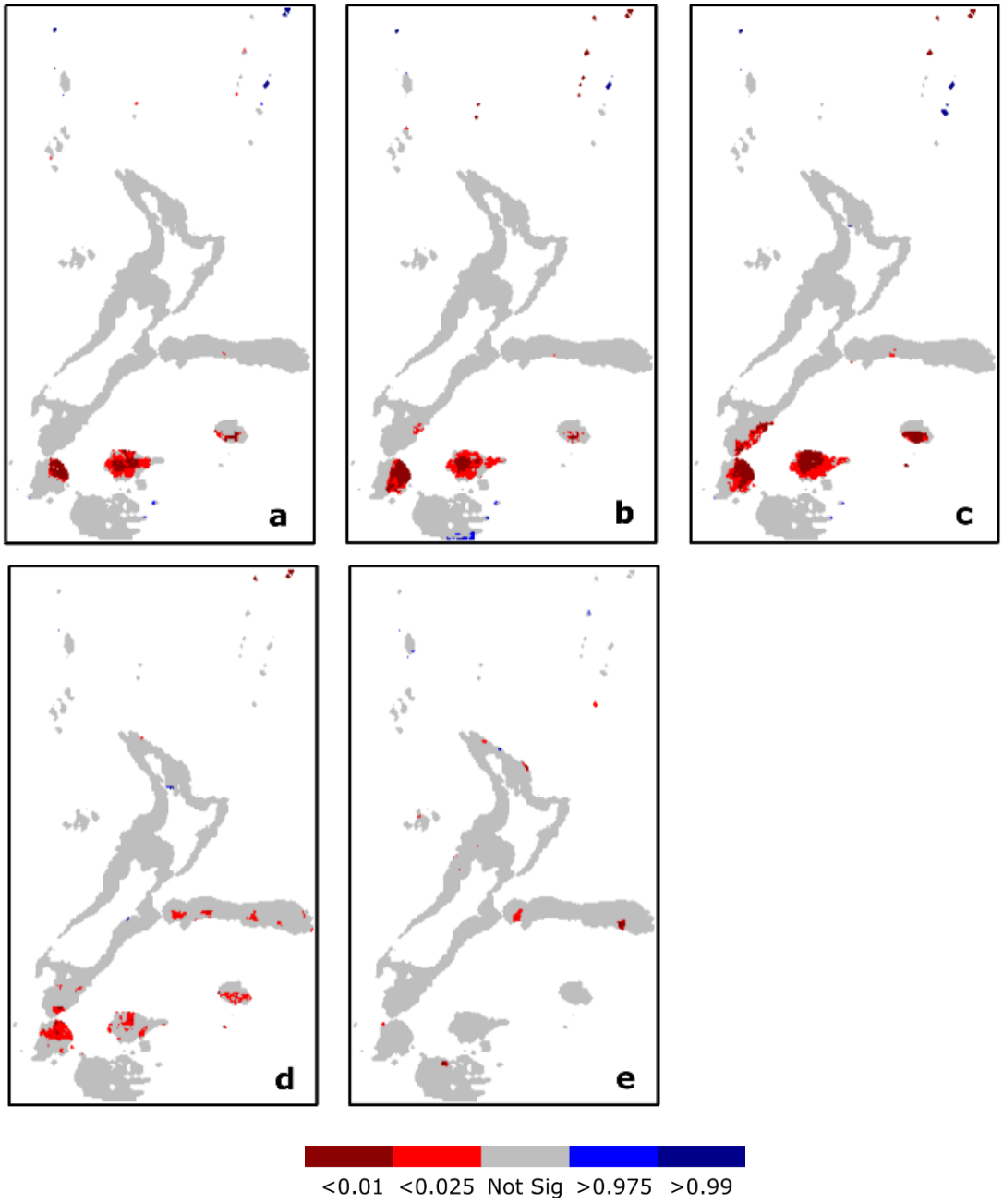

Figure 4.10S. Map of significance levels for relative phylogenetic endemism (RPE) after 999 randomization iterations. Maps based on five occurrence probability thresholds yielded by AquaMaps (a: 0.01, b: 0.25, c: 0.50, d: 0.75, and e: 1.00). Red cells are where observed values are significantly lower than expected based on species richness (two-tailed test; dark red <0.01, bright red p<0.025); blue cells are where observed values are significantly higher than expected based on species richness (two-tailed test; bright blue p>0.975, dark blue p>0.99).; and grey cells are where observed values are not significant.

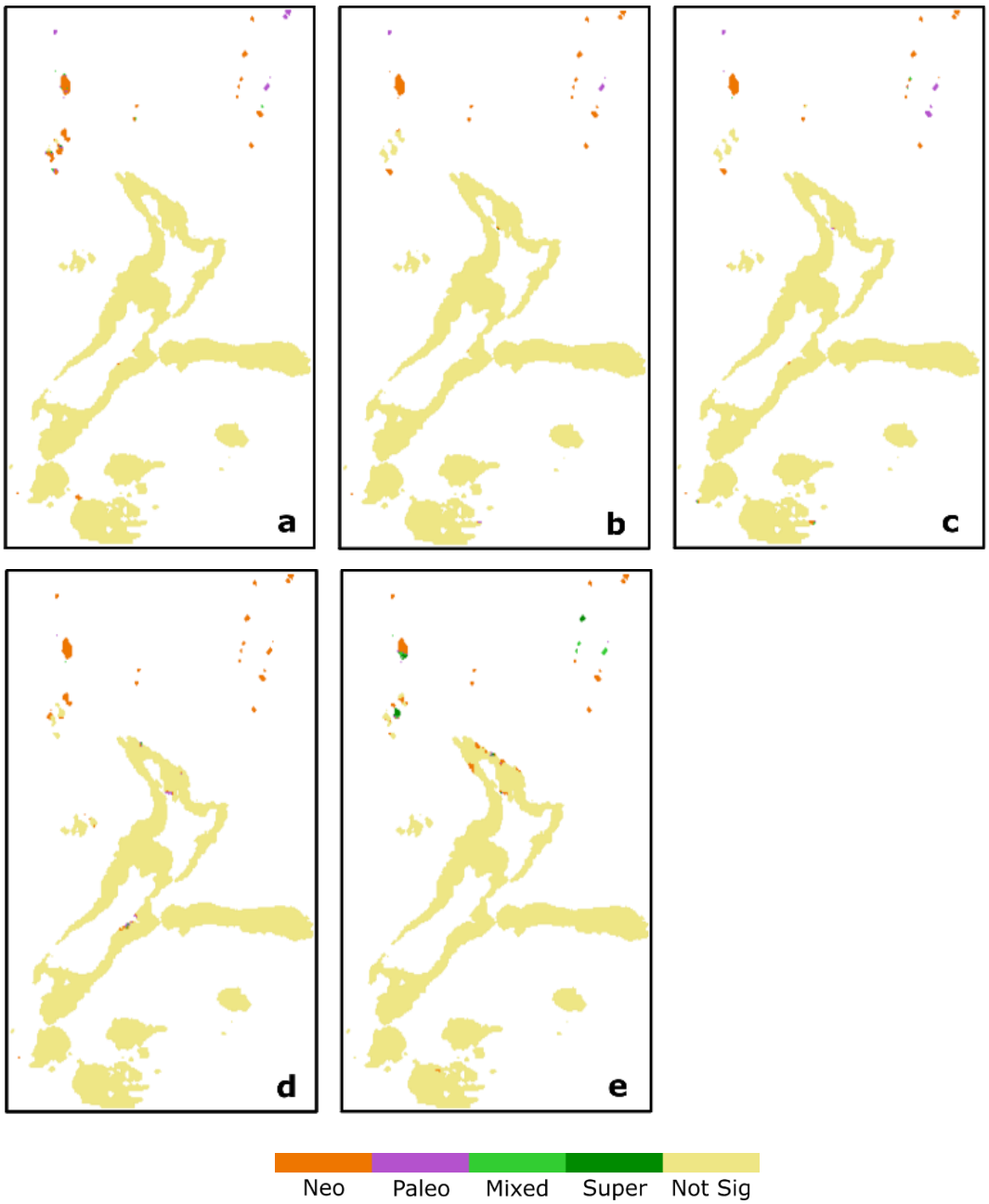

Figure 4.11S. Map derived from the categorical analysis of neo- and paleoendemism (CANAPE) for marine fishes occurring at 0-500 m around New Zealand using five occurrence probability thresholds yielded by AquaMaps. a: 0.01; b: 0.25, c: 0.50, d: 0.75, and e: 1.00).

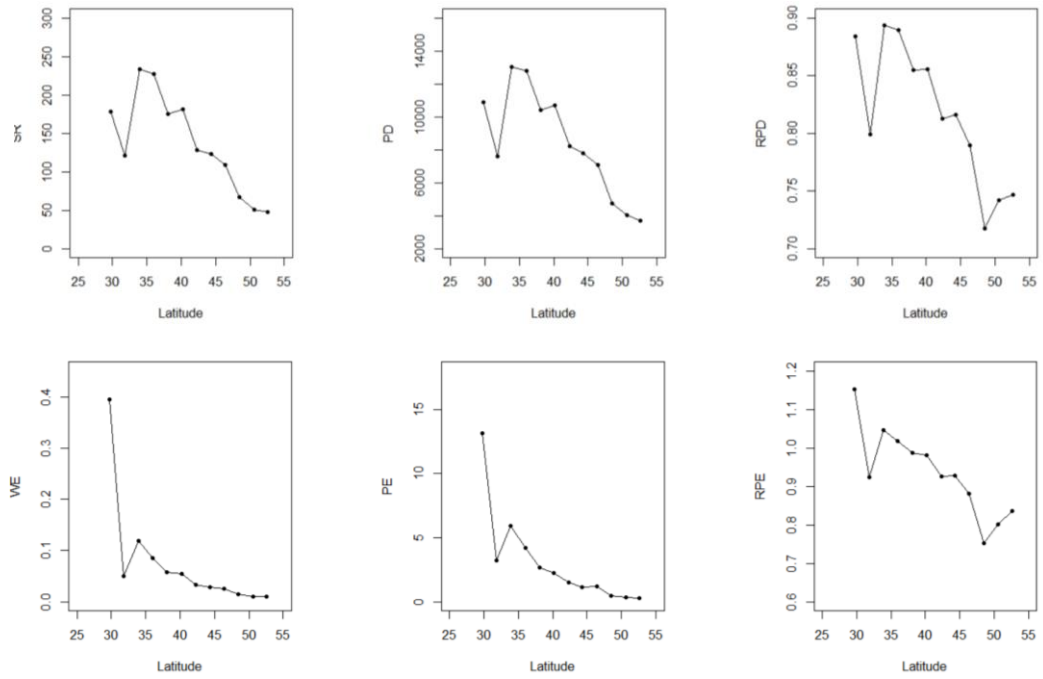

Figure 4.12S. Plots of biodiversity metrics against latitude based on an occurrence probability threshold of 0.01 to select ranges. SR: species richness; PD: phylogenetic diversity; RPD: relative phylogenetic diversity; WE: weighted endemism; PE: phylogenetic diversity; RPE: relative phylogenetic endemism. Latitudes are in degrees south.

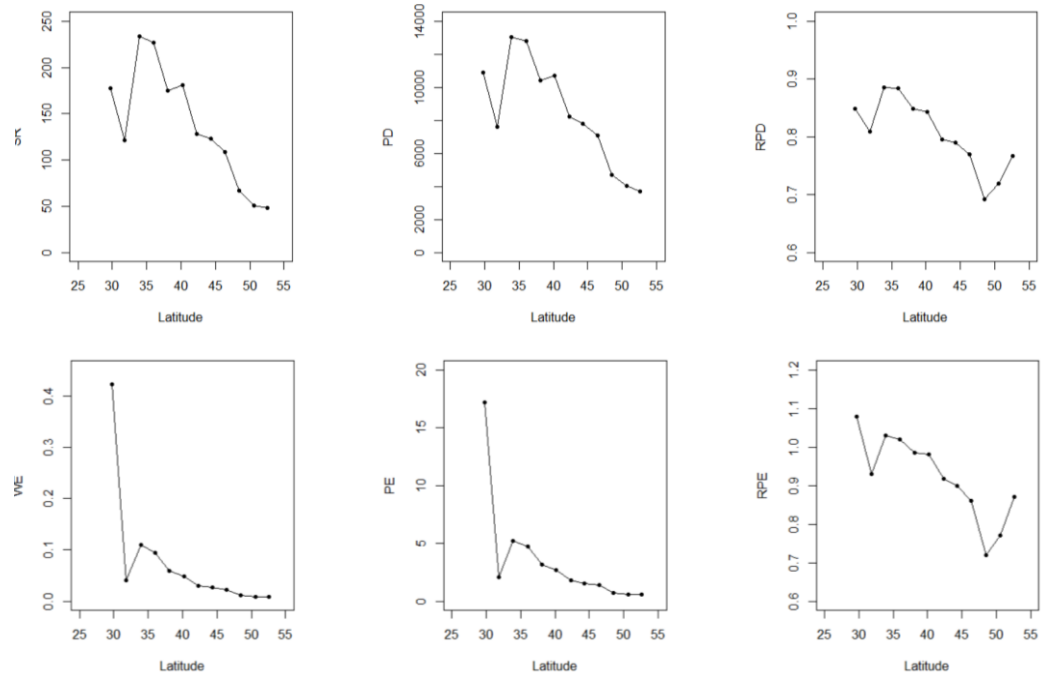

Figure 4.13S. Plots of biodiversity metrics against latitude based on an occurrence probability threshold of 0.25 to select ranges. SR: species richness; PD: phylogenetic diversity; RPD: relative phylogenetic diversity; WE: weighted endemism; PE: phylogenetic diversity; RPE: relative phylogenetic endemism. Latitudes are in degrees south.

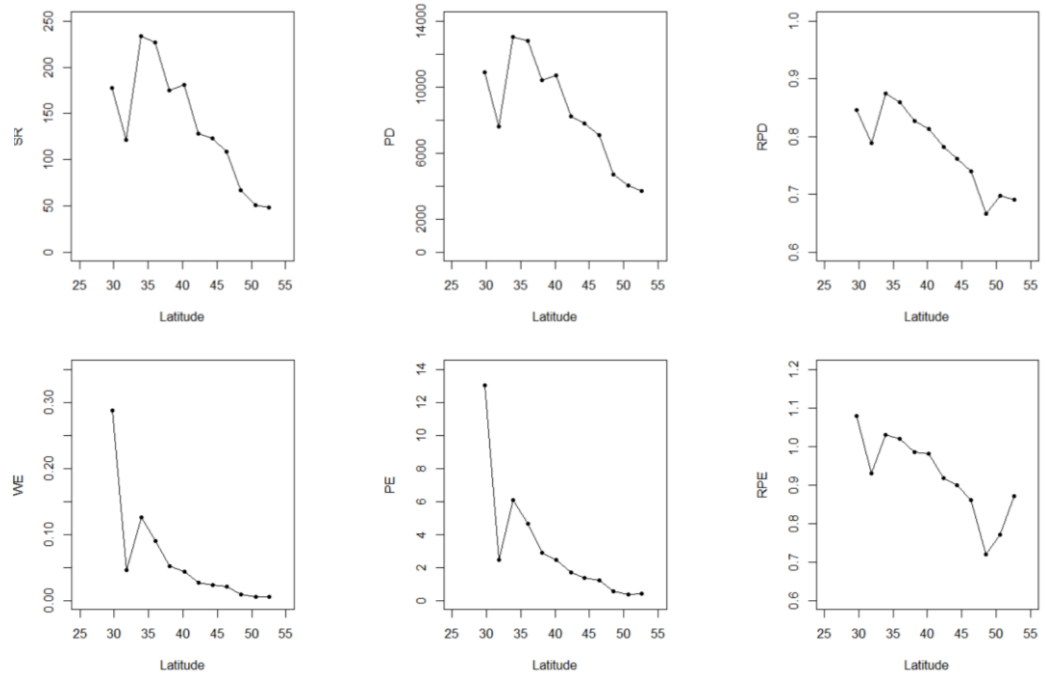

Figure 4.14S. Plots of biodiversity metrics against latitude based on an occurrence probability threshold of 0.50 to select ranges. SR: species richness; PD: phylogenetic diversity; RPD: relative phylogenetic diversity; WE: weighted endemism; PE: phylogenetic diversity; RPE: relative phylogenetic endemism. Latitudes are in degrees south.

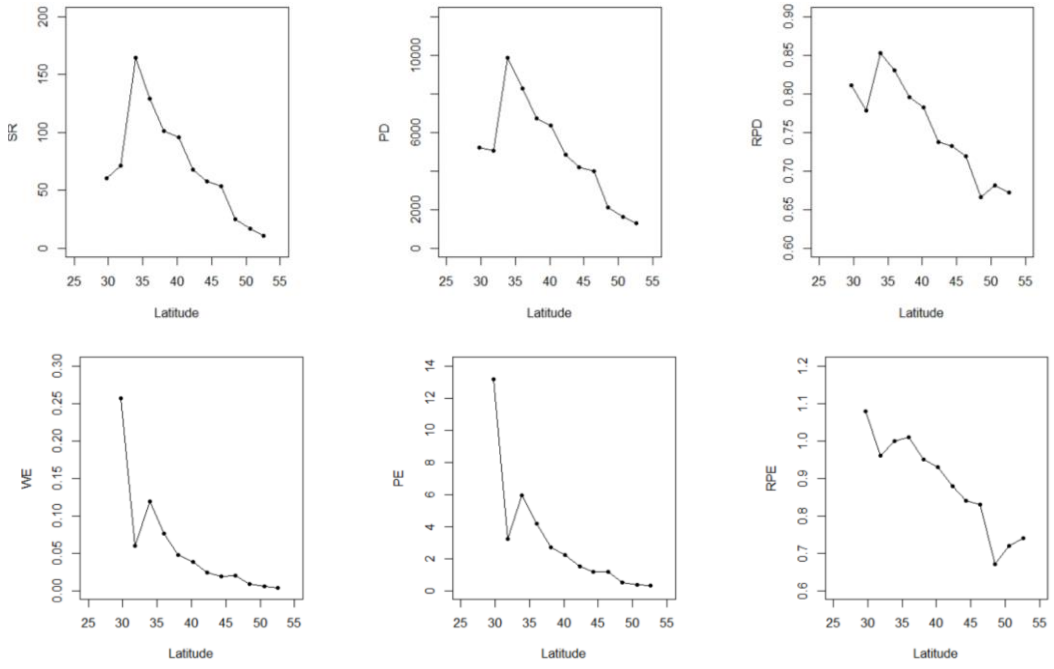

Figure 4.15S. Plots of biodiversity metrics against latitude based on an occurrence probability threshold of 0.75 to select ranges. SR: species richness; PD: phylogenetic diversity; RPD: relative phylogenetic diversity; WE: weighted endemism; PE: phylogenetic diversity; RPE: relative phylogenetic endemism. Latitudes are in degrees south.

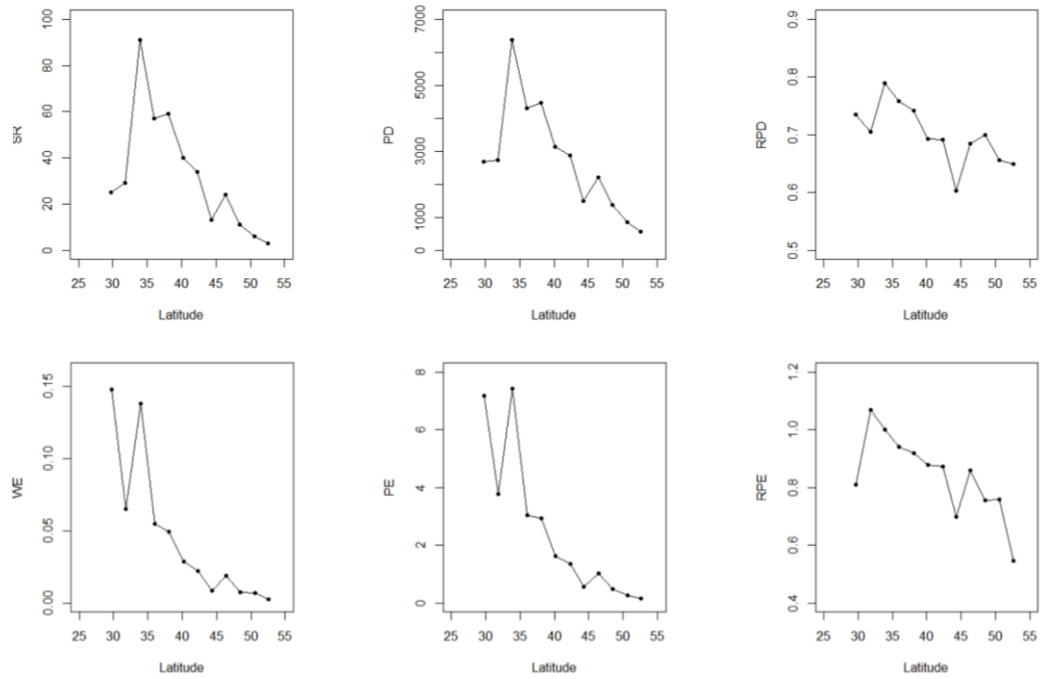

Figure 4.16S. Plots of biodiversity metrics against latitude based on an occurrence probability threshold of 1.00 to select ranges. SR: species richness; PD: phylogenetic diversity; RPD: relative phylogenetic diversity; WE: weighted endemism; PE: phylogenetic diversity; RPE: relative phylogenetic endemism. Latitudes are in degrees south.

5. General discussion

Climate change is impacting the current geographic distribution of marine biodiversity at a global scale (Chaudhary et al., 2021), and is expected to aggravate the loss of marine life already stressed by anthropogenic pressure (Beaugrand et al., 2015). Areas of high biodiversity have been recognized as conservation priorities (Myers, 1988, Myers et al., 2000, Roberts et al., 2002), with recent research showing that the evolutionary processes that shape biodiversity "hotspots" are equally valuable if we are to understand how life will cope with the current environmental pressures (Munday et al., 2013, Nielsen et al., 2017, Sgrò et al., 2011). To accurately identify the processes that have shaped the contemporary patterns of high endemism and elevated richness in marine environments, I used the latest tools and methods developed for historical biogeographic research. Because marine actinopterygians are highly diverse (Fricke et al., 2022), play critical ecological functions (Hayden et al., 2019), are economically valuable (Natale et al., 2013), and display resilience to climate change (Duffy et al., 2016), marine fishes are a good model to understand how marine biodiversity has evolved through time and space. To enhance our understanding of the evolutionary role that regions at the periphery of the Pacific Ocean play in the generation and maintenance of marine biodiversity, I focused on the Southwest Pacific, a highly diverse region with elevated marine fish endemism at a global scale (Costello et al., 2017), but where evolutionary research is in its infancy (Delrieu-Trottin et al., 2018, Eme et al., 2020, Liggins et al., 2022). To understand the evolutionary and ecological processes that shaped contemporary patterns of marine fish endemism and biodiversity in the Southwest Pacific, I generated empirical data across three research chapters using a variety of historical biogeographic approaches. Taken together, my major findings contribute to the academic knowledge of marine fish evolution in the Pacific. I end the discussion of my doctoral thesis by proposing future lines of investigation that derive from my research.

5. 1. Major findings

The study of the evolutionary history of marine fishes endemic to the subtropical islands of Lord Howe, Norfolk, and Rangitāhua (Chapter 2) suggested that the regional marine fish endemism originates predominantly from mainland Australia. Using time-calibrated phylogenies, I found that more than half of endemic taxa are closely related to Australian fauna, and for a small percentage of endemics, sister taxa occur in the East Pacific and northern Pacific locations. Additionally, the study established that the subtropical oceanic islands mainly act as centers of neoendemism: more than two-thirds of endemic lineages appear to have diverged after the emergence of the oldest of the three groups of islands.

The study of the historical biogeography of marine fishes endemic to the subtropical islands of the Southwest Pacific (Chapter 3) quantitatively showed that mainland Australia is the main source of endemic lineages in the region. For two-thirds of endemic lineages, the estimation of ancestral ranges locate the origin in mainland Australia, and for a smaller number of lineages, the origin is estimated to be in the East Pacific and northern Pacific locations. The biogeographic models highlighted vicariance and jump-dispersal as significant processes in the evolution of regional endemism, showing that geographic distance and climate zone differences are relevant factors that limit dispersal.

The phylogenetic study of the biogeographic patterns of marine fishes in shallow waters of New Zealand (Chapter 4) highlighted the difference in the geographic location of richness hotspots and centers of endemism, showing that these biogeographic patterns originate from distinct processes. For richness, I found that warmer locations, particularly around the northeast of the North Island, display high biodiversity, likely resulting from poleward range shifts of old tropical lineages. For endemism, I identified the subtropical oceanic islands as centers of neoendemism, confirming how the isolation of islands drives biodiversity origination, but also two centers of paleoendemism along

coastlines of the North and South Islands, possibly the result of local environmental stability over time.

5. 2. Knowledge contributions

The empirical data I have generated in my doctoral thesis significantly contributes to the understanding of the geographic distribution of marine fish biodiversity and endemism in the Southwest Pacific, as well as the historical processes that have generated contemporary patterns. I present nine major contributions nested within the theoretical background introduced in Chapter 1, and a set of phylogenetic contributions necessary for the partial development of this thesis, but that sit outside my main objectives.

Firstly, I bring evidence that richness hotspots and endemism centers do not co-occur geographically for marine fishes in the Southwest Pacific (Chapter 4), a similar biogeographic pattern observed in marine fishes at the larger Indo-Pacific scale (Cowman, 2014, Cowman et al., 2017).

I also detected higher taxonomic and phylogenetic diversities in warm, low-latitude waters within the Southwest Pacific, peaking at 35°S (Chapter 4), in congruence with phylogenetic and ecological research in the region (Eme et al., 2020, Middleton et al., in review, Myers et al., 2021), and the distribution of marine fish biodiversity in the Southern Hemisphere (Chaudhary et al., 2017). Altogether, these results likely translate the range overlap of tropical and mid-latitude species (Chaudhary et al., 2016).

My phylogenetic results show that the warmer waters of the North Island and northern subtropical oceanic islands act as “museums” for old marine fish lineages (Chapter 4), supporting models that explain the ‘Indo-Australian Archipelago hotspot’ based on the older age and habitat complexity of tropical environments (Miller et al., 2018, Pellissier et al., 2014, Siqueira et al., 2016).

Probabilistic biogeographic models suggest that both jump-dispersal and vicariance are significant drivers of endemism, where jump-dispersal is a relevant

process for lineages restricted to volcanic islands (Chapter 3). This inference supports historical biogeographic models that emphasize the synergy between vicariant and dispersal events over time and space (Sanmartín, 2012), as well as models of marine island biogeography that underline the relevance of colonization after the emergence of an island (Dawson, 2016, Hachich et al., 2015, Pinheiro et al., 2017, Whittaker et al., 2008).

The subtropical oceanic islands of the Southwest Pacific lie at the periphery of the Pacific Ocean. I provide evidence that such peripheral islands are generators of biodiversity novelty (Chapters 2, 3, and 4), supporting biogeographic models that assume the peripheral islands are engines of marine fish biodiversity in the Pacific (Bowen et al., 2013, Gaboriau et al., 2018).

I bring evidence that mainland Australia is the main source of endemic lineages in the Southwest Pacific, a pathway likely facilitated by the predominant eastward oceanic currents in the region (Chapters 2 and 3). Similar regional patterns are reported in other marine taxa (Bronstein et al., 2019, Brook, 1998a, Brook, 1999, Francis, 1993).

The last three of ten major contributions are methodological, given that my research has highlighted the efficacy of historical biogeographic tools and methods outlined in Chapter 1. Firstly, Chapter 2 confirms the preference of fossils to calibrate molecular phylogenies, and to estimate divergence timings (Powell et al., 2020), despite taxonomic and age uncertainties of some fossils (Heads, 2005). Secondly, Chapter 3 demonstrates the utility of probabilistic models that incorporate a jump-dispersal parameter (Matzke, 2014) given the congruence between what the models suggest and the ecological expectations in my dataset. My results support the validity of biogeographic models that parametrize jump-dispersal (Matzke, 2022) despite previous criticism (Ree and Sanmartín, 2018). Finally, Chapter 4 emphasizes the value of phylogenetic metrics in determining evolutionary processes uncaptured by species

richness alone (Faith, 2013), and in quantitatively delineating centers of endemism (Mishler et al., 2014).

Finally, the set of contributions that underpin part of my thesis (Chapters 2 and 3), but stay outside of my main objectives, is the inference of molecular phylogenies at the tips of the Fish Tree of Life, a necessary approach that also addresses biological shortfalls (Hortal et al., 2015). I clarified evolutionary relationships within 21 genera, eight of which were fully sampled, and four missed only one taxon. Moreover, I built the first comprehensively sampled phylogenies for four genera (*Enneapterygius*, *Lepidoperca*, *Hypoplectrodes*, and *Upeneus*). I confirmed the species status for 34 endemic taxa, 11 of which are positioned for the first time within a published molecular phylogeny, including 3 undescribed taxa (*Hypoplectrodes* sp. A, *Hypoplectrodes* sp. B, and *Nemadactylus* n.sp.). Additionally, I present novel molecular sequences for six endemics previously absent from open-access repositories.

Overall, my work has generated a historical biogeographic scenario for marine fishes of the Southwest Pacific where centers of endemism are not concordant with richness hotspots, suggesting the patterns originate from distinct historical processes. Biodiversity richness peaks at 35°S to decrease with increasing latitude, a pattern likely driven by the range overlap of tropical, subtropical, and temperate species, and expected to intensify with current poleward range shifts of highly diverse old tropical lineages. Endemism concentrates in subtropical oceanic islands, which act as peripheral islands that generate biodiversity novelty into the Pacific, and originates from mainland Australia lineages that colonized the recently emerged islands by jump-dispersal – following the predominant eastward oceanographic currents – to eventually diverge into endemic taxa.

5. 3. Future directions

Constructive research relies on the conscious identification of what we know, and what we do not know (Hortal et al., 2015). I conclude the discussion of my thesis by

acknowledging four major grounds of investigation that would enrich the inferences presented throughout the document.

First, the phylogenetic inference would improve with the addition of taxa within poorly sampled genera, clarifying the evolutionary relationships among all extant congeners, and avoiding the overestimation of divergence timings (Hodge and Bellwood, 2016). Such addition would derive from an improvement of specimen preservation for DNA analysis, and field surveys. Furthermore, the generation and inclusion of novel sequences for additional gene regions would improve topological resolution (Rubinoff and Holland, 2005) and benefit species identification (Dupuis et al., 2012). Finally, the exploration of phylogenomics is a promising, relatively inexpensive alternative to molecular phylogenetics by using genome-scale data to infer evolutionary relationships among taxa, estimate divergence times, and reconstruct ancestral ranges in biogeography (Young and Gillung, 2020).

Second, the full extension of the phylogenetic landscape of marine fishes in the shallow waters around New Zealand remains to be examined. I focused on richness and endemism metrics, which are a small proportion of the numerous indices measurable with a phylogenetic tree (Tucker et al., 2017). I encourage future investigators to explore measures of distance and evenness to enrich the phylogenetic landscape inferred in the present thesis. Furthermore, the estimation of divergence rates based on the phylogenies presented in this thesis would enhance our understanding of the evolutionary and ecological processes behind the biogeographic patterns detected in my thesis, as diversification rates bridge questions raised in macroevolution and macroecology (McGill et al., 2019). These lines of investigation will benefit from the ongoing molecular extension of New Zealand's marine fish phylogeny (Liggins, L., personal communication).

Third, the ecological aspects of the actinopterygian biogeography in the Southwest Pacific are yet to be fully explored. A short-term objective is the formal

description of undescribed endemic taxa, an ongoing work that uses part of my phylogenetic data for *Nemadactylus* and *Hypoplectrodes* (Roberts, C.D., personal communication). Field work in subtropical islands, particularly Lord Howe and Norfolk, would improve taxonomic inventories, and provide biological/ecological information on endemic taxa (e.g., dispersal capacities and reproductive success), offering an ecological background to contrast with the evolutionary inferences presented in my thesis.

Finally, the continuing curation of open-access repositories is a substantial work that provides a valuable amount of biological, ecological, and biogeographic data. My thesis exemplifies the capacity of using contemporary analytical tools to synthesize an ever-growing amount of data, and to improve our understanding of natural processes. Similar works to my thesis should provide constructive inferences if web-based datasets (e.g., occurrence and range information) are maintained and updated by expert opinions, as this is useful information for evolutionary, ecological, and biogeographic research.

As a final conclusion, it is considered that achieving a complete understanding of any natural process is highly unlikely (Ladle and Hortal, 2013). However, I believe that my doctoral research significantly contributes to a better understanding of the historical biogeography of marine fishes in the Southwest Pacific, and that my thesis represents a knowledge bridge for future work within the marine evolutionary ecology field.

6. Literature cited

AGUIRRE, J. D., BOLLARD-BREEN, B., CAMERON, M., CONSTANTINE, R., DUFFY, C. A., DUNPHY, B., HART, K., HEWITT, J. E., JARVIS, R. M. & JEFFS, A. 2016. Loved to pieces: toward the sustainable management of the Waitematā Harbour and Hauraki Gulf. *Regional Studies in Marine Science,* 8**,** 220-233. https://doi.org/10.1016/j.rsma.2016.02.009.

ALFARO, M. E., FAIRCLOTH, B. C., HARRINGTON, R. C., SORENSON, L., FRIEDMAN, M., THACKER, C. E., OLIVEROS, C. H., ČERNÝ, D. & NEAR, T. J. 2018. Explosive diversification of marine fishes at the Cretaceous–Palaeogene boundary. *Nature Ecology & Evolution,* 2**,** 688-696. https://doi.org/10.1038/s41559-018-0494-6.

ALLEN, G. R. 2008. Conservation hotspots of biodiversity and endemism for Indo-Pacific coral reef fishes. *Aquatic Conservation: Marine and Freshwater Ecosystems*, 18, 541–556. https://doi.org/10.1002/aqc.880.

ALLEN, G. R. & RANDALL, J. E. 1985. A new species of damselfish (Pomacentridae) from eastern Australia and the Norfolk Island Ridge. *Records of the Western Australian Museum*, 12,241-245.

ALLENDORF, F. W., HOHENLOHE, P. A. & LUIKART, G. 2010. Genomics and the future of conservation genetics. *Nature Reviews Genetics,* 11**,** 697-709. https://doi.org/10.1038/nrg2844.

ANDERSON, S. 1994. Area and endemism. *The quarterly review of biology,* 69**,** 451-471.

ANTONELLI, A., HETTLING, H., CONDAMINE, F. L., VOS, K., NILSSON, R. H., SANDERSON, M. J., SAUQUET, H., SCHARN, R., SILVESTRO, D. & TÖPEL, M. 2017. Toward a self-updating platform for estimating rates of speciation and migration, ages, and relationships of taxa. *Systematic Biology,* 66**,** 152-166.

AYRES, D. L., DARLING, A., ZWICKL, D. J., BEERLI, P., HOLDER, M. T., LEWIS, P. O., HUELSENBECK, J. P., RONQUIST, F., SWOFFORD, D. L. & CUMMINGS, M. P. 2012. BEAGLE: an application programming interface and high-performance computing library for statistical phylogenetics. *Systematic Biology,* 61**,** 170-173.

AZEVEDO, J. A., GUEDES, T. B., NOGUEIRA, C. D. C., PASSOS, P., SAWAYA, R. J., PRUDENTE, A. L., BARBO, F. E., STRÜSSMANN, C., FRANCO, F. L. & ARZAMENDIA, V. 2020. Museums and cradles of diversity are geographically coincident for narrowly distributed Neotropical snakes. *Ecography,* 43**,** 328-339. https://doi.org/ 10.1111/ecog.04815.

BARAF, L. M., PRATCHETT, M. S. & COWMAN, P. F. 2019. Ancestral biogeography and ecology of marine angelfishes (F: Pomacanthidae). *Molecular Phylogenetics and Evolution,* 140**,** 106596. https://doi.org/10.1016/j.ympev.2019.106596.

BARBER, P. H. & BELLWOOD, D. R. 2005. Biodiversity hotspots: evolutionary origins of biodiversity in wrasses (Halichoeres: Labridae) in the Indo-Pacific and new world tropics. *Molecular phylogenetics and evolution,* 35**,** 235-253.

BEAUGRAND, G., EDWARDS, M., RAYBAUD, V., GOBERVILLE, E. & KIRBY, R. R. 2015. Future vulnerability of marine biodiversity compared with contemporary and past changes. *Nature Climate Change,* 5**,** 695-701. https://doi.org/10.1038/NCLIMATE2650.

BEAUMONT, J., D'ARCHINO, R., MACDIARMID, A. & NIWA, W. 2009. Mapping the values of New Zealand's coastal waters. 4. A meta-analysis of environmental values. *Biosecurity New Zealand Technical Paper No: 2010,* 8.

BELDADE, R., LONGO, G. C., CLEMENTS, K. D., ROBERTSON, D. R., PEREZ-MATUS, A., ITOI, S., SUGITA, H. & BERNARDI, G. 2021. Evolutionary origin of the Atlantic Cabo Verde nibbler (*Girella stuebeli*), a member of a primarily Pacific Ocean family of antitropical herbivorous reef fishes. *Molecular Phylogenetics and Evolution,* 156**,** 107021. https://doi.org/10.1016/j.ympev.2020.107021.

BELLWOOD, D. R. & MEYER, C. P. 2009. Searching for heat in a marine biodiversity hotspot. *Journal of Biogeography*, 36, 569-576. https://doi.org/10.1111/j.1365-2699.2008.02029.x.

BELLWOOD, D. R., RENEMA, W. & ROSEN, B. R. 2012. Biodiversity hotspots, evolution and coral reef biogeography. In D. Gower, K. Johnson, J. Richardson, B. Rosen, L. Rüber,

and S. Williams (Eds.), *Biotic evolution and environmental change in Southeast Asia,* pp.2-32. Cambridge University Press.
BENESTAN, L., FIETZ, K., LOISEAU, N., GUERIN, P.-E., TROFIMENKO, E., RÜHS, S., SCHMIDT, C., RATH, W., BIASTOCH, A. & PÉREZ-RUZAFA, A. 2021. Restricted dispersal in a sea of gene flow. *Proceedings of the Royal Society B,* 288**,** 20210458. https://doi.org/10.1098/rspb.2021.0458.
BETANCUR-R, R., BROUGHTON, R. E., WILEY, E. O., CARPENTER, K., LÓPEZ, J. A., LI, C., HOLCROFT, N. I., ARCILA, D., SANCIANGCO, M. & CURETON II, J. C. 2013. The tree of life and a new classification of bony fishes. *PLoS Currents,* 5: ecurrents.tol.53ba26640df0ccaee75bb165c8c26288.
BETANCUR-R, R., WILEY, E. O., ARRATIA, G., ACERO, A., BAILLY, N., MIYA, M., LECOINTRE, G. & ORTI, G. 2017. Phylogenetic classification of bony fishes. *BMC Evolutionary Biology,* 17**,** 1-40. https://doi.org/ 10.1186/s12862-017-0958-3.
BETANCUR-R, R., ORTÍ, G. & PYRON, R. A. 2015. Fossil-based comparative analyses reveal ancient marine ancestry erased by extinction in ray-finned fishes. *Ecology Letters,* 18**,** 441-450.
BIRCH, J. L. & KEELEY, S. C. 2013. Dispersal pathways across the Pacific: the historical biogeography of *Astelia* s.l. (Asteliaceae, Asparagales). *Journal of Biogeography,* 40**,** 1914-1927.
BOUCKAERT, R. & XIE, D. 2017. Standard nucleotide substitution models v1. 0.1. https://doi.org/10.5281/zenodo.995740.
BOUCKAERT, R., VAUGHAN, T. G., BARIDO-SOTTANI, J., DUCHÊNE, S., FOURMENT, M., GAVRYUSHKINA, A., HELED, J., JONES, G., KÜHNERT, D. & DE MAIO, N. 2019. BEAST 2.5: An advanced software platform for Bayesian evolutionary analysis. *PLoS Computational Biology,* 15**,** e1006650. https://doi.org/10.1371/journal.pcbi.1006650.
BOWEN, B. W., GAITHER, M. R., DIBATTISTA, J. D., IACCHEI, M., ANDREWS, K. R., GRANT, W. S., TOONEN, R. J. & BRIGGS, J. C. 2016. Comparative phylogeography of the ocean planet. *Proceedings of the National Academy of Sciences,* 113**,** 7962-7969.
BOWEN, B. W., ROCHA, L. A., TOONEN, R. J. & KARL, S. A. 2013. The origins of tropical marine biodiversity. *Trends in Ecology & Evolution,* 28**,** 359-366.
BRIGGS, J. C. 2003. Marine centres of origin as evolutionary engines. *Journal of Biogeography,* 30**,** 1-18.
BRIGGS, J. C. & BOWEN, B. W. 2012. A realignment of marine biogeographic provinces with particular reference to fish distributions. *Journal of Biogeography,* 39**,** 12-30.
BRITO, P. H. & EDWARDS, S. V. 2009. Multilocus phylogeography and phylogenetics using sequence-based markers. *Genetica,* 135**,** 439-455.
BRITO-MORALES, I., SCHOEMAN, D. S., MOLINOS, J. G., BURROWS, M. T., KLEIN, C. J., ARAFEH-DALMAU, N., KASCHNER, K., GARILAO, C., KESNER-REYES, K. & RICHARDSON, A. J. 2020. Climate velocity reveals increasing exposure of deep-ocean biodiversity to future warming. *Nature Climate Change,* 10**,** 576-581. https://doi.org/10.1038/s41558-020-0773-5.
BRONSTEIN, O., KROH, A., MISKELLY, A. D., SMITH, S. D., DWORJANYN, S. A., MOS, B. & BYRNE, M. 2019. Implications of range overlap in the commercially important pan-tropical sea urchin genus *Tripneustes* (Echinoidea: Toxopneustidae). *Marine Biology,* 166**,** 1-5. https://doi.org/10.1007/s00227-019-3478-4.
BROOK, F. 1998a. The coastal molluscan fauna of the northern Kermadec Islands, Southwest Pacific Ocean. *Journal of the royal society of new Zealand,* 28**,** 185-233.
BROOK, F. 1998b. Stratigraphy and paleontology of Pleistocene submarine volcanic-sedimentary sequences at the northern Kermadec Islands. *Journal of the Royal Society of New Zealand,* 28**,** 235-257.
BROOK, F. 1999. The coastal scleractinian coral fauna of the Kermadec Islands, southwestern Pacific Ocean. *Journal of the Royal Society of New Zealand,* 29**,** 435-460.
BROUGH, T., MACTAVISH, T. & ZINTZEN, V. 2018. *Biological monitoring of marine protected areas at Banks Peninsula using baited underwater video (BUV)*. Department of Conservation, New Zealand.
BURRIDGE, C. 1999. Molecular phylogeny of *Nemadactylus* and *Acantholatris* (Perciformes: Cirrhitoidea: Cheilodactylidae), with implications for taxonomy and biogeography. *Molecular Phylogenetics and Evolution,* 13**,** 93-109.

BURRIDGE, C. P. 2000a. Biogeographic history of geminate cirrhitoids (Perciformes: Cirrhitoidea) with east–west allopatric distributions across southern Australia, based on molecular data. *Global Ecology and Biogeography,* 9**,** 517-525.

BURRIDGE, C. P. 2000b. Molecular phylogeny of the Aplodactylidae (Perciformes: Cirrhitoidea), a group of Southern Hemisphere marine fishes. *Journal of Natural History,* 34**,** 2173-2185.

BURRIDGE, C. P., ROBERTO, M. C. & DYER, B. S. 2006. Multiple origins of the Juan Fernández kelpfish fauna and evidence for frequent and unidirectional dispersal of cirrhitoid fishes across the South Pacific. *Systematic Biology,* 55**,** 566-578.

BURRIDGE, C. P. & SMOLENSKI, A. J. 2004. Molecular phylogeny of the Cheilodactylidae and Latridae (Perciformes: Cirrhitoidea) with notes on taxonomy and biogeography. *Molecular Phylogenetics and Evolution,* 30**,** 118-127.

CADOTTE, M. W. & DAVIES, T. J. 2010. Rarest of the rare: advances in combining evolutionary distinctiveness and scarcity to inform conservation at biogeographical scales. *Diversity and Distributions,* 16**,** 376-385. https://doi.org/10.1111/j.1472-4642.2010.00650.x.

CADOTTE, M. W., DAVIES, T.J., REGETZ, J., KEMBEL, S. W., CLELAND, E. & OAKLEY, T. H. 2010. Phylogenetic diversity metrics for ecological communities: integrating species richness, abundance and evolutionary history. *Ecology letters,* 13**,** 96-105. https://doi.org/10.1111/j.1461-0248.2009.01405.x.

CAMACHO, G. P., LOSS, A. C., FISHER, B. L. & BLAIMER, B. B. 2021. Spatial phylogenomics of acrobat ants in Madagascar—Mountains function as cradles for recent diversity and endemism. *Journal of Biogeography,* 48**,** 1706-1719. https://doi.org/10.1111/jbi.14107.

CAPELLA-GUTIÉRREZ, S., SILLA-MARTÍNEZ, J. M. & GABALDÓN, T. 2009. trimAl: a tool for automated alignment trimming in large-scale phylogenetic analyses. *Bioinformatics,* 25**,** 1972-1973.

CHAUDHARY, C., RICHARDSON, A. J., SCHOEMAN, D. S. & COSTELLO, M. J. 2021. Global warming is causing a more pronounced dip in marine species richness around the equator. *Proceedings of the National Academy of Sciences,* 118**,** e2015094118.

CHAUDHARY, C., SAEEDI, H. & COSTELLO, M. J. 2016. Bimodality of latitudinal gradients in marine species richness. *Trends in Ecology & Evolution,* 31**,** 670-676. https://doi.org/10.1016/j.tree.2016.06.001.

CHAUDHARY, C., SAEEDI, H. & COSTELLO, M. J. 2017. Marine species richness is bimodal with latitude: a reply to Fernandez and Marques. *Trends in Ecology & Evolution,* 32**,** 234-237. https://doi.org/10.1016/j.tree.2017.02.007.

CHISWELL, S. M. & RICKARD, G. J. 2011. Larval connectivity of harbours via ocean currents: a New Zealand study. *Continental Shelf Research,* 31**,** 1057-1074. https://doi.org/10.1016/j.csr.2011.03.012.

CLOUARD, V. & BONNEVILLE, A. 2005. Ages of seamounts, islands, and plateaus on the Pacific plate. In G. R. Foulger (Ed.), *Plates, plumes, and paradigms* (pp. 71-90). Geological Society of America.

COLL, M., PIRODDI, C., STEENBEEK, J., KASCHNER, K., BEN RAIS LASRAM, F., AGUZZI, J., BALLESTEROS, E., BIANCHI, C. N., CORBERA, J. & DAILIANIS, T. 2010. The biodiversity of the Mediterranean Sea: estimates, patterns, and threats. *PloS One,* 5**,** e11842. https://doi.org/10.1371/journal.pone.0011842.

COMMONWEALTH OF AUSTRALIA. 2012. Marine bioregional plan for the Temperate East Marine Region. *Department of Sustainability, Environment, Water, Population and Communities*. Australian Government.

CONWAY, K. W., KING, C. D., SUMMERS, A. P., KIM, D., HASTINGS, P. A., MOORE, G. I., IGLÉSIAS, S. P., ERDMANN, M. V., BALDWIN, C. C. & SHORT, G. 2020. Molecular phylogenetics of the clingfishes (Teleostei: Gobiesocidae)—implications for classification. *Copeia,* 108**,** 886-906. https://doi.org/ 10.1643/CI2020054.

CONWAY, K. W., STEWART, A. L. & SUMMERS, A. P. 2018. A new genus and species of clingfish from the Rangitāhua Kermadec Islands of New Zealand (Teleostei, Gobiesocidae). *ZooKeys***,** 786, 75-104. https://doi.org/ 10.3897/zookeys.786.28539.

COSTELLO, M. J. & CHAUDHARY, C. 2017. Marine biodiversity, biogeography, deep-sea gradients, and conservation. *Current Biology,* 27**,** R511-R527. https://doi.org/ https://doi.org/10.1016/j.cub.2017.04.060.

COSTELLO, M. J., COLL, M., DANOVARO, R., HALPIN, P., OJAVEER, H. & MILOSLAVICH, P. 2010. A census of marine biodiversity knowledge, resources, and future challenges. *PloS one,* 5**,** e12110. https://doi.org/ 10.1371/journal.pone.0012110.

COSTELLO, M. J., TSAI, P., WONG, P. S., CHEUNG, A. K. L., BASHER, Z. & CHAUDHARY, C. 2017. Marine biogeographic realms and species endemicity. *Nature Communications,* 8**,** 1-10. https://doi.org/ 10.1038/s41467-017-01121-2.

COWEN, R. K. & SPONAUGLE, S. 2009. Larval dispersal and marine population connectivity. *Annual Review of Marine Science,* 1**,** 443-466. https://doi.org/10.1146/annurev.marine.010908.163757.

COWMAN, P. F. 2014. Historical factors that have shaped the evolution of tropical reef fishes: a review of phylogenies, biogeography, and remaining questions. *Frontiers in Genetics,* 5**,** 394. https://doi.org/10.3389/fgene.2014.00394.

COWMAN, P. F. & BELLWOOD, D. R. 2013. Vicariance across major marine biogeographic barriers: temporal concordance and the relative intensity of hard versus soft barriers. *Proceedings of the Royal Society B: Biological Sciences,* 280**,** 20131541. http://dx.doi.org/10.1098/rspb.2013.1541

COWMAN, P. F., PARRAVICINI, V., KULBICKI, M. & FLOETER, S. R. 2017. The biogeography of tropical reef fishes: endemism and provinciality through time. *Biological Reviews,* 92**,** 2112-2130.

CRAME, J. A. 2018. Key stages in the evolution of the Antarctic marine fauna. *Journal of Biogeography,* 45**,** 986-994. https://doi.org/10.1111/jbi.13208.

CRISCI, J. V. 2001. The voice of historical biogeography. *Journal of Biogeography,* 28**,** 157-168.

CRISP, M. D., LAFFAN, S., LINDER, H. P. & MONRO, A. 2001. Endemism in the Australian flora. *Journal of Biogeography,* 28**,** 183-198. https://doi.org/10.1046/j.1365-2699.2001.00524.x.

CRISP, M. D., TREWICK, S. A. & COOK, L. G. 2011. Hypothesis testing in biogeography. *Trends in Ecology & Evolution,* 26**,** 66-72. https://doi.org/10.1016/j.tree.2010.11.005.

CUNHA, T. J., LEMER, S., BOUCHET, P., KANO, Y. & GIRIBET, G. 2019. Putting keyhole limpets on the map: phylogeny and biogeography of the globally distributed marine family Fissurellidae (Vetigastropoda, Mollusca). *Molecular Phylogenetics and Evolution,* 135**,** 249-269. https://doi.org/ https://doi.org/10.1016/j.ympev.2019.02.008.

DAGALLIER, L. P. M., JANSSENS, S. B., DAUBY, G., BLACH-OVERGAARD, A., MACKINDER, B. A., DROISSART, V., SVENNING, J. C., SOSEF, M. S., STÉVART, T. & HARRIS, D. J. 2020. Cradles and museums of generic plant diversity across tropical Africa. *New Phytologist,* 225**,** 2196-2213. https://doi.org/10.1111/nph.16293.

DALONGEVILLE, A., ANDRELLO, M., MOUILLOT, D., LOBREAUX, S., FORTIN, M. J., LASRAM, F., BELMAKER, J., ROCKLIN, D. & MANEL, S. 2018. Geographic isolation and larval dispersal shape seascape genetic patterns differently according to spatial scale. *Evolutionary Applications,* 11**,** 1437-1447.

DARU, B. H., FAROOQ, H., ANTONELLI, A. & FAURBY, S. 2020. Endemism patterns are scale dependent. *Nature Communications,* 11**,** 1-11. https://doi.org/10.1038/s41467-020-15921-6.

DAWSON, M. N. 2016. Island and island-like marine environments. *Global Ecology and Biogeography,* 25**,** 831-846.

DECK, J., GAITHER, M. R., EWING, R., BIRD, C. E., DAVIES, N., MEYER, C., RIGINOS, C., TOONEN, R. J. & CRANDALL, E. D. 2017. The Genomic Observatories Metadatabase (GeOMe): A new repository for field and sampling event metadata associated with genetic samples. *PLoS Biology,* 15**,** e2002925. https://doi.org/10.1371/journal.pbio.2002925.

DELRIEU-TROTTIN, E., WILLIAMS, J., BACCHET, P., KULBICKI, M., MOURIER, J., GALZIN, R., DE LOMA, T. L., MOU-THAM, G., SIU, G. & PLANES, S. 2015. Shore fishes of the Marquesas Islands, an updated checklist with new records and new percentage of endemic species. *Check List*, 11, 1-13. http://dx.doi.org/10.15560/11.5.1758.

DELRIEU-TROTTIN, E., LIGGINS, L., TRNSKI, T., WILLIAMS, J. T., NEGLIA, V., RAPU-EDMUNDS, C., PLANES, S. & SAENZ-AGUDEULO, P. 2018. Evidence of cryptic species in the blenniid *Cirripectes alboapicalis* species complex, with zoogeographic implications for the South Pacific. *Zookeys*, 810, 127-138. https://doi.org/ 10.3897/zookeys.810.28887.

DELRIEU-TROTTIN, E., BROSSEAU-ACQUAVIVA, L., MONA, S., NEGLIA, V., GILES, E. C., RAPU-EDMUNDS, C. & SAENZ-AGUDELO, P. 2019. Understanding the origin of the most isolated endemic reef fish fauna of the Indo-Pacific: Coral reef fishes of Rapa Nui. *Journal of Biogeography,* 46**,** 723-733. https://doi.org/ 10.1111/jbi.13531.

DUFFY, C. A. & AHYONG, S. T. 2015. Annotated checklist of the marine flora and fauna of the Kermadec Islands Marine Reserve and northern Kermadec Ridge, New Zealand. *Bulletin of the Auckland Museum,* 20**,** 19-124.

DUFFY, J. E., LEFCHECK, J. S., STUART-SMITH, R. D., NAVARRETE, S. A. & EDGAR, G. J. 2016. Biodiversity enhances reef fish biomass and resistance to climate change. *Proceedings of the National Academy of Sciences,* 113**,** 6230-6235. https://doi.org/10.1073/pnas.1524465113.

DUPUIS, J. R., ROE, A. D. & SPERLING, F. A. 2012. Multi-locus species delimitation in closely related animals and fungi: one marker is not enough. *Molecular Ecology,* 21**,** 4422-4436. https://doi.org/10.1111/j.1365-294X.2012.05642.x.

EARL, C., BELITZ, M. W., LAFFAN, S. W., BARVE, V., BARVE, N., SOLTIS, D. E., ALLEN, J. M., SOLTIS, P. S., MISHLER, B. D. & KAWAHARA, A. Y. 2021. Spatial phylogenetics of butterflies in relation to environmental drivers and angiosperm diversity across North America. *iScience,* 24**,** 102239. https://doi.org/10.1016/j.isci.2021.102239.

EBACH, M. C. 2004. Forum on biogeography: introduction. *Taxon,* 53**,** 889-891.

EME, D., ANDERSON, M. J., STRUTHERS, C. D., ROBERTS, C. D. & LIGGINS, L. 2019. An integrated pathway for building regional phylogenies for ecological studies. *Global Ecology and Biogeography,* 28**,** 1899-1911. https://doi.org/ 10.1111/geb.12986.

EME, D., ANDERSON, M., MYERS, E., ROBERTS, C. & LIGGINS, L. 2020. Phylogenetic measures reveal eco-evolutionary drivers of biodiversity along a depth gradient. *Ecography,* 43**,** 689-702. https://doi.org/10.1111/ecog.04836.

FAIRCLOTH, B. C., ALDA, F., HOEKZEMA, K., BURNS, M. D., OLIVEIRA, C., ALBERT, J. S., MELO, B. F., OCHOA, L. E., ROXO, F. F. & CHAKRABARTY, P. 2020. A target enrichment bait set for studying relationships among ostariophysan fishes. *Copeia,* 108**,** 47-60. https://doi.org/ 10.1643/CG-18-139.

FAITH, D. P. 1992. Conservation evaluation and phylogenetic diversity. *Biological Conservation,* 61**,** 1-10.

FAITH, D. P. 2013. Biodiversity and evolutionary history: useful extensions of the PD phylogenetic diversity assessment framework. *Annals of the New York Academy of Sciences,* 1289**,** 69-89. https://doi.org/ 10.1111/nyas.12186.

FLEMING, C. 1973. Kermadec Island giant limpet occurring fossil in New Zealand, and relict distributions in the tropics. *New Zealand Journal of Marine and Freshwater Research,* 7**,** 159-164.

FLOWER, B. P. & KENNETT, J. P. 1994. The middle Miocene climatic transition: East Antarctic ice sheet development, deep ocean circulation and global carbon cycling. *Palaeogeography, Palaeoclimatology, Palaeoecology,* 108**,** 537-555.

FONTENELLE, J. P., PORTELLA LUNA MARQUES, F., KOLMANN, M. A. & LOVEJOY, N. R. 2021. Biogeography of the Neotropical freshwater stingrays (Myliobatiformes: Potamotrygoninae) reveals effects of continent-scale paleogeographic change and drainage evolution. *Journal of Biogeography,* 48**,** 1406-1419. https://doi.org/ 10.1111/jbi.14086.

FOREST, F., GRENYER, R., ROUGET, M., DAVIES, T. J., COWLING, R. M., FAITH, D. P., BALMFORD, A., MANNING, J. C., PROCHEŞ, Ş. & VAN DER BANK, M. 2007. Preserving the evolutionary potential of floras in biodiversity hotspots. *Nature,* 445**,** 757-760. https://doi.org/10.1038/nature05587.

FRANCIS, M. P. 1993. Checklist of the coastal fishes of Lord Howe, Norfolk, and Kermadec Islands, Southwest Pacific Ocean. *Pacific Science*, 47, 136-170.

FRANCIS, M. 2019. Checklist of the coastal fishes of Lord Howe, Norfolk, and Kermadec Islands, southwest Pacific Ocean. https://doi.org/10.6084/m9.figshare.c.4428305.v1.

FRANCIS, M. P. & DUFFY, C. A. 2015. New records, checklist and biogeography of Kermadec Islands' coastal fishes. *Bulletin of the Auckland Museum,* 20**,** 481-495.

FRÉDÉRICH, B., SORENSON, L., SANTINI, F., SLATER, G. J. & ALFARO, M. E. 2013. Iterative ecological radiation and convergence during the evolutionary history of damselfishes (Pomacentridae). *The American Naturalist,* 181**,** 94-113. https://doi.org/10.1086/668599.

FRICKE, R. 1994. Tripterygiid Fishes of Australia, New Zealand and the Southwest Pacific Ocean: With Descriptions of 2 New Genera and 16 New Species (Teleostei). Lubrecht & Cramer Limited.

FRICKE, R., ESCHMEYER, W.N. & VAN DER LAAN, R. 2021. *Eschmeyer's Catalog of Fishes: Genera, Species, References*. Available at:

http://researcharchive.calacademy.org/research/ichthyology/catalog/fishcatmain.asp (Accessed: 8 November 2021).
FRICKE, R., ESCHMEYER, W.N. & VAN DER LAAN, R. 2022. *Eschmeyer's Catalog of Fishes: Genera, Species, References*. Available at: http://researcharchive.calacademy.org/research/ichthyology/catalog/fishcatmain.asp (Accessed: May 2022).
FRIEDLANDER, A. M., BALLESTEROS, E., CASELLE, J. E., GAYMER, C. F., PALMA, A. T., PETIT, I., VARAS, E., MUÑOZ WILSON, A. & SALA, E. 2016. Marine biodiversity in Juan Fernández and Desventuradas Islands, Chile: global endemism hotspots. *PLoS One,* 11**,** e0145059. https://doi.org/ 10.1371/journal.pone.0145059.
FRITZ, S. A. & RAHBEK, C. 2012. Global patterns of amphibian phylogenetic diversity. *Journal of Biogeography,* 39**,** 1373-1382. https://doi.org/10.1111/j.1365-2699.2012.02757.x.
FROESE, R. & PAULY, D. 2021. *FishBase*. World Wide Web electronic publication. org. version (06/2021). Available at: http://www. fishbase. org (Accessed: 8 November 2021).
FROESE, R. & PAULY, D. 2022. *FishBase*. World Wide Web electronic publication. org. version (06/2021). Available at: http://www. fishbase. org (Accessed: May 2022).
FUJIWARA, K., CONWAY, K. W. & MOTOMURA, H. 2021. First record of the Kermadec Clingfish, *Flexor incus* Conway, Stewart & Summers, 2018 (Gobiesocidae), from New Caledonia and Australia. *Check List,* 17**,** 769-773. https://doi.org/10.15560/17.3.769.
GABORIAU, T., LEPRIEUR, F., MOUILLOT, D. & HUBERT, N. 2018. Influence of the geography of speciation on current patterns of coral reef fish biodiversity across the Indo-Pacific. *Ecography,* 41**,** 1295-1306. https://doi.org/10.1111/ecog.02589.
GANACHAUD, A., CRAVATTE, S., MELET, A., SCHILLER, A., HOLBROOK, N., SLOYAN, B., WIDLANSKY, M., BOWEN, M., VERRON, J. & WILES, P. 2014. The Southwest Pacific Ocean circulation and climate experiment (SPICE). *Journal of Geophysical Research: Oceans,* 119**,** 7660-7686. https://doi.org/ 10.1002/2013JC009678.
GANDOLFO, M. A., NIXON, K. C. & CREPET, W. L. 2008. Selection of fossils for calibration of molecular dating models. *Annals of the Missouri Botanical Garden,* 95**,** 34-42.
GARCIA–R, J. C., GONZALEZ-OROZCO, C. E. & TREWICK, S. A. 2019. Contrasting patterns of diversification in a bird family (Aves: Gruiformes: Rallidae) are revealed by analysis of geospatial distribution of species and phylogenetic diversity. *Ecography,* 42**,** 500-510. https://doi.org/10.1111/ecog.03783.
GASTON, K. J. 1996. Species richness: measure and measurement. *Biodiversity: A Biology of Numbers and Difference***,** 77-113.
GASTON, K. J. 2007. Latitudinal gradient in species richness. *Current Biology,* 17**,** R574. https://doi.org/10.1016/j.cub.2007.05.013.
GHEDOTTI, M. J., DEKAY, H. M., MAILE, A. J., SMITH, W. L. & DAVIS, M. P. 2021. Anatomy and evolution of bioluminescent organs in the slimeheads (Teleostei: Trachichthyidae). *Journal of Morphology,* 282**,** 820-832. https://doi.org/10.1002/jmor.21349.
GILLESPIE, R. G. & RODERICK, G. K. 2002. Arthropods on Islands: Colonization, Speciation, and Conservation. *Annual Review of Entomology,* 47**,** 595-632.
GOLDBERG, J., TREWICK, S. A. & PATERSON, A. M. 2008. Evolution of New Zealand's terrestrial fauna: a review of molecular evidence. *Philosophical Transactions of the Royal Society B: Biological Sciences,* 363**,** 3319-3334.
GOMON, M. F. & ROBERTS, C. D. 2011. A second New Zealand species of the stargazer genus *Kathetostoma* (Trachinoidei: Uranoscopidae). *Zootaxa,* 2776**,** 1-12. https://doi.org/10.11646/zootaxa.2776.1.1.
GORDON, D. P., BEAUMONT, J., MACDIARMID, A., ROBERTSON, D. A. & AHYONG, S. T. 2010. Marine biodiversity of Aotearoa New Zealand. *PloS One,* 5**,** e10905. https://doi.org/10.1371/journal.pone.0010905.
GRANDCOLAS, P., MURIENNE, J. M., ROBILLARD, T., DESUTTER-GRANDCOLAS, L., JOURDAN, H., GUILBERT, E. & DEHARVENG, L. 2008. New Caledonia: a very old Darwinian island? *Philosophical Transactions of the Royal Society B: Biological Sciences,* 363**,** 3309-3317.
GRANDE, T. C., BORDEN, W. C., WILSON, M. V. & SCARPITTA, L. 2018. Phylogenetic relationships among fishes in the order Zeiformes based on molecular and morphological data. *Copeia,* 106**,** 20-48. https://doi.org/ 10.1643/CG-17-594.
HACHICH, N. F., BONSALL, M. B., ARRAUT, E. M., BARNECHE, D. R., LEWINSOHN, T. M. & FLOETER, S. R. 2015. Island biogeography: patterns of marine shallow-water organisms

in the Atlantic Ocean. *Journal of Biogeography,* 42**,** 1871-1882. https://doi.org/10.1111/jbi.12560.
HASTINGS, R. A., RUTTERFORD, L. A., FREER, J. J., COLLINS, R. A., SIMPSON, S. D. & GENNER, M. J. 2020. Climate change drives poleward increases and equatorward declines in marine species. *Current Biology,* 30**,** 1572-1577. https://doi.org/10.1016/j.cub.2020.02.043.
HARRISON, S. & NOSS, R. 2017. Endemism hotspots are linked to stable climatic refugia. *Annals of Botany,* 119**,** 207-214. https://doi.org/10.1093/aob/mcw248.
HAYDEN, B., PALOMARES, M. L. D., SMITH, B. & POELEN, J. 2019. Biological and environmental drivers of trophic ecology in marine fishes-a global perspective. *Scientific Reports,* 9**,** 1-10. https://doi.org/10.1038/s41598-019-47618-2.
HEADS, M. 2005. Dating nodes on molecular phylogenies: a critique of molecular biogeography. *Cladistics,* 21**,** 62-78.
HEADS, M. 2011. Old taxa on young islands: a critique of the use of island age to date island-endemic clades and calibrate phylogenies. *Systematic Biology,* 60**,** 204-218.
HEBERT, P. D., RATNASINGHAM, S. & DE WAARD, J. R. 2003. Barcoding animal life: cytochrome c oxidase subunit 1 divergences among closely related species. *Proceedings of the Royal Society of London. Series B: Biological Sciences,* 270**,** S96-S99.
HEDGES, S. B. 1996. Historical biogeography of West Indian vertebrates. *Annual Review of Ecology and Systematics***,** 163-196.
HEENAN, P. B., MILLAR, T. R., SMISSEN, R. D., MCGLONE, M. S. & WILTON, A. D. 2017. Phylogenetic measures of neo-and palaeo-endemism in the indigenous vascular flora of the New Zealand archipelago. *Australian Systematic Botany,* 30**,** 124-133. https://doi.org/10.1071/SB17009.
HIJMANS, R.J. & VAN ETTEN, J. 2012. Geographic analysis and modeling with raster data. R package version 3.5-15.
HOBAN, M. L. & WILLIAMS, J. T. 2020. *Cirripectes matatakaro*, a new species of combtooth blenny from the Central Pacific, illuminates the origins of the Hawaiian fish fauna. *PeerJ,* 8**,** e8852. https://doi.org/10.7717/peerj.8852.
HOBAN, S., BRUFORD, M., FUNK, W. C., GALBUSERA, P., GRIFFITH, M. P., GRUEBER, C. E., HEUERTZ, M., HUNTER, M. E., HVILSOM, C. & KALAMUJIC, S. B. 2021. Global commitments to conserving and monitoring genetic diversity are now necessary and feasible. *BioScience*. 71, 964-976. https://doi.org/10.1093/biosci/biab054.
HODGE, J. R. & BELLWOOD, D. R. 2016. The geography of speciation in coral reef fishes: The relative importance of biogeographical barriers in separating sister-species. *Journal of Biogeography,* 43**,** 1324-1335. https://doi.org/10.1111/jbi.12729.
HODGE, J. R., VAN HERWERDEN, L. & BELLWOOD, D. R. 2014. Temporal evolution of coral reef fishes: global patterns and disparity in isolated locations. *Journal of Biogeography,* 41**,** 2115-2127. https://doi.org/10.1111/jbi.12356.
HOEKSEMA, B. W. 2007. Delineation of the Indo-Malayan centre of maximum marine biodiversity: the Coral Triangle. In: Renema, W. (ed.) *Biogeography, time, and place: distributions, barriers, and islands* (pp. 117-178). Dordrecht: Springer.
HOESE, D. F. & STEWART, A. L. 2012. A new species of the gobiid genus *Eviota* (Teleostei: Gobioidei) from the Kermadec Islands, New Zealand. *Zootaxa,* 3418**,** 61-67. https://doi.org/10.11646/zootaxa.3418.1.5.
HORTAL, J., DE BELLO, F., DINIZ-FILHO, J. A. F., LEWINSOHN, T. M., LOBO, J. M. & LADLE, R. J. 2015. Seven shortfalls that beset large-scale knowledge of biodiversity. *Annual Review of Ecology, Evolution, and Systematics,* 46**,** 523-549. https://doi.org/0.1146/annurev-ecolsys-112414-054400.
HUGHES, A. C., ORR, M. C., MA, K., COSTELLO, M. J., WALLER, J., PROVOOST, P., YANG, Q., ZHU, C. & QIAO, H. 2021. Sampling biases shape our view of the natural world. *Ecography,* 44**,** 1259-1269. https://doi.org/10.1111/ecog.05926.
HUGHES, L. C., ORTÍ, G., HUANG, Y., SUN, Y., BALDWIN, C. C., THOMPSON, A. W., ARCILA, D., BETANCUR-R, R., LI, C. & BECKER, L. 2018. Comprehensive phylogeny of ray-finned fishes (Actinopterygii) based on transcriptomic and genomic data. *Proceedings of the National Academy of Sciences,* 115**,** 6249-6254. https://doi.org/10.1073/pnas.1719358115.
HUGHES, T. P., BELLWOOD, D. R. & CONNOLLY, S. R. 2002. Biodiversity hotspots, centres of endemicity, and the conservation of coral reefs. *Ecology Letters,* 5**,** 775-784. https://doi.org./10.1046/j.1461-0248.2002.00383.x.

HUNN, C. A. & UPCHURCH, P. 2001. The importance of time/space in diagnosing the causality of phylogenetic events: towards a 'chronobiogeographical'paradigm? *Systematic Biology,* 50**,** 391-407. https://doi.org/ 10.1093/sysbio/50.3.391.

HUSON, D. H. & SCORNAVACCA, C. 2012. Dendroscope 3: an interactive tool for rooted phylogenetic trees and networks. *Systematic Biology,* 61**,** 1061-1067. https://doi.org/10.1093/sysbio/sys062.

IVANOVA, N. V., ZEMLAK, T. S., HANNER, R. H. & HEBERT, P. D. 2007. Universal primer cocktails for fish DNA barcoding. *Molecular Ecology Notes,* 7**,** 544-548. https://doi.org/10.1111/j.1471-8286.2007.01748.x.

IWATSUBO, H. & MOTOMURA, H. 2018. *Chromis katoi*, a new species of damselfish from the Izu Islands, Japan, with a key to species in the *Chromis notata* species complex (Perciforms: Pomacentridae). *International Journal of Ichthyology*, 24, 27-34.

JIANG, W., CHEN, S.-Y., WANG, H., LI, D.-Z. & WIENS, J. J. 2014. Should genes with missing data be excluded from phylogenetic analyses? *Molecular Phylogenetics and Evolution,* 80**,** 308-318. https://doi.org/10.1016/j.ympev.2014.08.006.

JONES, G., ALMANY, G., RUSS, G., SALE, P., STENECK, R., VAN OPPEN, M. & WILLIS, B. 2009. Larval retention and connectivity among populations of corals and reef fishes: history, advances and challenges. *Coral Reefs,* 28**,** 307-325. https://doi.org/10.1007/s00338-009-0469-9.

JONES, J. & MCDOUGALL, I. 1973. Geological history of Norfolk and Philip islands, southwest Pacific Ocean. *Journal of the Geological Society of Australia,* 20**,** 239-254.

KASCHNER, K., TITTENSOR, D. P., READY, J., GERRODETTE, T. & WORM, B. 2011. Current and future patterns of global marine mammal biodiversity. *PLoS One,* 6**,** e19653. https://doi.org/10.1371/journal.pone.0019653.

KASCHNER, K., KESNER-REYES, K., GARILAO, C., SEGSCHNEIDER, J., RIUS-BARILE, J., REES, T. & FROESE, R. 2019. *AquaMaps: Predicted range maps for aquatic species*. World Wide Web electronic publication, www.aquamaps.org, version 10/2019 (final).

KATOH, K., MISAWA, K., KUMA, K. I. & MIYATA, T. 2002. MAFFT: a novel method for rapid multiple sequence alignment based on fast Fourier transform. *Nucleic Acids Research,* 30**,** 3059-3066. https://doi.org/10.1093/nar/gkf436.

KIER, G., KREFT, H., LEE, T. M., JETZ, W., IBISCH, P. L., NOWICKI, C., MUTKE, J. & BARTHLOTT, W. 2009. A global assessment of endemism and species richness across island and mainland regions. *Proceedings of the National Academy of Sciences,* 106**,** 9322-9327. https://doi.org/10.1073/pnas.081030610.

KLEIN, C. J., BROWN, C. J., HALPERN, B. S., SEGAN, D. B., MCGOWAN, J., BEGER, M. & WATSON, J. E. 2015. Shortfalls in the global protected area network at representing marine biodiversity. *Scientific Reports,* 5**,** 1-7. https://doi.org/10.1038/srep17539.

KNUDSEN, S. W., CHOAT, J. H. & CLEMENTS, K. D. 2019. The herbivorous fish family Kyphosidae (Teleostei: Perciformes) represents a recent radiation from higher latitudes. *Journal of Biogeography,* 46**,** 2067-2080. https://doi.org/10.1111/jbi.13634.

KNUDSEN, S. W. & CLEMENTS, K. D. 2016. World-wide species distributions in the family Kyphosidae (Teleostei: Perciformes). *Molecular Phylogenetics and Evolution,* 101**,** 252-266. https://doi.org/10.1016/j.ympev.2016.04.037.

KULBICKI, M., PARRAVICINI, V., BELLWOOD, D. R., ARIAS-GONZÀLEZ, E., CHABANET, P., FLOETER, S. R., FRIEDLANDER, A., MCPHERSON, J., MYERS, R. E. & VIGLIOLA, L. 2013. Global biogeography of reef fishes: a hierarchical quantitative delineation of regions. *PloS One,* 8**,** e81847. https://doi.org/10.1371/journal.pone.0081847.

LACHNER, E. A. & KARNELLA, S. J. 1980. Fishes of the Indo-Pacific genus *Eviota* with descriptions of eight new species (Teleostei, Gobiidae). *Smithsonian Contributions to Zoology*. Smithsonian Insitution Press, Washington.

LADD, H. 1960. Origin of the Pacific Island Molluscan Fauna. *American Journal of Science, Bradley Volume***,** 137-150.

LADLE, R. & HORTAL, J. 2013. Mapping species distributions: living with uncertainty. *Frontiers of Biogeography,* 5. https://doi.org/10.21425/F5FBG12942.

LAFFAN, S. W., LUBARSKY, E. & ROSAUER, D. F. 2010. Biodiverse, a tool for the spatial analysis of biological and related diversity. *Ecography,* 33**,** 643-647. https://doi.org/10.1111/j.1600-0587.2010.06237.x.

LAMM, K. S. & REDELINGS, B. D. 2009. Reconstructing ancestral ranges in historical biogeography: properties and prospects. *Journal of Systematics and Evolution,* 47**,** 369-382. https://doi.org/10.1111/j.1759-6831.2009.00042.x.

LANDIS, M. J., MATZKE, N. J., MOORE, B. R. & HUELSENBECK, J. P. 2013. Bayesian analysis of biogeography when the number of areas is large. *Systematic Biology,* 62**,** 789-804. https://doi.org/10.1093/sysbio/syt040.

LANFEAR, R., FRANDSEN, P. B., WRIGHT, A. M., SENFELD, T. & CALCOTT, B. 2017. PartitionFinder 2: new methods for selecting partitioned models of evolution for molecular and morphological phylogenetic analyses. *Molecular Biology and Evolution,* 34**,** 772-773. https://doi.org/10.1093/molbev/msw260.

LE FEUVRE, M. C., DEMPSTER, T., SHELLEY, J. J., DAVIS, A. M. & SWEARER, S. E. 2021. Range restriction leads to narrower ecological niches and greater extinction risk in Australian freshwater fish. *Biodiversity and Conservation,* 30**,** 2955-2976. https://doi.org/10.1007/s10531-021-02229-0.

LEATHWICK, J., ELITH, J., FRANCIS, M., HASTIE, T. & TAYLOR, P. 2006. Variation in demersal fish species richness in the oceans surrounding New Zealand: an analysis using boosted regression trees. *Marine Ecology Progress Series,* 321**,** 267-281. https://doi.org/10.3354/meps321267.

LEE, A. C. & MISHLER, B. 2014. Phylogenetic diversity and endemism: metrics for identifying critical regions of conifer conservation in Australia. *Berkeley Scientific Journal,* 18. 48-58. https://doi.org/10.5070/BS3182022486.

LEPRIEUR, F., DESCOMBES, P., GABORIAU, T., COWMAN, P. F., PARRAVICINI, V., KULBICKI, M., MELIÁN, C. J., DE SANTANA, C. N., HEINE, C. & MOUILLOT, D. 2016. Plate tectonics drive tropical reef biodiversity dynamics. *Nature Communications,* 7**,** 1-8. https://doi.org/10.1038/ncomms11461.

LESTER, S. E., RUTTENBERG, B. I., GAINES, S. D. & KINLAN, B. P. 2007. The relationship between dispersal ability and geographic range size. *Ecology Letters,* 10**,** 745-758. https://doi.org/10.1111/j.1461-0248.2007.01070.x.

LI, X., SHEN, X., CHEN, X., XIANG, D., MURPHY, R. W. & SHEN, Y. 2018. Detection of potential problematic Cytb gene sequences of fishes in GenBank. *Frontiers in Genetics,* 9**,** 30. https://doi.org/10.3389/fgene.2018.00030.

LIGGINS, L., KILDUFF, L., TRNSKI, T., DELRIEU-TROTTIN, E., CARVAJAL, J. I., ARRANZ, V., PLANES, S., SAENZ-AGUDELO, P. & AGUIRRE, J. D. 2022. Morphological and genetic divergence supports peripheral endemism and a recent evolutionary history of *Chrysiptera* demoiselles in the subtropical South Pacific. *Coral Reefs,* 41**,** 797-812. https://doi.org/10.1007/s00338-021-02179-7.

LIGGINS, L., SWEATMAN, J. A., TRNSKI, T., DUFFY, C. A., EDDY, T. D. & AGUIRRE, J. D. 2020. Natural history footage provides new reef fish biodiversity information for a pristine but rarely visited archipelago. *Scientific Reports*, 10, 1-7. https://doi.org/10.1038/s41598-020-60136-w.

LIN, H.-Y., CORKREY, R., KASCHNER, K., GARILAO, C. & COSTELLO, M. J. 2021. Latitudinal diversity gradients for five taxonomic levels of marine fish in depth zones. *Ecological Research,* 36**,** 266-280. https://doi.org/10.1111/1440-1703.12193.

LIU, H., LI, S., UGOLINI, A., MOMTAZI, F. & HOU, Z. 2018. Tethyan closure drove tropical marine biodiversity: Vicariant diversification of intertidal crustaceans. *Journal of Biogeography,* 45**,** 941-951. https://doi.org/10.1111/jbi.13183.

LOHMAN, D. J., DE BRUYN, M., PAGE, T., VON RINTELEN, K., HALL, R., NG, P. K., SHIH, H.-T., CARVALHO, G. R. & VON RINTELEN, T. 2011. Biogeography of the Indo-Australian archipelago. *Annual Review of Ecology, Evolution and Systematics,* 42**,** 205-226. https://doi.org/10.1146/annurev-ecolsys-102710-145001.

LÓPEZ, J. A., CHEN, W.-J. & ORTÍ, G. 2004. Esociform phylogeny. *Copeia,* 2004**,** 449-464. https://doi.org/10.1643/CG-03-087R1.

LÓPEZ-AGUIRRE, C., HAND, S. J., LAFFAN, S. W. & ARCHER, M. 2018. Phylogenetic diversity, types of endemism and the evolutionary history of New World bats. *Ecography,* 41**,** 1955-1966. https://doi.org/10.1111/ecog.03260.

LORREY, A. M., VANDERGOES, M., ALMOND, P., RENWICK, J., STEPHENS, T., BOSTOCK, H., MACKINTOSH, A., NEWNHAM, R., WILLIAMS, P. W. & ACKERLEY, D. 2012. Palaeocirculation across New Zealand during the last glacial maximum at~ 21 ka. *Quaternary Science Reviews,* 36**,** 189-213. https://doi.org/ https://doi.org/10.1016/j.quascirev.2011.09.025.

LOTZE, H. K., LENIHAN, H. S., BOURQUE, B. J., BRADBURY, R. H., COOKE, R. G., KAY, M. C., KIDWELL, S. M., KIRBY, M. X., PETERSON, C. H. & JACKSON, J. B. 2006.

Depletion, degradation, and recovery potential of estuaries and coastal seas. *Science,* 312**,** 1806-1809. https://doi.org/10.1126/science.1128035.
LOUIS, M., SKOVRIND, M., SAMANIEGO CASTRUITA, J. A., GARILAO, C., KASCHNER, K., GOPALAKRISHNAN, S., HAILE, J. S., LYDERSEN, C., KOVACS, K. M. & GARDE, E. 2020. Influence of past climate change on phylogeography and demographic history of narwhals, *Monodon monoceros*. *Proceedings of the Royal Society B,* 287**,** 20192964. https://doi.org/10.1098/rspb.2019.2964.
LUDT, W. B., BURRIDGE, C. P. & CHAKRABARTY, P. 2019. A taxonomic revision of Cheilodactylidae and Latridae (Centrarchiformes: Cirrhitoidei) using morphological and genomic characters. *Zootaxa,* 4585, 121-141. https://doi.org/10.11646/zootaxa.4585.1.7.
MACARTHUR, R. H. & WILSON, E. O. 1963. An equilibrium theory of insular zoogeography. *Evolution***,** 373-387.
MACARTHUR, R. H. & WILSON, E. O. 1967. The theory of island biogeography. NJ: Princeton University Press.
MANES, S., COSTELLO, M. J., BECKETT, H., DEBNATH, A., DEVENISH-NELSON, E., GREY, K.-A., JENKINS, R., KHAN, T. M., KIESSLING, W. & KRAUSE, C. 2021. Endemism increases species' climate change risk in areas of global biodiversity importance. *Biological Conservation,* 257**,** 109070. https://doi.org/10.1016/j.biocon.2021.109070.
MATSCHINER, M., MUSILOVÁ, Z., BARTH, J. M., STAROSTOVÁ, Z., SALZBURGER, W., STEEL, M. & BOUCKAERT, R. 2017. Bayesian phylogenetic estimation of clade ages supports trans-Atlantic dispersal of cichlid fishes. *Systematic Biology,* 66**,** 3-22. https://doi.org/10.1093/sysbio/syw076.
MATZKE, N. J. 2013. Probabilistic historical biogeography: new models for founder-event speciation, imperfect detection, and fossils allow improved accuracy and model-testing. *Frontiers of Biogeography,* 5**,** 242-248. https://doi.org/10.21425/F55419694.
MATZKE, N. J. 2014. Model selection in historical biogeography reveals that founder-event speciation is a crucial process in island clades. *Systematic Biology,* 63**,** 951-970. https://doi.org/10.1093/sysbio/syu056.
MATZKE, N. J. 2022. Statistical comparison of DEC and DEC+ J is identical to comparison of two ClaSSE submodels, and is therefore valid. *Journal of Biogeography,* 49**,** 1805-1824. https://doi.org/10.1111/jbi.14346.
MCCLYMONT, E. L., ELMORE, A. C., KENDER, S., LENG, M. J., GREAVES, M. & ELDERFIELD, H. 2016. Pliocene-Pleistocene evolution of sea surface and intermediate water temperatures from the southwest Pacific. *Paleoceanography,* 31**,** 895-913. https://doi.org/10.1002/2016PA002954.
MCCORD, C. L. & WESTNEAT, M. W. 2016. Phylogenetic relationships and the evolution of BMP4 in triggerfishes and filefishes (Balistoidea). *Molecular Phylogenetics and Evolution,* 94**,** 397-409. https://doi.org/10.1016/j.ympev.2015.09.014.
MCCORD, C.L., NASH, C.M., COOPER, W.J. & WESTNEAT, M.W. 2021. Phylogeny of the damselfishes (Pomacentridae) and patterns of asymmetrical diversification in body size and feeding ecology. *PLoS One,* 16, e0258889. https://doi.org/10.1371/journal.pone.0258889.
MCDOUGALL, I., EMBLETON, B. & STONE, D. 1981. Origin and evolution of Lord Howe Island, southwest Pacific Ocean. *Journal of the Geological Society of Australia,* 28**,** 155-176.
MCGILL, B. J., CHASE, J. M., HORTAL, J., OVERCAST, I., ROMINGER, A. J., ROSINDELL, J., BORGES, P. A., EMERSON, B. C., ETIENNE, R. S. & HICKERSON, M. J. 2019. Unifying macroecology and macroevolution to answer fundamental questions about biodiversity. *Global Ecology and Biogeography,* 28**,** 1925-1936.
MIDDLETON, I., AGUIRRE, J. D., TRNSKI, T., FRANCIS, M., DUFFY, C. & LIGGINS, L. 2021. Introduced alien, range extension or just visiting? Combining citizen science observations and expert knowledge to classify range dynamics of marine fishes. *Diversity and Distributions,* 27**,** 1278-1293. https://doi.org/10.1111/ddi.13273.
MIDDLETON, I., FRANCIS, M., AGUIRRE, J. D., STRUTHERS, C., TRNSKI, T., DUFFY, C., ANDERSON, J., CARNEY, M., COX, N., HEMSTALK, S., HERBERT, B., JOHNSTON, C., MIDDLETON, C., OLDFIELD, T., ROBINSON, R., SHEATH, C., SKIPWORTH, I., STANCICH, J., WHITTINGTON, H. & LIGGINS, L. In review. Spatio-temporal variability in occurrences of tropical, subtropical and rare marine fishes in Aotearoa New Zealand. *Journal of Biogeography*.

MILLER, E. C., HAYASHI, K. T., SONG, D. & WIENS, J. J. 2018. Explaining the ocean's richest biodiversity hotspot and global patterns of fish diversity. *Proceedings of the Royal Society B,* 285**,** 20181314. https://doi.org/10.1098/rspb.2018.1314.

MIRANDE, J. M. 2017. Combined phylogeny of ray-finned fishes (Actinopterygii) and the use of morphological characters in large-scale analyses. *Cladistics,* 33**,** 333-350. https://doi.org/10.1111/cla.12171.

MISHLER, B. D., GURALNICK, R., SOLTIS, P. S., SMITH, S. A., SOLTIS, D. E., BARVE, N., ALLEN, J. M. & LAFFAN, S. W. 2020. Spatial phylogenetics of the North American flora. *Journal of Systematics and Evolution,* 58**,** 393-405. https://doi.org/10.1111/jse.12590.

MISHLER, B. D., KNERR, N., GONZÁLEZ-OROZCO, C. E., THORNHILL, A. H., LAFFAN, S. W. & MILLER, J. T. 2014. Phylogenetic measures of biodiversity and neo-and paleo-endemism in Australian Acacia. *Nature Communications,* 5**,** 1-10. https://doi.org/10.1038/ncomms5473.

MOORE, G. & CHAPLIN, J. 2014. Contrasting demographic histories in a pair of allopatric, sibling species of fish (Arripidae) from environments with contrasting glacial histories. *Marine Biology,* 161**,** 1543-1555. https://doi.org/10.1007/s00227-014-2439-1.

MORA, C., TITTENSOR, D. P. & MYERS, R. A. 2008. The completeness of taxonomic inventories for describing the global diversity and distribution of marine fishes. *Proceedings of the Royal Society B: Biological Sciences,* 275**,** 149-155. https://doi.org/10.1098/rspb.2007.1315.

MORITZ, C. 2002. Strategies to protect biological diversity and the evolutionary processes that sustain it. *Systematic Biology,* 51**,** 238-254.

MORTIMER, N., CAMPBELL, H. J., TULLOCH, A. J., KING, P. R., STAGPOOLE, V. M., WOOD, R. A., RATTENBURY, M. S., SUTHERLAND, R., ADAMS, C. J. & COLLOT, J. 2017. Zealandia: Earth's hidden continent. *GSA today,* 27**,** 27-35. https:doi.org/10.1130/GSATG321A.1.

MUNDAY, P. L., WARNER, R. R., MONRO, K., PANDOLFI, J. M. & MARSHALL, D. J. 2013. Predicting evolutionary responses to climate change in the sea. *Ecology Letters,* 16**,** 1488-1500. https://doi.org/ 10.1111/ele.12185.

MYERS, E. M., ANDERSON, M. J., LIGGINS, L., HARVEY, E. S., ROBERTS, C. D. & EME, D. 2021. High functional diversity in deep-sea fish communities and increasing intraspecific trait variation with increasing latitude. *Ecology and Evolution,* 11**,** 10600-10612. https://doi.org/10.1002/ece3.7871.

MYERS, N. 1988. Threatened biotas:" hot spots" in tropical forests. *Environmentalist,* 8**,** 187-208.

MYERS, N. 1990. The biodiversity challenge: expanded hot-spots analysis. *Environmentalist,* 10**,** 243-256.

MYERS, N., MITTERMEIER, R. A., MITTERMEIER, C. G., DA FONSECA, G. A. & KENT, J. 2000. Biodiversity hotspots for conservation priorities. *Nature,* 403**,** 853-858.

NATALE, F., HOFHERR, J., FIORE, G. & VIRTANEN, J. 2013. Interactions between aquaculture and fisheries. *Marine Policy,* 38**,** 205-213. https://doi.org/10.1016/j.marpol.2012.05.037.

NAVARRETE, A. H., LAGOS, N. A. & OJEDA, F. P. 2014. Latitudinal diversity patterns of Chilean coastal fishes: searching for causal processes. *Revista Chilena de Historia Natural,* 87**,** 1-11. https://doi.org/10.1186/0717-6317-87-2.

NEALL, V. E. & TREWICK, S. A. 2008. The age and origin of the Pacific islands: a geological overview. *Philosophical Transactions of the Royal Society B: Biological Sciences,* 363**,** 3293-3308. https://doi.org/10.1098/rstb.2008.0119.

NEAR, T. J., DORNBURG, A., EYTAN, R. I., KECK, B. P., SMITH, W. L., KUHN, K. L., MOORE, J. A., PRICE, S. A., BURBRINK, F. T. & FRIEDMAN, M. 2013. Phylogeny and tempo of diversification in the superradiation of spiny-rayed fishes. *Proceedings of the National Academy of Sciences,* 110**,** 12738-12743. https://doi.org/10.1073/pnas.1304661110.

NEAR, T. J., EYTAN, R. I., DORNBURG, A., KUHN, K. L., MOORE, J. A., DAVIS, M. P., WAINWRIGHT, P. C., FRIEDMAN, M. & SMITH, W. L. 2012. Resolution of ray-finned fish phylogeny and timing of diversification. *Proceedings of the National Academy of Sciences,* 109**,** 13698-13703. https://doi.org/10.1073/pnas.1206625109.

NELSON, C. S. & COOKE, P. J. 2001. History of oceanic front development in the New Zealand sector of the Southern Ocean during the Cenozoic—a synthesis. *New Zealand Journal of geology and geophysics,* 44**,** 535-553. https://doi.org/10.1080/00288306.2001.9514954.

NEW ZEALAND DEPARTMENT OF CONSERVATION. 2019. New Zealand marine protected areas. Gaps analysis. *Department of Conservation, Ministry for the Environment, Ministry for Primary Industries*. New Zealand Government.

NIELSEN, E. S., BEGER, M., HENRIQUES, R., SELKOE, K. A. & VON DER HEYDEN, S. 2017. Multispecies genetic objectives in spatial conservation planning. *Conservation Biology,* 31**,** 872-882. https://doi.org/10.1111/cobi.12875.

NORMAN, M. 2003. Biodiversity hotspots revisited. *BioScience,* 53**,** 916-917.

NUNEZ, S., ARETS, E., ALKEMADE, R., VERWER, C. & LEEMANS, R. 2019. Assesing the impacts of climate change on biodiversity: is below 2 ºC enough? *Climate Change,* 154**,** 351-365. https://doi.org/10.1007/s10584-019-02420-x.

Ó FOIGHIL, D., MARSHALL, B. A., HILBISH, T. J. & PINO, M. A. 1999. Trans-Pacific range extension by rafting is inferred for the flat oyster *Ostrea chilensis*. *The Biological Bulletin,* 196**,** 122-126.

ORME, C. D. L., DAVIES, R. G., BURGESS, M., EIGENBROD, F., PICKUP, N., OLSON, V. A., WEBSTER, A. J., DING, T.-S., RASMUSSEN, P. C. & RIDGELY, R. S. 2005. Global hotspots of species richness are not congruent with endemism or threat. *Nature,* 436**,** 1016-1019. https://doi.org/10.1038/nature03850.

PANTE, E., & SIMON-BOUHET, B. 2013. marmap: A Package for Importing, Plotting and Analyzing Bathymetric and Topographic Data in R. *PLoS One*, 8, e73051. https://doi.org/10.1371/journal.pone.0073051.

PAPA, Y., HALLIWELL, A. G., MORRISON, M. A., WELLENREUTHER, M. & RITCHIE, P. A. 2021. Phylogeographic structure and historical demography of tarakihi (*Nemadactylus macropterus*) and king tarakihi (*Nemadactylus* n. sp.) in New Zealand. *New Zealand Journal of Marine and Freshwater Research***,** 1-25. https://doi.org/10.1080/00288330.2021.1912119.

PARADIS, E. & SCHLIEP, K. 2019. ape 5.0: an environment for modern phylogenetics and evolutionary analyses in R. *Bioinformatics,* 35**,** 526-528. https://doi.org/10.1093/bioinformatics/bty633.

PAULIN, C. 1993. Review of the Australian fish family Arripididae (Percomorpha), with the description of a new species. *Marine and Freshwater Research,* 44**,** 459-471.

PAVOINE, S. & BONSALL, M. B. 2011. Measuring biodiversity to explain community assembly: a unified approach. *Biological Reviews,* 86**,** 792-812. https://doi.org/10.1111/j.1469-185X.2010.00171.x.

PEBESMA, E. J. 2018. Simple features for R: standardized support for spatial vector data. *R J.,* 10**,** 439.

PELLISSIER, L., LEPRIEUR, F., PARRAVICINI, V., COWMAN, P. F., KULBICKI, M., LITSIOS, G., OLSEN, S. M., WISZ, M. S., BELLWOOD, D. R. & MOUILLOT, D. 2014. Quaternary coral reef refugia preserved fish diversity. *Science,* 344**,** 1016-1019. https://doi.org/10.1126/science.1249853.

PINHEIRO, H. T., BERNARDI, G., SIMON, T., JOYEUX, J.-C., MACIEIRA, R. M., GASPARINI, J. L., ROCHA, C. & ROCHA, L. A. 2017. Island biogeography of marine organisms. *Nature,* 549**,** 82-85. https://doi.org/10.1038/nature23680.

PIÑEROS, V. J., BELTRÁN-LÓPEZ, R. G., BALDWIN, C. C., BARRAZA, E., ESPINOZA, E., MARTÍNEZ, J. E. & DOMÍNGUEZ-DOMÍNGUEZ, O. 2019. Diversification of the genus *Apogon* (Lacepède, 1801) (Apogonidae: Perciformes) in the tropical eastern Pacific. *Molecular Phylogenetics and Evolution,* 132**,** 232-242. https://doi.org/10.1016/j.ympev.2018.12.010.

POSADAS, P., CRISCI, J. V. & KATINAS, L. 2006. Historical biogeography: a review of its basic concepts and critical issues. *Journal of Arid Environments,* 66**,** 389-403. https://doi.org/10.1016/j.jaridenv.2006.01.004.

POWELL, C. L. E., WASKIN, S. & BATTISTUZZI, F. U. 2020. Quantifying the error of secondary vs. distant primary calibrations in a simulated environment. *Frontiers in Genetics,* 11**,** 252. https://doi.org/10.3389/fgene.2020.00252.

PROVOOST, P. & BOSCH, S. 2020. robis: R Client to access data from the OBIS API. *Ocean Biogeographic Information System. Intergovernmental Oceanographic Commission of UNESCO, R package version,* 2.

PYRON, R. A. & BURBRINK, F. T. 2010. Hard and soft allopatry: physically and ecologically mediated modes of geographic speciation. *Journal of Biogeography,* 37**,** 2005-2015. https://doi.org/10.1111/j.1365-2699.2010.02336.x.

QUILTY, P. G. 2007. Origin and evolution of the sub-Antarctic islands: the foundation. *Papers and Proceedings of the Royal Society of Tasmania*, 141, 35-58. https://doi.org/10.26749/rstpp.141.1.35.
R CORE TEAM. 2020. *R: A language and environment for statistical computing*. R Foundation for Statistical Computing, Vienna, Austria. https://www.R-project.org/.
R CORE TEAM. 2022. *R: A language and environment for statistical computing*. R Foundation for Statistical Computing, Vienna, Austria. https://www.R-project.org/.
RABOSKY, D. L. 2020. Speciation rate and the diversity of fishes in freshwaters and the oceans. *Journal of Biogeography,* 47**,** 1207-1217. https://doi.org/10.1111/jbi.13839.
RABOSKY, D. L., CHANG, J., TITLE, P. O., COWMAN, P. F., SALLAN, L., FRIEDMAN, M., KASCHNER, K., GARILAO, C., NEAR, T. J. & COLL, M. 2018. An inverse latitudinal gradient in speciation rate for marine fishes. *Nature,* 559**,** 392-395. https://doi.org/10.1038/s41586-018-0273-1.
RAMBAUT, A., DRUMMOND, A. J., XIE, D., BAELE, G. & SUCHARD, M. A. 2018. Posterior summarization in Bayesian phylogenetics using Tracer 1.7. *Systematic Biology,* 67**,** 901. https://doi.org/ 10.1093/sysbio/syy032.
RANDALL, J. 2007. Reef fishes of Hawaii. University of Hawaii Press, Honolulu.
RANDALL, J. E. & CEA, A. 2011. Shore fishes of Easter Island. University of Hawaii Press, Honolulu.
REE, R. H., MOORE, B. R., WEBB, C. O. & DONOGHUE, M. J. 2005. A likelihood framework for inferring the evolution of geographic range on phylogenetic trees. *Evolution,* 59**,** 2299-2311. https://doi.org/10.1111/j.0014-3820.2005.tb00940.x.
REE, R. H. & SANMARTÍN, I. 2018. Conceptual and statistical problems with the DEC+ J model of founder-event speciation and its comparison with DEC via model selection. *Journal of Biogeography,* 45**,** 741-749. https://doi.org/10.1111/jbi.13173.
REE, R. H. & SMITH, S. A. 2008. Maximum likelihood inference of geographic range evolution by dispersal, local extinction, and cladogenesis. *Systematic Biology,* 57**,** 4-14. https://doi.org/10.1080/10635150701883881.
REID, W. V. 1998. Biodiversity hotspots. *Trends in Ecology & Evolution,* 13**,** 275-280.
RIGINOS, C., CRANDALL, E. D., LIGGINS, L., GAITHER, M. R., EWING, R. B., MEYER, C., ANDREWS, K. R., EUCLIDE, P. T., TITUS, B. M. & THERKILDSEN, N. O. 2020. Building a global genomics observatory: Using GEOME (the Genomic Observatories Metadatabase) to expedite and improve deposition and retrieval of genetic data and metadata for biodiversity research. *Molecular Ecology Resources,* 20**,** 1458-1469. https://doi.org/10.1111/1755-0998.13269.
RIGINOS, C., DOUGLAS, K. E., JIN, Y., SHANAHAN, D. F. & TREML, E. A. 2011. Effects of geography and life history traits on genetic differentiation in benthic marine fishes. *Ecography,* 34**,** 566-575. https://doi.org/10.1111/j.1600-0587.2010.06511.x.
ROBERTS, C. D., STEWART, A.L. & STRUTHERS, C.D. 2015. The Fishes of New Zealand. Te Papa Press, Wellington.
ROBERTS, C. D., PAULIN, C. D., STEWART, A. L., MCPHEE, R. P. & MCDOWALL, R. M. 2009. Checklist of New Zealand Chordata: Living lancelets, jawless fishes, cartilaginous, and bony fishes (Vol. 1). In D. P. Gordon (Ed.), *New Zealand inventory of biodiversity. Vol. 1. Kingdom Animalia* (pp. 527-536). Canterbury University Press.
ROBERTS, C.D., STEWART, A.L., STRUTHERS, C.D., BARKER, J.J. & KORTET, S. 2020. Checklist of the Fishes of New Zealand. Online version 1.2. Museum of New Zealand Te Papa Tongarewa, Wellington. https://collections.tepapa.govt.nz/document/10564.
ROBERTS, C. M., MCCLEAN, C. J., VERON, J. E., HAWKINS, J. P., ALLEN, G. R., MCALLISTER, D. E., MITTERMEIER, C. G., SCHUELER, F. W., SPALDING, M. & WELLS, F. 2002. Marine biodiversity hotspots and conservation priorities for tropical reefs. *Science,* 295**,** 1280-1284. https://doi.org/ 10.1126/science.1067728.
ROBERTSON, D. R., GROVE, J. S. & MCCOSKER, J. E. 2004. Tropical transpacific shore fishes. *Pacific Science,* 58**,** 507-565.
ROE, A. D., RICE, A. V., BROMILOW, S. E., COOKE, J. E. & SPERLING, F. A. 2010. Multilocus species identification and fungal DNA barcoding: insights from blue stain fungal symbionts of the mountain pine beetle. *Molecular Ecology Resources,* 10**,** 946-959. https://doi.org/10.1111/j.1755-0998.2010.02844.x.
RONQUIST, F. 1997. Dispersal-vicariance analysis: a new approach to the quantification of historical biogeography. *Systematic Biology,* 46**,** 195-203.

RONQUIST, F. & SANMARTÍN, I. 2011. Phylogenetic methods in biogeography. *Annual Review of Ecology, Evolution, and Systematics,* 42**,** 441-464. https://doi.org/10.1146/annurev-ecolsys-102209-144710.

ROSAUER, D., LAFFAN, S. W., CRISP, M. D., DONNELLAN, S. C. & COOK, L. G. 2009. Phylogenetic endemism: a new approach for identifying geographical concentrations of evolutionary history. *Molecular Ecology,* 18**,** 4061-4072. https://doi.org/10.1111/j.1365-294X.2009.04311.x.

ROSENBLATT, R. H. & WAPLES, R. S. 1986. A genetic comparison of allopatric populations of shore fish species from the eastern and central Pacific Ocean: dispersal or vicariance? *Copeia***,** 1986, 275-284.

RSTUDIO TEAM. 2019. RStudio: Integrated Development for R. RStudio, Inc., Boston, MA. http://www.rstudio.com/.

RSTUDIO TEAM. 2022. RStudio: Integrated Development for R. RStudio, Inc., Boston, MA. http://www.rstudio.com/.

RUBINOFF, D. & HOLLAND, B. S. 2005. Between two extremes: mitochondrial DNA is neither the panacea nor the nemesis of phylogenetic and taxonomic inference. *Systematic Biology,* 54**,** 952-961. https://doi.org/10.1080/10635150500234674.

SAFI, K., CIANCIARUSO, M. V., LOYOLA, R. D., BRITO, D., ARMOUR-MARSHALL, K. & DINIZ-FILHO, J. A. F. 2011. Understanding global patterns of mammalian functional and phylogenetic diversity. *Philosophical Transactions of the Royal Society B: Biological Sciences,* 366**,** 2536-2544. https://doi.org/10.1098/rstb.2011.0024.

SAMAYOA, A. P., STRUTHERS, C. D., TRNSKI, T., ROBERTS, C. D. & LIGGINS, L. 2022. Molecular phylogenetics reveals the evolutionary history of marine fishes (Actinopterygii) endemic to the subtropical islands of the Southwest Pacific. *Molecular Phylogenetics and Evolution,* 176**,** 107584. https://doi.org/10.1016/j.ympev.2022.107584.

SAMAYOA, A.P., AGUIRRE, J.D., DELRIEU-TROTTIN, E., & LIGGINS, L. In review. The origins of marine fishes endemic to subtropical islands of the Southwest Pacific. *Journal of Biogeography*.

SANCIANGCO, M. D., CARPENTER, K. E. & BETANCUR-R, R. 2016. Phylogenetic placement of enigmatic percomorph families (Teleostei: Percomorphaceae). *Molecular Phylogenetics and Evolution,* 94**,** 565-576. https://doi.org/10.1016/j.ympev.2015.10.006.

SANMARTÍN, I. 2012. Historical biogeography: evolution in time and space. *Evolution: Education and Outreach,* 5**,** 555-568. https://doi.org/10.1007/s12052-012-0421-2.

SANTAQUITERIA, A., SIQUEIRA, A. C., DUARTE-RIBEIRO, E., CARNEVALE, G., WHITE, W. T., POGONOSKI, J. J., BALDWIN, C. C., ORTÍ, G., ARCILA, D. & RICARDO, B.-R. 2021. Phylogenomics and historical biogeography of seahorses, dragonets, goatfishes, and allies (Teleostei: Syngnatharia): Assessing factors driving uncertainty in biogeographic inferences. *Systematic Biology,* 70**,** 1145-1162. https://doi.org/10.1093/sysbio/syab028.

SAUQUET, H. 2013. A practical guide to molecular dating. *Comptes Rendus Palevol,* 12**,** 355-367. https://doi.org/10.1016/j.crpv.2013.07.003.

SCHMIDT-LEBUHN, A. N., KNERR, N. J., MILLER, J. T. & MISHLER, B. D. 2015. Phylogenetic diversity and endemism of Australian daisies (Asteraceae). *Journal of Biogeography,* 42**,** 1114-1122. https://doi.org/10.1111/jbi.12488.

SCOTT, J. M. & TURNBULL, I. M. 2019. Geology of New Zealand's sub-Antarctic islands. *New Zealand Journal of Geology and Geophysics,* 62**,** 291-317. https://doi.org/10.1080/00288306.2019.1600557.

SEEHAUSEN, O. & WAGNER, C. E. 2014. Speciation in freshwater fishes. *Annual Review of Ecology, Evolution, and Systematics,* 45**,** 621-651. https://doi.org/10.1146/annurev-ecolsys-120213-091818.

SELIG, E. R., TURNER, W. R., TROËNG, S., WALLACE, B. P., HALPERN, B. S., KASCHNER, K., LASCELLES, B. G., CARPENTER, K. E. & MITTERMEIER, R. A. 2014. Global priorities for marine biodiversity conservation. *PloS One,* 9**,** e82898. https://doi.org/10.1371/journal.pone.0082898.

SGRÒ, C. M., LOWE, A. J. & HOFFMANN, A. A. 2011. Building evolutionary resilience for conserving biodiversity under climate change. *Evolutionary Applications,* 4**,** 326-337. https://doi.org/ 10.1111/j.1752-4571.2010.00157.x.

SIQUEIRA, A. C., BELLWOOD, D. R. & COWMAN, P. F. 2019. Historical biogeography of herbivorous coral reef fishes: the formation of an Atlantic fauna. *Journal of Biogeography,* 46**,** 1611-1624. https://doi.org/10.1111/jbi.13631.

SIQUEIRA, A. C., OLIVEIRA-SANTOS, L. G. R., COWMAN, P. F. & FLOETER, S. R. 2016. Evolutionary processes underlying latitudinal differences in reef fish biodiversity. *Global Ecology and Biogeography,* 25**,** 1466-1476. https://doi.org/10.1111/geb.12506.

SKOVRIND, M., LOUIS, M., WESTBURY, M. V., GARILAO, C., KASCHNER, K., CASTRUITA, J. A. S., GOPALAKRISHNAN, S., KNUDSEN, S. W., HAILE, J. S. & DALÉN, L. 2021. Circumpolar phylogeography and demographic history of beluga whales reflect past climatic fluctuations. *Molecular Ecology,* 30**,** 2543-2559. https://doi.org/10.1111/mec.15915.

SMITH, P. J., MCPHEE, R. P. & ROBERTS, C. D. 2006. DNA and meristic evidence for two species of giant stargazer (Teleostei: Uranoscopidae: *Kathetostoma*) in New Zealand waters. *New Zealand Journal of Marine and Freshwater Research,* 40**,** 379-387. https://doi.org/10.1080/00288330.2006.9517429.

STAMATAKIS, A. 2014. RAxML version 8: a tool for phylogenetic analysis and post-analysis of large phylogenies. *Bioinformatics,* 30**,** 1312-1313. https://doi.org/10.1093/bioinformatics/btu033.

STEWART, A. L. 2015. Family Gobiesocidae. Clingfishes (Vol. 4). In C. D. Roberts, A. L. Stewart & C. D. Struthers (Eds), *The Fishes of New Zealand*, (pp. 1539-1555). Te Papa Press, Wellington.

STUART-SMITH, J., PECL, G., PENDER, A., TRACEY, S., VILLANUEVA, C. & SMITH-VANIZ, W. F. 2018. Southernmost records of two *Seriola* species in an Australian ocean-warming hotspot. *Marine Biodiversity,* 48**,** 1579-1582. https://doi.org/10.1007/s12526-016-0580-4.

STUART-SMITH, R. D., EDGAR, G. J. & BATES, A. E. 2017. Thermal limits to the geographic distributions of shallow-water marine species. *Nature Ecology & Evolution,* 1**,** 1846-1852. https://doi.org/10.1038/s41559-017-0353-x.

TANG, K. L., STIASSNY, M. L., MAYDEN, R. L. & DESALLE, R. 2021. Systematics of Damselfishes. *Ichthyology & Herpetology,* 109**,** 258-318. https://doi.org/10.1643/i2020105.

TEA, Y.-K. & GILL, A. C. 2020. Systematic reappraisal of the anti-equatorial fish genus *Microcanthus* Swainson (Teleostei: Microcanthidae), with redescription and resurrection of *Microcanthus joyceae* Whitley. *Zootaxa,* 4802**,** 41-60. https://doi.org/10.11646/zootaxa.4802.1.3.

TEA, Y.-K., XU, X., DIBATTISTA, J. D., LO, N., COWMAN, P. F. & HO, S. Y. 2022. Phylogenomic analysis of concatenated ultraconserved elements reveals the recent evolutionary radiation of the fairy wrasses (Teleostei: Labridae: *Cirrhilabrus*). *Systematic Biology,* 71**,** 1-12. https://doi.org/10.1093/sysbio/syab012.

TEA, Y.-K., VAN DER WAL, C., LUDT, W. B., GILL, A. C., LO, N. & HO, S. Y. 2019. Boomeranging around Australia: Historical biogeography and population genomics of the anti-equatorial fish *Microcanthus strigatus* (Teleostei: Microcanthidae). *Molecular Ecology,* 28**,** 3771-3785. https://doi.org/10.1111/mec.15172.

TEMPLETON, A. R. 2008. The reality and importance of founder speciation in evolution. *BioEssays,* 30**,** 470-479. https://doi.org/10.1002/bies.20745.

THACKER, C. E. 2015. Biogeography of goby lineages (Gobiiformes: Gobioidei): origin, invasions and extinction throughout the Cenozoic. *Journal of Biogeography,* 42**,** 1615-1625. https://doi.org/10.1111/jbi.12545.

THORNHILL, A. H., MISHLER, B. D., KNERR, N. J., GONZÁLEZ-OROZCO, C. E., COSTION, C. M., CRAYN, D. M., LAFFAN, S. W. & MILLER, J. T. 2016. Continental-scale spatial phylogenetics of Australian angiosperms provides insights into ecology, evolution and conservation. *Journal of Biogeography,* 43**,** 2085-2098. https://doi.org/10.1111/jbi.12797.

TITTENSOR, D. P., MORA, C., JETZ, W., LOTZE, H. K., RICARD, D., BERGHE, E. V. & WORM, B. 2010. Global patterns and predictors of marine biodiversity across taxa. *Nature,* 466**,** 1098-1101. https://doi.org/10.1038/nature09329.

TREWICK, S. A., PATERSON, A. M. & CAMPBELL, H. J. 2007. Hello New Zealand. *Journal of Biogeography*, 34, 1-6. https://doi.org/10.1111/j.1365-2699.2006.01643.x.

TRNSKI, T. & DE LANGE, P. J. 2015. Introduction to the Kermadec Biodiscovery Expedition 2011. *Bulletin of the Auckland Museum,* 20**,** 1-18.

TRNSKI, T., DUFFY, C. A., FRANCIS, M. P., MCGROUTHER, M. A., STEWART, A. L., STRUTHERS, C. D. & ZINTZEN, V. 2015. Recent collections of fishes at the Kermadec Islands and new records for the region. *Bulletin of the Auckland Museum,* 20**,** 463-480.

TUCKER, C. M., CADOTTE, M. W., CARVALHO, S. B., DAVIES, T. J., FERRIER, S., FRITZ, S. A., GRENYER, R., HELMUS, M. R., JIN, L. S. & MOOERS, A. O. 2017. A guide to

phylogenetic metrics for conservation, community ecology and macroecology. *Biological Reviews,* 92**,** 698-715. https://doi.org/10.1111/brv.12252.

UIBLEIN, F. & HEEMSTRA, P. C. 2010. A taxonomic review of the Western Indian Ocean goathfishes of the genus *Upeneus* (Family Mullidae), with descriptions of four new species. *Smithiana Bulletin*, 11, 35-71.

UIBLEIN, F. & MOTOMURA, H. 2021. Three new goatfishes of the genus *Upeneus* from the Eastern Indian Ocean and Western Pacific, with an updated taxonomic account for *U. itoui* (Mullidae: *japonicus*-species group). *Zootaxa,* 4938**,** 298-324. https://doi.org/10.11646/zootaxa.4938.3.2.

VAN DAM, M. H. & MATZKE, N. J. 2016. Evaluating the influence of connectivity and distance on biogeographical patterns in the south-western deserts of North America. *Journal of Biogeography,* 43**,** 1514-1532. https://doi.org/10.1111/jbi.12727.

VAN DER MEER, M. H., BERUMEN, M. L., HOBBS, J.-P. & VAN HERWERDEN, L. 2015. Population connectivity and the effectiveness of marine protected areas to protect vulnerable, exploited and endemic coral reef fishes at an endemic hotspot. *Coral Reefs,* 34**,** 393-402. https://doi.org/10.1007/s00338-014-1242-2.

VENEGAS-LI, R., LEVIN, N., MORALES-BARQUERO, L., KASCHNER, K., GARILAO, C. & KARK, S. 2019. Global assessment of marine biodiversity potentially threatened by offshore hydrocarbon activities. *Global Change Biology,* 25**,** 2009-2020. https://doi.org/10.1111/gcb.14616.

VISALLI, M. E., BEST, B. D., CABRAL, R. B., CHEUNG, W. W., CLARK, N. A., GARILAO, C., KASCHNER, K., KESNER-REYES, K., LAM, V. W. & MAXWELL, S. M. 2020. Data-driven approach for highlighting priority areas for protection in marine areas beyond national jurisdiction. *Marine Policy,* 122**,** 103927. https://doi.org/10.1016/j.marpol.2020.103927.

VOSKAMP, A., BAKER, D. J., STEPHENS, P. A., VALDES, P. J. & WILLIS, S. G. 2017. Global patterns in the divergence between phylogenetic diversity and species richness in terrestrial birds. *Journal of Biogeography,* 44**,** 709-721. https://doi.org/10.1111/jbi.12916.

WARD, R. D., ZEMLAK, T. S., INNES, B. H., LAST, P. R. & HEBERT, P. D. 2005. DNA barcoding Australia's fish species. *Philosophical Transactions of the Royal Society B: Biological Sciences,* 360**,** 1847-1857. https://doi.org/10.1098/rstb.2005.1716.

WATERS, J. M. 2008. Driven by the West Wind Drift? A synthesis of southern temperate marine biogeography, with new directions for dispersalism. *Journal of Biogeography,* 35**,** 417-427. https://doi.org/10.1111/j.1365-2699.2007.01724.x.

WATERS, J. M. & ROY, M. S. 2004. Out of Africa: the slow train to Australasia. *Systematic Biology,* 53**,** 18-24. https://doi.org/10.1080/10635150490264671.

WEBB, T. J., VANDEN BERGHE, E. & O'DOR, R. 2010. Biodiversity's big wet secret: the global distribution of marine biological records reveals chronic under-exploration of the deep pelagic ocean. *PloS One,* 5**,** e10223. https://doi.org/10.1371/journal.pone.0010223.

WERNBERG, T., BENNETT, S., BABCOCK, R. C., DE BETTIGNIES, T., CURE, K., DEPCZYNSKI, M., DUFOIS, F., FROMONT, J., FULTON, C. J. & HOVEY, R. K. 2016. Climate-driven regime shift of a temperate marine ecosystem. *Science,* 353**,** 169-172. https://doi.org/10.1126/science.aad8745.

WHITTAKER, R. J., TRIANTIS, K. A. & LADLE, R. J. 2008. A general dynamic theory of oceanic island biogeography. *Journal of Biogeography,* 35**,** 977-994. https://doi.org/10.1111/j.1365-2699.2008.01892.x.

WHITTAKER, R. J., TRIANTIS, K. A. & LADLE, R. J. 2010. A general dynamic theory of oceanic island biogeography: extending the MacArthur–Wilson theory to accommodate the rise and fall of volcanic islands. In J. B. Losos & R. E. Ricklefs (Eds.), *The theory of island biogeography revisited,* (pp. 88-115). Princeton University Press.

WICKS, L. C., GARDNER, J. P. & DAVY, S. K. 2010. Spatial patterns and regional affinities of coral communities at the Kermadec Islands Marine Reserve, New Zealand—a marginal high-latitude site. *Marine Ecology Progress Series*, 400, 101-113. https://doi.org/10.3354/meps08398.

WIENS, J. J. & DONOGHUE, M. J. 2004. Historical biogeography, ecology and species richness. *Trends in Ecology & Evolution,* 19**,** 639-644. https://doi.org/10.1016/j.tree.2004.09.011.

WILLIG, M. R., KAUFMAN, D. M. & STEVENS, R. D. 2003. Latitudinal gradients of biodiversity: pattern, process, scale, and synthesis. *Annual Review of Ecology, Evolution, and Systematics***,** 273-309.

WILSON, A. C., CANN, R. L., CARR, S. M., GEORGE, M., GYLLENSTEN, U. B., HELM-BYCHOWSKI, K. M., HIGUCHI, R. G., PALUMBI, S. R., PRAGER, E. M. & SAGE, R. D. 1985. Mitochondrial DNA and two perspectives on evolutionary genetics. *Biological Journal of the Linnean Society,* 26**,** 375-400.

WOODLAND, D. 1983. Zoogeography of the Siganidae (Pisces): an interpretation of distribution and richness patterns. *Bulletin of Marine Science,* 33**,** 713-717.

WORMS EDITORIAL BOARD. 2021. *World Register of Marine Species*. http://www.marinespecies.org at VLIZ. doi:10.14284/170 (accessed 8 November 2021).

WORMS EDITORIAL BOARD. 2022. *World Register of Marine Species*. http://www.marinespecies.org at VLIZ. doi:10.14284/170 (accessed May 2022).

YANCEY, P. H., GERRINGER, M. E., DRAZEN, J. C., ROWDEN, A. A. & JAMIESON, A. 2014. Marine fish may be biochemically constrained from inhabiting the deepest ocean depths. *Proceedings of the National Academy of Sciences,* 111**,** 4461-4465. https://doi.org/10.1073/pnas.1322003111.

YOUNG, A. D. & GILLUNG, J. P. 2020. Phylogenomics—principles, opportunities and pitfalls of big-data phylogenetics. *Systematic Entomology,* 45**,** 225-247. https://doi.org/10.1111/syen.12406.

ZHENG, Y. & WIENS, J. J. 2015. Do missing data influence the accuracy of divergence-time estimation with BEAST? *Molecular Phylogenetics and Evolution,* 85**,** 41-49. https://doi.org/10.1016/j.ympev.2015.02.002.

ZIELSKE, S., PONDER, W. F. & HAASE, M. 2017. The enigmatic pattern of long-distance dispersal of minute freshwater gastropods (Caenogastropoda, Truncatelloidea, Tateidae) across the South Pacific. *Journal of Biogeography,* 44**,** 195-206. https://doi.org/10.1111/jbi.12800.

ZINTZEN, V., ANDERSON, M. J., ROBERTS, C. D., HARVEY, E. S. & STEWART, A. L. 2017. Effects of latitude and depth on the beta diversity of New Zealand fish communities. *Scientific Reports,* 7**,** 1-10. https://doi.org/10.1038/s41598-017-08427-7.